INFORMATION TO USERS

This manuscript has been reproduced from the microfilm master. UMI films the text directly from the original or copy submitted. Thus, some thesis and dissertation copies are in typewriter face, while others may be from any type of computer printer.

The quality of this reproduction is dependent upon the quality of the copy submitted. Broken or indistinct print, colored or poor quality illustrations and photographs, print bleedthrough, substandard margins, and improper alignment can adversely affect reproduction.

In the unlikely event that the author did not send UMI a complete manuscript and there are missing pages, these will be noted. Also, if unauthorized copyright material had to be removed, a note will indicate the deletion.

Oversize materials (e.g., maps, drawings, charts) are reproduced by sectioning the original, beginning at the upper left-hand corner and continuing from left to right in equal sections with small overlaps.

Photographs included in the original manuscript have been reproduced xerographically in this copy. Higher quality 6" x 9" black and white photographic prints are available for any photographs or illustrations appearing in this copy for an additional charge. Contact UMI directly to order.

Bell & Howell Information and Learning
300 North Zeeb Road, Ann Arbor, MI 48106-1346 USA
800-521-0600

Université d'Ottawa • University of Ottawa

STRUCTURE AND ACTIVITY OF HUMAN CLUSTERIN

Thesis submitted to the Department of Biochemistry in partial fulfillment of the requirements for the degree of Doctor of Philosophy

University of Ottawa
Ottawa, Ontario, Canada
September, 1998

National Library
of Canada

Acquisitions and
Bibliographic Services

395 Wellington Street
Ottawa ON K1A 0N4
Canada

Bibliothèque nationale
du Canada

Acquisitions et
services bibliographiques

395, rue Wellington
Ottawa ON K1A 0N4
Canada

Your file Votre référence

Our file Notre référence

0-612-45178-X

Canada

Abstract

Clusterin is a heterodimeric disulfide linked glycoprotein secreted by many epithelia in adult and developing tissues. Clusterin is also induced in response to diverse injury or cell death stimuli. The protein interacts with, and is suggested to have, a relatively non specific affinity for markedly hydrophobic/amphipathic ligands including terminal complement components, Alzheimer's disease amyloid β (Aβ) peptides, and apo AI-HDL in addition to immunoglobulins, TGFβ receptors, heparin and the endocytic receptor LRP2.

Little is known of clusterin structure and function. Sequences modeled as amphipathic α helices have been proposed as promiscous binding sites(s) for hydrophobic ligands. A reanalysis of these sequences using the COIL algorithm predicts a single conserved coiled-coil helix in each of the α and β chains. These overlap, with heptads aligned, when each chain is aligned (antiparallel) with respect to the pattern of interchain disulfide bonds, and may reflect formation of an antiparallel coiled-coil with a cationic face that is proposed as an LRP2\heparin binding site. Distinct α and β chain amphipathic helices encoded by exon 5 may constitute the hydrophobic ligand binding site. Partial proteolysis predominantly within or near these latter helices accompanies expression of human clusterin in *Pichia pastoris* and is associated with significant decreases in specific binding activity to IgG and $A\beta_{1-40}$ but not to LRP2 overexpressing differentiated F9 cells, in agreement with these binding site assignments. Although Zn^{+2} polymerized C9 (poly C9) and $A\beta_{1-40}$ are mutual heterologous competitive clusterin-binding inhibitors, the specific binding of the recombinant protein to poly C9 is not as

significantly diminished, suggesting a distinct but nearby binding site for this presumptive hydrophobic ligand. The C9 binding site is likely to be distinct from that of LRP2 since like IgG and $A\beta_{1-40}$ but unlike F9 cell surface binding poly C9 binding is not inhibited by anti-human clusterin monoclonal antibody G7.

Distinct interactions may also mediate clusterin recognition of IgG and $A\beta_{1-40}$ since mild acidification and diethylpyrocarbonate (DEPC) modification of clusterin histidine side chains had markedly different effects on each interaction. Binding to $A\beta_{1-40}$ is singularly and dramatically enhanced by mild acidification and diminished by DEPC modification suggesting that a salt bridge between a clusterin imidazole and an acidic side chain of $A\beta_{1-40}$, reminiscent of electrostatic interactions postulated to stabilize $A\beta$ peptide monomers in polymeric fibrils, in addition to hydrophobic interactions may be important in the stability of the clusterin-$A\beta_{1-40}$ complex. These findings support the hypothesis that the interaction of clusterin with some hydrophobic ligands is highly specific and suggest conversely a physiological function specifically related to these interactions.

Acknowledgements

I would like to acknowledge the support of a number of individuals without whom I could not have completed this work. To my supervisor, Dr. Martin Tenniswood I owe a large debt of thanks for allowing me to pursue my Doctoral work under his mentorship and for his guidance, patience, perseverence, and encouragement. The members of Dr. Tenniswood's laboratory, past and present, have been a constant source of advice, practical help, and friendship. In particular it is necessary to single out the friendship of Dr. Sean Guenette, with whom I started my Doctoral work and who has been a constant source of support, both practical and emotional. No less were friendships with Dr. Esther Nitsche, Dr. Paul Wong, Dr. Mark Wilson, Dr. Steffany Bennett, Dan Taillefer, Zheng Qi Wang, Jacintha O'Sullivan, Colm Morrissey, Amy Moquin, and Pamela Scott Adams. In addition to friendship several individuals also helped out directly with experimental work. Dr. Mark Wilson provided invaluable reagents and advice, including his own direct experience with clusterin, and by this helped focus the objectives of my thesis. Colm Morrissey and Dr. Steffany Bennett provided much help in characterization of the anti-rat clusterin monoclonal antibodies. Dr. Tenniswood's excellent technicians at the Adirondack Biomedical Research Center, Amy Moquin and Pamela Scott Adams provided invaluable support in oligonucleotide synthesis and DNA sequencing.

Several individuals outside of Dr. Tenniswood's laboratory also deserve especial mention. Amino acid analyses, peptide synthesis and protein sequencing were done in the Protein Core Facility of Dr. John Crabb at the Adirondack Biomedical Research

Center, by his excellent technician Karen West. I have had a particularly fruitful and enjoyable collaboration with Dr. Jim Kapron, a Postdoctoral Fellow in Dr. Crabb's laboratory, who did much work characterizing N-linked carbohydrate on human serum clusterin and has done preliminary work, together with Karen West, characterizing sites of proteolysis in recombinant clusterin. Dr. Dennis Williamson, at the University of Ottawa provided much useful advice, comic relief, and generously allowed me access to the equipment in his laboratory at a time when my experience, or lack thereof, was such as to place it in constant jeopardy. Dr. Denry Sato, at the Adirondack Biomedical Research Center was also a fount of good humor, useful advice, and practical help, particularly in the cell surface binding studies and in preparation of monoclonal antibodies. Dr. Marianna Sikorska Walker at the National Research Council in Ottawa made me feel particularly welcome in her laboratory and spent much time teaching me peptide synthesis, and the preparation and characterization of anti-peptide polyclonal antibodies in rabbits. Dr. Mina Bissell and Dr. Ruth Lupu at the Lawrence Berkeley National Laboratories in California generously allowed me to conduct experiments related to my Doctoral work in their laboratories.

There have also been many people working further behind the scenes that have in countless ways helped directly or indirectly in pursuit of my Doctoral studies. Of the many I would like to extend singular notes to Marina La Duke and Alice Vera in the audiovisual department at the Adirondack Biomedical Research Center who did all of the photography for this thesis. The secreteries for the Dept. of Biochemistry, at the University of Ottawa; Julie Normand and Joanne Barlow also deserve especial mention.

Julie earlier, and Joanne most recently, have done much work to keep my relationship with the School of Graduate Studies and Research on an even keel during my time on campus but more particuarly, for the last few years while off campus.

Lastly I cannot fail to acknowledge the enormous debt I owe to my wife, Dr. Valerie Weaver, whom without her love, patience, understanding, and encouragement during the long years of my graduate work I could never have found the fortitude to finish.

Dedication

This thesis is dedicated to my family: my mother, Jill, my brother Andrew, sister, Joanna, and in memory of my father, John and to my wife, Valerie.

TABLE OF CONTENTS

LIST OF FIGURES AND ILLUSTRATIONS

CHAPTER ONE

CHAPTER THREE

CHAPTER FOUR

LIST OF TABLES

LIST OF ABBREVIATIONS

^{1}H NMR	Proton Nuclear Magnetic Resonance
α_2M	Alpha 2 Macroglobulin
$A\beta_{10-35}$	Amyloid Beta Peptide Amino Acids 10-35
$A\beta_{1-16}$	Amyloid Beta Peptide Amino Acids 1-16
$A\beta_{1-28}$	Amyloid Beta Peptide Amino Acids 1-28
$A\beta_{1-40}$	Amyloid Beta Peptide Amino Acids 1-40
$A\beta_{1-42}$	Amyloid Beta Peptide Amino Acids 1-42
$A\beta_{17-28}$	Amyloid Beta Peptide Amino Acids 17-28
Aβ4	Amyloid Beta Peptides of 4 kDa
$A\beta_{9-25}$	Amyloid Beta Peptide Amino Acids 9-25
ApoAI	Apolipoprotein AI
ApoAII	Apolipoprotein AII
ApoD	Apolipoprotein D
ApoE	Apolipoprotein E
APP	Amyloid Beta Peptide Precursor Protein
ATCC	American Type Culture Collection
ATP	Adenosine 5'-triphosphate
BSA	Bovine Serum Albumin
cAMP	Adenosine 3':5' -cyclic Monophosphate
CETP	Cholesterol Ester Transfer Protein
dATP	Deoxyadensoine 5'-triphosphate
dCTP	Deoxycytosine 5'-triphosphate
DEAE-Sephacel	Diethylaminoethyl-Sephacel
DEPC	Diethyl Pyrocarbonate
dGTP	Deoxyguanosine 5'-triphosphate
DMSO	Dimethylsulfoxide
dNTP	Deoyxynucleotide 5'-triphosphate; 4 dNTP's are dGTP, dCTP, dTTP, and dATP
DTT	Dithiothreitol
dTTP	Deoxythymidine 5'-triphosphate
EDTA	Ethylenediaminetetraacetic Acid
EGF	Epidermal Growth Factor
FBS	Fetal Bovine Serum
HCHWA-D	Hereditary Cerebral Hemorrhage with Amyloidosis of the Dutch Type
HDC	Heat Denatured Casein
HDL	High Density Lipoprotein
HEPES	(N-[2-Hydroxyethyl]piperazine-N'-[4-ethanesulfonic acid])
HRP	Horseradish Peroxidase
IC_{50}	50% Inhibitory Concentration
IgA	Immunoglobulin A
IgG	Immunoglobulin G
IgM	Immunoglobulin M

IPTG	Isopropyl β-D-Thiogalactopyranoside
LCMS	Liquid Chromatography Mass Spectrometry
LDL	Low Density Lipoprotein
LDLR	Low Density Lipoprotein Receptor
LRP	Low Density Lipoprotein Receptor Related Protein
LRP2/gp330	Low Density Lipoprotein Receptor Related Protein/Glycoprotein 330
MALDI-TOF	Matrix Assisted Laser Desorption Time of Flight Mass Spectrometry
MDCK	Madin Darby Canine Kidney Cells
OPD	o-Phenylenediamine
PAGE	Polyacrylamide Gel Electrophoresis
PBS	Phosphate Buffered Saline
PEG	Polyethylene Glycol
PMSF	Phenylmethylsulfonyl Flouride
PTH	Phenylthiocarbamyl
PVDF	Polyvinylidene Diflouride
RAP	Receptor Associated Protein
RP-HPLC	Reverse Phase-High Pressure Liquid Chromatography
RT-PCR	Reverse Transcriptase-Polymerase Chain Reaction
SDS	Sodium Dodecyl Sulphate
TAE	Tris-Acetate/EDTA Buffer
TCA	Trichloroacetic acid
TE	Tris-HCl\EDTA Buffer
TEMED	N,N,N',N'-tetramethylethylenediamine
TFA	Trifluoroacetic Acid
TGFβ	Transforming Growth Factor Beta
TGFβRI	Transforming Growth Factor Beta Receptor Type I
TGFβRII	Transforming Growth Factor Beta Receptor Type II
TNFα	Tumor Necrosis Factor Alpha
Tris	Tris(hydroxymethyl)aminomethane
UTR	Untranslated Region
VBS	Veronal Buffered Saline
VLDLR	Very Low Density Lipoprotein Receptor

UNITS

TIME	
h	Hour
min	Minute
sec	Second
MASS	
g	Gram
mg	Milligram (10^{-3} g)
µg	Microgram (10^{-6} g)
ng	Nanogram (10^{-9} g)
pmol	Picomoles (10^{-12} moles)
VOLUME	
L	Liter
mL	Milliliter (10^{-3} L)
µL	Microliter (10^{-6} L)
EXTENSION	
nm	Nanometer (10^{-9} m)
TEMPERATURE	
°C	Degrees Centigrade
CONCENTRATION	
M	Molar (Moles of solute/Liter of solution)
mM	Millimolar (10^{-3} M)
µM	Micromolar (10^{-6} M)
nM	Nanomolar (10^{-9} M)
mg/mL	Milligram of solute/Milliliter of solution
µg/mL	Microgram of solute/Milliliter of solution
% (v/v)	Volume of solute as a percentage of volume of solution
% (w/v)	g of solute per 100 mL of solution
% (w/w)	Mass of solute as a percentage of mass of solution
ELECTRICAL	
A	Amp
mA	Milliamp (10^{-3} A)
V	Volt
CENTRIFUGATION	
xg	Times Gravity

CHAPTER ONE

1. *Introduction*

1.1. Background

Ovine clusterin and its homologs in other species has been independently isolated by a number of groups at the protein level, as an expressed glycoprotein, ligand or biochemical activity, and at the mRNA level as an upregulated message associated with a number of biological processes, or as a cDNA encoding a ligand binding domain (Table 1.1). This has lead to a number of distinct names/acronyms and proposed functions as suggested by the context of identification. As agreed at the first Workshop on Clusterin held at Cambridge, UK, in 1990 the gene and gene products are referred to as clusterin in deference to its initial identification and in the absence of any clear concensus on its biological function(s).

1.2. Gene structure and regulation

Clusterin is encoded by a single copy gene located on chromosome 8 in the human (Slawin et al., 1990; Eddy and Fritz, 1991; Purrello et al., 1991) refined to p21 near the gene for lipoprotein lipase (Dietzsch et al., 1992; Fink et al., 1993; Wong et al., 1994a), chromosome 14 in the mouse (Birkenmeier et al., 1993; Jordan-Starck et al., 1994), and chromosome 15 in the rat (Goldner-Sauve et al., 1991). The gene has been isolated and characterized from the human (Wong et al., 1994a), rat (Wong et al., 1993; Rosemblit and Chen, 1994), mouse (Jordan-Starck et al., 1994), and quail (Michel et al., 1995) and has a similar structure of nine exons and eight introns in which the relative positioning of exon boundaries in relation to multiple species protein alignments is strongly conserved. Primer extension analysis obtained evidence for only one functional promoter in the rat gene (Wong et al., 1993). In the quail gene two functional promoters

Table 1.1. Clusterin isolation and context of identification

Identification as a purified protein or antigen			
Source	Name (Acronym)	Proposed Function	Reference
ram rete testis fluid	clusterin	cell-cell interactions in spermatogenesis	(Blaschuk *et al.*, 1983)
rat Sertoli cell secreted glycoprotein	sulfated glycoprotein 2 (SGP-2)	spermatogenesis	(Collard and Griswold, 1987)
human serum terminal complement complex associated protein	complement lysis inhibitor (CLI), serum protein 40.40 (SP40.40)	complement lysis inhibitor	(Jenne and Tschopp, 1989) (Kirszbaum *et al.*, 1989)
human serum component of HDL subclass	apolipoprotein j (apoj), NA1/NA2	lipid transport /metabolism	(de Silva *et al.*, 1990a) (Jenne *et al.*, 1991) (James *et al.* 1991)
Alzheimer's Aβ4 binding protein in human serum and CSF		regulation of Alzheimer's amyloid plaque formation	(Ghiso *et al.*, 1993)
human serum Ig binding protein		regulation of Ig function	(Wilson *et al.*, 1991)
apically secreted glycoprotein from polarized MDCK cells	glycoprotein 80 (gp80)	marker of apical secretion in polarized epithelia	(Hartmann *et al.*, 1991)
soluble and membrane associated component of bovine chromaffin granules	glycoprotein III (gpIII)	formation/exocytosis /recycling of secretory granules	(Palmer and Christie, 1990)
human serum protein binding streptococcal inhibitor of complement (SIC)		screen for serum ligands of SIC	(Akesson *et al.*, 1996)
LRP-2 ligand in human milk		ligands of LRP-2 in human milk	(Kounnas *et al.*, 1995)

Identification as an upregulated mRNA (differential expression)			
Source	Name (Acronym)	Upregulation with	Reference
involuting rat ventral prostate following castration	testosterone repressed prostate message 2 (TRPM-2)	programmed cell death (apoptosis)	(Léger *et al.*, 1987)
Rous sarcoma virus transformed quail neuroretinal cells	T64	morphological transformation	(Michel *et al.*, 1989)
Alzheimer associated hippocampal cDNA	Alzheimer disease hippocampal cDNA (ADHC-9)	neurodegeneration	(May *et al.*, 1990)
cDNA overexpressed in glioma cell line	TB16	transformed cells of CNS origin and epileptic foci	(Danik *et al.*, 1991)
scrapie infected hamster brain		neurodegeneration accompanying scrapie infection	(Duguid *et al.*, 1989)
porcine smooth muscle cells		nodule formation in cultures of primary vascular smooth muscle cells	(Diemer *et al.*, 1992)

Identification as a translated cDNA			
Source	Name (Acronym)	Proposed Function	Reference
stromal cDNA encoding a secreted protein binding to the surface of pre-B lymphocyte cell lines		stromal secretory protein influencing B lymphocyte development	(Oritani and Kincade, 1996)
cDNA interacting with TGF β receptor cytoplasmic domain in genetic screen		possible cytoplasmic protein involved in TGF β receptor signalling	(Reddy *et al.*, 1996)

have been described: a TATAless promoter in intron I and, as in the mammalian gene, a classical TATA promoter upstream of exon I (Michel et al., 1995). Several consensus transcriptional elements in both mammalian and quail promoters are present upstream of exon I and in intron I of both mammalian (Wong et al., 1993; Jordan-Starck et al., 1994; Rosemblit and Chen, 1994; Wong et al., 1994a) and quail genes (Michel et al., 1995) and it is probable that both of these regions are important in overall clusterin transcriptional regulation in both vertebrate groups. For the most part, with the exception of the quail, the clusterin gene appears to give rise to a single mRNA in most tissues. Recently, increases in an alternatively spliced mRNA lacking exon 5 were detected by RT PCR in a number of tissues of the rat following treatment with protein synthesis inhibitors (Kimura and Yamamoto, 1996). The significance of this alternate transcript is unknown.

1.3. Expression

1.3.1. Expression of clusterin in adult tissues

Clusterin is expressed constitutively, but at widely varying levels, in most adult organs. Higher levels of clusterin have been observed in such organs as normal adult testis, epididymis, brain, and liver, while moderate levels are detected in stomach, heart, and ovary and low to undetectable levels in skeletal muscle, skin, bone, lung, thymus, thyroid, kidney, uterus, prostate, intestine, and colon of various species (French et al., 1993; Wong et al., 1993; Jordan-Starck et al., 1994; Wong et al., 1994a). In general, expression is spatially restricted to the epithelial compartment in most tissues (Aronow et al., 1993; French et al., 1993). Clusterin is expressed at high levels in select epithelia that form the barrier at tissue-fluid interfaces (Aronow et al., 1993). Some of these face

particularly harsh environments including select epithelia of the gastrointestinal, urinary, and female reproductive tracts (Aronow et al., 1993). In most expressing cell lines and tissues clusterin is constitutively secreted and in all polarized epithelia studied to date, secretion has a pronounced apical bias (Urban et al., 1987; Grima et al., 1992). Given this secretory pattern it is not surprising that the protein is found at significant levels in many extracellular fluids including blood (Murphy et al., 1988), urine (Aulitzky et al., 1992), cereberal spinal fluid (Ghiso et al., 1993; Polihronis et al., 1993), milk (Kounnas et al., 1995), aqueous and vitreous humor of the eye (Reeder et al., 1995) and seminal fluid (O'Bryan et al., 1990; Law and Griswold, 1994). However, in some expressing cell types with a regulated exocytic pathway, including platelets (Tschopp et al., 1993; Witte et al., 1993), and in endocrine and neuroendocrine secretory tissues (Palmer and Christie, 1990; Laslop et al., 1993; Appel et al., 1996) clusterin is stored in secretory granules and released upon stimulated exocytosis.

Constitutive expression of clusterin has been well characterized in the rat male reproductive tract. Clusterin was identified as the major protein secreted by primary cultures of rat Sertoli cells (Kissinger et al., 1982; Sylvester et al., 1984; Griswold et al., 1986; Collard and Griswold, 1987). It is expressed by Sertoli cells of the seminiferous epithelium (Hugly et al., 1988; Vaishnav and Moudgal, 1991) and is secreted apically where it binds to the surfaces of late spermatids and spermatozoa throughout the male reproductive tract (Sylvester et al., 1984; Mattmueller and Hinton, 1991; Sylvester et al., 1991). Clusterin is also synthesized and secreted at high levels by the principal cells of the epididymis with a marked regional heterogeneity within the gland varying from high

levels in the caput to very low levels in the corpus and cauda (Sylvester et al., 1984; Hermo et al., 1991; Mattmueller and Hinton, 1991; Sylvester et al., 1991; Cyr and Robaire, 1992; Zakeri et al., 1992; Ahuja et al., 1996). A remarkable reorganization of spermatozoan associated clusterin occurs in transit from the testis to epididymis. In the rat, testicular clusterin associated with testicular spermatozoa is quantitatively removed by endocytosis mediated by the low density lipoprotein receptor related protein, LRP2 expressed at high levels on the apical surface of epithelial cells of the efferent duct and replaced in the caput by a lower molecular weight epididymal form of the protein (Hermo et al., 1991; Sylvester et al., 1991; Morales et al., 1996). The association of clusterin expression with spermatogenic supporting cells in the testis and epididymis, its immunolocalization on spermatozoa and reorganization has suggested a potentially important role for the protein in the process of spermatogenesis. Interestingly, although not as well characterized, clusterin is expressed in the oogenic supporting granulosa cells of the female reproductive tract, where it is synthesized and secreted into the follicular fluid and localized to the zona pellucida (Ahuja et al., 1994), suggesting possibly analogous roles in oogenesis.

1.3.2. Expression of clusterin during development

In the developing mouse embryo clusterin is expressed transiently in decidua during postimplantation decidualization and, in the embryo, is first expressed at 12.5 days and onwards, predominantly in epithelia during organogenesis (French et al., 1993). In some tissues, such as the liver, once turned on clusterin expression persists into the adult. In others expression may be transient during development. In the lung expression

is transiently induced in the more differentiated cuboidal cells of the developing bronchial buds, and in the kidney transiently in areas of the nephric unit in association with epithelial cell polarization (French et al., 1993). In certain developing epithelia that spatially and/or temporally have well delineated proliferative and differentiating zones or temporal phases, expression has been noted selectively in differentiating compartments prior to attainment of the terminally differentiated state. This includes skin, villi of duodenum, and enamel secreting ameloblasts during tooth development (French et al., 1993). Based on these observations it has been suggested that clusterin may be a marker of early epithelial differentiation during organogenesis and may play a role during this process.

1.3.3. Expression of clusterin in cell death and tissue injury

A central focus of research has and continues to be the involvement of clusterin in tissue injury, cell death, and disease. This perspective derives from the frequent isolation of clusterin as an upregulated message in differential cross screens of healthy, normal tissues and their diseased or regressing counterparts (Table 1.1). These include the regressing rat ventral prostate following castration (Léger et al., 1987), in the hippocampus of Alzheimer disease brain (May et al., 1990) and in the Scrapie infected hamster brain (Duguid et al., 1989). Subsequent use of the cDNA in a variety of other experimental and spontaneous models of tissue injury, cell death, and disease in numerous tissues *in vivo* and cells *in vitro* identifies a proximal upregulation of clusterin as a frequent response in these processes. These include tissue injury and cell death in the central nervous system (Day et al., 1990; Lampert-Etchells et al., 1991; Laping et al.,

1991; Pasinetti and Finch, 1991; May et al., 1992; Danik et al., 1993; Pasinetti et al., 1993; Schreiber et al., 1993; Wiessner et al., 1993; Rozovsky et al., 1994; Liu et al., 1995; Walton et al., 1996; Popper et al., 1997), kidney (Sawczuk et al., 1989; Harding et al., 1991; Rosenberg and Paller, 1991; Correa-Rotter et al., 1992a; Correa-Rotter et al., 1992b; Schumer et al., 1992; Calvet and Chadwick, 1994; Dvergsten et al., 1994; Nath et al., 1994; Rosenberg et al., 1995a), heart (Swertfeger et al., 1996), and retina (Jones et al., 1992; Wong et al., 1994b; Wong et al., 1994c; Jomary et al., 1995; Smith et al., 1995; Popper et al., 1997) among others. The diversity of physical and chemical agents inducing injury and the range of biological responses to injury suggest that the clusterin gene is responsive to a wide variety of stimulating agents that may involve one or more convergent biochemical pathways and that it may have a general role(s) to play in response to, or recovery from, tissue injury. The time course of clusterin expression appears to mirror biochemical or morphological signs of injury. It can be slow and sustained in chronically developing injury or rapid and transient in acute injury (Nath et al., 1994). Clusterin can also be upregulated in response to systemic disease and has been identified as an acute phase serum protein showing increases in hepatic synthesis in response to endotoxins and cytokines (Hardardottir et al., 1994) and cardiovascular disease (Navab et al., 1997). The recent identification of a functional heat shock element conserved in all clusterin promoters (Michel et al., 1997a) and of clusterin as a heat shock inducible gene (Clark and Griswold, 1997a; Michel et al., 1997a) is also consistent with the view of clusterin as a gene involved in coping with the consequences of stresses related to tissue injury.

1.3.3.1. Expression of clusterin in association with apoptosis

Early studies suggested that clusterin may play a role as a genetic component of the cell autonomous program of apoptotic cell death. Clusterin was identified as an mRNA induced transiently and to very high levels in the rat ventral prostate following castration (Montpetit et al., 1986; Léger et al., 1987; Wong et al., 1993; Russo et al., 1994) or treatment with anti-androgens (Léger et al., 1988). Temporally, induction of clusterin mRNA reaches a maximum between the third and fourth day after castration in the tall columnar epithelial cells of the distal and intermediate zones of the prostatic ducts (Rouleau et al., 1990; Guenette et al., 1994a). Similar transient increases in the protein have been measured in organ extracts (Grima et al., 1990), and by Western (Sensibar et al., 1993), and immunohistochemical analysis (Sensibar et al., 1991). Castration induces dramatic shrinkage of the ventral prostate, attributed in large part to loss by apoptosis of up to 90% of the epithelial cells of the distal and intermediate zones and reaches a maximal rate between the third and fourth day post castration (Tenniswood et al., 1992; Colombel and Buttyan, 1995). Thus clusterin expression is spatially and temporally associated with apoptosis in the rat ventral prostate. Similar observations have been noted for epithelial induction of clusterin expression and subsequent epithelial apoptosis during involution of rat mammary gland following weaning (Guenette et al., 1994b). Thus clusterin has been considered a candidate component of the apoptotic program, a suggestion that has lead in hindsight to its premature widespread adoption as a molecular marker for the identification of apoptosis in different tissues (Tenniswood et al., 1992). However, clusterin is clearly expressed in non apoptotic cells and upregulated expression in other *in vivo* models of apoptosis is either not observed or not observed specifically in

cells undergoing apoptosis. For example, there is a general lack of correspondence noted between upregulated expression and known episodes of neuronal as well as non-neuronal cell death during development (Garden et al., 1991).

Studies of the association of clusterin expression with apoptosis in cell lines *in vitro* and of tumors derived from cell lines also provide conflicting results. Clusterin is frequently expressed at detectable levels in most but not all cell lines *in vitro*. The quail homolog of clusterin, T64 has been cloned as an mRNA transcriptionally upregulated in association with transformation of neuroretinal, myoblast, and fibroblast cells by Rous Sarcoma virus carrying oncogenic forms of src as well as other avian viruses carrying activated forms of protein kinases fps and mil (Michel et al., 1989; Herault et al., 1992). Constitutive expression of clusterin in cell lines and tumors may thus be a consequence of transformation. In general, those cell lines *in vitro*, and tumors *in vivo*, that demonstrate a variable upregulation of clusterin mRNA and/or protein in association with induction of apoptosis, derive from those that are either sex steroid hormone-dependent or originally derived from tissues that respond to sex steroid hormones (Rennie et al., 1988; Kyprianou and Isaacs, 1989; Kyprianou et al., 1990; Kyprianou et al., 1991a; Sklar et al., 1993; Warri et al., 1993; Kyprianou et al., 1994; Furuya et al., 1995; Chen et al., 1996; Narvaez et al., 1996; Simboli-Campbell et al., 1996; Wright et al., 1996). Other cell types and models of apoptosis *in vitro* reportedly show, in some cases, induction of expression (Kyprianou et al., 1991b; Guenal and Mignotte, 1995) and in others, either no change or decreases in expression (Martin et al., 1992; French et al., 1994; Flach et al., 1995; Chiesa et al., 1996). Taken together these data suggest that clusterin is not an

integral component of a conserved cell autonomous genetic apoptotic program.

In one study it has been reported that in cell lines induced to die *in vitro* clusterin expression corresponds to cells that survive and suggested that it may serve a cell autonomous protective function promoting cell survival (French et al., 1994). Few studies have directly examined the effects of experimentally manipulating levels of clusterin expression on cell death and survival. In human prostatic LNCaP cells overexpression of clusterin protected only modestly against TNF-α induced cell death and oligonucleotide directed antisense inhibition enhanced spontaneous cell death in untreated cultures (Sensibar et al., 1995). A similar result was found for clusterin overexpression in protection against TNF-α induced mixed apoptotic/necrotic cell death of L929 cells (Humphreys et al., 1997). However, this effect was specific as no protection was observed in apoptosis induced by cholchicine or staurosporine or necrotic cell death induced by azide. Although the mechanism of protection against TNF-α is not understood addition of exogenous clusterin was ineffectual suggesting that the active form must be synthesized by the cell, and may act intracellularly (Humphreys et al., 1997).

In vivo studies of neurodegeneration provide an additional insight into the role of clusterin in cell death and tissue injury. In several such models clusterin mRNA is observed to increase in glial fibillary acid-protein positive, reactive astrocytes proximal to the sites of neurodegeneration, but not the dying neurons themselves (Day et al., 1990; Lampert-Etchells et al., 1991; Laping et al., 1991; Pasinetti and Finch, 1991; Danik et al.,

1993; Pasinetti et al., 1993; Schreiber et al., 1993; Rozovsky et al., 1994; Chiesa et al., 1996; Walton et al., 1996). Because of the role of reactive astrocytes as supporting cells in neural tissue reorganization, this suggests a role for clusterin in response to, or recovery from, tissue injury rather than in either the initial cell death cascade or as a factor promoting cell survival in a strictly cell autonomous fashion.

Interestingly, in several models characterized by apoptotic cell death clusterin that may be synthesized and secreted by neighboring cells appears to be bound or taken up by dying cells. This has been reported in both neural (Agarwal et al., 1996; Michel et al., 1997b), and non neural (Clark et al., 1997b) models of apoptosis. Although the mechanism of clusterin localization in non expressing cells is unknown this suggests a complicated relationship between dying and responding cells in an integrated tissue. Understanding the regulation and mechanisms of this event may shed light on the process of cell death as well as the function served by clusterin.

1.1.4. Null expression of clusterin in transgenic knockout mice

Despite patterns of expression *in vivo*, suggesting roles for clusterin in development, reproduction, and normal epithelial cell function, recent studies of transgenic mice in which clusterin expression has been abrogated have not revealed any particularly striking developmental or reproductive phenotype in animals either hetero- or homozygous for the null mutation, indicating that clusterin does not have a unique "make or break" function in these complex, integrated processes (Aronow, 1997). Similarly, no genetic studies have chanced across clusterin mutations associated with a specific

phenotype. Thus, the physiological role of clusterin remains to be clarified. There is, however, a marked inclination towards the view that it may be an accessory factor having a protective and/or supportive role in the diverse biological contexts of its expression. This general hypothesis is based largely on what is known of the biochemistry of clusterin and its relation to specific ligands.

1.4. Protein structure

Full length cDNAs for clusterin have been isolated for human (Jenne and Tschopp, 1989; Kirszbaum et al., 1989; de Silva et al., 1990a; Wong et al., 1994a), rat (Collard and Griswold, 1987; Wong et al., 1993), mouse (French et al., 1993; Lee et al., 1993; Jordan-Starck et al., 1994), dog (Hartmann et al., 1991), pig (Diemer et al., 1992), cow (Palmer and Christie, 1990), and quail (Michel et al., 1989), and a partial sequence for the hamster (Duguid et al., 1989). These cDNAs have open reading frames encoding proteins of 439 to 451 amino acids (Fig. 1.1). The mature clusterin protein is a secreted disulfide bonded N-linked glycoprotein of non homologous, but similarly sized, α and β chains (Fig. 1.2). Both chains are encoded by the single mRNA which is translated by endoplasmic reticulum bound ribosomes as a preproprotein. The short N-terminal secretory signal sequence is cleaved by signal peptidase and the soluble proprotein is processed by endoproteolytic cleavage between the centrally located dipeptide R-S/N/E (αR205-βS1 in the human; numbering according to the mature protein) (Fig.1.1) prior to secretion into the extracellular space.

Clusterin homologs show good conservation of sequence, ranging from 45%

Figure 1.1. Multiple species alignment of clusterin homologs

Clusterin homologs from the indicated species were aligned using the program CLUSTAL using the following parameters: K-tuple = 1; Gap Penalty = 5; Window Size = 10; Filtering Level = 2.5; Open Gap Cost = 10; Unit Gap Cost = 10.

"*", conserved and "·" , nearly conserved in identity and "-" represents gaps introduced to optimize the alignment. Cysteines are in red, asparagines of consensus sites of N-linked glycosylation are in blue, the site of proteolysis to generate the αβ heterodimer is in green with an overlying green arrow. The overlying black line indicates the secretory signal sequence. Inverted triangles, the initial position and number of the corresponding exons in the human clusterin gene (Wong et al., 1994a). Two numbering systems are given. In the first +1 is the number assigned to the N-terminal amino acid of the preproprotein. In the second, given in parenthesis the sequences are numbered relative to the N-termini of the mature (processed) sequences of the respective α and β chains. These N-termini are known for the human (Kirszbaum et al., 1989), rat (Cheng et al., 1988a), and bovine (Palmer and Christie, 1990) homologs. The N-terminal secretory signal sequence of murine, canine, and porcine homologs is similar to that of human clusterin allowing alignment and prediction of the α N-terminus for these homologs. The N-terminal secretory signal sequence of the quail homolog is similar to that of bovine clusterin and a partial sequence from ovine clusterin (Cheng et al., 1988b; Tsuruta et al., 1990) allowing alignment and prediction of the α N-terminus for this homolog. Alignment and conservation of the α-β cleavage site allowed prediction of the β N-terminus from murine, porcine, canine and quail homologs.

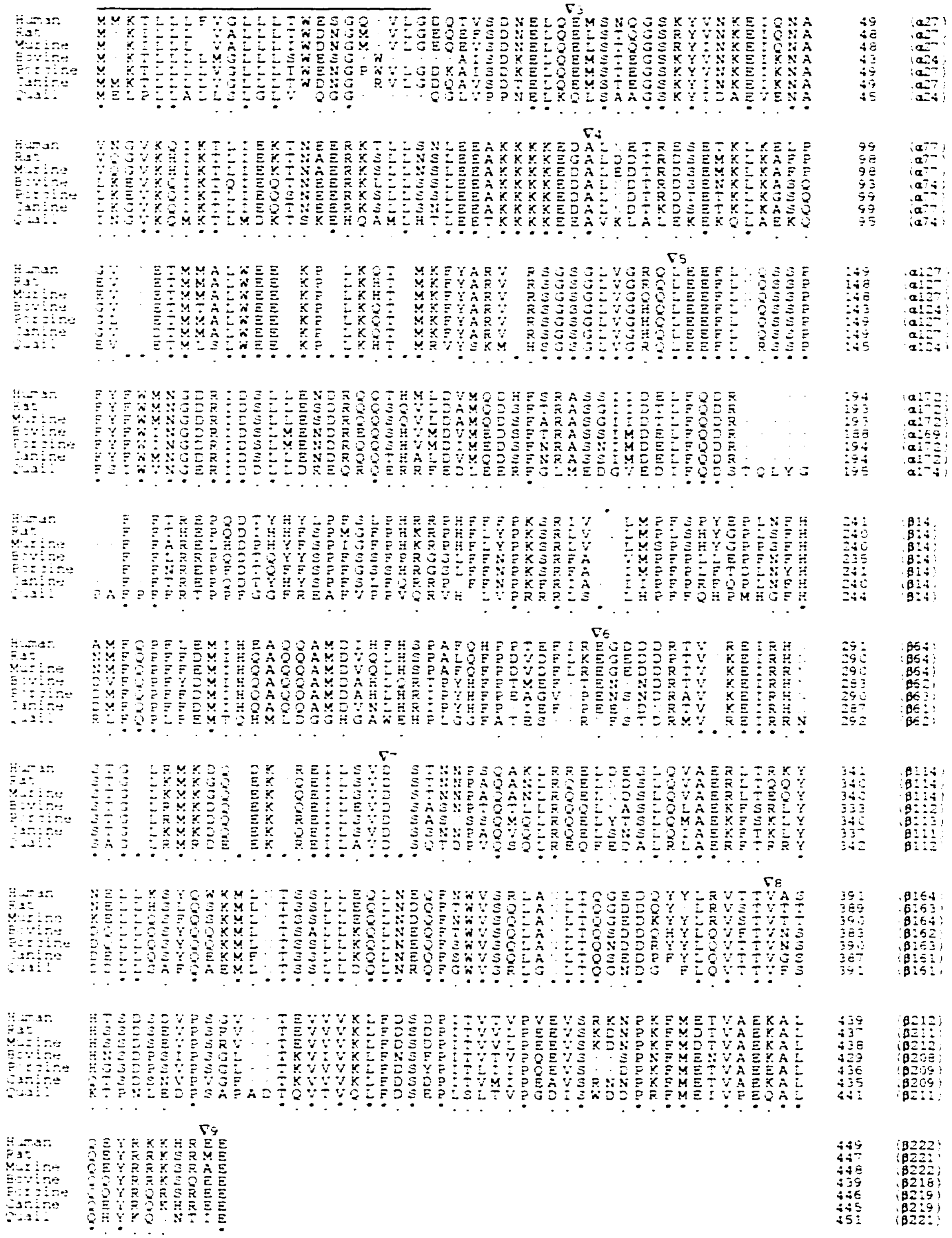

Figure 1.2. Proposed structure of clusterin

Human clusterin α and β chains are drawn to scale (fixed unit length/amino acid) and depicted in antiparallel orientation aligned with respect to the known disulfide αC80-βC86. Known disulfide bonds are shown as solid lines while that inferred is shown as a dotted line (Choi-Miura et al., 1992a; Kirszbaum et al., 1992). "Y", known sites of N-linked glycosylation (Choi-Miura et al., 1992a; Kirszbaum et al., 1992; Kapron et al., 1997). Myosin homology domains are shown as red boxes and amphipathic α helices identified using the AMPHI algorithm (Cornette et al., 1987; Margalit et al., 1987) are shown as yellow boxes. These were identified for rat clusterin (Tsuruta et al., 1990) and positioned in the human sequence based on the multiple species alignment (Fig. 1.1) . Amphipathic α helices identified using helical wheels (Schiffer and Edmundson, 1967) are shown as blue boxes (de Silva et al., 1990a). Synthetic peptides that inhibit the binding of clusterin to $A\beta_{1-40}$ (Choi-Miura et al., 1994) are shown as grey boxes located near the respective chains. Numbers in corresponding colors denote the boundaries of these sequence elements in human clusterin based on position relative to the N-terminus of the respective α and β chains.

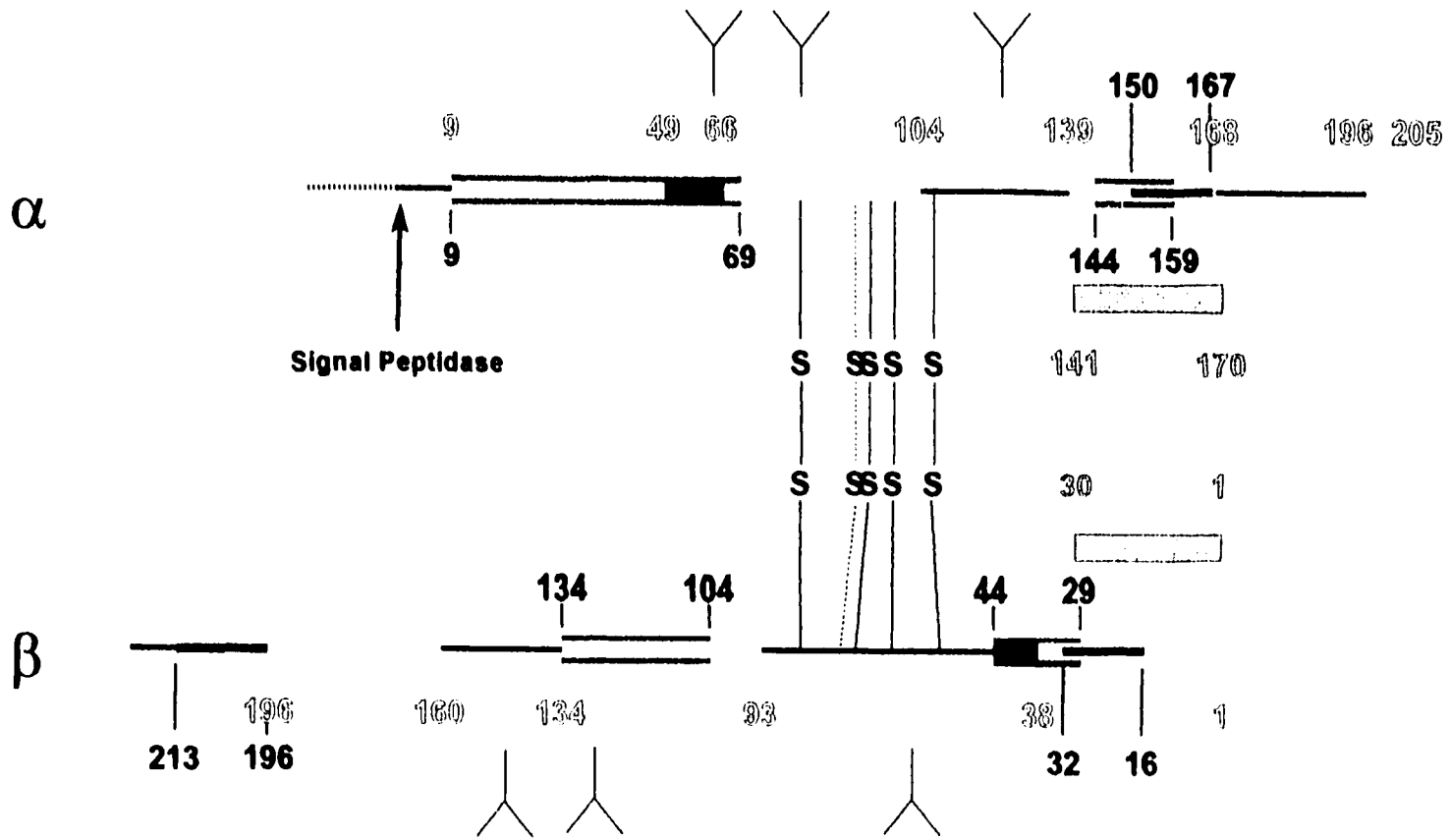
α
β
9
49
66
104
139
150
167
168
196
205
9
69
144
159
Signal Peptidase
S
S
S
S
S
S
S
S
141
170
30
1
134
104
44
29
213
196
196
160
134
93
38
1
32
16

overall identity between porcine and quail to 93% between murine and rat. This homology is not however, distributed uniformly over the protein sequence. The greatest homology is seen between the N-terminal two thirds of the α chain and C-terminal two thirds of the β chain while the greatest divergence, including the occurrence of most gaps introduced to optimize species alignments is found in the C-terminal third of the α chain and N-terminal third of the β chain, and is encoded by a single exon (exon 5, Fig.1.1). Scans for homology in current protein databases have revealed no extensive identity to other known proteins. However, short regions of homology have been described to the rod-like tail domain of myosin heavy chain (Jenne and Tschopp, 1989; Tsuruta et al., 1990) (Fig. 1.2) and to the cysteine rich N-terminal thrombospondin-like domain of terminal complement attack complex components C7, C8β, and C9 (Kirszbaum et al., 1989). In addition segments of the α and β chains have been modeled as amphipathic α helices (Fig. 1.2) (de Silva et al., 1990a; Tsuruta et al., 1990). Clusterin has a unique arrangement of disulfide bonds. Each chain contains a short sequence of 28 (α) or 29 (β) amino acids encoded nearly entirely by a single exon (4 and 6, respectively) that features 5 cysteine residues spaced at nearly identical intervals, though in reverse orientation (Fig. 1.1). The cysteine residues involved in 4 of the 5 disulfide bonds have been positively assigned for human serum clusterin (Choi-Miura et al., 1992a; Kirszbaum et al., 1992). All four disulfide bonds are interchain, involving cysteines from the α and β chains that are aligned when both chains are arranged in a linear antiparallel orientation with respect to these domains (Fig. 1.2). Since no free sulfhydryl is detected in clusterin (Choi-Miura et al., 1992a) it is assumed that the unmapped disulfide is also an interchain disulfide bond completing the "ladder-like" disulfide structure.

Secreted clusterin from different species and tissue sources shows substantial variation in molecular weights and isoelectric points. These are probably due to differences in N-linked glycosylation. There are 5 to 7 predicted N-linked glycosylation sites in the different species homologs and it is probable that variable numbers of sites in different species are used (Fig. 1.1). In the human there are 6 sites of N-linked glycosylation, three in each chain and in human serum clusterin all are known to be used (Kirszbaum et al., 1989; Choi-Miura et al., 1992a; Kirszbaum et al., 1992; Kapron et al., 1997). Similarities in the chain length and in the number and structure of N-linked carbohydrates of α and β chains accounts for their close migration on reducing SDS PAGE. In contrast, in the rat homolog there are only two such sites in the α, and four in the β chain, and these differences probably account for the resolution of the higher molecular weight β from lower molecular weight α chains by reducing SDS PAGE (Griswold et al., 1986). Smaller differences in the length and composition of complex N-linked glycans probably account for differences in molecular weight and isoelectric points between clusterin isolated from different tissues of the same species (Laslop et al., 1993; Sensibar et al., 1993), and have been used as a signature of the biosynthetic origin. In the rat, testicular and epididymal clusterin have higher and lower molecular weights, respectively, and are the result of differences in tissue specific N-glycosylation (Sylvester et al., 1991). Less easily resolvable by one dimensional SDS PAGE, single tissue sources typically show multiple resolvable acidic isoelectric forms on 2D gels. This is the consequence of microheterogeneity in N-linked carbohydrate sialyation (Kamboh et al., 1991; Kapron et al., 1997) and/or sulfation (Sylvester et al., 1984; Urban et al., 1987; Appel et al., 1996). Clusterin does not appear to be modified by O-linked carbohydrates

(Burkey et al., 1991). It is unknown whether tissue specific differences in N-linked carbohydrate have any functional consequences.

While it has widely been assumed that the function of clusterin relates to its extracellular localization, whether in secretory granules, endocytic vesicles, or secreted, recent evidence has demonstrated the existence of a specifically induced nuclear-cytoplasmic form (Reddy et al., 1996). In the mink lung epithelial CCL-64 and HepG2 cells TGF-β1 treatment induces upregulation of clusterin mRNA, and specific accumulation of a non glycosylated 43 kDa immunologically related protein in nuclei and cytoplasm. In untreated cells only N-glycosylated secreted forms are present in cell lysates. An in frame ATG start codon 99 nucleotides downstream of the first ATG in the human cDNA would result in a protein without the N-terminal secretory signal sequence if used as the translation start. Downstream of the corresponding methionine lies a putative nuclear localization signal (Fig. 1.1) and may mediate translocation from the cytoplasm to the nucleus of a form lacking the signal sequence. If translation is engineered to initiate at this site *in vitro* and *in vivo* the resulting product is related by size, immunoreactivity, and V8 protease peptide maps to the nuclear 43 kDa antigen in TGF-β1 treated cells (Reddy et al., 1996). Most importantly ectopic expression in CCL-64 cells, of such an engineered human clusterin expression construct, results in nuclear accumulation of the human protein demonstrating its competence for nuclear sorting (Reddy et al., 1996).

The function of the nuclear form of clusterin is unclear. There are no reports of specific biological effects resulting from ectopic expression and nuclear accumulation in

CCL-64 cells independent of TGF-β1 treatment (Reddy et al., 1996). The general importance of this event is also uncertain since, of the cDNAs isolated for different species, those of the rat, mouse, and quail do not conserve ATG at the hypothesized start position, although they do have ATGs downstream (quail) or upstream (mouse and rat) that might substitute. Alternative mRNAs, perhaps specifically induced by TGF-β1, may also be possible.

1.5. Protein function

1.5.1. Cell aggregation *in vitro*

Clusterin was first purified as the active factor in the aggregation of suspended cells *in vitro* elicited by ram rete testis fluid (Blaschuk et al., 1983; Fritz et al., 1983). It induces aggregation of numerous eukaryotic cell types or lines with no apparent specificity, including red blood cells, murine testicular derived TM-4 cells, primary cultures of immature rat Sertoli cells, guinea pig epididymal spermatozoa, and porcine kidney derived LLC-PK1 cells (Blaschuk et al., 1983; Fritz et al., 1983; Fritz and Burdzy, 1989; O'Bryan et al., 1990; Mattmueller and Hinton, 1991; Tung et al., 1992; Silkensen et al., 1994; Schwochau et al., 1997). There are no reported differences in aggregation of erythrocytes from different ABO blood groups, or species (Fritz et al., 1983; O'Bryan et al., 1990). Glutaraldehyde fixed erythrocytes, and erythrocyte ghosts are also susceptible to aggregation (Fritz and Burdzy, 1989; Fritz et al., 1991; Tung et al., 1992). The final aggregated state does, however, depend upon the cell type. Erythrocytes form loose spherical compacts easily disrupted by mechanical agitation (Fritz et al., 1983) and no evidence of close intercellular contacts (Fritz and Burdzy, 1989). On the

other hand, TM-4 cells eventually form well compacted structures with sharply demarcated borders resistant to mechanical disruption (Fritz et al., 1983) and LLC-PK1 aggregates reportedly formed tight junctions and lumen (Silkensen et al., 1994). Aggregation occurs at clusterin concentrations of the order of 10^{-7} to 10^{-8} M suggesting a recognition mechanism of appreciable affinity (Blaschuk et al., 1983). However, no specific high affinity cell surface clusterin binding sites have been measured on TM-4 cells (Tung et al., 1992) or erythrocytes and the mechanism of aggregation remains unknown. It is possible that clusterin-induced cell aggregation is mediated by binding to a low affinity, high capacity and/or abundant non-cell type specific surface structure.

Recently, human serum clusterin has been shown to specifically mediate the aggregation of clinical isolates of *Staphylococcus aureus* (Partridge et al., 1996). In this case, clusterin has been shown to bind specifically and saturably to the cell surface and this was eliminated by protease treatment of intact cells. Interestingly, unlike results from eukaryotic cells, clusterin induced aggregation demonstrates specificity and is not observed with either a gram negative *Escherichia coli* line JM109 or gram positive *Bacillus subtilis* line BR151, which do not specifically bind clusterin under the same conditions (Partridge et al., 1996). This suggests that unlike eukaryotic cells clusterin-induced aggregation of *S.aureus* isolates may be mediated by interaction with a high affinity specific cell surface receptor. This receptor, however, has yet to be identified.

The possible interaction of clusterin with cell surfaces has suggested that clusterin, in addition to cell-cell interactions, may also be involved in cell-substratum

interactions. Clusterin is present in the laminin-rich basement membrane preparation of Matrigel (Thomas-Salgar and Millis, 1994). In the only reported direct measurement of a possible role of clusterin in mediating cell-substratum interactions, clusterin-coated tissue culture plates significantly enhanced the attachment of a single cell suspension of LLC-PK1 cells to a level equivalent to collagen type I- or fibronectin-coated plates. This effect was reversible in the presence of an anti-clusterin polyclonal antibody (Silkensen et al., 1994).

At this time it is not clear that clusterin-induced cell aggregation or effects on cell adherence are physiologically important. It has been suggested that clusterin may be one factor promoting cell-cell and cell-substratum interactions in cases of tissue remodeling in development or in the reformation of tissue architecture during recovery from tissue injury (Silkensen et al., 1994; Rosenberg and Silkensen, 1995b).

1.1.2. Terminal complement components

Complement is a major effector arm of the humoral immune system and consists in its broadest extent of a number of distinct plasma proteins constituting activators, effectors, and regulators, as well as cell surface-bound receptors and regulators (Muller-Eberhard, 1986; Muller-Eberhard, 1988). It exists in a latent form in plasma and is activated by means of two distinct pathways; the classical pathway, commonly activated by the formation of antibody-antigen immune complexes, and the alternate pathway, activated by a structurally diverse group of substances including certain particulate polysaccharides, fungi, bacteria, viruses, and some mammalian cells and aggregates of

immunoglobulins. The classical and alternate pathways converge in the formation of a structurally analogous highly specific serine protease, the C5 convertase which cleaves a single bond in the plasma protein C5 to produce two fragments C5a and C5b. C5b displays a metastable binding site for plasma C6 to form the C5b6 complex. C5b in C5b6 then displays a binding site for plasma C7 and bound C7 undergoes a conformational change resulting in display of a metastable membrane binding site and if available nearby, C5b-7 inserts into the target membrane. Bound C7 also displays a binding site for plasma C8, and membrane bound C5b-8 subsequently serves as a binding site for C9. C9 undergoes a conformational change that reveals a further membrane binding site, as well as a binding site for another C9 molecule. 12 to 18 molecules of C9 can be incorporated into the complex, polymerizing at the highest multiplicities to form tubular polyC9. The resulting C5b-9_n complex is referred to as the terminal complement complex and results in an increase in target cell membrane permeability, that is thought to be the proximate cause of cytotoxic activity.

Clusterin was identified in association with the terminal complement complex independently by three groups. Murphy *et al.* identified clusterin as a novel antigen in kidney glomerular basement membrane preparations deposited together with components of the complement pathway in a patient with membranous glomerulonephritis (Murphy et al., 1988). Jenne and Tschopp (Jenne et al., 1985; Jenne and Tschopp, 1989) and Choi *et al.* (Choi et al., 1989) identified clusterin in purified preparations of the soluble terminal complement complex, sC5b-9 which forms in serum when complement is activated in the absence of target cell membranes. A more recent connection of clusterin and complement

is less direct. Clusterin has been found together with histidine rich glycoprotein to be the major serum proteins binding to an affinity matrix of streptococcal inhibitor of complement (SIC), a gene product secreted by *Streptococcus pyogenes* having complement mediated hemolysis inhibitory activity *in vitro* (Akesson et al., 1996).

In addition to the identification of clusterin in association with sC5b-9, a physiological role for clusterin in relation to complement is suggested by its immunological colocalization with the terminal complement complex during experimental and spontaneous tissue injury. This includes codeposition specifically in histopathologically infarcted but not normal myocardium (Vakeva et al., 1993), in epithelial cells of proximal tubules of infarcted renal tissue (Vakeva et al., 1995), variously in tubules and glomeruli in kidney biopsies of patients with clinically distinct renal pathologies (French et al., 1992a), in skin biopsies of lesional and non lesional patients with a positive lupus band test (French et al., 1992b), in terminal complement complex deposits of human liver allographs (Scoazec et al., 1997), and in the glomerular epimembranous deposits of rats with experimental passive Heymann nephritis (Eddy and Fritz, 1991). In the latter study, clusterin deposition was shown to be dependent on that of the terminal complement complex since complement depletion by intravenous injection of cobra venom factor prior to induction of nephritis yielded neither deposition of terminal complement complex or clusterin (Eddy and Fritz, 1991). Similarly, clusterin deposition on the membranes of erythrocytes (Wilson et al., 1991) or the surface of agarose beads (Berge et al., 1997) incubated with human serum is dependent on complement activation and deposition. Thus, under (patho)physiological conditions

clusterin demonstrates an interaction with complement.

Clusterin has been found to inhibit complement dependent hemolysis *in vitro* (Choi et al., 1989; Jenne and Tschopp, 1989; Murphy et al., 1989; O'Bryan et al., 1990; Oda et al., 1994). In early studies inhibition was observed when clusterin was added with or before addition of C7. In one report, if C5b-7 complexes were preassembled on target erythrocytes prior to addition of clusterin, C8, and C9, no effect on hemolysis was observed (Jenne and Tschopp, 1989). Clusterin is present in complexes of soluble sC5b-7, sC5b-8, and sC5b-9 indicating that it is incorporated before or after addition of C7 to C5b6 (Choi et al., 1990). These results have lead to the hypothesis that clusterin inhibits terminal complement complex attack principally by masking the membrane binding site of C5b-7 thereby rendering it soluble. However, the dependency of clusterin codeposition with terminal complement components in membrane particulate fractions (Wilson et al., 1991) argues that clusterin does not merely compete with membranes for binding metastable C5b-7 since the membrane binding site is presumably already occupied. Recent experiments indicate that clusterin also inhibits complement at later stages of terminal complement complex assembly and that these events take place after the assembling complex has bound to target membranes. These studies suggest additional interactions with latent binding sites on C8 and C9 that might be revealed during the conformational transitions that accompany assembly in the complex. Solution phase clusterin has been shown to specifically bind to immobilized, denatured forms of C7, C8β, and C9 (Tschopp et al., 1993). These interactions are not competed by native monomeric C7 and C8 but the interaction with denatured C9 is competed by polymeric

C9 prepared by treatment of C9 with Zn^{+2} *in vitro*, a reaction structurally analogous to C9 polymerization mediated by C5b-8 (Tschopp et al., 1993). Complement activation by incubation of human serum with agarose beads results in codepostion of clusterin with the terminal complement complex, but not with C9 deficient serum, suggesting that C9 is the principal site of clusterin binding to the bead bound complement complexes (Berge et al., 1997). It has also been shown that clusterin binds to C8 and C9 in the context of the assembling terminal complement complex on model membranes (McDonald and Nelsestuen, 1997). Clusterin was found to reversibly inhibit the rate of a first order, flourescent quenching, process associated with the irreversible unfolding of FITC labeled C9 following binding to C5b-8 or C5b-9_1 preassembled on small unilamellar vesicles (SUV) (McDonald and Nelsestuen, 1997). These results suggested that clusterin reversibly binds to latent C9 binding sites on incorporated C8 and C9 and inhibits further incorporation of C9. In fact, clusterin has been shown to inhibit C9 polymerization induced either by Zn^{+2} (Tschopp et al., 1993) or mediated by C5b-8 preassembled on SUVs (McDonald and Nelsestuen, 1997). These results suggest that clusterin inhibits the terminal attack complex by binding to C5b-7 in solution and to C5b-8 and C5b-9_n on target membranes.

Thus, clusterin may be a physiological regulator of complement at the level of the assembling terminal complement complex. It may attentuate the cytolytic potential of complement directly through interactions with components of the assembling terminal complement complex and indirectly by limiting tissue damage which releases, or exposes additional activators of the complement pathway. Clusterin binding and inactivation of

the membrane binding site of fluid phase C5b-7, may be particulary important in preventing bystander lysis of healthy cells, a potential problem since C5b-7 is assembled in the fluid phase where diffusion may carry it away from the intended target to an otherwise healthy cell. In cases of tissue injury in general, clusterin may be one of several inhibitors that limit unrestrained activation of complement. During apoptosis, there is no strong development of an inflammatory response, and the local upregulation of clusterin expression, whether in dying or surviving cells, may be one of several anti-inflammatory complement limiting mechanisms. In support of this hypothesis in a more physiologically relevant model, glomerular damage caused by experimentally induced complement activation in the rat kidney is specifically enhanced by clusterin immunodepletion of plasma perfusates (Saunders et al., 1994).

Despite this, it has been argued that clusterin may not be a physiologically significant complement inhibitor. In studies using human serum as a source of complement rather than purified terminal complement components, concentrations of clusterin required to achieve more than modest inhibitory effects on hemolysis were estimated to exceed by a factor of 10^4 those known to exist in serum (Hochgrebe et al., 1997). However, since the hemolytic assays used in these and earlier studies used single end points of the order of 10^3 seconds and erythrocytes are lysed by small numbers of terminal complement complexes of low C9 multiplicity per cell, these studies may have underestimated the complement inhibitory potential of clusterin. Clusterin appears to be a *reversible* inhibitor, on the order of 10^1 to 10^2 seconds, of the *rate of irreversible* incorporation of C9 into the terminal complement complex and inhibits incorporation of

not just one but each successive C9 molecule (McDonald and Nelsestuen, 1997). Thus, these hemolytic studies likely only revealed clusterin inhibitory effects at the level of C7. Dramatic differences have been modeled in the rate of cytolysis by terminal complement complex of nucleated cells requiring a multiplicity of C9 of three compared to erythrocytes with a multiplicity of one at concentrations of clusterin significantly below plasma levels (McDonald and Nelsestuen, 1997). Kinetic inhibition of terminal complement complex by clusterin could be a significant mechanism, particularly for nucleated cells, if combined with dynamic terminal complement complex inactivating processes involving longer time scales, for example by membrane blebbing or endocytosis.

In addition, or as an alternative to a complement inhibitor, it has been suggested that clusterin incorporated in the membrane bound terminal complement complex may function as a receptor. In this context it may function as a recognition receptor for a mechanism(s) involved in clearance of debris from sites of tissue injury. Such possibilities include clusterin as an opsonin for a phagocytic cell, as an adaptor for receptor mediated endocytosis of complexes of the terminal complement complex with cellular debris, or as an adaptor for ApoAI-HDL binding to active terminal complement complex, efficiently linking ongoing cytolysis to binding and packaging of released lipids and lipophilic products (Wilson et al., 1995). In this latter regard, it has been shown that apoAI incorporation into sCb5-9 is dependent on incorporation of clusterin, raising the possibility that apoAI-HDL via clusterin may be localized to the membrane bound terminal complement complex (Choi-Miura et al., 1993a).

1.1.3. Apolipoprotein AI-HDL, serum paraoxonase, and atherogenesis

Several groups, using monospecific antibodies to plasma clusterin or to apoAI, have independently described an association of clusterin with apoAI-HDL in human plasma. Clusterin has been identified as a 70 kDa antigen, designated apolipoprotein J, recognized by a monoclonal antibody obtained against affinity purified preparations of plasma cholesterol ester transfer protein (CETP) (de Silva et al., 1990b). Immunoaffinity purification of clusterin from plasma was shown to copurify apoAI (de Silva et al., 1990b; de Silva et al., 1990c). Identical results have been reported using monoclonal antibodies obtained against clusterin associated with the terminal complement complexes (Ehnholm et al., 1991; Jenne et al., 1991). Using a complementary approach clusterin was identified on 2D gels as a minor plasma protein enriched in immunoaffinity preparations of apoAI-HDL with or without apoAII (James et al., 1988; James et al., 1991).

Immunoaffinity purified human clusterin-apoAI-HDL from plasma is lipid poor, containing 10 to 20% lipid by weight (de Silva et al., 1990b; Jenne et al., 1991). These preparations contain high proportions of cholesterol and cholesterol esters, phospholipid, and are very poor in triglycerides (de Silva et al., 1990b; Jenne et al., 1991). Electron micrographs of negatively stained preparations show spherical particles with a diameter falling in the range of HDL (de Silva et al., 1990b; Jenne et al., 1991). ApoAI is present in plasma at concentrations at least twenty times that of clusterin and accordingly substoichiometric levels of clusterin have been found to copurify with apoAI by anti-apoAI immunoaffinity chromatography (James et al., 1988). Thus, clusterin has been

referred to as a marker of a small, lipid poor subclass of HDL. Conversely, the proportion of plasma clusterin that is associated with apoAI-HDL also appears to be relatively minor. Based on yields of apoAI by anti-clusterin immunoaffinity chromatography and comigration of clusterin with apoAI-HDL in analytical fractionations of plasma including isotachophoresis and gel filtration chromatography (Jenne et al., 1991) and single spin density ultracentrifugation (de Silva et al., 1990b) earlier studies suggested that a significant proportion of clusterin in plasma may be associated with apoAI-HDL. However, a two dimensional separation using native agarose gel and gradient gel electrophoresis in successive dimensions, found very little clusterin in human plasma comigrating with apoAI (Stuart et al., 1992). Similarly, single spin density gradient separation of rat seminiferous tubule and epididymal tubule fluid also estimated that only a small proportion of clusterin may be associated with apoAI in these fluids (Law and Griswold, 1994).

Although apoAI is the most abundant apolipoprotein component of anti-clusterin immunoaffinity preparations small amounts of apoAII, apoE, and apoD have also been reported by Western analysis (de Silva et al., 1990b; Jenne et al., 1991). Similarly, anti-apoE columns retain a small proportion of clusterin from cerebrospinal fluid (Borghini et al., 1995) and anti-apoAII columns retain small proportions of clusterin from plasma (James et al., 1988). Recently, disulfide oxidized and reduced forms of serum paraoxonase have been identified as a component of immunoaffinity purified preparations of both apoAI-HDL and clusterin apoAI-HDL from plasma (Blatter et al., 1993; Kelso et al., 1994). Estimates of the proportion of plasma clusterin associated with

serum paraoxonase and vice versa vary from significant, estimated from proportional yields on anti-clusterin and anti-serum paraoxonase supports (Blatter et al., 1993), to little, based on the small degree of overlap when plasma was resolved by native agarose gel, followed by gradient gel electrophoresis (Kelso et al., 1994).

The relationship of plasma clusterin levels to levels of markers of lipid metabolism has been studied to illuminate a possible role for clusterin in lipid metabolism. Surprisingly, plasma clusterin levels were not found to be correlated with plasma apoAI or HDL-cholesterol in normolipemic healthy adults of either sex (Jenkins et al., 1996). In fact, clusterin levels are in the normal range in patients with Tangier's disease that have severe deficiencies of HDL, apoAI, and AII (Choi-Miura et al., 1993b). These results suggest no simple direct structural and/or functional relationship of clusterin to apoAI-HDL and are consistent with experiments that demonstrate that only a small proportion of plasma clusterin may be associated with apoAI-HDL. In contrast, clusterin levels were reportedly positively correlated with total plasma triglycerides, LDL-cholesterol, apoE, and apoB in normolipemic adults (Jenkins et al., 1996). Recent results suggest that these correlations may be indirect, with plasma clusterin levels reflecting molecular and cellular events associated with vascular damage directly or indirectly related to these markers. Employing several genetic and/or dietery animal models of atheromatous vascular lesions, it has been found that clusterin plasma levels are elevated in association with lesion development (Navab et al., 1997). These increases may be the result of an upregulation of clusterin expression in the liver mediated by oxidized-LDL (Navab et al., 1997), stimulus secretion of clusterin stored in the α-

granules of platelets (Tschopp et al., 1993; Witte et al., 1993) and/or synthesis locally in developing lesions by foam cells (Jordan-Starck et al., 1994). The latter two sources and the specific immunolocalization of clusterin to atheromatous endothelium in human and mouse supports a direct functional relationship to events associated with atherogenesis (Witte et al., 1993; Jordan-Starck et al., 1994; Mackness et al., 1997). Interestingly, serum paraoxonase levels are negatively correlated to LDL (Blatter et al., 1993) and in the animal models of atherogenesis referred to above, serum paraoxonase levels show associated decreases with conditions that led to lesion development (Navab et al., 1997). Thus, unlike apoAI-HDL, the physical association suggested between clusterin and serum paraoxonase appears to be reflected in a significant inverse (patho)physiological correlation.

To date there are scant *in vitro* biochemical studies that have addressed possible roles of clusterin in relation to lipoproteins. Clusterin is enriched in affinity preparations of CETP and clusterin immunodepletion resulted in some increase in neutral lipid transfer activity in these preparations (de Silva et al., 1990b). Based on the lipid poor characteristics of clusterin apoAI-HDL it has been suggested that clusterin may be specialized for the reverse transport of cholesterol from extrahepatic tissues. In support of such a role it has been recently reported that clusterin, like apoAI, stimulates the efflux of cholesterol from cholesterol loaded peritoneal macrophages *in vitro* (Gelissen et al., 1998). Clusterin also appears to have an anti-atherogenic activity at the level of LDL oxidation in a tissue culture model of atherogenesis (Navab et al., 1997). Clusterin has been shown to inhibit in a dose dependent manner, the oxidation of freshly prepared LDL

by cocultures of human aortic endothelial and smooth muscle cells, thereby reducing its monocyte/macrophage infiltration-inducing activity (Navab et al., 1997). Preincubation of clusterin with cocultures has the same effect suggesting that clusterin does not directly interact with LDL but rather with target cells (Navab et al., 1997). It is unclear whether this reflects a clusterin lipid binding activity, but it is possible that clusterin may directly bind and sequester oxidized lipids generated in target cells. Immunoprecipitates of clusterin, newly synthesized and secreted by human hepatoma HepG2 cells *in vitro* are associated with lipids, but not with significant amounts of other proteins, suggesting that clusterin may bind lipids directly (Burkey et al., 1992).

It has been noted that many of the biological contexts of clusterin expression and localization correspond to processes involving dynamic tissue and membrane remodeling. These include involution of hormone dependent tissues, (re)organization of tissues during development, and during tissue injury and repair. It has been suggested that an associated clusterin lipid transport function may be required for and/or facillitate these remodeling processes and thus underlie these expression patterns.

1.1.4. Alzheimer's Disease amyloid β peptide

Alzheimer's disease is one of the leading causes of progressive senile dementia. It is characterized histopathologically by the presence of lesions in various regions of the brain including hippocampus, entorhinal cortex, amygdala, cerebral cortex, and certain subcortical nuclei that project to the hippocampus and neocortex (Selkoe, 1991). These lesions include intranuclear neurofibrillary tangles, which are distinguished

ultrastructurally and immunohistochemically as extramembranous deposits of paired helical filaments of polymerized, hyperphosphorylated forms of the neuron-specific microtubule associated protein, tau and parenchymal and cereberovascular extracellular deposits of a 39-43 amino acid peptide, amyloid β (Aβ4). Diffuse amorphous focal deposits of Aβ4 are found immunohistochemically in the brains of elderly individuals without cognitive defects. However, in brains from Alzheimer patients, Aβ4 is also found in numerous focal compacted and fibrillar forms with the characteristic histochemical properties of amyloid, referred to as senile plaques. Senile plaques show various degrees of glial involvement, including glial fibrillar-associated protein-positive reactive astrocytes and microglia. Neuritic plaques are associated with neurite outgrowths into the plaque and local dystrophic neurons. The etiology of sporadic and familial Alzheimer's disease is thought to converge with the deposition of Aβ4 in fibrillar form. Fibrillar Aβ4, in addition to its own direct neurotoxic effects (Pike et al., 1993), may participate in initiation, organization, and amplification of a chronic and unresolvable inflammatory response (Cotman et al., 1996) which results in progressive neural loss and its clinical manifestation, progressive cognitive dysfunction. As a result, a great deal of research interest has centered on the cellular origins, pathways of production and regulation of levels of Aβ4 peptides, the structural requirements, cofactors, and physicochemical conditions of its aggregation into fibrillogenic and other morphological forms, and the direct and indirect consequences of these different soluble and aggregated states on the form and function of neurons and glia.

Aβ4 peptides derive via proteolysis of a larger, ubiquitously expressed type I

plasma membrane glycoprotein of uncertain function, encoded by chromosome 21 in the human, named the amyloid precursor protein (APP) (Selkoe, 1994). Aβ4 is heterogeneous in length with the principal forms including 28 amino acids of the juxtamembrane extracellular domain of APP and 12 to 14 amino acids of the predicted transmembrane domain. APP is proteolytically processed by two pathways. Most APP is cleaved in the extracellular domain within the Aβ4 sequence by an unknown protease(s), α secretase, giving rise to a soluble secreted form of APP precluding generation of amyloidogenic peptides. A minor proportion of APP is processed by another unknown protease(s), referred to as β secretase, principally 17-18 amino acids N-terminal to this site, giving rise to a truncated form of APP_s and a membrane associated C-terminal fragment that is the direct precursor of Aβ4. The Aβ4 precursor is internalized by endocytosis and cleaved at a heterogeneous site in the transmembrane domain, by another unknown protease(s) referred to as γ secretase, releasing soluble Aβ4. The most abundant Aβ4 peptides are $A\beta_{1-40}$ and $A\beta_{1-42}$, produced as alternate cleavage products of γ secretase. Recycling vesicles return these peptides to the cell surface, resulting in secretion. The Aβ4 pathway is found in all cells accounting for the finding of diffuse deposits of Aβ4 in normal aged brain as well as diseased brain and the presence of low concentrations of these peptides in blood plasma and cereberal spinal fluid of normal as well as diseased individuals. $A\beta_{1-42}$ is the principal peptide in senile plaques, and overproduction of $A\beta_{1-42}$ in particular provides a coherent explanation of all presently known autosomal dominant forms of familial Alzheimer's disease for which the mutation has been identified (Hardy, 1997).

Clusterin was identified as an mRNA upregulated by approximately three fold in

Alzheimer's hippocampus compared to age matched controls (May et al., 1990). Induction of clusterin expression is not specific for Alzheimer's disease. In many different models of spontaneous and experimental brain injury clusterin expression is upregulated in reactive astrocytes proximal to the site of neurodegeneration suggesting that clusterin may be upregulated secondarily in Alzheimer's disease as a molecular component of a general cellular and molecular response to neurodegeneration. Thus the upregulated expression of clusterin, specifically in astrocytes that perform supportive functions in neuronal maintenance and repair, is consistent with the idea that clusterin plays protective and/or supportive functions in neurodegeneration. A complement inhibitory, anti-inflammatory activity is one possible function in neurodegenerative responses and is consistent with the colocalization of clusterin with complement components in dystrophic neurites of senile plaques and neuropil threads in Alzheimer's disease (McGeer et al., 1992). Alternatively, it has been suggested that clusterin may function in local lipid transport in clearance and/or repair processes associated with synaptic reorganization.

However, biochemical studies have independently identified a more specific association between clusterin and Alzheimer's disease. Clusterin has been found to be the major protein in serum and cerebro-spinal fluid bound to an affinity matrix of synthetic $A\beta_{1-40}$ (Ghiso et al., 1993). Clusterin-Aβ4 complexes have been demonstrated in both cerebro-spinal fluid (Ghiso et al., 1993) and plasma (Koudinov et al., 1994) by coimmunoprecipitation. *In vitro* ligand binding studies show that the interaction of clusterin with $A\beta_{1-40}$ and $A\beta_{1-42}$ is specific, saturable, and of high affinity (Matsubara et

al., 1995; Matsubara et al., 1996). And of several known serum Aβ4 binding proteins, clusterin may have the highest affinity for both $A\beta_{1-40}$ or $A\beta_{1-42}$ (Matsubara et al., 1995; Matsubara et al., 1996). Thus, clusterin may be the principal binding protein of Aβ4 peptides in extracelullar fluids. Interestingly, it has recently been shown that clusterin-Aβ4 complexes can be bound and taken up by a high affinity LRP2 related receptor (see section 1.5.6) on cerebral microvessels and choroid plexus (Zlokovic, 1996a; Zlokovic et al., 1996b). Thus uptake of clusterin-Aβ4 complexes in plasma and cerebro-spinal fluid into the brain may serve some normal function and/or may increase amyloid load contributing to Alzheimer's disease pathogenesis.

Immunolocalization studies of clusterin in Alzheimer's cortical sections have also shown that clusterin is present in diffuse and compacted amyloid deposits apparently free from complement components (Choi-Miura et al., 1992b; McGeer et al., 1992). Thus, clusterin may interact directly with Aβ4 in deposits in the central nervous system and locally secreted clusterin in Alzheimer's disease may also directly influence the course of Aβ4 deposition, fibrillogenesis, and/or neurotoxicity. It has been shown that clusterin forms a stable 1:1 stoichiometric complex with $A\beta_{1-40}$ and $A\beta_{1-42}$ *in vitro* (Matsubara et al., 1995; Matsubara et al., 1996) suggesting that clusterin may inhibit formation of fibrillar Aβ by lowering the concentration of free Aβ4. *In vitro*, clusterin inhibits the formation of sedimentable aggregates of synthetic $A\beta_{1-42}$ in a dose dependent manner (Oda et al., 1994; Oda et al., 1995; Matsubara et al., 1996). Since clusterin maintains solubility when used at substoichiometric ratios (1:20 to 1:50) it is likely that $A\beta_{1-42}$ solubility may be maintained not only by sequestration of unincorporated monomer but

also by binding to incipient $A\beta_{1-42}$ aggregates in ways that interfere with aggregate development. Cosedimentation of clusterin with larger aggregates of $A\beta_{1-42}$ suggests that clusterin does have affinity for $A\beta_{1-42}$ once aggregated (Oda et al., 1995). Using atomic force microscopy it has been shown that $A\beta_{1-42}$ aggregated in the presence of clusterin results in an increase of shorter and thicker fibrillar forms as well as globular forms reminiscent of clusterin alone (Oda et al., 1995). This is consistent with clusterin binding to developing fibrils preventing incorporation of further $A\beta_{1-42}$ monomers and fibril elongation.

Treatment of neurons in culture with aggregated $A\beta_{1-42}$ has a direct neurotoxic effect via an increase in oxidative stress (Pike et al., 1993). Opposite effects have been reported for the neurotoxic potential of aggregates of Aβ4 peptides formed in the presence of clusterin. In one study both sedimentable and non sedimentable fractions of $A\beta_{1-42}$ aggregated in the presence of clusterin increased the level of oxidative stress in rat PC12 pheochromocytoma cells beyond the level produced by aggregated $A\beta_{1-42}$ alone (Oda et al., 1994; Oda et al., 1995). In another study, however, it was reported that addition of substoichiometric concentrations of clusterin together with micromolar levels of unaggregated $A\beta_{1-40}$ nearly quantitatively attenuated cytotoxicity in rat hippocampal primary mixed glial/neuronal cultures mediated by $A\beta_{1-40}$ alone (Boggs et al., 1996). There are substantial methodological differences in these studies and these may have influenced, in particular the structure, and hence neurotoxicity, of Aβ4 aggregates formed in both the presence and absence of clusterin in each study. However, it does leave uncertain whether clusterin expressed locally in Alzheimer's brain might aggravate or

alleviate Aβ4 induced neuropathology.

1.1.5. Immunoglobulins

Spatial proximity of immunoglobulins (IgG) facilitated by binding to multiple copies of a surface antigen are functionally important in the immune response. In searching for plasma molecules that might influence this process polyethelene glycol fractionated plasma was passed over a column bearing immobilized human IgGs crosslinked with glutaraldehyde to mimic spatial clustering and clusterin was identified as a major binding protein (Wilson et al., 1991). Clusterin in the bound fraction was subsequently purified as a Protein A non-binding and Concanavalin A bound protein. These preparations were initially observed to enhance the rate of formation of high molecular weight immune complexes of anti-ovalbumin and ovalbumin *in vitro* (Wilson et al., 1991). Subsequently, however, this activity was identified not with clusterin but with copurifying plasma complement activator C1q (Roeth and Easterbrook-Smith, 1996). Nonetheless, the interaction of clusterin with crosslinked IgGs was direct as C1q free immunoaffinity preparations bind purified IgGs in solid phase ligand binding assays (Wilson and Easterbrook-Smith, 1992). Multiple clusterin binding sites appear to exist on IgGs as clusterin binds to both Fab and Fc IgG fragments and binding sites exist on all isotypes tested, with orders of affinity of $IgG_3 > IgG_4 > IgM > IgG_1 > IgG_2$, IgA (Wilson and Easterbrook-Smith, 1992). Since Fab and Fc fragments and all isotypes consist of domains having a common immunoglobulin fold clusterin may recognize a structural feature that is well conserved in these folds.

It has been suggested that the functional form of clusterin interacting with IgGs is a non covalent oligomer, each monomer bearing a single low affinity IgG binding site. Binding isotherms are sigmoidal, and clusterin concentrations obtaining half maximal saturation, which estimate the affinity of the interaction, decreased with increasing immunoglobulin coating concentration. Furthermore, only heat aggregated but not monomeric IgG was found to be an effective solution phase inhibitor of the binding of clusterin to immobilized IgG (Wilson and Easterbrook-Smith, 1992).

The physiological significance of binding to immunoglobulins has received little attention, in part because there is no evidence to suggest that the complex exists *in vivo*. It has been suggested that spatial colocalization of immunoglobulins bound to cell surface antigens might present a multivalent ligand for a complex of clusterin apoAI-HDL facilitating uptake of lipids, as suggested for binding of clusterin to membrane bound terminal complement complex (Wilson et al., 1995). Interestingly, analysis of the codeposition of clusterin, terminal complement complex, and immunoglobulins in renal biopsies of patients with various kidney pathologies has shown that clusterin has a stronger tendancy to deposit with terminal complement complex in which immunoglobulins are colocalized (French et al., 1992a). It is possible that this relates in some way to the ability of clusterin to bind to immunoglobulins as well as complement although the functional significance of this is unclear.

1.1.6. LRP2

gp330/megalin/Heymann nephritis autoantigen (now LRP2) is a large type I

transmembrane glycoprotein belonging to the low density lipoprotein receptor (LDLR) superfamily that includes, in addition to the LDLR, the very low density lipoprotein receptor (VLDLR), α_2 macroglobulin (α_2M) receptor/LDLR related protein (now LRP), the LRP-like protein from *C.elegans*, and several avian receptors such as the vitellogenin receptor (Saito et al., 1994). Each of these family members has in common one or more NPXY motifs in their cytoplasmic domain important in clathrin coated pit internalization. Like other members of the family, LRP2 is found in clathrin coated pits, and binds and mediates the endocytic internalization of a multitude of distinct ligands (Farquhar et al., 1994; Kounnas et al., 1994; Moestrup et al., 1994; Zheng et al., 1994). The large extracellular domain of LRP2 is constituted of repeats of three types of cysteine rich domains common to all members of the family and separated by spacer regions characterized by repeats of a short YWTD consensus repeat (Saito et al., 1994). The three cysteine rich repeats include those homologous to the epidermal growth factor (EGF) (B.1 motif), a second type of growth factor related repeat (B.2 motif), and a cysteine rich repeat referred to as the LDLR ligand binding repeat on the basis of homology to the ligand binding domain of the LDLR .

LRP2 is found on mammary epithelium (Zheng et al., 1994) and in a search for LRP2 ligands in human milk, chromatography on a LRP2 affinity matrix identified clusterin as the principal constituent binding protein (Kounnas et al., 1995). Clusterin binding to LRP2 in solid phase binding assays is specific, high affinity, and saturable, and is inhibited by other LRP2 binding proteins including the receptor associated protein (RAP), apoE3, and lipoprotein lipase C (Kounnas et al., 1995). Unlike a number of other

ligands including apoE3, clusterin does not bind to LRP (Kounnas et al., 1995). LRP2 on differentiated F9 murine teratocarcinoma cells specifically binds and internalizes clusterin leading to its degradation in an acidic, probably lysosomal compartment (Kounnas et al., 1995).

Clusterin is probably a ligand of LRP2 *in vivo*. As described above, in the rat, testicular clusterin in the lumen, and associated with spermatozoa of the rete testis and excurrent ducts, is known to be endocytosed and targeted to the lysosomal compartment of non-ciliated epithelial cells of the efferent ducts of the epididymis (Hermo et al., 1991; Igdoura et al., 1994). LRP2 has been identified on the apical surface of the efferent duct epithelial and principal cells of the epididymis, and is associated with coated pits and endocytic vesicles in these cells (Zheng et al., 1994; Morales et al., 1996). Uptake of clusterin into the endocytic and lysosomal compartments can be prevented by injection of RAP into the efferent duct lumen, suggesting that uptake is mediated by LRP2 (Morales et al., 1996). In cerebral microvessels and choroid plexus in a guinea pig brain perfusion model labeled clusterin and clusterin complexes with $A\beta_{1-40}$ are taken up specifically with high K_m and with one of the highest unidirectional transport rates measured for any protein (Zlokovic, 1996a; Zlokovic et al., 1996b). Immunoreactive LRP2 is found in extracts of both choroid plexus and brain microvasculature and clusterin uptake is inhibited by simultaneous perfusion of unlabeled RAP or a function inhibitory anti-LRP2 monoclonal antibody (Zlokovic et al., 1996b), suggesting that clusterin-Aβ4 complexes may be specifically endocytosed by LRP2. Colocalization of clusterin (Hartmann et al., 1991) and LRP2 (Zheng et al., 1994) immunoreactivity in the brush border of proximal

tubule epithelial cells of the adult kidney nephron may also reflect a clusterin-LRP2 interaction.

These data suggest that LRP2 may have a physiological role as a receptor for clusterin and/or clusterin ligand complexes. *In vitro* binding of $A\beta_{1-40}$ to LRP2 is mediated by clusterin and the ability of cell surface LRP2 to mediate internalization and degradation of labeled $A\beta_{1-40}$ depends on complex formation with clusterin (Hammad et al., 1997). LRP2 mediated uptake in brain microvasculature and choroid plexus of complexes of labeled clusterin with $A\beta_{1-40}$ is inhibited by unlabeled clusterin but not by unlabeled $A\beta_{1-40}$ (Zlokovic et al., 1996b). Interestingly, the clusterin-$A\beta_{1-40}$ complex had an estimated 2.4 to 10.2 fold higher affinity for the transport system than clusterin alone, suggesting that clusterin complexes may be the preferred *in vivo* substrate (Zlokovic et al., 1996b). Thus, clusterin may serve as an adaptor for LRP2 in clearance of a number of extracellular ligands. Alternatively, LRP2 may function in transcytosis of clusterin and clusterin ligand complexes across epithelial and/or endothelial barriers. Following perfusion of labeled clusterin in the guinea pig brain model a significant amount of radiolabel is found in the brain depleted of cerebral microvasculature, and this appears to correspond to an intact form of clusterin (Zlokovic et al., 1996b). Thus, LRP2 may actually mediate transcytosis across the blood brain barrier and into the parenchyma without lysosomal targeting. As described, transcytosis of clusterin-Aβ4 complexes has been suggested as a possible pathological mechanism contributing to an increased amyloid load in Alzheimer's disease although it may serve some other purpose related to a normal function for Aβ4.

1.1.7. TGF-β Receptors Type I and Type II

A clusterin cDNA from a human placental library was identified as a candidate for interaction with the TGF-β type I and II receptor cytoplasmic domains (Reddy et al., 1996). Direct specific binding to both receptors was confirmed *in vitro* by showing that plasma clusterin was the principal binding protein to fusions of glutathione S-transferase with type I and II cytoplasmic domains immobilized on an affinity matrix, and by showing that purified unlabeled clusterin specifically inhibited binding to these matrices (Reddy et al., 1996).

The physiological significance of the interaction of clusterin with the cytoplasmic domains of the TGF-β receptors is at present unclear. There is no evidence at the moment for a mechansim to transport extracellular clusterin into the cellular cytoplasm. The nuclear-cytoplasmic form of clusterin induced by TGF-β1, as described above, provides a previously unacknowledged subcellular localization that is spatially compatible with an interaction with this domain of the receptor (Reddy et al., 1996). It is thus concievable that an intracellular form of clusterin may have some role to play in the TGF-β signal transduction pathway, either as an effector, a recruitment protein or perhaps as a signal modulator. It has not yet been demonstrated that such a complex does in fact exist *in vivo*, particularly under the obvious conditions in which it might be expected, that is in TGF-β1 treated cells that feature formation of the nuclear-cytoplasmic form.

1.1.8. Heparin

It has recently been described that clusterin binds heparin *in vitro* with

submicromolar affinity (Pankhurst et al., 1997), confirming the suggestion that at least some contiguous linear basic sequences in clusterin may constitute heparin binding sites (de Silva et al., 1990a). Of the clusterin α and β chains only the α chain is retained by a heparin affinity matrix suggesting that the heparin binding site resides in this chain (Pankhurst et al., 1997). Interestingly, a small 5' cDNA fragment that contains part of the α chain was selected based on binding to the cell surface of the pre B lymphocyte cell line BCB10 (Oritani and Kincade, 1996). It is possible that this represents an interaction with cell surface proteoglycans. Binding of clusterin to heparin proteoglycans may be important in cell-cell, in cell-substratum interactions and/or concentrating clusterin at the surface of cells.

1.6. Thesis objectives and perspectives

The broad objective of my thesis project was to develop a model of clusterin structure and to study the relationship between clusterin structure and function. Accurate models of this kind are required for the design of meaningful, readily interpretable, experiments directed to a number of questions relating structure to function at the biochemical, cellular, and physiological levels of organization. When I began these studies there was a general concensus that clusterin was a hydrophobic/amphipathic extracellular glycoprotein that bound to other hydrophobic/amphipathic ligands by means of hydrophobic interactions. Clusterin was associated with apoAI-HDL (de Silva et al., 1990b; James et al., 1991; Jenne et al., 1991) and the complex could be dissocated with non ionic detergents (Jenne et al., 1991). It was also found in association with lipids in the absence of other proteins suggesting that it was capable of binding lipids directly (Burkey et al., 1992). Clusterin was also found associated with sC5b-9 (Murphy et al., 1988; Choi et al., 1989; Jenne and Tschopp, 1989), incorporating at the level of C7 during complex assembly (Choi et al., 1990), and inhibited complement dependent hemolysis at the level of C7 (Jenne and Tschopp, 1989; Murphy et al., 1989). The widely accepted interpretation was that clusterin bound to the C7 membrane binding site in fluid phase metastable C5b-7 and thereby maintained solubility (forming sC5b-7). Clusterin was found in membrane fractions of adrenal medullary chromaffin granules (Palmer and Christie, 1990), and in association with the surface of spermatids and spermatozoa (Sylvester et al., 1984; Sylvester et al., 1991) and in both cases, complete solubilization required use of membrane disrupting agents. Segments of clusterin sequence could be

modeled as amphipathic α helices (de Silva et al., 1990a; Tsuruta et al., 1990) and were suggested as functional elements in these hydrophobic binding interactions.

During the course of my thesis further studies have been interpreted as confirming this view. Thus, clusterin has been found associated with hydrophobic Aβ4 peptides (Ghiso et al., 1993; Koudinov et al., 1994) and shown to inhibit the aggregation of Aβ4 peptides (Oda et al., 1994; Oda et al., 1995; Matsubara et al., 1996). Moreover, the binding interaction can be inhibited by synthetic peptides that correspond to the putative amphipathic α helices in both the α and β chains of clusterin (Fig. 1.2) (Choi-Miura et al., 1994). By ligand blot, clusterin has been shown to bind specifically and saturably to denatured forms of complement components C7, C8β, and C9 and to Zn^{+2} polymerized C9 (Tschopp et al., 1993). Binding to denatured and activated forms of these components suggests an interaction with a latent binding site, such as the putative membrane binding sites of these components. Each separated α and β chain of clusterin also inhibits complement dependent hemolysis (Tschopp et al., 1993), an observation that echoes the Aβ4 clusterin binding inhibitory activity of the α and β chain synthetic peptides. A similar observation has been made recently made for the activity of α and β chains in the interaction of clusterin with the cytoplasmic domain of TGF β type I and II receptors (Reddy et al., 1996). Thus, it has been suggested that many clusterin ligand interactions may be based on hydrophobic interactions. The implication of this view is that clusterin has a promiscuous binding site constituted of amphipathic α helices, and it has been suggested that clusterin serves a general cytoprotective role by binding to structurally diverse hydrophobic surface active molecules (Aronow et al., 1993).

In addition, a few years ago LRP2 was identified as a cell surface endocytic receptor for clusterin (Kounnas et al., 1995). ApoE specifically inhibits the binding of clusterin to LRP2 (Kounnas et al., 1995). ApoE appears to bind to LRP2 on the basis, in large part, of electrostatic interactions between a cationic domain in its N-terminal domain and an anionic domain of the cysteine rich LDL ligand binding receptor-related repeats of LRP2 (Weisgraber, 1994; Daly et al., 1995; Orlando et al., 1997). Thus clusterin may bind to LRP2 at the same site as ApoE and with a similar physicochemical basis and it is likely that, in addition to a hydrophobic binding site, a distinct binding site exists on clusterin for the interaction with LRP2. Similarly, cationic-anionic electrostatic interactions are likely to underlie binding of clusterin to heparin.

There has not been any significant attempt to integrate these observations in any detailed way into a model of clusterin structure. The first specific aim of this thesis, developed in Chapter 3, is an attempt to integrate these and other observations into a sufficiently detailed model to serve as a useful experimental guide, in lieu of an atomic scale structure, for refining approaches to questions of structure and function. The model that I have developed relies heavily on the linear antiparallel ladder like pattern of interchain disulfide bonding (Choi-Miura et al., 1992a; Kirszbaum et al., 1992). The idea of α and β chain structural symmetry and antiparallelism within this domain are extended by a re-analysis of the structure of amphipathic α helices identified previously (de Silva et al., 1990a; Tsuruta et al., 1990) (Fig. 1.2). I suggest that this re-analysis identifies two pairs of helices, one from each chain per pair, as structurally distinct, and use this to

develop specific, and novel, structural and functional implications. The model reflects the view of the two binding sites implied above, although it has become likely, in light of results reported in this thesis and from other investigators that there are probably more than two binding sites.

The second specific aim of this thesis was to develop a recombinant expression system for clusterin that could serve as a model source for biophysical studies, and structure-function studies using a mutagenic approach. In Chapter 4, I describe the structural and functional characterization of human clusterin expressed in the methylotrophic yeast, *Pichia pastoris*. Transformation with an expression construct for the human clusterin cDNA resulted in high level secretion of an N-glycosylated α:β disulfide linked heterodimer structurally analogous to serum/plasma clusterin, and which retains some of the binding activities of the latter, suggesting that it should have some utility as a model recombinant source. However, this may be limited given that proteolysis at aberrant sites accompanying clusterin expression results in a heterogeneous mix of heterodimers in immunoaffinity purified preparations and is associated with deficiencies in specific binding interactions. Nonetheless, characterization of these patterns of proteolysis is justified by its implications for clusterin structure and function, and has compelling relationship(s) to the model developed in Chapter 3.

One of the most interesting observations in Chapter 4 is that proteolysis of the recombinant is associated with differential effects on distinct hydrophobic/amphipathic clusterin ligands $A\beta_{1-40}$ and Zn^{+2} polymerized C9, suggesting that the respective binding

sites are distinct. In other studies detailed in Chapter 4, I have attempted to implicate a general role for histidine(s) and histidine ionization in regulation of clusterin interactions with hydrophobic/amphipathic ligands. Dramatic differences observed in the stable binding of clusterin to $A\beta_{1-40}$ as a function of pH and the sensitivity of this interaction to modification of histidine residues with diethyl pyrocarbonate (DEPC), may reflect the importance of specific salt bridge(s) in this interaction. These examples of specificity suggests that the physiological role of clusterin may relate to interactions with specific ligands, and not as a generic binding protein for hydrophobic ligands.

Clusterin ligand interactions have for the most part been defined in humans for which monospecific immunoprecipitating antibodies exist. For obvious reasons these studies have been restricted to certain tissues and fluids, such as serum and cerebro-spinal fluid. It is possible that clusterin may be physiologically multifunctional. This multifunctionality may relate to specificity in ligand interactions, suggesting that identifying and characterizing ligands in different tissues and under different physiological conditions is necessary to clarify its role. These analyses may reciprocally provide insights into molecular mechanisms and processes underlying these contexts. Development of monospecific immunoprecipitating anti-clusterin monoclonal antibodies in a more experimentally tractable animal model will permit such questions to be addressed. The last specific aim, described in Chapter 5, involved the preparation and characterization of murine anti-rat clusterin monoclonal antibodies, including those that recognize native epitopes with high affinity which should be of use for this, and other purposes. These antibodies have been used to characterize the expression of clusterin in

the involuting rat ventral prostate following castration. Future studies will use these to identify coimmunoprecipitating ligands associated with this process.

CHAPTER TWO

2. *Methods and Materials*

2.1. Animals

Male Sprague-Dawley rats (Taconic, Germanstown, NY) and female BALB/c mice (Taconic) were maintained in a controlled environment (14 h light, 10 h dark) and provided food and water *ad libitum*. All animal protocols were approved by the Institutional Animal Care and Utilization Committee at the W.Alton Jones Cell Science Center.

2.2. Antibodies and proteins

The hybridoma secreting anti-human (serum) clusterin monoclonal antibody G7 was a generous gift of Dr. Brendan Murphy (St. Vincents Hospital, Australia). G7 IgG_1 was purified from serum free conditioned RD medium by chromatography on Protein G Sepharose (Pharmacia Biotech, Piscataway, NJ). The hybridoma secreting anti-human (serum) clusterin monoclonal antibody 78E was a generous gift of Dr. Mark Wilson (University of Wollongong, Australia). Protein A affinity purified rabbit anti-rat (Sertoli cell) clusterin was a generous gift of Drs. Michael Griswold and Steven Sylvester (Washington State University, WA). Murine monoclonal antibody 1H2 to rat (nephric) gp330/LRP2 was a generous gift of Dr. Robert McCluskey (Harvard/Massachusetts General Hospital, Boston, MA). Monomeric human complement C9 and human IgG (Reagent Grade) were purchased from Sigma Chemical Company (St. Louis, MO). Synthetic Alzheimer's amyloid β_{1-40} ($A\beta_{1-40}$) was obtained both from Sigma and by in house solid phase peptide synthesis using an Applied Biosystems model 430A automatic peptide synthesizer (Protein Core Facility, W.Alton Jones Cell Science Center, Lake Placid, NY). The peptide from the latter source was purified by RP-HPLC and

lyophilized. The expected molecular mass was verified by electrospray mass spectrometry, and composition by amino acid analysis. Human IgG was dissolved at 2 mg/mL in PBS (10 mM Na_2HPO_4, 1.8 mM KH_2PO_4, 137 mM NaCl, 2.7 mM KCl pH 7.4), 2 mM NaN_3. $A\beta_{1-40}$ was prepared fresh at regular intervals as a 1 mg/mL solution in 0.5 M sodium borate pH 8.6 and monomeric human complement C9 was supplied as a 1 mg/mL solution in 15 mM Na_2HPO_4-NaH_2PO_4, 135 mM NaCl, pH 7.4. Human serum/plasma clusterin, recombinant human and rat clusterin, sC5b-9, and murine anti-rat (recombinant) clusterin monoclonal antibodies were prepared and/or purified as described below. All proteins and antibody stocks were stored at 4 °C.

2.3. Cells

Cholesterol auxotrophic murine myeloma NS-1-Ag4-1 (NS-1) cells (ATCC, Rockville, MD) were propagated in RD medium (Sato et al., 1987) supplemented to 5 to 10% (v/v) with Fetal Bovine Serum (FBS) (Sigma). RD medium consisted of 8.1 g/L RPMI 1640 (Gibco BRL, Grand Island, NY), and 4.99 g/L DME (Gibco BRL) supplemented with 2.2 g/L $NaHCO_3$, 0.595 g/L HEPES, 45 mg/L sodium pyruvate, 3 g/L glucose, 20 mg/L penicillin G, 45 mg/L streptomycin sulfate, and 40 mg/L ampicillin. Murine teratocarcinoma F9 cells (ATCC) were propagated in an undifferentiated state in 10% (v/v) FBS and 90% (v/v) DMEM (Gibco BRL) supplemented with glucose to 4.5 g/L, 4.3 g/L $NaHCO_3$, 100 U/mL penicillin G, and 117 mg/L streptomycin sulfate pH 7.3-7.5 in tissue culture plates coated with 0.1% (w/v) gelatin (J.T. Baker, Phillipsburg, NJ). Differentiation of F9 cells is described below. Murine hybridomas G7 and 78E were initially propagated in 10% (v/v) FBS and 90% (v/v) DMEM/F12. G7 was later adapted

to growth in serum free RD based medium selective for cholesterol prototrophy as were all hybridomas generated in this thesis. All cells were grown at 37 °C in a humid atmosphere containing 5% (v/v) CO_2.

2.4. Protein concentrations

Protein concentrations were routinely estimated by the Bicinchoninic Assay using BSA (Fraction V) (Sigma) as a standard (Smith et al., 1985). To compare relative activities of immunoaffinity purified preparations of human plasma and *P.pastoris* recombinant human clusterin stock concentrations were estimated by amino acid analysis. Depending upon the preparation, 5 to 20 pmol of purified clusterin was analyzed by automated phenylthiocarbamyl amino acid analysis using an Applied Biosystems model 420H/130/920 essentially as described (Kapron et al., 1997). Concentrations of immunoglobulin fractions were estimated by absorbance at 280 nm using an extinction coefficient ε_{280} = 1.35/(mg/mL)-cm for IgG (Harlow and Lane, 1988).

2.5. SDS polyacrylamide gel electrophoresis (PAGE)

Protein samples were analayzed by separation on both continuous linear gradient and discontinuous sodium dodecyl sulfate (SDS) polyacrylamide gels (Laemmli, 1970). Separated protein bands were fixed and stained with Coomassie Blue R250 (Eastman Kodak, Rochester, NY) or silver nitrate as described (See and Jackowski, 1989) or were electroblotted to nitrocellulose membranes for immunological detection or polyvinylidene diflouride (PVDF) membranes for N-terminal sequencing. Bands were sized by interpolation of cubic spline fits generated using software supplied by Graphpad

Prism™ (GraphPad Software Inc., San Diego, CA) to plots of $\log_{10}$(molecular weights) of standard proteins (Bio-Rad Labs., Hercules, CA) run in parallel versus migration distance.

2.6. Transverse urea gradient PAGE

The denaturation/renaturation profile of human clusterin was analyzed on a transverse linear 0 to 8 M urea gradient superimposed on a transverse linear gradient of 15% to 11% total acrylamide:bisacrylamide (T), 2.65% bisacrylamide (C) in 50 mM Tris-25 mM boric acid pH 8.7 (Creighton, 1979; Goldenberg, 1989). 37 µg of G7 immunoaffinity purified human plasma clusterin was made 50 mM Tris-25 mM boric acid pH 8.7, 0.02% (w/v) bromophenol blue, and either 7 M in deionized urea to denature, or 10% (w/v) in glycerol to maintain the native state, in a final volume of 60 µL and incubated for 45 min at room temperature. Samples were loaded carefully on individual gels in a continuous well and run at 10 mA constant current for 4 h at room temperature. Proteins bands were fixed and visualized by staining with Coomassie Blue as described (Goldenberg, 1989).

2.7. Electroblotting of proteins separated by SDS PAGE

Proteins separated by SDS PAGE were transferred electrophoretically to supported nitrocellulose membranes (Bio-Rad) submerged in a buffer of 25 mM Tris-192 mM glycine, 20% (v/v) methanol, and 0.1% (w/v) SDS at either 100 mA overnight at room temperature or at 400 mA for 2 h with cooling. Transfer was confirmed by reversibly staining with Ponceau S. Transfer to PVDF membranes (Immobilon-P^{SQ}, Millipore, Bedford, MA) was essentially the same except that PVDF membranes were wetted first

in methanol, then water and finally transfer buffer. Following transfer, membranes were stained with Coomassie Blue to visualize protein bands or spots for excision. Briefly, membranes were stained 5 min at room temperature with 0.5% (w/v) Coomassie Blue R250 in 40% (v/v) methanol and destained to develop contrast by multiple washes with methanol. Desired spots or bands were excised and stored at -20°C prior to N-terminal sequencing.

2.8. N-terminal sequencing of polypeptides immobilized on PVDF membranes

Automated Edman N-terminal sequence determinations were performed on selected PVDF immobilized polypeptides with an Applied Biosystems Gas-phase Sequencer (Models 470/120/900) using the PVDF sequenator program of Speicher (Speicher, 1989).

2.9. Immunodetection of human and rat clusterin and murine LRP2 on nitrocellulose

Nitrocellulose membranes were blocked in 1% (w/v) casein (Sigma) dissolved in PBS at 95 to 100 °C (HDC PBS). Blots were incubated 1 to 2 h at room temperature or overnight at 4 °C in undiluted hybridoma conditioned medium at different times as complete RD medium or 90% (v/v) DMEM/F12, 10% FBS or as a dilution of Protein G or Protein A purified and concentrated rabbit polyclonal or mouse monoclonal respectively, in blocking buffer. Blots were then rinsed several times in PBS and incubated 1 to 2 h at room temperature or overnight at 4 °C with 1 in 5000 to 1 in 8000 dilution in blocking buffer of horseradish peroxidase (HRP) conjugated goat anti-mouse γ chain polyclonal (human γ chain adsorbed; Caltag, Mississauga, Ont.) or goat anti-rabbit IgG heavy and light chains (Caltag) for murine and rabbit antibodies, respectively. Blots were rinsed

several times in PBS then twice for 10 min each at room temperature with 0.1% (v/v) Triton X-100 in PBS with vigorous agitation and finally rinsed several times again with PBS. Immunoreactive bands were developed by Enhanced Chemiluminescence™ (ECL) (Amersham Life Science, Cleveland, OH) essentially as described by the manufacturer employing exposure times varying from a few seconds to 30 min to overnight on Kodak X-OMAT R film (Eastman Kodak).

1.10. Plasmids for expression of rat and human clusterin in *Pichia pastoris* and *Escherichia coli*

Plasmids for the expression of rat and human clusterin in *P.pastoris* and *E.coli* were prepared by subcloning of the clusterin open reading frame or that of individual α and β chains generated by polymerase chain reaction (PCR) into the appropriate vector. Mapping of α and/or β chain murine anti-rat clusterin monoclonal antibody specificities was performed using Western analysis of appropriate fusion proteins expressed in *E.coli*. Recombinant rat clusterin proprotein (amino acids 22-447), and α (amino acids 22-226; or 1-205), and β (amino acids 227-447; or 1-221) chains were amplified from plasmid pG17H by PCR and subcloned in frame as C-terminal fusions with the maltose binding protein in the *E.coli* expression vector pMalpR1 (New England Biolabs, Beverly, MA). Forward primers, GCGAATTCGAGCAGGAGTTCTCTGACAATGAG for the α chain and proprotein, and GCGAATTCAGCCTCATGCCTCTCTCCCACT for the β chain, had 5' extensions with an EcoR1 site in frame with both the clusterin and MalE coding sequences. Reverse primers GCGGATC-**CTA**TTCCATGCGGCTTTTCCTGCGGT for the β chain and proprotein, and GCGGATC-**CTA**GCGGACCAAGCGGGACTTG for

the α chain had a 5' extension with a BamHI site following a stop codon (underlined). The template was amplified on a Hybaid Thermocycler (Hybaid, Teddington, UK) using Taq DNA polymerase (Boehringer Mannheim, Indianapolis, IN) in a buffer supplied by the manufacturer using 30 cycles of 95°C for 1 min, 54°C for 1 min and 72°C for 2 min and a final extension of 10 min at 72°C. The purified PCR products were digested with an excess of EcoRI and BamHI and ligated initially into the vector pMalcR1 (New England Biolabs) at these sites. Proprotein or chain encoding fragments were subsequently excised by EcoRI and SalI and ligated into these sites in pMalpRI. This plasmid was then used to transform competent DH5αF' using standard protocols. Recombinant forms of human and rat clusterin were prepared as secreted proteins in the methylotrophic yeast *P. pastoris*. The complete open reading frame of the respective clusterin cDNAs including the N-terminal secretory signal sequence was amplified by PCR and subcloned into the *P. pastoris* expression vector pHIL-D2 (Invitrogen, San Diego, CA) via DNA ligase free homologous recombination in a *recA E. coli* host (Jones and Howard, 1991). The forward primers were ACTAATTATTCGAAACG-**ATG** AAGATTCTCCTGCTGTGTGT and ACTAATTATTCGAAACG-**ATG**AAGACTCTG CTGCTGTTTG for the rat and human cDNAs respectively and consisted of 23 and 22 bases of the respective clusterin 5' sequence beginning with the start codon (underlined) and a 5' extension of 17 bases homologous to the 5' untranslated region of the *P.pastoris* AOX1 mRNA immediately upstream of the AOX1 start codon in pHIL-D2. The reverse primers were CAGTCATGTCTAAGGCG-**TCA**TTCCATGCGGCTTTTCCTG and CAGTCATGTCTAAGGCG-CATC**TCA**CTCCTCCCGGTGCT for the rat and human cDNAs, respectively and consisted of 22 and 21 bases of the respective clusterin 3'

sequence including the termination codon (underlined) and a 5' extension of 17 bases homologous to the 5' end of the AOX1 3' transcription termination fragment in pHIL-D2. Templates were amplified on a Hybaid Thermocycler using $Vent_R$ DNA Polymerase (New England Biolabs) in a buffer supplied by the manufacturer and supplemented to a final concentration of 6 mM $MgSO_4$. Amplification was for 30 cycles of denaturation at 95°C for 1 min, annealing at 54°C for 1 min and elongation at 72°C for 2 min and final extension for 10 min at 72°C. The purified PCR products were transformed together with alkaline phosphatase treated pHIL-D2 linearized at the unique EcoRI site into competent Top10F' cells (Invitrogen). Low frequency recombination between the homologous ends of the PCR products and the vector resulted in site specific directional insertion eliminating the EcoRI site and precisely replacing the 5' untranslated region (UTR) and most (human) or all (rat) of the 3' UTR of clusterin with that of the AOX1 5' UTR and 3' coding and non coding sequence. These steps were thought to improve expression of clusterin by possible positive effects of the 5' UTR, in particular, of AOX1 on translation. These constructs were then linearized at the unique SalI site in the HIS4 gene and used to stably transform *P. pastoris* host line GS115 spheroplasts to histidine prototrophy as described by the manufacturer (Invitrogen). Transformants that secreted rat or human clusterin at high levels in the presence of methanol were selected for further use.

1.11. Expression of human and rat clusterin in *Pichia pastoris*

HIS+ transformants of GS115 secreting high levels of rat or human clusterin were inoculated and grown in a shaking incubator for 2 days at 30°C to saturation in non inducing BMGY medium as described by the manufacturer (Invitrogen). Cells were

pelleted by centrifugation at 5000 x g for 15 min at room temperature and resuspended in 1/5 to 1/6 of the original culture volume with BMMY containing methanol to induce recombinant protein expression. Alternatively, cells were resuspended in BMMY supplemented to 1% (w/v) with casein (Sigma) dissolved at near boiling temperatures (HDC BMMY). Induction was for 3 days at 30°C in a shaking incubator with an additional supplement of 1/10 volume of 5% (v/v) methanol after 36 h. Cells were pelleted as above and discarded. Conditioned BMMY was used as a source of recombinant clusterin partially purified by ethanol precipitation. HDC BMMY was used as a source of recombinant clusterin purified by immunoaffinity chromatography.

1.12. Quantification of human clusterin in conditioned BMMY by immunodot blot assay

Human recombinant and plasma clusterin in various fractions were diluted in PBS and applied to supported nitrocellulose membranes directly with the aid of a mild vacuum at 100 µL/dot using a commercially available 96 well vacuum manifold (Bio-Rad). Membranes were allowed to air dry and then were processed for immunodetection as described for Western analysis. To estimate unknown concentrations of clusterin in conditioned BMMY and other samples serial dilutions in PBS of the unknown sample were compared to dilutions of G7 immunoaffinity purified human plasma clusterin of known concentration applied and processed simultaneously.

1.13. Quantification of human clusterin in conditioned HDC BMMY by competitive antigen capture assay

96 well polystyrene microtitre plates (Corning, Corning, NY) were coated overnight at 4°C with 50 µL/well of 2.5 µg/mL Protein G purified mouse monoclonal G7 in 0.1 M Na_2CO_3-$NaHCO_3$ pH 9.5. Non specific binding sites were blocked for 1 h at 37°C with 100 µL/well of 1% (w/v) BSA, 0.02% Thimerosal in PBS pH 7.5 (at 37°C). The pH of conditioned HDC BMMY was adjusted to 7.5 at 37°C and volumes of medium from 10 nL to 25 µL made 1% (w/v) BSA, 0.1% (v/v) Triton X-100 and 500 ng/mL biotin labeled human clusterin and incubated at 50 µL/well for 1.5 h at 37°C. A standard curve was run in parallel using 0 to 50 µg/mL of immunoaffinity purified human plasma clusterin as unlabeled competitor. The wells were washed three times 200 µL/well with PBS, three times 200 µL/well with PBS containing 0.1% (v/v) Triton X-100 and three times 200 µL/well with PBS. The plates were incubated for 1.5 h at 37°C with 50 µL/well of 1 µg/mL streptavidin (Sigma) and 1 µg/mL biotin labeled HRP in blocking buffer and washed as described above. Plates were developed at room temperature with 100 µL/well of 2.5 mg/mL O-phenylenediamine (1,2-benzenediamine) (OPD; Sigma) and 0.03% (v/v) H_2O_2 in 50 mM citric acid, 100 mM Na_2HPO_4 pH 5. Color development was stopped by addition of 50 µL/well of 2 M HCl and the end point absorbance was measured at 490 nm using a microtitre plate reader. The data were fitted by non linear regression analysis to an equation for one site competition using a program supplied by GraphPad Prism™ (GraphPad Software). Concentrations of human clusterin in conditioned HDC BMMY were obtained by comparison of the estimated IC_{50}s of standard and unknowns.

1.14. G7 immunoaffinity purification of human clusterin

Clusterin was immunoaffinity purified at different times from human serum or plasma or recombinant *P.pastoris* conditioned HDC BMMY by immunoaffinity chromatography on a column of purified monoclonal antibody G7 linked to CNBr activated Sepharose 4B (Pharmacia). No differences were noted between serum and plasma as sources of non recombinant human clusterin in activity assays. The preparation of the affinity matrix has been described (Wilson and Easterbrook-Smith, 1992) and was a generous gift of Dr. Mark Wilson (University of Wollongong, Australia). All steps were performed at 0-4°C unless otherwise noted. Typically serum or plasma were prepared from 100 to 140 ml of venous blood obtained fresh from a healthy male volunteer. Blood was made 5 mM in EDTA and centrifuged at 1000 x g for 10 min to obtain plasma. To prepare serum, blood was clotted at room temperature for 1 h and then centrifuged at 15000 x g for 15 min at 4°C. Recombinant clusterin was prepared from up to 75 mL of HDC BMMY conditioned by a *P.pastoris* transformant secreting immunoreactive human clusterin. Cells were removed by centrifugation at 5000 x g for 15 min at room temperature. Serum and conditioned medium were made 5 mM in EDTA and all sources were diluted with one volume of cold PBS supplemented to a final concentration of 0.5 M with NaCl and 5 mM with EDTA (high PBSE) and benzamidine-HCl, phenyl methyl sulfonyl flouride (PMSF), and NaN_3, were added to 1 mM. The pH of diluted conditioned HDC BMMY was adjusted to pH 7.4. All sources were clarified by centrifugation at 15000 x g for 15 min and loaded onto a 2 ml column of G7 Sepharose 4B pre-equilibrated with high salt PBSE at a flow rate of 0.5 ml/min. The column was washed with high salt PBSE until the absorbance at 280 nm reached baseline and then was washed successively with PBS

supplemented to 5 mM with EDTA (low salt PBSE), low salt PBSE supplemented to 0.5% with Triton X-100, and finally low salt PBSE to remove the detergent. Bound material was eluted with 0.2 M glycine-HCl pH 2.74 monitored at 280 nm, collected as 2 ml fractions into tubes containing 150 µL of 2 M Tris-HCl pH 8.0 and immediately mixed to neutralize. Fractions containing the bulk of the absorbing material were pooled, concentrated, and spin dialyzed against three successive 10 fold dilutions of PBS in a CM-30 ultrafiltration unit (Amicon, Beverly, MA). The yield of clusterin from each source was typically of the order of 1 to 4 mg.

1.15. Ethanol precipitation of *P.pastoris* recombinant rat and human clusterin

Different experiments in this thesis used variations of the method outlined below for the precipitation of recombinant rat or human clusterin. All variations resulted in quantitative precipitation of clusterin. 3/5 volume of water was added to conditioned BMMY and diluted medium was supplemented to final concentrations of 1 mM NaN_3, 0.5 mM EDTA, 1 mM PMSF, and 1 mM benzamidine-HCl. Dilution with water prevented formation of a large flocculent pellet due to precipitation of components of the media. Diluted medium was clarified by centrifugation at 18000 x g for 30 min at 4°C. The pH of the supernatant was adjusted to pH 5.5 and the solution was cooled to just below 0°C in a dry ice/ethanol bath. Before appreciable ice formation 100% ethanol at -80°C was added slowly with stirring to give a final ethanol concentration of 25% (v/v). The medium was allowed to cool to -10°C and maintained at that temperature with stirring for 30 min. Clusterin was quantitatively precipitated with 25% (v/v) ethanol at pH 5.5, but required 35% (v/v) ethanol if precipitated at pH 6.5 or 7.0. The precipitate was recovered

by centrifugation at 30000 x g for 30 min at -10°C and dissolved on ice in a buffer of physiological ionic strength and neutral or near neutral pH containing 1 mM NaN_3, 0.5 mM EDTA, 1 mM PMSF, 1 mM benzamidine-HCl, 1 μg/mL Pepstatin A, and 1 μg/mL leupeptin. To prepare recombinant rat clusterin as immunogen and primary screening antigen, the pellet was dissolved in 1/40 volume of the total culture volume of PBS, dialyzed against four 1 L changes of PBS and filter sterilized through a 0.22 μm syringe filter. This preparation was stored at 4 °C.

1.16. Reversed phase high performance liquid chromatography (RP HPLC) separation of *P.pastoris* recombinant clusterin

100 μg of immunoaffinity purified *P.pastoris* recombinant human clusterin was diluted with 3 volumes of 10% (v/v) acetonitrile, 0.1% (v/v) triflouroacetic acid (TFA) to 1 mL and loaded on a 4.6 mm by 25 cm C4 RP HPLC column (Vydac, Hesperia, CA) operating at a flow rate of 0.5 mL/min. Separation was effected by a 5 min linear gradient of 10 to 25% acetonitrile, 0.1% TFA followed by a 60 min linear gradient from 25 to 58% and monitored continuously at 230 nm. One min fractions were neutralized immediately with 250 μL of 1 M NH_4HCO_3, and subsequently dried to approximately 120 μL with a Speed Vac concentator (Savant Instruments, Farmingdale, NY). 50 μL of each concentrated fraction was freeze dried overnight, redissolved in 1% (w/v) SDS, 2.5% (v/v) β-mercaptoethanol in 50 mM Tris HCl pH 6.8 and treated with N-glycosidase F as described.

1.17. N-linked deglycosylation of recombinant and plasma clusterin

Particular details of deglycosylation experiments varied depending upon the experiment. These differences did not appear to substantially affect the efficiency of deglycosylation. Briefly, different preparations containing up to 50 μg of recombinant and plasma clusterin were made 0.8 to 1% (w/v) SDS with or without 2 to 2.8% (v/v) β-mercaptoethanol and 50 mM Tris-HCl pH 6.8 and denatured by heating 10 min in a boiling water bath. Denatured samples were diluted such that the SDS concentration was 0.15% (w/v) and made 0.75% (v/v) NP40, 30 to 150 mM in Na_2HPO_4-NaH_2PO_4 or K_2HPO_4-KH_2PO_4 pH 8.3, 0 to 2 mM in EDTA, 1 mM in PMSF and 0.2 to 2.4 units of N-glycosidase F (Boehringer Mannheim, Indianapolis, IN). Deglycosylation was overnight at 37°C. Samples were diluted directly in sample reducing or non-reducing buffer for SDS PAGE such that the final NP40 concentration was less than 0.6% (v/v) and analyzed by one ore two dimensional SDS PAGE.

1.18. 2 dimensional (non-reducing followed by reducing) SDS PAGE of N-deglycosylated clusterin

α and β chain structures of human recombinant and plasma clusterin were analyzed by two dimensional SDS PAGE. Non-reduced N-deglycosylated samples were separated on 10% T, 2.65% C discontinuous SDS polyacrylamide gels in the first dimension. Lanes were excised and proteins reduced *in situ* by incubation for 30 min at room temperature with 0.125 M Tris-HCl pH 6.8, 2% (w/v) SDS, 65 mM DTT, 10% (v/v) glycerol, 0.001% (w/v) bromophenol blue and separated in the second dimension on 7% T to 20% T, 2.65% C continuous linear SDS polyacrylamide gels. Gels were stained either with

Coomassie Blue or transfered to nitrocellulose membranes for Western analysis or to PVDF membranes for N-terminal protein sequencing as described. Marker proteins were run in parallel in both dimensions.

1.19. Purification of sC5b-9

The soluble form of the terminal attack complex, sC5b-9 was prepared from inulin activated human serum essentially as described (Bhakdi and Roth, 1981). Briefly 75 mL of human serum was prepared from approximately 150 mL of freshly drawn venous blood from a fasted male volunteer. To generate sC5b-9, 2.17 g of inulin (Sigma) was added to serum and maintained in suspension by continuous gentle stirring at 37°C for 24 h. All subsequent steps were performed at 0–4°C. Inulin was removed by centrifugation at 18000 x g for 5 min. 20% (w/v) polyethelene glycol (PEG)-4000, 10 mM EDTA, in veronal buffered saline (VBS) (4.9 mM disodium barbital, 142 mM NaCl pH 7.4) was added incrementally to plasma to a concentration of 5% (w/v) PEG and incubated with gentle stirring for 30 min. Precipitated proteins were removed by centrifugation at 27000 x g for 20 min and the supernatant made 10% (w/v) PEG by incremental addition of the 20% (w/v) PEG solution with continuous stirring for a further 30 min. Precipitated proteins were collected by centrifugation at 27000 x g for 20 min and redissolved in 10 mL of 25 mM veronal-HCl, 100 mM NaCl pH 7.0. Unredissolved material was removed by centrifugation at 20000 x g for 30 min and the supernatant loaded at a flow rate of 1 mL/min on a 2.5 cm x 13 cm DEAE-Sephacel column (Pharmacia) preequilibrated in solubilization buffer (Appendix, Fig. 6.2). The column was washed with 70 mL 25 mM veronal-HCl pH 7.0 before elution of the bound proteins with a 450 mL linear gradient of

of 50 mM to 500 mM NaCl buffered by 25 mM veronal-HCl pH 7.0. Absorbance was monitored continuously at 280 nm and 9 mL fractions were collected. sC5b-9 elutes free of the bulk of contaminating serum proteins at 220 to 410 mM NaCl, estimated from specific conductances as reported (Bhakdi and Roth, 1981). Fractions were analyzed by Coomassie Blue stained SDS polyacrylamide gels run under non-reducing conditions and those that contained the distinctive polypeptide composition of sC5b-9, and that contained C9 as judged from comigration with purified C9 run in parallel, were pooled. Pooled fractions were made 2 mM in NaN_3, 1 mM in PMSF, and 1 mM in benzamidine-HCl, 1 μg/mL leupeptin, 1 μg/mL pepstatin, and 0.5 mM EDTA and concentrated to approximately 3 mL by ultrafiltration on a YM-10 membrane in a stirred cell apparatus (Amicon, Beverly, MA). Concentrated protein was diluted with 17 volumes of 5 mM Tris-HCl, 25 mM NaCl, 7.5 mM NaN_3, pH 7.75 and reconcentrated to 4 mL. Denatured proteins were removed by centrifugation at 20000 x g for 30 min and the supernatant diluted with a further 4 mL of the same buffer. 1 mL aliquots were overlayed on 11.3 mL 10% to 43% (w/v) linear sucrose gradients buffered with 5 mM Tris-HCl, 25 mM NaCl, 7.5 mM NaCl pH 7.75 in 14 mm x 89 mm Ultraclear™ tubes (Beckman Instruments, Columbia, MD) and centrifuged for 16 h at 35000 rpm at 8° C in a SW41 Ti rotor in a Class H L8M-70 ultracentrifuge (Beckman). Gradients were fractionated from the top into approximately 21 equal fractions. The refractive index at 20 °C of each fraction was converted to concentrations of sucrose using standard tables (CRC Handbook of Chemistry and Physics) and protein concentration was measured by BCA. Two protein containing peaks centered at about 16.69% and 27.95% (w/v) sucrose were well resolved from each other (Appendix, Fig. 6.3). By a similar analysis of fractions by SDS PAGE

sC5b-9 was found in the faster sedimenting peak as expected. Fractions corresponding to 25.31% (w/v) sucrose on the leading edge to 32.6% (w/v) sucrose on the trailing edge of this peak were pooled and concentrated by centrifugation at 3200 x g on a CM-30 ultrafiltration unit to a volume of approximately 200 µL. Purified sC5b-9 was stored in this form at 4 °C. The yield of sC5b-9 was estimated by BCA at 3.5 mg.

1.20. Biotin labeling of human clusterin

G7 immunoaffinity purified *P.pastoris* recombinant human and human plasma clusterin in 25 mM K_2HPO_4-KH_2PO_4, 100 mM NaCl pH 7.5 were biotinylated with a 20 fold molar excess of NHS-LC-biotin (Pierce Chemical Co., Rockford, IL) for 2 h on ice. Excess unreacted reagent was removed in different experiments by dialysis against 25 mM K_2HPO_4-KH_2PO_4, 100 mM NaCl pH 7.5 or VBS made 1 mM in NaN_3 and stored at 4 °C.

1.21. Incorporation of biotin labeled clusterin into sC5b-9 in inulin activated serum

50 µL of human serum was diluted 1:1 (v/v) with 2 x VBS supplemented to 2 mM with each of $CaCl_2$ and $MgCl_2$ and 2.5 µg of biotinylated human recombinant or human serum clusterin. After preincubating for 15 min at 37°C 2.85 mg of inulin was added to each sample and incubation at 37°C continued for a further 6-8 h with end over end mixing. Controls contained all components except inulin. 40 µL of VBS was added to each sample and inulin was removed by centrifugation for 2 min in a microcentrifuge. 100 µL of each supernatant was carefully layered on a 5-5.2 mL linear 10%-40% (w/w) sucrose gradient buffered with 5 mM Tris-HCl, 25 mM NaCl, 5 mM EDTA, 7.5 mM NaN_3 pH

7.75. Gradients were centrifuged for 12 h at 65000 rpm at 5°C in a SW65 rotor in an L8M-70 Ultracentrifuge (Beckman) using an acceleration and deceleration setting of 7. Gradients were fractionated from the top into 17-18 equal fractions of 290-310 µL. The refractive index at 20°C of each fraction was converted to % (w/w) sucrose using standard tables (CRC Handbook of Chemistry and Physics). Aliquots of fractions were seperated by 11% T, 2.65% C discontinuous SDS PAGE and electroblotted to nitrocellulose membranes as described. To detect biotin-labeled clusterin membranes were blocked 1 h at room temperature in 5% (w/v) skim milk dissolved in PBS and then incubated a further 1-2 h with 1 µg/mL streptavidin and 1 µg/mL biotin labeled HRP in HDC PBS. Membranes were processed as described for Western blots and biotinylated bands visualized by ECL.

1.22. Culture and differentiation of F9 cells

Differentiated F9 cells were prepared essentially as described (Kounnas et al., 1995). Briefly, 6.1 x 10^4 undifferentiated cells were seeded into gelatin coated 100 mm plastic tissue culture dishes in 15 mL of non-differentiating medium and allowed to attach overnight. Medium was then replaced with 15 mL of the same medium supplemented with 0.1 µM retinoic acid (Sigma) and 0.2 µM dibutyrl cAMP (Sigma) and grown for a total of eight days. Differentiating medium was changed every two days and after four days cells confluent cultures were subcultured at a density of 1 x 10^6 cells. After eight days confluent cultures contained 3-4 x 10^7 morphologically differentiated F9 cells (Strickland and Mahdavi, 1978; Strickland et al., 1980) were subcultured into gelatin coated 24 well plastic tissue culture dishes (Corning) at 1.7-1.8 x 10^5 cells/well in 500

μL/well differentiating medium and allowed to attach for 24-30 h prior to use in clusterin cell surface binding experiments.

1.23. Labeling of human plasma clusterin with $Na^{125}I$

20 μg of G7 immunoaffinity purified human plasma clusterin was labeled with $Na^{125}I$ using chloramine T as oxidant (Hunter and Greenwood, 1962). Labeling was for 90 sec at room temperature in a final volume of 180 μL consisting of 146 μL 0.3 M NaH_2PO_4/Na_2HPO_4 pH 7.4 , and 10 μL of 50 μM $Na^{125}I$ (15.9 mCi $^{125}I/\mu g$ I, Amersham, Cleveland, OH) and initiated by addition of 20 μL of 2.56 mg/mL chloramine T (Sigma) in water. To stop the reaction 8 μL of 8.26 mg/mL sodium metabisulfate was added to each reaction. Unincorporated ^{125}I was removed by size exclusion chromatography through spun columns. Briefly, 2 μL of 1 M $Na^{127}I$ and 10 μL of 2% (w/v) BSA, 1% (v/v) Triton X-100, 10 mM NaH_2PO_4/Na_2HPO_4, 150 mM NaCl pH 7.4 were added to the terminated reaction and then centrifuged through 1.3 mL spun columns of Sephadex G-25 medium grade (Pharmacia) pre-equilibrated in 0.1% (w/v) BSA, 0.05% (v/v) Triton X-100, 10 mM NaH_2PO_4/Na_2HPO_4, 150 mM NaCl pH 7.4 for 1 min at 250 x g. The specific activity of ^{125}I-labeled clusterin was 7.76 x 10^4 cpm/ng. Labeled products were stored at 4°C until used and specific activity was always corrected using theoretical rates of decay at the time of use.

1.24. Competition assay for high affinity clusterin binding to differentiated F9 cells

Differentiating medium was aspirated and differentiated F9 monolayers washed once carefully at room temperature, then incubated for 2 hrs at 37°C with 500 μL/well of

serum free medium consisting of 1% (v/v) Nutridoma^{TM}-SP (Boehringer-Mannheim), and 99% (v/v) binding buffer (serum free non differentiating medium with 1.5% (w/v) BSA, and 25 mM HEPES pH 7.35). Plates were then placed on ice and medium replaced with 240 µL/well binding buffer at 4 °C containing 0.49 µg/mL ^{125}I-labeled clusterin (specific activity 7.0 x 10^4 cpm/ng) and from 0 to 100 fold excess unlabeled immunoaffinity purified human plasma clusterin or *P.pastoris* recombinant human clusterin and incubated for 2.5 h at 4°C. To determine the effect of G7 on cell surface binding ^{125}I-labeled clusterin was preincubated with purified antibody at 52.5 µg/mL (47 fold molar excess) on ice for 1 hr before addition to monolayer. Monolayers were then washed carefully four times with 500 µL/well ice cold binding buffer and lysed with 300 µL/well of 0.1 N NaOH. Lysates were counted for 60 sec in a LKB gamma counter. Non specific binding to F9 monolayers was considered to be bound counts in the presence of 100 fold molar excess of unlabeled clusterin and was subtracted from the total bound counts at each experimental condition. Specifically bound counts were normalized to the mean number of cells/well obtained from additional wells processed in parallel and converted to ng specifically bound ^{125}I-labeled clusterin. The data were fitted by non linear regression analysis to an equation for one site competition using a program supplied by GraphPad Prism^{TM} (GraphPad Software).

1.25. Interaction of human clusterin with monoclonal antibody G7, Amyloid β_{1-40}, IgG, and Zn^{+2} polymerized C9

Human IgG, $A\beta_{1-40}$, and Zn^{+2} polymerized C9 were coated at concentrations ranging from 0.5 to 10 µg/mL at 50 µL/well in 96 well polystyrene microtitre plates (Corning) for

1 to 2 h at 37°C and overnight at 4 °C. Human IgG and purified monoclonal antibody G7 were coated in 0.1 M Na_2CO_3-$NaHCO_3$ pH 9.5 and $A\beta_{1-40}$ in 0.1 M Na_2CO_3-$NaHCO_3$ pH 8.6 and Zn^{+2} polymerized C9 in TBS (10 mM Tris-HCl, 150 mM NaCl, pH 7.5). C9 was freshly polymerized with Zn^{+2} prior to each binding experiment as described (Tschopp et al., 1993). Briefly, monomeric C9 was diluted to 100 µg/mL in TBS and incubated for 2 h at 37°C in the presence of 100 µM $ZnCl_2$. Polymerized C9 was then diluted to the appropriate concentration in TBS for coating microtitre plates. Coated plates were blocked with 110 µL/well of 1% (w/v) BSA, in PBS for 1 h at 37°C. Wells were washed once with 50 µL of binding buffer consisting of 1% (w/v) BSA, 0.1% (v/v) Triton X-100, 0.02% (w/v) NaN_3 in PBS at the pH used subsequently in the clusterin binding phase (pH 5 to 7.5 at 37°C). Biotin labeled human plasma clusterin was bound to immobilized ligands at concentrations ranging from 0 to 500 ng/mL in binding buffer at the appropriate pH in the presence of DEPC modified or unmodified unlabeled clusterin in a total of 50 µL/well for 1.5 h at 37°C. In heterologous competitive binding assays labeled clusterin was preincubated with Zn^{+2} polymerized C9, $A\beta_{1-40}$, or monoclonal antibody G7 (as described in the appropriate Fig. legend) prior to addition to ligand coated wells. For direct binding assays unlabeled clusterin was bound at concentrations ranging from 0 to 200 µg/mL and 0.5 to 20 µg/mL under identical conditions. Plates were washed at room temperature nine times with 150 µL/well using a wash buffer made fresh as 1% (w/v) BSA in PBS with or without 0.1% (v/v) Triton X-100. In order, these were three times without detergent, three times with detergent and lastly three times again without. Bound biotin labeled clusterin was detected with 50 µL/well 1 µg/mL streptavidin (Sigma) and 1 µg/mL biotin labeled HRP (Sigma) in detergent free wash buffer incubated for 1.5 h at

37°C. Bound unlabeled clusterin was detected with 50 µL/well 2 µg/mL monoclonal antibody G7 followed by 50 µL/well 1/1000 dilution of HRP linked goat anti-mouse γ chain (human γ chain adsorbed; Caltag), both diluted in detergent free wash buffer and incubated for 1.5 h at 37°C. Plates were washed three times 150 µL/well with detergent free wash buffer after G7 incubation, and as per post-clusterin binding phase following HRP-linked detecting reagent. Plates were developed using OPD as substrate as described for the clusterin G7 antigen capture assay. For competitive inhibition experiments the data were fitted by non linear regression analysis to an equation for one site competition using a program supplied by GraphPad Prism™ (GraphPad Software).

1.26. DEPC modification of clusterin

Immunoaffinity purified human plasma clusterin at 200 µg/mL in 20 mM K_2HPO_4-KH_2PO_4, 50 mM NaCl pH 6 or 7 was modified with 0.5 mM DEPC (Sigma) for times ranging from 0 to 20 min at room temperature. Modification of histidine residues was followed by the change in absorbance at 240 nm. At timed intervals after addition of DEPC aliquots were withdrawn and the reaction quenched by rapid mixing with 1 µL 0.1 M imidazole-HCl pH 7 (at 37°C) and dilution by a factor of 20 to a final concentration of 10 µg/mL clusterin in binding buffer (1% (w/v) BSA, 0.1% (v/v) Triton X-100, 0.02% (w/v) NaN_3 in PBS pH 7.0 (at 37 °C)) containing 500 ng/mL biotin labeled human plasma clusterin and added to wells coated with $A\beta_{1-40}$, IgG, or Zn^{+2} polymerized C9. An aliquot was withdrawn and processed identically prior to addition of DEPC and as time 0. Bound biotin labeled clusterin was detected with streptavidin and biotin labeled HRP as described. Competitive inhibition binding experiments performed in parallel using

unlabeled unmodified serum/plasma clusterin were used to obtain standard curves from which equivalent effective concentrations of DEPC modified clusterin could be calculated.

1.27. Preparation of anti-rat clusterin monoclonal antibodies

4-6 week old female BALB/c mice were injected intraperitoneally a total of five times each at one site with an estimated 20 to 100 μg of rat recombinant clusterin in 150 to 200 μL of MPL+TDM adjuvant (RIBI Immunochem Res., Hamilton, MT). The first two boosts were at 2 week intervals, the third after a period of a month and the fourth after an additional 2 weeks. 3 days after the last boost mice were sacrificed by cervical dislocation, and spleenocytes prepared for and fused with NS-1 cells at a ratio of cells of 1 to 10 as described (Myoken et al., 1989). Hybridomas were grown in 96 well plates with selection for cholesterol prototrophy in serum free RD medium containing 5 μg/mL bovine insulin-HCl (Sigma), 5 μg/mL human transferrin (Sigma), 10 μM ethanolamine (Sigma), 10 μM 2-mercaptoethanol (Sigma), 10 nM sodium selenite (Sigma), and 0.5 mg/mL BSA with 2 moles oleic acid conjugated/mol protein (Sigma) (Myoken et al., 1989). Hybridomas were screened for reactivity by ELISA to rat recombinant clusterin bound to 96 well polystyrene plates (Corning) coated at an estimated concentration of 5 to 10 μg/mL in PBS. Wells were blocked with 1% (w/v) BSA in PBS then incubated with hybridoma conditioned medium. After washing with PBS and PBS supplemented with 0.1% (v/v) Triton X-100 (PBST) wells were incubated with 1/2000 dilution of HRP-linked goat anti-mouse γ chain (human γ chain adsorbed; Caltag) in HDC PBS and then washed with PBS and PBST prior to detection. Positive wells were identified after

development using OPD as a substrate as described for the clusterin G7 antigen capture assay. Positive hybridomas were cloned and rescreened by ELISA and positive sublines selected for expansion. The corresponding monoclonal antibodies were typed using a Mouse MonoAb ID/SP kit (Zymed, So. San Francisco, CA) as described by the manufacturer. Conditioned medium from selected sublines was used for immunoprecipitation, immunohistochemistry, and Western analysis.

1.28. Preparation of rat ventral prostate for immunological analyses

Male Sprague Dawley rats weighing 250-300 g were castrated via the scrotal route under light halothane anaesthesia. Untreated control animals and animals 1 to 4 days following castration were sacrificed by cervical dislocation. Prostate glands were excised, flash-frozen in liquid N_2- chilled isopentane, and stored in liquid N_2 until prepared for Western analysis or immunoprecipitation. Thawed prostates were homogenized with a hand held polytron in 500 µL ice cold 50 mM Tris-HCl pH 7.4, 150 mM NaCl, 1% (v/v) NP40, 0.1% (w/v) SDS, 0.25% (w/v) sodium deoxycholate (RIPA) for Western analysis or 90% (v/v) PBS pH 7.4, 10% (v/v) glycerol (PBS-glycerol) supplemented with 1 mM EDTA, 1 mM benzamidine-HCl, 1 µg/mL leupeptin, and 1 mM PMSF for immunoprecipitation. RIPA extracts were clarified by centrifugation in a microcentrifuge and used directly for Western analysis. Clarified PBS-glycerol extracts were combined with a 400 µL PBS-glycerol wash of the pellet and further clarified by centrifugation at 55000 rpm for 30 min at 4°C in a TLA 100A rotor in a Optima TL Benchtop Ultracentrifuge (Beckman) for immunoprecipitations. Alternatively excised prostates were fixed for 24 h in 4% (v/v) paraformaldehyde in 100 mM Na_2HPO_4-NaH_2PO_4 pH 7.5 followed by routine paraffin

embedding. 10 μm sections were cut on a rotary microtome and mounted on sterile gelatin-coated, positively charged microscope slides (Fisher, Pittsburgh, PA) for immunohistochemistry.

1.29. Expression of rat clusterin proprotein, α and β chain MalE fusions in *E.coli*

To prepare fusion proteins for mapping of murine anti-rat clusterin monoclonal antibody epitopes a DH5αF' transformant of each fusion construct was grown to an OD_{600} of 0.4 in Rich Broth at 37°C in a shaking incubator as described by the manufacturer (New England Biolabs) at which time recombinant protein expression was induced with 0.3 mM IPTG. After 2 h cells were recovered by centrifugation and lysed by heating to 100°C for 10 min in 1.25% (w/v) SDS in 30 mM Tris-HCl pH 6.8. 35 μg total protein in each lysate was analyzed by Western analysis as described.

1.30. Immunoprecipitation of clusterin from rat ventral prostate lysates

To immobilize monoclonal antibodies 1.2 mL of the corresponding hybridoma conditioned serum free complete RD medium was incubated with 25 μL settled Protein G agarose (Pierce) overnight at 4 °C and beads were washed 3 times with 1 mL each of ice cold PBS. 500 μg of total soluble prostatic protein was diluted into PBS supplemented with 1 mM EDTA, 1 mM PMSF, and 1 mM benzamidine-HCl in a final volume of 500 μL and incubated with the washed beads for 6-8 h with end over end mixing at 4 °C. Beads were pelleted by centrifugation and washed successively with 1 ml volumes of ice cold PBS supplemented to 0.5 M with NaCl (4 times), with PBS (1 time), with PBS supplemented to 0.1% (v/v) Triton X-100 (3 times), and finally with PBS (3 times).

Bound proteins were eluted by heating at 100°C in SDS PAGE non-reducing sample buffer and eluted proteins separated by SDS PAGE.

1.31. Immunohistochemical analysis of clusterin in the rat ventral prostate

Sections were deparaffinized, rehydrated, and equilibrated in 10 mM Na_2HPO_4-NaH_2PO_4, 154 mM NaCl pH 7.2 (10 mM PBS). Immunoperoxidase staining was used to localize immunoreactivity. After overnight incubation with diluted hybridoma conditioned serum free RD medium at 4 °C, sections were incubated for 1 h at room temperature with biotin labeled goat anti-mouse IgG (1:300; Sigma), and reacted with 1 mg/mL diaminobenzidine in 50 mM Tris-HCl pH 8.0 containing 0.003% (v/v) H_2O_2. The secondary antibody and hybridoma conditioned medium were diluted in 10 mM PBS, 0.3% (v/v) Triton X-100, 3% (w/v) BSA, pH 7.2. For each hybridoma serial dilutions (neat, 1:10, 1:100, 1:1000) were tested to obtain the optimal dilutions shown.

CHAPTER THREE

2. *Structural symmetries in α and β chain amphipathic α helices suggest a novel model of clusterin structure and function*

2.1. Background

Presently, little is known of clusterin structure or of the relationship between structure and function. Clusterin demonstrates no extensive homology to any proteins in current databases. Some limited homologies have been identified to repetitive sequences of the rod-like tail domain of myosin heavy chains (Fig. 3.1) (Jenne and Tschopp, 1989; Tsuruta et al., 1990). Visual (de Silva et al., 1990a) and computer assisted analysis (Tsuruta et al., 1990) have identified segments of clusterin sequence that can be modeled as amphipathic α helices (Fig. 3.1). In view of the interaction of clusterin with apoAI-HDL, terminal complement components, and Aβ4 peptides in particular, the non polar faces of amphipathic α helices have been proposed as functional elements in the binding of hydrophobic/amphipathic ligands. More recently, clusterin has been identified as a ligand of the low density lipoprotein receptor related protein, LRP2, both *in vivo* (Morales et al., 1996; Zlokovic et al., 1996b) and *in vitro* (Kounnas et al., 1995) and of heparin *in vitro* (Pankhurst et al., 1997). By analogy to other proteins, such as apoE, that bind LRP2 and/or heparin it is likely that clusterin binds to these by an electrostatic interaction, through a distinct binding site (Weisgraber, 1994).

While the α and β chains of clusterin display little detectable sequence homology, there are interesting interchain similarities in structure and function. This is particularly evident in the pattern of interchain disulfide bonding. The conservation of number and spacing of cysteine residues in the cysteine rich domains of each chain, reflects a unique linear, antiparallel, arrangement of five interchain disulfide bonds (Choi-Miura et al., 1992a; Kirszbaum et al., 1992) (Fig. 3.1). At the genomic level each of these domains is

Figure 3.1. Correspondance of clusterin structural elements with coding exons

Human clusterin α and β chains are presented as given in Figure 1.2 with myosin homology domains (red boxes) and amphipathic α helices (yellow and blue boxes) as previously described (de Silva et al., 1990a; Tsuruta et al., 1990). Depicted are boundaries that correspond to coding exons in the human clusterin gene (Wong et al., 1994a).

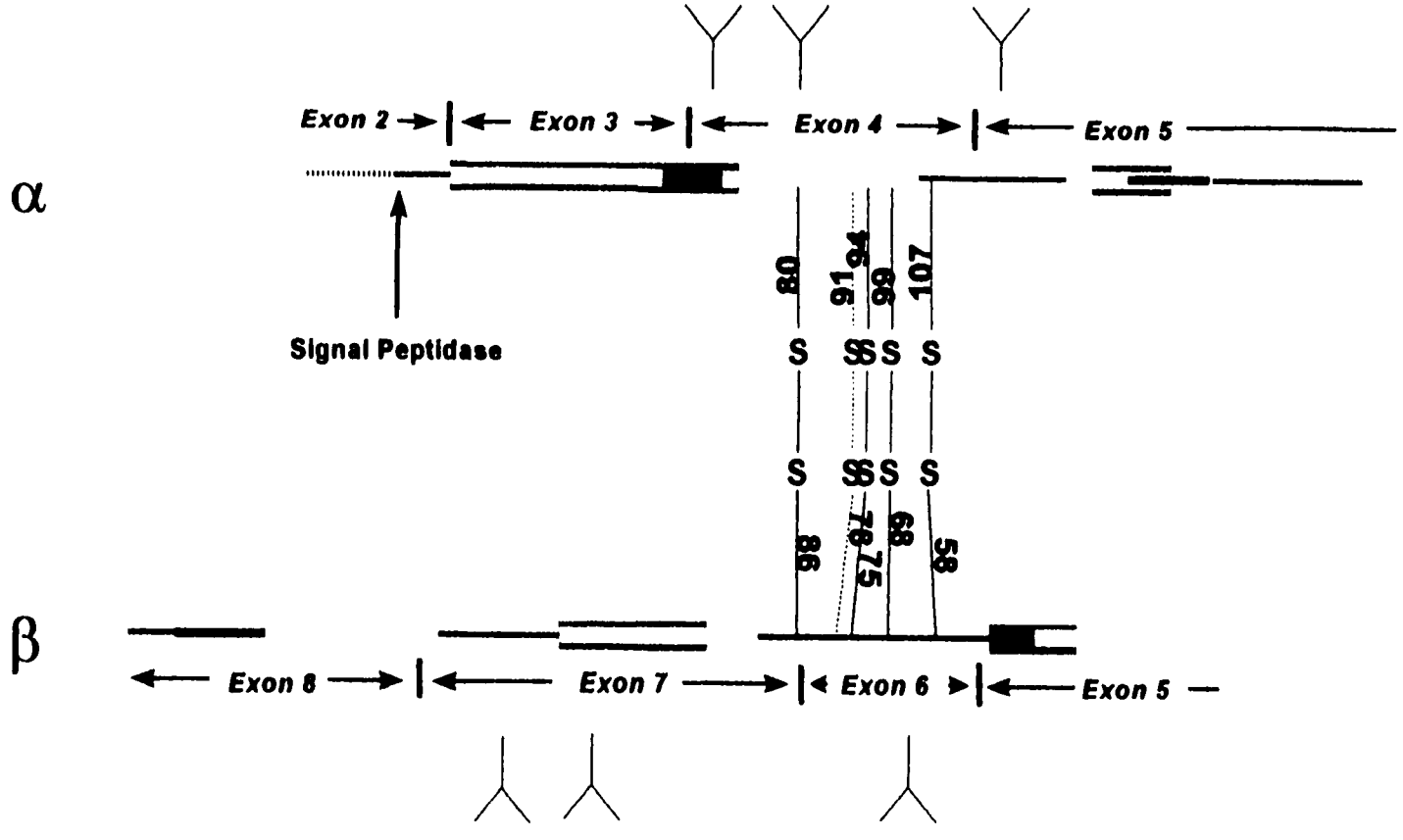
α
β
Exon 2
Exon 3
Exon 4
Exon 5
Signal Peptidase
80
91
94
99
107
S
S
S
S
S
S
S
S
86
78
75
68
58
Exon 8
Exon 7
Exon 6
Exon 5

encoded essentially by a single exon (α, exon 4; β, exon 6) suggesting a possible common evolutionary origin for these α and β chain domains (Wong et al., 1993; Jordan-Starck et al., 1994; Wong et al., 1994a; Michel et al., 1995). Outside of this domain there are other suggestive interchain structural similarities. There are two regions of homology to the myosin heavy chain tail reported in each of the α and β chains (Tsuruta et al., 1990) (Fig. 3.1). The AMPHI algorithm (Cornette et al., 1987; Margalit et al., 1987) identified three sequences in each chain having periodic hydrophobic moments corresponding to an α helix (Tsuruta et al., 1990) and helical wheels (Schiffer and Edmundson, 1967) identified three sequences, one in the α chain and two in the β chain, that can be modeled as amphipathic α helices (de Silva et al., 1990a) (Fig. 3.1).

Interchain functional symmetries also appear to reflect, at some level, a structural symmetry. Both the α and β chains inhibit binding of the clusterin heterodimer to denatured complement C9, and inhibit complement dependent hemolysis *in vitro* (Tschopp et al., 1993). In addition, they inhibit binding of the heterodimer to the C-terminal domain of the transforming growth factor β receptor type II (Reddy et al., 1996) and to $A\beta_{1-40}$ (Choi-Miura et al., 1994). Synthetic peptides corresponding to part of the putative α and β amphipathic α helices encoded by exon 5 have $A\beta_{1-40}$ binding inhibitory activity (Choi-Miura et al., 1994) suggesting that the basis of these α and β chain functional symmetries in each case may be the respective amphipathic α helices in each chain (Fig. 1.2).

1.2. Objective

There has been no concerted attempt to synthesize these and other observations into a more detailed and integrated model of clusterin structure and function. The development of such a model would have heuristic value in focusing and directing specific experimental approaches to understanding these relationships in clusterin and can have important implications for its physiological role. This chapter represents an attempt at such a synthesis. In addition to the studies referred to above I make use of an analysis of amphipathic α helices using the COIL algorithm (Lupas et al., 1991) and consider the results in relation to topological constraints introduced by the pattern of interchain disulfide bonds. The implications of these analyses, I believe, is a deeper understanding of the significance of structural and functional symmetries between α and β chains and leads to a compelling and novel hypothesis of the domain structure of clusterin. The model is developed with proposals for specific binding sites, in particular a novel suggestion for the structure and identity of the LRP2 binding site, and predictions of possible structure-function relationships that might be observed in the binding to hydrophobic/amphipathic ligands. Much of the experimental data in Chapter 4 has been interpreted in light of this model.

1.3. Results

1.3.1. α and β chain symmetries emphasized in a 2D model of clusterin structure

The symmetry of the α and β chains of in the myosin homology/amphipathic helical domains is emphasized in a simple model of clusterin in which the chains are drawn to scale (fixed unit length/amino acid) fully extended and aligned in an antiparallel

orientation with respect to the disulfide bond formed between the first cysteine of the α chain, C80, (all numbering is relative to the mature N-terminus of the respective α and β chains of human clusterin unless otherwise noted) and to the last cysteine of the β chain, C86 (Fig. 3.1). Symmetry is reflected in the spatial overlap of pairs of putative amphipathic α helices. Putative helices encoded by exon 3/4 in the α and by exon 7 in the β overlap spatially as do those in each chain encoded by exon 5. Additionally, the N-terminal boundary of the polypeptide sequence encoded by exon 3 and the C-terminal boundary of that encoded by exon 7 as well the N and C-terminal boundaries, respectively of the polypeptide sequence encoded by exon 4 and exon 6, are very nearly colinear (Fig. 3.1). This suggests a possible two dimensional spatial context in which to understand the one dimensional description of the distribution of amphipathic α helices and of evolutionary relationships that might exist amongst exons of each chain. I therefore explored the possible significance of this model in greater detail.

1.1.2. Analysis of clusterin structure using the COIL algorithm

Based on the apparent homologies to the rod-like tail domain of myosins, which consists of two parallel amphipathic α helices paired to form a long, stable coiled-coil, the sequences of all homologs of clusterin were analyzed using the program COIL (Fig. 3.2) (Lupas et al., 1991). Coiled-coil domains of α filamentous proteins are characterized by a heptad repeating pattern, a-b-c-d-e-f-g where the "a" and "d" residues are usually hydrophobic, with the other positions commonly hydrophilic and frequently charged (Fig. 3.3). When folded as a typical α helix these sequences give rise to an amphipathic structure with a non-polar face characterized by a "knobs and holes" alternation of

Figure 3.2. COIL analysis of clusterin

A. Species homologs of clusterin were analyzed by the program COIL without modification (proline and tryptophan included) (Lupas et al., 1991) using a window size of 28. The probability of forming a coiled-coil amphipathic α helix is plotted for each species as a function of position in the multiple species alignment (Fig. 1.1).

B. Identical to A. showing only the predictions for sequences coding for exon 7, the extent of which is delineated by the overlying line.

C. Plot of COIL scores using a 28 amino acid window for the helices encoded by human exon 7 for three different continuous heptad (a-b-c-d-e-f-g) phase relations. Red line, phase I (βN89 as "a"), blue, phase II (βN89 as "d"), and green, a reference third phase (βN89 as "e"). Calculation of COIL scores was modified by the exclusion of proline (βP91) and tryptophan (βW123 and βW141) which have relative frequencies of either 0 or sufficiently low in the heptad positions in which they fall in these phases to exert a dominant negative effect on the geometric mean. Each amino acid is assigned the score of the highest scoring 28 amino acid window containing it. A score of 1.24 represents a probability of about 0.1 of forming a coiled-coil and increases rapidly for higher scores (COIL score of 1.50 corresponds to a probability of 0.94). For reference the circles with error bars are the mean ± standard deviation of the scores of all 28 amino acid windows in the coiled-coil domains of α fibrous proteins: myosins, keratins, and tropomyosins (open circle, 1.63 ± 0.24) and of globular proteins as a whole (closed circle, 0.77 ± 0.2) each fit to a Gaussian distribution (Lupas et al., 1991).

A.

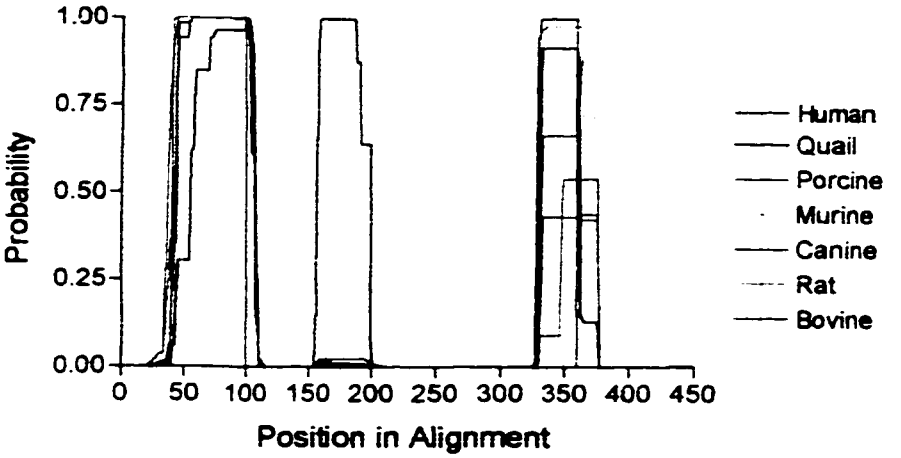
1.00
0.75
0.50
0.25
0.00
Probability
0
50
100
150
200
250
300
350
400
450
Position in Alignment
Human
Quail
Porcine
Murine
Canine
Rat
Bovine

B.

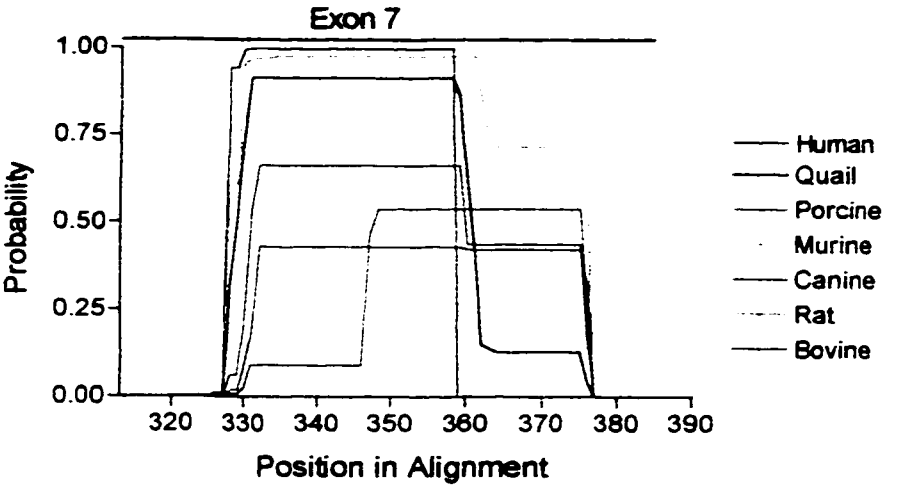
Exon 7
1.00
0.75
0.50
0.25
0.00
Probability
320
330
340
350
360
370
380
390
Position in Alignment
Human
Quail
Porcine
Murine
Canine
Rat
Bovine

C.

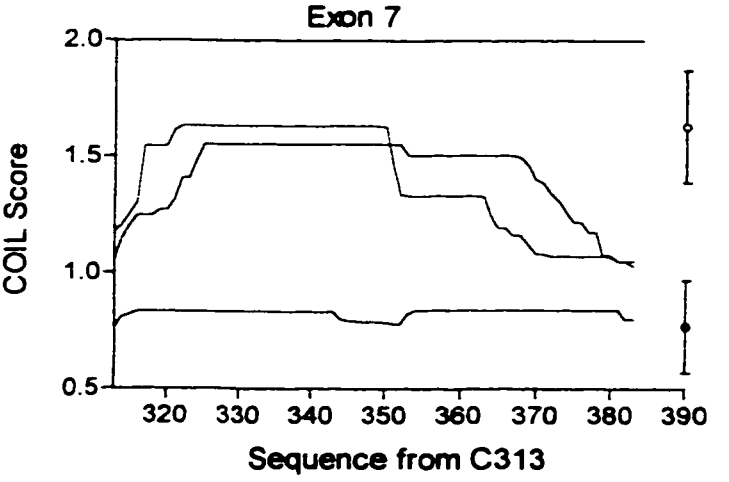
Exon 7
2.0
1.5
1.0
0.5
COIL Score
320
330
340
350
360
370
380
390
Sequence from C313

Figure 3.3. "Knobs and Holes" pairing in parallel and antiparallel coiled-coils

End on view of two coiled-coil amphipathic regular (100°/residue) right handed α helices oriented with axes parallel and antiparallel to show the distribution of amino acids at each heptad position in two helical turns and the differences in "knobs" to "holes" packing of "a" and "d" hydrophobes. In parallel orientation "a" and "a′" and "d" and "d′" are aligned while in the antiparallel orientation "a" and "d′" and "d" and "a′" are aligned. "a" and "d" are interfacial, while "e" and "g" are juxtafacial, and "b", "c", and "f" are extrafacial.

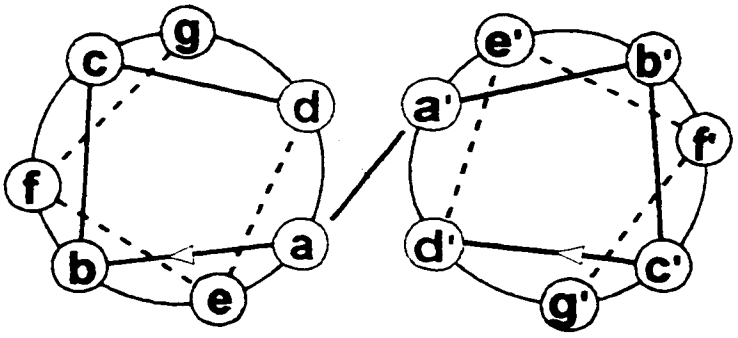

Parallel

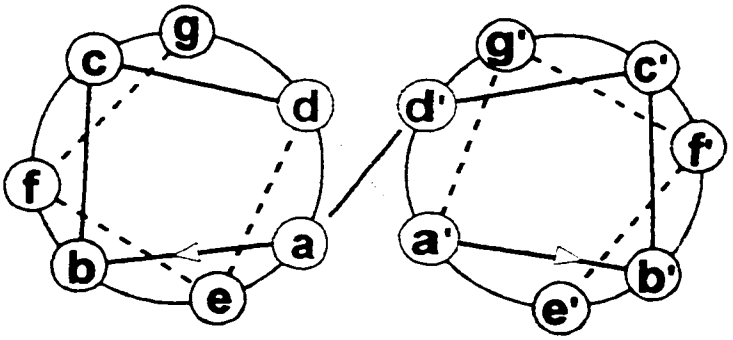

Antiparallel

hydrophobic residues. Two such helices pair with the "knobs" of one helix filling the "holes" of the other driven in large part by the hydrophobic effect (Fig. 3.3). The COIL algorithm calculates a geometric mean (score) taken over a sliding window of 14, 21, or 28 residues (2 , 3 ,or 4 successive heptad repeats), of the relative frequencies of each successive amino acid of the query sequence based on its assignment of a position in the heptad relative to the start of the window. The relative frequencies are the frequency of the given amino acid for the given heptad position estimated from the database of known coiled-coils of myosins, tropomyosins, and keratins relative to its frequency in all known proteins. The given residue is assigned the position and score of the phase of the window producing the highest score, and is converted to a probability of forming a coiled-coil α helix by a probability function based on Gaussian distribution "best" fits to the distribution of all scores for known coiled-coils, known globular proteins and to all proteins in GenBank (Lupas et al., 1991).

Using a window size of 28 residues, only the helices encoded by exon 3/4 and 7 display a significant probability of forming a coiled-coil helix that is conserved across species (Fig. 3.2, A and B). Using a probability cut off of 0.1 the predicted coiled-coil α helix encoded by exon 3/4 varied from 57 amino acids for mouse and rat to 78 amino acids for bovine clusterin and for most of this extent the COIL scores are very high corresponding to probability values of between 0.9 and 1. In the human this region extends from αS17 to αL76 (39 to 98 in alignment of Fig. 3.2, A), of which αV20 to αL76 (42 to 98 in alignment of Fig. 3.2A) corresponds to the maximum extent of overlap of the individual species predictions. In addition, in all species except the quail, the

constitutive heptads are all predicted to be in phase, without discontinuities, and with the same phase predicted for all species in the alignment (Fig. 3.4). In the quail sequence a discontinuity is predicted for the heptad, αH42 to αT48, but this does not alter the phase relations between preceeding and succeeding heptads.

The COIL probabilities for the helix encoded by exon 7 were more species-variable, both in predicted extent and magnitude, than those encoded by exon 3/4 (Fig. 3.2B). Using a cut off of 0.1, the sequence with the greatest predicted continuous extent is 49 amino acids for mouse and rat clusterin and that with the least, 31 amino acids for the human protein. COIL scores range from very high, with probability values between 0.9 to 1 for the human, rat and canine clusterin to a probability maximum of 0.43 for bovine clusterin. Unlike that for the helices encoded by exon 3/4 COIL does not predict an identical heptad phase relation for the helices encoded by exon 7 for each homolog. Rather two phases, designated I and II, are represented (Fig. 3.4). For all species except the human and porcine, a discontinuity is predicted, at a species variable position at which the N-terminal phase I is succeeded toward the C-terminus by phase II. Based on conservation of hydrophobes at "a" and "d" positions exon 7 can plausibly be modeled as a succession of 7 to 8 continuous heptads using either phase relation. 11 of 16 amino acids at "a" or "d" for either phase for the 8 heptads from βN90 to βA146 of human clusterin (326 to 382 in alignment of Fig. 3.2A and B) have relative frequencies greater than 1.24 and 8 and 9 of 16 for phases I and II, respectively have relative frequencies greater than 1.63, corresponding to probabilities of 0.1 and 0.99 if scored for a 28 residuewindow (Lupas et al., 1991).

Figure 3.4. Heptad phase predictions of COIL for sequences encoded by exon 3/4 and 7

Prediction of the extent (COIL probability ≥ 0.1) and heptad position for the helices encoded by exon 3/4 (Top) and 7 (Bottom) using the unmodified COIL algorithm (Fig. 3.2, A and B) and aligned on the basis of the multiple species alignment (Fig.1.1). "a" and "d" residues are in blue and red, respectively and are boxed in the same color. Horizontal black underlines indicate a discontinuity or change in the predicted phase. The heptad position predictions are aligned with the corresponding human sequences; the helices encoded by exon 3/4 species predictions (Top) with the sequence α (Q10 to L87) given in II and exon 7 species predictions (Bottom) with the sequence β (S92 to N140) given in I. At the center of the figure the helices encoded by exon 7 are shown with either of the two plausible continuous heptad phases (I and II; amino acids corresponding to predicted "a" and "d" positions are in blue and red, respectively) suggested by analysis with the modified COIL algorithm (Fig 3.2, C) while exon 3/4 is given the highest scoring heptad phase relation given in Figure 3.2 A. The two plausible antiparallel arrangements (I and II) of the helices encoded by exon 3/4 and exon 7 helices are shown. Both these arrangements maintain close spatial proximity of the cystine halves of the nearby αC80 and βC86 disulfide and align "a" and "d′" and "d" and "a′" with maximal overlap of COIL predictions. Exon 7 heptad phase prediction I gives rise to antiparallel arrangement I while heptad phase prediction II gives rise to antiparallel arrangement II. The sequences are numbered relative to the N-terminal amino acid of the mature α and β chains of the human clusterin protein.

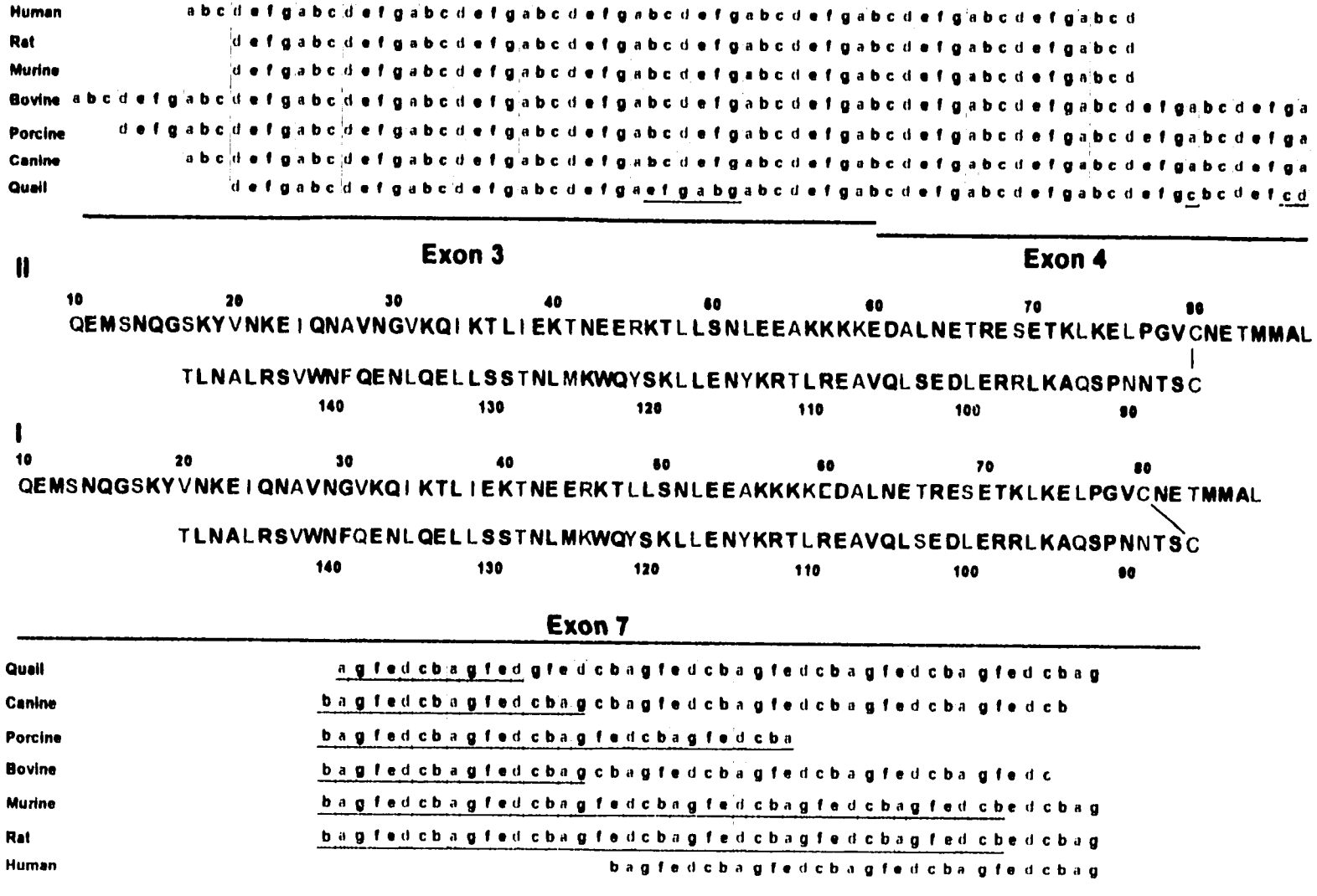
Human
Rat
Murine
Bovine
Porcine
Canine
Quail
Exon 3
Exon 4
II
I
QEMSNQGSKYVNKEIQNAVNGVKQIKTLIEKTNEERKTLLSNLEEAKKKKEDALNETRESETKLKELPGVCNETMMAL
TLNALRSVWNFQENLQELLSSTNLMKWQYSKLLENYKRTLREAVQLSEDLERRLKAQSPNNTSC
QEMSNQGSKYVNKEIQNAVNGVKQIKTLIEKTNEERKTLLSNLEEAKKKKCDALNETRESETKLKELPGVCNETMMAL
TLNALRSVWNFQENLQELLSSTNLMKWQYSKLLENYKRTLREAVQLSEDLERRLKAQSPNNTSC
Exon 7
Quail
Canine
Porcine
Bovine
Murine
Rat
Human

Phase I and II were compared using calculations of COIL, for a window of 28 amino acids, assuming that each phase is continuous over the extent of the sequence encoded by exon 7. To analyze this data the COIL algorithm was modified because the original algorithm attaches a dominant negative predictive effect on windows that contained proline or tryptophan at particular heptad positions. Proline at position "b" (βP91, Phase II) and "f" (βP91, Phase I) has a relative frequency, R_f 0.008 and 0, respectively while tryptophan at position "c" (βW123, Phase I and βW141, Phase II), "f" (βW123, Phase II) and "g" (βW141, Phase II) have R_f 0 (Lupas et al., 1991) (Fig. 3.4). In the modified algorithm the contribution of these to computation of the geometric mean has been eliminated by assigning them a relative frequency of one and reducing the degree of the root of the product of the relative frequencies for each of these present within the given window. The single non-conserved proline is present at the amino teminal end of the helix encoded by exon 7 and is predicted to occur within the first helical turn, a position in which it is "permitted" without disrupting regular helical geometry. It is somewhat more arbitrary to ignore tryptophan. However, the relative frequency statistics which COIL uses is based on a data set limited to the single coiled-coil structural class represented by the α filamentous proteins. While there are shared structural properties with other coiled-coil classes (Cohen and Parry, 1986; Lupas et al., 1991) there are also differences reflected at all structural levels. For example, the four helix coiled-coil of the 22 kDa N-terminal thrombolytic fragment of apolipoprotein E3 contains three tryptophans within the first helix (Wilson et al., 1991). This suggests that the singular absolute injunctions imposed by COIL on tryptophan may not be appropriate for the analysis of clusterin. Fig. 3.2C shows that for both phases I and II for the

sequence encoded by exon 7 in human clusterin using a window size of 28 there is a single broad peak of relatively high COIL scores, although phase I is clearly favored in the N-terminal half and phase II in the C-terminal half. Using a COIL score cut off of 1.24 (probability of approximately 0.1), phase I predicts a continuous coiled-coil helix extending from βT88 to βN140 (7.5 heptads) (315 to 367 in Fig. 3.2C) while phase II predicts one extending from βN89 to βL148 (8.5 heptads) (316 to 375 in Fig. 3.2C). For contrast a distinct third phase has lower scores more typical of "globular" proteins (Fig. 3.2C). These results indicate that either phase I or II represents plausible continuous coiled-coil amphipathic α helices over much of the extent of the segment encoded by exon 7 when the preferences of all heptad positions are considered.

Of the other predicted amphipathic helices (Tsuruta et al., 1990) (Fig. 3.1) only that in the α chain encoded by exon 5 and specifically in the quail (αV129 to αL172; 155 to 198 in alignment of Fig. 3.2A) is there a high predicted probability of forming such a helix. The heptad phase of the quail sequence is predicted to be continuous over this extent. For all other species the corresponding segment has very low probability (< 0.1). This difference is due in large part to the very large number of substitutions of charged amino acids in the quail for neutral amino acids that are neither highly polar or non-polar in the mammalian sequences, and the strong statistical preference for charged amino acids at these positions in the α filamentous proteins (Lupas et al., 1991).

1.1.3. Analysis of clusterin structure using helical nets

The presentation of amphipathic α helices as helical nets (Lim, 1978) facilitates

visual analysis of important structural features including the distribution of polar and non-polar residues particulary in long helices. In the helical net method the helix is visualized as a cylinder whose axis is colinear with the helical axis and with the amino acid side chains projected on the cylinder surface at the point corresponding to that of the C_α atom in a regular, ideal α helix. The cylinder is cut along the surface parallel to the axis and "flattened" into two dimensions. Panel A of Fig. 3.5 shows this presentation for the segments αS139 to αD171 and βS1 to βF40 (human) and the corresponding sequences from the quail, which displays the greatest divergence in identity from the better conserved mammalian sequences (Fig. 1.1). These are compared to helical net presentations of the α helices encoded by exon3/4 and 7 (Fig.3.5B). Of the former, two shorter sequences, one in each chain, have a conserved structure consistent with formation of an amphipathic α helix. These are identified visually as extending from αH152 to αD171and βN12 to βS36 and correspond in large part to those identified previously using helical wheels (de Silva et al., 1990a). There are some interesting similarities between the predicted properties of these helices that contrast with the properties of those predicted for the helices encoded by exon 3/4 and 7. The predicted length for each is similar (23 and 26 amino acids for α and β chains, respectively), roughly half the size of the predicted coiled-coil helices. The exon 5 encoded helices have wide predicted non-polar faces subtending an angle perpendicular to the helical axis of approximately 150° and are aligned with the helical axis (Fig. 3.5A). In contrast, typical of the coiled-coil, the non-polar face for exon 3/4 and exon 7 encoded helices is narrow subtending an angle perpendicular to the helical axis of 50° to 100° and is inclined at an angle of about 20° to the helical axis (Fig. 3.5B). In addition, the polar and

Figure 3.5. Helical net diagrams of predicted clusterin amphipathic α helices

A. Human clusterin sequences αS139 to αD171 and βS1 to βF40 and the corresponding quail sequence based on the multiple species alignment (Fig. 1.1) corresponding to the exon 5 amphipathic α helices (Tsuruta et al., 1990) depicted as helical nets (Lim, 1978). Hydrophobic amino acids (L,V,I,M,F,Y,W) are shown in blue. Boxed areas delimit the non-polar faces of the predicted amphipathic α helices. Exon 5 encoded amphipathic α helices are estimated visually to extend from αH148 to αD171 (Human) and βN11 to βH36 (Human). Numbering is relative to the mature N-termini of α and β chains of human and quail clusterin.

B. Coiled-coil amphipathic α helical predictions for human clusterin αS17 to αL76 and β N90 to βT149 chains are depicted as in A. The coiled-coil amphipathic α helices are aligned in antiparallel orientation on the basis of alignment of the αC80 and βC86 disulfide (arrangement II, Fig. 3.4). Numbering is relative to the mature N-termini of α and β chains of human clusterin.

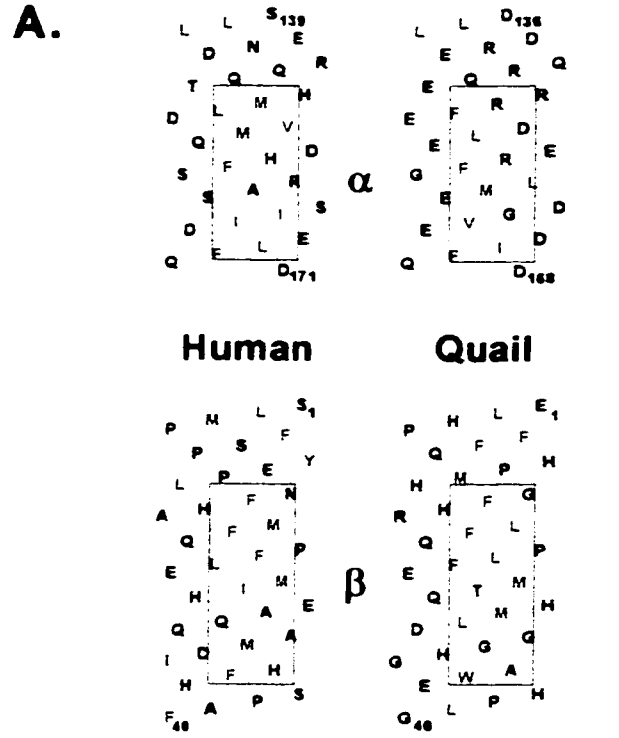
A.
α
Human
Quail
β
B.
Human α
Human β

non-polar faces of exon 5 encoded helices have similar amino acid compositions, conserved among species and contrasting with the compostions of the coiled-coil helices. These include higher compositions of methionine and phenylalanine in the non-polar faces. In the polar faces histidine is relatively abundant and the acidic amino acids, aspartate and glutamate predominate over arginine and lysine.

The differentiation of amphipathic helices predicted by COIL and the helical net analysis is especially interesting in relation to the linear antiparallel model of clusterin structure as it correlates with the spatial distribution of helical pairs implicit in the model (Fig. 3.1). While the putative exon 5 encoded helices as redefined above are not quite colinear in this model those encoded by exon 3/4 and 7 are nearly precisely colinear (Fig. 3.6). The possibility that the latter may pair specifically to form an antiparallel α helical coiled-coil was explored further. To obtain a "knobs" to "holes" packing of the hydrophobic "a" and "d" residues of two antiparallel right handed α helices the "a" residue of one helix must be aligned and paired with the "d'" residue of the other helix and vice versa, in contrast to the more frequently observed parallel coiled-coil in which "a" and "a'" and "d" and "d'" residues align and pair (Monera et al., 1993; Monera et al., 1994) (Fig. 3.3). Given the single continuous heptad phase relationship predicted by COIL for the exon 3/4 encoded helix and the two phases suggested for exon 7 encoded helices there are a number of possible relative arrangements, which satisfy the above condition. However, of these, two arrangements are most attractive as they are permissive to maintenance of the close spatial proximity of the nearby αC80 and βC86 linked as an interchain disulfide pair. These two arrangements are designated I and II according to the

heptad phase relationship for the exon 7 encoded helix (Fig. 3.5). The former requires that αC80 and βC86 be staggered by three residues but would allow alignment of downstream disulfide pairs, αC91and βC78 and αC94 and βC75. The latter results in alignment of αC80 and βC86, but requires staggering of the downstream pairs. Significantly, both arrangements represent the maximum possible overlap of the COIL predictions in each chain for each predicted phase of the exon 7 encoded helix. Arrangement II obtains a larger possible overlap of predictions than I (8.5 vs 6.5 heptads) constituted of αS17 to αL76 and βN90 to βN149 (Fig. 3.5). It is interesting that if one assumes a regular helical geometry to extend to αC80 and βC86 in either arrangement these amino acids are predicted to be interfacial, compatible with the formation of a disulfide bond.

Since the structure of clusterin appears to reflect some of the main features of the linear antiparallel model, I hypothesized that clusterin may be constituted by multiple, possibly independently folding structural and/or functional domains. Using the model as guide leads to the suggestion that there are three or four such domains (Fig. 3.6). The disulfide bonds formed between the cysteine rich sequences of exon 4 and exon 6/7 may represent one such domain (Domain 2b), while the putative antiparallel α helical coiled-coil may represent another (Domain 2a). Alternatively, since exon 4 encodes part of the α chain coiled-coil amphipathic α helix and exon 7 encodes part of the β chain cysteine rich domain, this suggests that Domain 2a and Domain 2b represent a single domain ancestrally encoded by a single exon in each chain that was subsequently assymetrically bisected with an intron at different relative points in each. Since in the model, exon 8 has

Figure 3.6. Correspondance of redefined amphipathic α helices with the genomic structure and proposed domain structure of clusterin

Human clusterin α and β chains are presented as given in Figure 3.1. Predicted coiled-coil amphipathic α helices are shown in blue. Predicted exon 5 encoded amphipathic α helices are shown in green. Numbers in corresponding colors denote the boundaries of the respective sequence elements and are given relative to the N-termini of the mature α and β chains. A four domain structure is proposed for clusterin. Segments of clusterin α and/or β chains proposed to interact physically and\or functionally are denoted by boxes with broken lines in distinct colors corresponding to the defining structural element in each and/or defined by coding exons. The putative coiled-coil α helical domain (blue) and disulfide domain (yellow) are designated 2a and 2b respectively, to reflect the possibility that both elements together consitute a single antiparallel symmetry domain. Exon 5 encoded amphipathic α helices (Domain 3) are proposed as binding sites for hydrophobic ligands. Grey boxes correspond to synthetic peptides in each chain that inhibit the interaction of clusterin with $A\beta_{1-40}$. The proposed LRP2 and\or heparin binding site lies in the α chain coiled-coil helix.

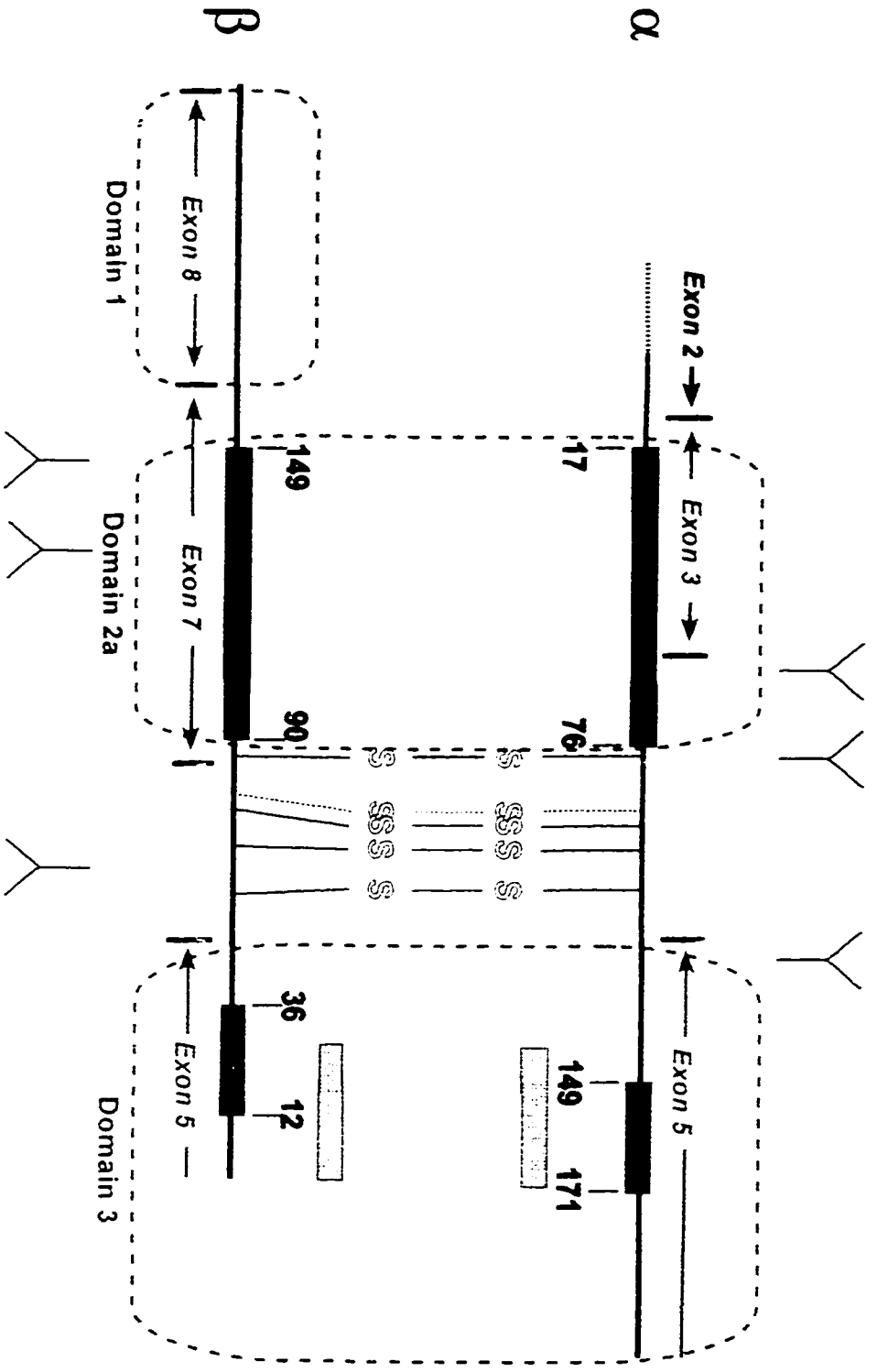
β
α
Exon 8
Domain 1
Exon 2
Exon 3
149
17
Exon 7
Domain 2a
90
76
36
12
Exon 5
Domain 3
149
171
Exon 5

no implied α chain structural partner it may encode an additional domain (Domain 1), while Exon 5 may also encode an independent domain (Domain 3).

1.1.4. Transverse urea gradient gel electrophoresis of clusterin

The existence of independently folding domains in proteins can manifest itself as multiple phases in the denaturation/renaturation profiles. One method for obtaining such profiles is transverse urea gradient electrophoresis (Creighton, 1979; Goldenberg, 1989), which was used to search for evidence of a domain structure in clusterin. In this method the electrophoretic mobility of a protein is obtained as a function of a linear, continuous change in the concentration of urea, and relatively sharp discontinuities in this mobility are interpreted as changes in effective hydrodynamic volume occasioned by unfolding and refolding events. Non denatured immunoaffinity purified human plasma clusterin runs at the lowest urea concentrations predominately as a single slightly diffuse Coomassie Blue stained band (Fig. 3.7). Several other bands with lower mobility, including a significant amount of stained material that was present at the gel origin, were also observed. The major band is presumed to be monomeric, while the slower migrating forms are probably aggregated forms and/or glycoforms with lower degrees of sialyation (Kapron et al., 1997). Increasing urea concentration results in a separation of the predominant band into three bands designated 1, 2, and 3. On the basis of staining, the slower migrating bands 1 and 2 represent the majority while a proportionally smaller amount is represented by the faster migrating band 3. Electrophoresis of human plasma clusterin on native 4 to 22% linear gradient polyacrylamide gels also resolves three bands with the same separation and relative abundance (data not shown). Moreover, two major

Figure 3.7. Transverse urea gradient gel electrophoresis of human clusterin

36 μg each of immunoaffinity purified human clusterin was treated with (Denatured) or without (Native) 7 M urea in 50 mM Tris-25 mM boric acid pH 8.7 at room temperature and separated on 0 to 8 M urea transverse, continuous linear gradient gels with an inverse linear gradient of 15% to 11% T polyacrylamide in the same buffer and fixed and stained with Coomassie Blue.

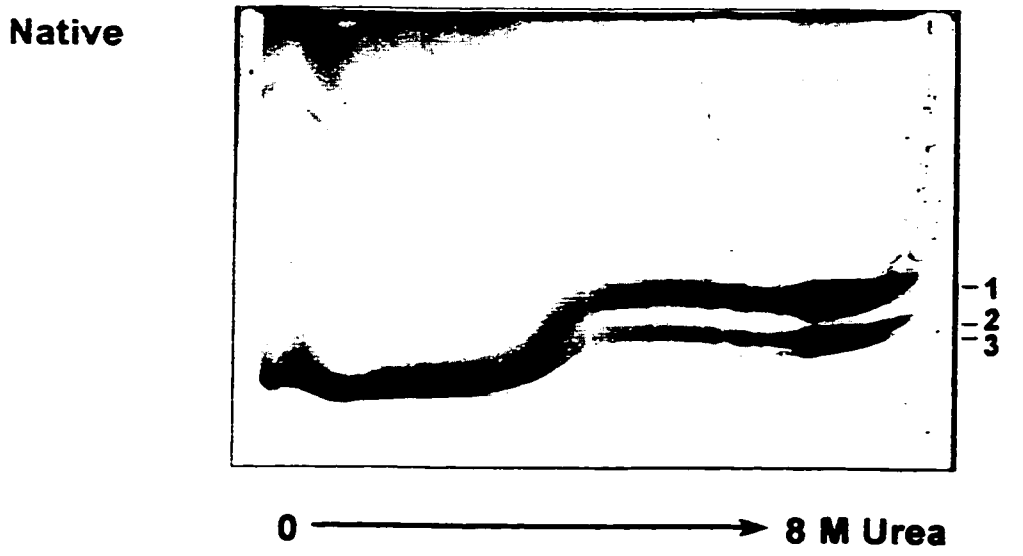
Native
1
2
3
0
8 M Urea

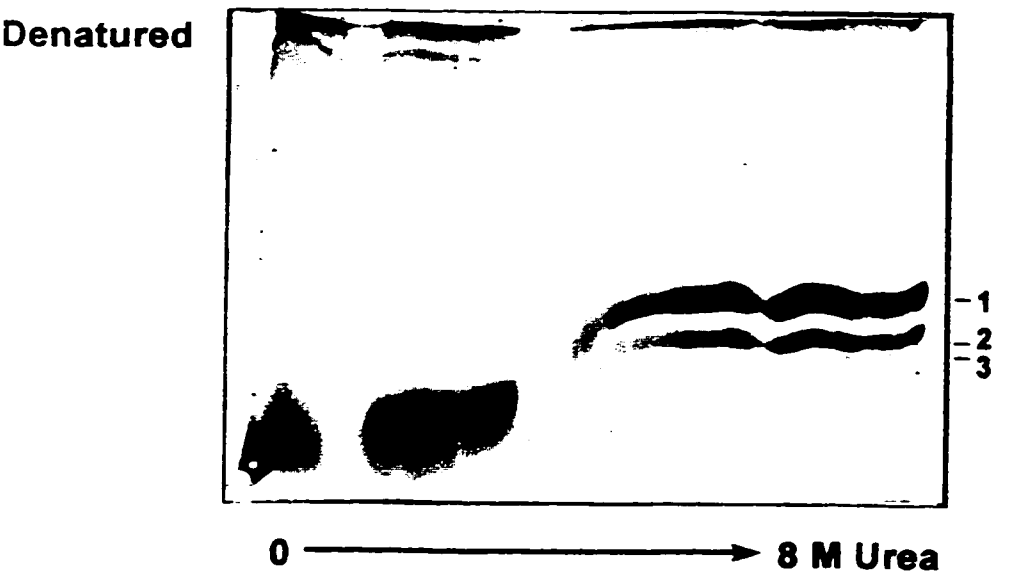
Denatured
1
2
3
0
8 M Urea

mass isoforms of the human plasma clusterin dimer have recently been detected using MALDI-TOF mass spectrometry (58.5 and 63.5 kDa), and of the purified α and β chains, one mass isoform of the β chain (32.8 kDa) and three mass isoforms of the α chain (24.2, 26.5, and 31.4 kDa), with the two largest of greatest abundance (Kapron et al., 1997). Thus bands 1, 2, and 3 probably represent monomeric clusterin isoforms differing in N-linked carbohydrate associated with the α chain. Between 3 to 5 M urea a sudden continuous decrease in mobility is seen for all three bands, suggesting an unfolding transition. The degree of change in mobility follows the order of band separation at urea concentrations below 3 M. Band 1, which shows the largest change in mobility is the first to separate from the original band present at low urea concentrations. This is followed by band 2 and finally band 3 which display intermediate and the smallest changes in mobility, respectively. No further mobility transitions are evident over concentrations of urea ranging from 5 to 8 M urea.

The same preparation of clusterin, denatured in 7 M urea prior to electrophoresis (Fig. 3.7) in large part recapitulates the pattern of native clusterin. At urea concentrations above 5 M the relative mobility and abundance of bands 1, 2, and 3 is essentially the same as seen using native clusterin. Over the range of 3 to 5 M there is an abrupt continuous increase in electrophoretic mobility to faster migrating forms suggesting a refolding transition. However, in this case bands 1, 2, and 3 do not converge to a single migrating species at urea concentrations less than 3 M. The observation of a continuous band of rapidly varying electrophoretic mobility in the region of the sharp transition with or without prior denaturation is compatible with a rapidly reversible, two state model of

urea induced denaturation (Creighton, 1979). There is however no indication at the resolution of this experiment that this large change in mobility contains any fine structure suggestive of a multiphasic renaturation/denaturation process.

1.4. Discussion

1.1.1. Implications of antiparallel coiled-coil structure

Application of the COIL algorithm using a window size of 28 predicts that of the amphipathic α helices previously identified (Tsuruta et al., 1990) only those encoded by exon 3/4 and 7 have a conserved probability of forming a coiled-coil α helix. Those helices identified in the sequences encoded by exon 5 (Tsuruta et al., 1990) show no such conserved probability. This distinction appears to have been evident in the original myosin homology studies but was ignored (Tsuruta et al., 1990). In this study the helices encoded by exon 3/4 and 7 display much longer and more significant homology to the multiple repeats of the tail domain of myosin, while those encoded by exon 5 showed shorter and more punctuated homology. The possible significance of this distinction is suggested by a simple two dimensional model of clusterin structure in which the chains are drawn to scale as antiparallel lines aligned with respect to the first known interchain disulfide pair (αC80-βC86). In this simple presentation exon 3/4 in the α chain and exon 7 encoded helices in the β chain overlap spatially. This suggests that α and β chain structural symmetry extends beyond the cysteine-rich domains and might reflect a physical pairing of these two helices in the form of an antiparallel α helical coiled-coil. The relation of the primary structure of amphipathic α helices of the coiled-coil type to their secondary structure and the mutual "knobs" to "holes" pairing of hydrophobes at the

tertiary structural level is comparatively well understood. In addition, constraints imposed by the fact that the cystine halves of the proximal disulfide pair on each chain of clusterin must be near each other leads to a small number of proposed specific helical pairings. A pairing with the proximal half cystines "staggered" (I) by three residues is suggested by the heptad phase prediction of COIL for exon 3/4 and phase I for exon 7 encoded helices and a pairing with these proximal half cystines "aligned" (II) is suggested by the prediction of phase II for the helix encoded by exon 7. The "aligned" arrangement stands out since it provides the largest possible overlap of the COIL predictions for each chain. The limits of the coiled-coil domains may be dictated by the non conserved αP77 and βP91 (human) as a result of its known disruptive effects on regular helical geometry. The other end of this domain has no such suggestive landmark, however, the conservation of "a" and "d" hydrophobes, the predictions of COIL, and the length of the exons, suggest that both the putative α and β coiled-coil amphipathic α helices may extend 6.5 to 8.5 continuous heptads. A tentative proposal for the boundaries of this coiled-coil domain is from αS17 to αL76 and βN90 to βT149 (Fig. 3.6). Collectively, based on the congruence of predicted amphipathic α helical type, length, heptad phase relation, and spatial relation to the first disulfide pair, the proposed formation of an antiparallel coiled-coil α helical pair is compelling.

The proposed coiled-coil may be considered as a rationalization of a number of "negative" structural features. In the multiple species alignment no proline is present at internal positions of the proposed coiled-coil helices (Fig. 1.1 and Fig. 3.6), a position where it would disrupt regular helical geometry and possibly compromise the proposed

helical pairing. Second, while alignment gaps are necessary at several positions in segments encoded by exon 5, and exon 8, and at the junctions of exons 5 and 6 and exons 7 and 8 there are no such gaps within either the cysteine rich domains or the coiled-coil helices in either chain (Fig. 1.1), consistent with the importance of conservation in the spacing of critical structural elements. In the putative coiled-coil domain, for example, most insertions or deletions would be expected to disrupt the phase relation of heptads preceding and succeeding it with likely detrimental effects on helical pairing. As another prediction of this model asparagines within the coiled-coil known to be modified by glycosylation should be localized to extra or juxtafacial positions in the heptad since such a modification to the relatively small asparagine side chain is likely to be sterically incompatible with burial in interfacial positions ("a" or "d"). N-linked glycosylation sites within clusterin are relatively well conserved, although there are several interspecies differences (Fig. 1.1). In human plasma clusterin there is one known site of N-linked glycosylation in the coiled-coil domain of the α chain (αN64) and two in the β chain (βN127 and βN147) (Kapron et al., 1997). In the rat, mouse, and bovine proteins there is another conserved N-linked glycosylation site at βN101 (rat corresponding to human βD101) and one in the porcine at βN89 (human βN90) which may or may not be used. Given the predicted heptad phases, only the porcine βN89 is in an interfacial position in phase II ("a" in phase II and "e" in phase I). The rest, including all those known to be modified, are in non interfacial positions. In phase I of the exon 7 encoded helix βN127 is juxtafacial ("e" or "g") and βN147 and βN101 (in rat, bovine, and mouse) is extrafacial ("b", "c", or "f") while the former two are extrafacial and the latter juxtafacial in phase II. αN64 is extrafacial.

At present there are few physical observations relevant to the question of clusterin structure generally and to the proposal of the coiled-coil structure specifically. A circular dichroic spectrum of human clusterin has recently been reported (Zlokovic et al., 1996b) and is typical of a protein with high α helical content compatible with the helical components of the coiled-coil. The formation of a long continuous coiled-coil in the central region of the protein may impart an elongate geometry to the protein compatible with sedimentation rates that are reportedly two fold lower than expect for a globular protein of similar size (Tsuruta et al., 1990).

The structure of disulfide and coiled-coil domains implies that covalent and non-covalent interactions between, rather than within the α and β chains, may be dominant in determining the overall structure and stability of clusterin. This suggests that other segments of α and β chains may fold and form (a) stable structure(s) on the basis of local interactions implied as being physically proximal in the linear antiparallel model (Fig. 3.6). It is interesting then that the sequences flanking the central disulfide/coiled-coil domain are encoded by distinct exons, and may constitute physically and/or functionally independent domains. The absence of α chain sequences that overlap those encoded by exon 8 in the model suggests that it may fold without mutually symmetrical interchain interactions. Exon 5 encodes sequences from both the α and β chains which overlap in the model, and may form a stable structure based on interchain interactions between these segments. The exon 5 encoded amphipathic α helices only partly overlap in the model, and while their structural similarity defines an additional symmetry between chains, there are no compelling circumstances, analogous to the coiled-coil domain, that would

suggest that pairing to the two helices results in mutual stabilization.

1.1.2. Implications of urea induced folding/unfolding of clusterin

We have looked for evidence of a multiphasic denaturation/renaturation profiles for human plasma clusterin on continuous urea transverse linear gradient gels as an indication of more than one independently folding domain. There is a large relatively well defined continuous change in mobility over a urea concentration range of 3 to 5 M whether or not clusterin is denatured with urea prior to electrophoresis. This is a pattern compatible with a model of a rapidly reversible transition between folded and unfolded states (Creighton, 1979). There is however, no convincing evidence of further distinct transitions at urea concentrations outside this range, and no indication of a fine structure to the large transition that would suggest a multiphasic process and the presence of more than one independently folding domain. It is possible that this experiment was not sufficiently resolving to identify more than one phase to the unfolding/refolding transition. Alternatively, under these experimental conditions domains may have similar stabilities or are not entirely independent but unfold/refold in a concerted manner. The rapid reversibility of the unfolding/refolding process, although not direct evidence of, is at least consistent, with urea induced separation of α and β chain amphipathic α helices in the coiled-coil. Rapid reversibility in unfolding/refolding of the coiled-coil might be expected given that the adjacent disulfide bonded domain should reduce the number of degrees of freedom in the search for the appropriate alignment of adjacent helices. Interestingly, rapid reversibility in folding is observed in model peptides that form antiparallel α helical coiled-coils in solution studied by incorporating a pair of cysteines

residues that form a disulfide bond at one end of the helical pair and that are in phase with the heptad predictions for each, identical to the structure suggested for clusterin (Monera et al., 1993; Monera et al., 1994). Rapid reversiblity in folding of these model peptides is thought to be due in large part to the alignment compelled by the disulfide bond.

1.1.3. Relationship of proposed structure to function of clusterin

Clusterin binds to a number of distinct ligands *in vitro* and *in vivo* including apoAI-HDL, terminal complement complex components, Alzheimers disease amyloid β peptides, serum paraoxonase, TGF β receptor type I and II cytoplasmic domains, streptococcal inhibitor of complement, immunoglobulins, LRP2, and heparin (Chapter 1). Several of these ligands, in particular apoAI-HDL, terminal complement complex components and amyloid β peptides, have hydrophobic/amphipathic domains. Because segments of clusterin could be modeled as amphipathic α helices it has been suggested that the non-polar faces of such helices could be functional in these interactions (de Silva et al., 1990a; Tsuruta et al., 1990). This suggestion is also supported by some biochemical studies. Thus, clusterin apoAI-HDL complexes are reportedly dissociated by non ionic detergents (Jenne et al., 1991). Clusterin inhibits complement dependent hemolysis at the level of C7 addition to C5b6 and binding to target membranes (Jenne and Tschopp, 1989; Murphy et al., 1989) and incorporates into the soluble terminal attack complex at the level of C7 (Choi et al., 1990). Thus, clusterin may bind to the membrane binding site of metastable C5b-7 rendering it soluble. Clusterin also inhibits the formation of insoluble aggregates of $A\beta_{1-42}$ *in vitro* (Oda et al., 1994; Oda et al., 1995;

Matsubara et al., 1996), suggesting that it might bind to a hydrophobic domain necessary for aggregation.

The pairing of coiled-coil amphipathic α helices encoded by exon 7 and exon 3/4 suggested here, predicts that the non-polar faces of these helices are mutually buried and do not participate in interaction with hydrophobic/amphipathic ligands, in contrast to an earlier suggestion (Jenne and Tschopp, 1989). Thus, the amphipathic α helices in each chain encoded by exon 5, may be more likely candidates. This is supported by the observation that a disulfide linked lysylendopeptidase-C fragment of human plasma clusterin consisting largely of exon 5 [α(Q97 to K200):β(S206 to K277)] binds to $A\beta_{1-40}$ and synthetic peptides that correspond to the putative exon 5 encoded helices in the α and β chains inhibit the interaction of the heterodimer with $A\beta_{1-40}$ (Choi-Miura et al., 1994) (Fig. 3.6). The capacity of both the α and β chains to independently inhibit the interaction of the heterodimer with the cytoplasmic tail of the TGF β type II receptor (Reddy et al., 1996), denatured C9, and to inhibit terminal complement dependent hemolysis (Tschopp et al., 1993) has also been proposed to be due to exon 5 encoded amphipathic α helices in both chains. However, beyond sharing an amphipathic structure it has not been previously appreciated, as described here, that these helices are similar in structure, including length, size of non-polar face, and amino acid composition. It is possible that amphipathicity alone is not sufficient for the observed functional symmetry, but that it reflects, at least in part, these specific structural similarities.

The implication that the interaction between clusterin and several ligands appears

to be hydrophobic has suggested to some that clusterin may have a promiscuous binding site for hydrophobic/amphipathic ligands with little discernable structural specificity. In this regard the conserved presence of methionine residues (Fig. 3.5) in the non-polar faces of these helices, among the different species is perhaps significant. Methionine, in the methionine rich (M) domain of signal recognition particle protein 54 has been suggested as the ideal amino acid for sequence/structure independent recognition of a hydrophobic surface (Bernstein et al., 1989). The long, unbranched non-polar side chain of methionine and the nature of its sulfur-carbon bond results in a relatively high degree of conformational flexibility that may be uniquely adaptive to a potentially wide variety of differently shaped hydrophobic surfaces (Bernstein et al., 1989; Gellman, 1991). Additionally, it has been proposed that the relatively high polarizability of the sulfur atom in methionine may allow it to contribute significantly to the binding energy through greater attractive dispersion forces (Gellman, 1991). Thus, it is possible that the methionine residues in exon 5 helices of clusterin may play a similar role in adaptive recognition in the binding to a number of ligands with structurally distinct hydrophobic domains.

Another interesting amino acid within or near to the helices encoded by exon 5 is histidine. There is a higher density of histidines in sequences encoded by exon 5 than in any other exon (Fig. 1.1). 11 of the 13 histidine residues in human clusterin are encoded by exon 5 (with one each in exons 6 and 8). While there is no conservation in position or content of histidine in, or proximal to, the amphipathic helix in the α chain, in the β chain there are 3 to 5 histidines between βL11 to βP38 (human), including βH14, which is the

only one absolutely conserved in the species alignments, and βH25 that is conserved in position in all the mammals and may be conserved in the alignment as the next amino acid in the quail, βH26. These latter are predicted to lie at the polar/non-polar interface of the helix (Fig. 3.5). The proximity of histidines to the putative clusterin ligand binding site suggests that ionization of histidine, at acidic pH, may influence the ligand binding properties of clusterin. Clusterin is localized *in vivo* in biological contexts associated with a constitutive or induced local acidosis such as sites of tissue injury, which may become significantly acidic (pH 5.5-6) (Punnia-Moorthy, 1988), and epididymal fluid (pH 6.5-6.8) (Hinton, 1995). It is possible that histidine ionization may represent a physiological mechanism by which clusterin activity is modulated. Alternatively, many of these histidines are close to the site of endoproteolytic maturation of α and β chains and may play some role in regulation of protein trafficking and/or maturation in acidic (pH 5) post-Golgi secretory compartments (Darnell et al., 1986).

Tentative localization of the hydrophobic binding site to sequences proximal to the site of limited proteolysis between αR205 and βS1, also suggests a possible relation of this event to activity. It has recently been reported that purified unprocessed human plasma clusterin has one hundred times the complement dependent inhibitory hemolytic activity of the processed form (Personal Communication, Dr. Judith Harmony) suggesting that proteolysis may have functional significance and that this relationship deserves greater attention in defining the structural basis of clusterin function.

Not all clusterin ligands are likely to bind on the basis of hydrophobic

interactions. Studies of other proteins with affinity for heparin and LRP2 suggest that the physicochemical basis for these interactions is largely electrostatic, between a cationic domain of the former and anionic groups of the latter (Weisgraber, 1994). Binding of heparin is in large part dependent on interactions between anionic sulfate and carboxylate groups on the polysaccharide and basic side chains of the protein (Cardin et al., 1991; van Boeckel et al., 1991; Margalit et al., 1993). To date, there is no high resolution 3D structure of a complex between heparin and a heparin binding domain that would serve as a paradigm for specific interactions between clusterin and heparin. However, heparin binding domains that have been mapped feature a spatial clustering of basic residues. In apoE, the heparin binding domain is present in a long 35 residue amphipathic α helix embedded in a four helix coiled-coil and features a solvent exposed face rich in basic residues (Weisgraber, 1994).

LRP2 contains multiple copies of two types of cysteine rich repeats in its extracellular domain : growth factor and LDL receptor ligand binding repeats (Saito et al., 1994). In the N-terminal ligand binding repeat from the LDL receptor the six conserved cysteines form three intramolecular disulfide bonds and the typical cluster of acidic residues present at the C-terminus presents an acidic face in the 3D structure (Daly et al., 1995). The binding of a number of ligands to LRP and other members of the LDL receptor superfamily is consistent with the importance of positive charges contributed by basic residues of the ligand, and it has been proposed that electrostatic interactions between basic residues of the ligand and acidic residues of the ligand binding repeats play an important role in the binding interaction (Weisgraber, 1994). In LRP2, the apoE

ligand binding domain has recently been mapped to the second cluster of eight tandem LDL receptor ligand binding repeats (Orlando et al., 1997). ApoE is a competitive inhibitor for the binding of clusterin to LRP2 suggesting that they share the same binding site on LRP2 (Kounnas et al., 1995). In apoE, the LDL receptor binding site overlaps the N-terminal heparin binding site in the basic rich sequences of helix 4 (Weisgraber, 1994).

The hydrophilic face of the predicted antiparallel, amphipathic, α helical coiled-coil domain of clusterin may harbor the binding site for both heparin and LRP2. This domain contains a large number of basic amino acids and their presentation in the context of an extended helix(ces) in the context of a coiled-coil is notably similar to apoE. It has been suggested that binding of heparin to basic residues presented on an α helical structural scaffold could occur with the long dimension of the polysaccharide colinear with the helical axis (Margalit et al., 1993).

The predicted clusterin α chain coiled-coil amphipathic α helix has a higher density of basic residues than that of the β chain suggesting that most, if not all, of the residues implicated in heparin and/or LRP2 binding might reside in the α chain (Fig.3.8). This is consistent with the observation that only the reduced and alkylated α chain is retained on a heparin affinity matrix (Pankhurst et al., 1997). In the folded structure, however, it is possible that basic residues of the β chain also form salt bridges with the heparin and/or LRP2 acidic residues. There are between 13 and 15 basic residues and between 10 and 12 acidic residues in the interval αS17 to αL76 (human) among the species homologs with seven of the basic residues positionally conserved in sequence

Figure 3.8. Distribution of lysine\arginine in α chain coiled-coil amphipathic α helices

Corresponding segments of the α chain coiled-coil amphipathic α helix of the human (S17 to L76), bovine (S14 to S73), and quail clusterin sequences (S14 to K73) as given by the multiple species alignment (Fig. 1.1), are depicted as helical nets. Basic amino acids (K,R) are in red. The boxed area delimits all residues lying within or at the edge of the same 180° face ("d", "b", "e", and "f") in relation to the non-polar face. Overall the quail sequence contains the fewest basic residues in this boxed, basic rich face while the bovine sequence, particulary at the N-terminus, the most. As proposed this basic face may be a heparin and\or LRP-2 binding site. The human β chain coiled-coil amphipathic α helix (N90 to T149) is shown in antiparallel orientation for comparison.

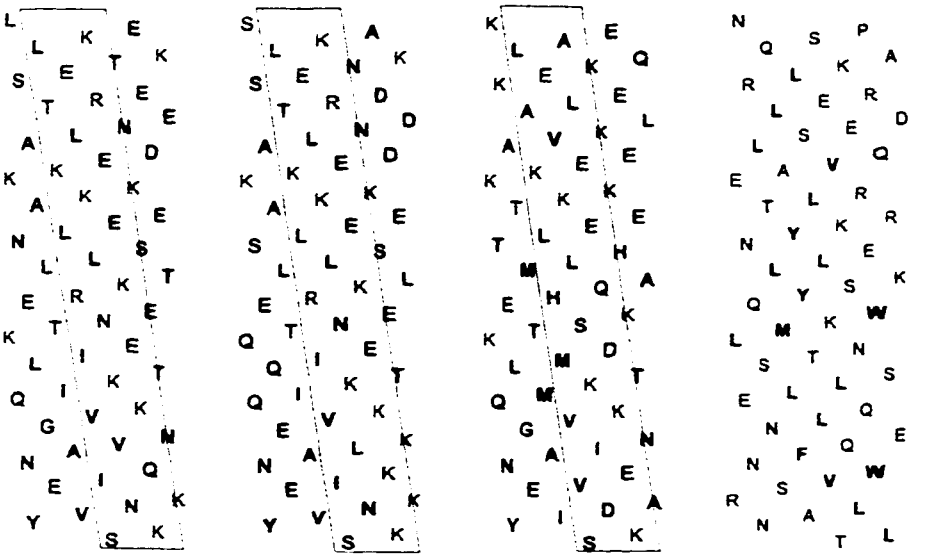

Human α Bovine α Quail α Human β

alignments. There is however, a relatively conserved and apparently non random radial distribution of basic residues observed in this segment when analyzed using helical nets, taking into account the presumed position of the non-polar face (Fig. 3.8). These basic residues are located predominatly on the face of this helix defined by heptad positions "a", "b", "e", and "f" (boxed area, Fig. 3.8) and although they are not positionally conserved in linear alignments, there is a reasonable conservation in distribution of basic residues in this face along the length of the helix. Owing to the geometry of a regular helix, lysines linearly separated in alignments by ±3 residues are on adjacent turns of the helix and on the same face. Given the long, unbranched, flexible side chain of lysine this positioning in space may represent some degree of functional conservation. This is consistent with the extended dimension of this basic face and on this basis suggests that it is a reasonable candidate for the heparin and/or LRP2 binding domain of clusterin.

It is thus likely that there are at least two ligand binding sites on clusterin; what might be a promiscuous hydrophobic/amphipathic ligand binding site and a cationic domain for the interaction of clusterin with heparin and/or LRP2. That these sites are physically distinct is supported by the recent observations that the interaction of $A\beta_{1-40}$ with LRP2 is clusterin dependent (Hammad et al., 1997) and that preformed clusterin $A\beta_{1-40}$ complexes are capable of being bound and internalized by a receptor immunologically related to LRP2 (Zlokovic et al., 1996b; Hammad et al., 1997). This supports a role for clusterin as an adaptor for targeting of specific ligands to LRP2.

1.5. Summary

This chapter develops a structure-function model of clusterin. This represents the most detailed and specific model yet developed and it is anticipated that it will serve as a guide in the design of experimental approaches to questions of structure and function. The model contains two major proposals:

1. Structural symmetry in the α and β chains, present in, and reflected by, the pattern of disulfide bonding between the respective cysteine rich domains, can be extended outside this domain. Exon 3/4 and exon 7 encoded amphipathic α helices in α and β chains are modeled as an antiparallel α helical coiled-coil with a very specific pattern of association based on presumed constraints introduced by known chain topology and the pattern of disulfide bonding. Exon 5 encoded amphipathic α helices in both α and β chains are noted to be structurally similar but the structure of their association, if any, is unknown. When related to a two dimensional model of clusterin structure in which the α and β chains are presented as fully extended antiparallel lines aligned by interchain disulfide bonds the colinearity of these interchain symmetry relations compels the view that far from mere visual convenience, this model may actually reflect the physical pattern of interchain association. Thus, I have hypothesized a three to four domain model of clusterin structure. Disulfide linked clusterin is rapidly and reversibly denatured in urea but at the resolution of present experiments no evidence of multiphasic transitions, that might suggest such a multidomain model, are observed.

2. I have hypothesized that there are at least two ligand binding sites; a cationic

domain constituted of the hydrophilic face of the presumed antiparallel coiled-coil and specific for LRP2 and heparin, and a promiscuous binding site for hydrophobic/amphipathic ligands constituted of exon 5 encoded amphipathic α helices. Methionine in the non polar faces of these latter helices may be important for promiscuity, and ligand binding may be reversibly regulated by histidine ionization and irreversibly by partial proteolysis of αR205-βS1 during biosynthesis to generate the mature heterodimer.

CHAPTER FOUR

3. *Structure activity correlations in recombinant and plasma clusterin : Evidence for distinct binding sites for LRP2, complement C9, and* $A\beta_{1-40}$

3.1. Background and Objectives

In the previous chapter a model of clusterin structure and function was developed. In order to test and refine specific aspects of this model it is useful to develop a source of recombinant clusterin. An ideal source, in addition to producing sufficiently high levels of expression must also be otherwise identical to the natural protein in respect of structure and function. Clusterin is a secreted, proteolytically processed, heterodimeric disulfide bonded N-linked glycoprotein. To faithfully reproduce these complex patterns of post-translational processing we decided to express clusterin in an eukaryotic system. This chapter describes the structural and functional characterization of human clusterin expressed as a constitutively secreted recombinant protein in the methylotrophic yeast *Pichia pastoris*. While several of the more significant structural and functional hallmarks of human clusterin are reproduced in this organism, aberrant proteolysis of clusterin accompanying expression will likely limit the usefulness of this system. Nevertheless, characterization of this proteolysis and its association with specific deficiencies in binding to ligands, including $A\beta_{1-40}$, IgG, complement C9, and LRP2, may have important structural and functional implications for the model presented in the previous chapter.

This chapter also describes studies directed at testing aspects of this model using purified plasma clusterin. In particular, the effects of pH and N-carbethoxylation of histidines on ligand binding were studied to elucidate the importance of histidines and/or histidine ionization in regulation of clusterin activity. In addition, patterns of heterologous ligand competition assays were used to directly test for the possibility of

structurally distinct binding sites.

Collectively, these studies support important structural and functional aspects of the model. However, they also suggest the possibility of greater specificity in interactions with presumptive hydrophobic/amphipathic ligands than previously suspected. In particular, complement C9 may interact, not with exon 5 encoded amphipathic α helices, but at a distinct site and perhaps with a distinct physicochemical basis. The stability of clusterin-Aβ4 complexes may involve an electrostatic interaction between one or more ionized histidine residues on clusterin and one or more ionized acidic residues on Aβ4 peptides, in addition to hydrophobic interactions. If the interaction of clusterin with certain hydrophobic/amphipathic ligands is not generic it suggests that the physiological function(s) of clusterin may be specific, relating to interactions with specific ligands.

1.2. Results

1.2.1. Preparation and structural characterization of human clusterin

It was necessary to obtain clusterin as a purified preparation from natural sources, both to provide a standard to which the structure and activity of recombinant forms of clusterin could be directly compared, and for biochemical characterization in its own right. Human clusterin was chosen as the full length human cDNA had been cloned (Wong et al., 1994a), the majority of biochemical studies have been undertaken with the human protein, anti-human monoclonal antibodies were available with proven utility in immunoaffinity purification (Murphy et al., 1988) and an abundant natural source was readily available in serum or plasma (Jenkins et al., 1996).

In the course of these studies clusterin was purified from five independent preparations of freshly drawn venous blood from a single fasted (Preparations II, IV, and V; Table 4.1) or post-prandial (Preparations I and III) male volunteer. Human clusterin was purified from EDTA-plasma or serum on a monoclonal antibody sepharose immunoaffinity column, prepared using G7, a murine IgG_1 with high affinity for human clusterin under non-denaturing conditions (Murphy et al., 1988). To dissociate clusterin apoAI-HDL complexes prior to low pH elution, columns were washed with three to five volumes of 0.5% Triton X-100 in PBS (Jenne et al., 1991). The concentrations and purity of the preparations were estimated by amino acid analysis. The experimental compositions of individual preparations differed by an estimated 10 to 20% (average 15%) from the known composition, depending upon the preparation (Table 4.1). By RP HPLC non-reduced clusterin ran as a single peak, and reduced and carboxymethylated clusterin as two similarly sized peaks that were verified by N-terminal sequencing as the expected α and β chains (Kirszbaum et al., 1989)(data not shown).

Serum/plasma clusterin preparations ran predominantly as a single band of 68-70 kDa under non-reducing conditions (Fig. 4.1A, lane 5 and Fig. 4.1B, lane 8) and as a cluster of closely spaced bands at 37-39 kDa under reducing conditions on SDS polyacrylamide gels (Fig. 4.1A, lane 1 and Fig. 4.1B, lane 3). Western blotting with a cocktail of anti-human clusterin monoclonal antibodies G7 and 78E detected these same bands (Fig. 4.1A, lanes 2 and 6).

Treatment of human serum/plasma clusterin with N-glycosidase F, an enzyme

Table 4.1. Concentrations and composition of stock preparations of immunoaffinity purified human recombinant and serum\plasma clusterin

Preparation[a]	Amino Acid Analysis			Bicinchoninic Acid Assay
	pmol/μL ± SD; n[b]	μg/μL ± SD; n[b]	Mean % Dif. in Composition ± SD; n[c]	μg/μL ± SD; n= 3
I. Recombinant	114 ± 8; 8	5.69 ± 0.39; 8	14.7 ± 12.1; 15	10.28 ± 0.25
	106 ± 11; 6	5.31 ± 0.55; 6	19.9 ± 11.6; 15	
II. Recombinant	65 ± 7; 9	3.23 ± 0.33; 9	17.9 ± 16.5; 15	4.03 ± 0.20
	56 ± 3; 8	2.79 ± 0.16; 8	14.9 ± 12.7; 15	
I. Plasma	57 ± 4; 11	2.83 ± 0.21; 11	11.8 ± 13.4; 15	4.30 ± 0.07
	58 ± 5; 8	2.89 ± 0.23; 8	12.7 ± 8.5; 15	
	63 ± 4; 12	3.15 ± 0.19; 12	10.4 ± 13.2; 15	
II. Plasma	48 ± 3; 8	2.39 ± 0.17; 8	16.4 ± 14.8; 15	5.00 ± 0.14
	45 ± 5; 9	2.25 ± 0.23; 9	16.8 ± 14.0; 15	
III. Plasma	167 ± 14; 12	8.35 ± 0.69; 12	10.3 ± 7.9; 15	11.26 ± 0.09
	170 ± 14; 11	8.52 ± 0.68; 11	13.3 ± 14.0; 15	
	176 ± 17; 10	8.79 ± 0.85; 10	13.2 ± 8.3; 15	
IV. Serum	39 ± 3; 7	1.93 ± 0.14; 7	15.9 ± 12.5; 15	3.76 ± 0.06
	46 ± 3; 8	2.32 ± 0.16; 8	15.3 ± 11.8; 15	
V. Plasma	61 ± 3; 4	3.06 ± 0.14; 4	20.7 ± 16.9; 14	7.13 ± 0.09
	73 ± 9; 8	3.66 ± 0.44; 8	17.0 ± 9.8; 14	

[a] Human clusterin was independently prepared by immunaffinity chromatography from recombinant *P. pastoris* conditioned media supplemented with 1% (w/v) heat denatured casein, or from fresh EDTA plasma or serum as indicated.

[b] n, number of different PTH amino acids used to calculate mean and standard deviation. The estimate of concentration was the mean of 2 or 3 independent amino acid analyses. For each analysis the final estimate of concentration was based only on those specific PTH amino acids which gave concentration estimates ± 15% of the mean of concentration estimates from all PTH amino acids excluding cysteine, glycine, tryptophan, and in the case of preparation V. methionine.

[c] Mean and standard deviation of the values for all the amino acids (except those excluded in [b]) of the % difference between known and experimental composition as a proportion of the known composition.

Figure 4.1. 1D SDS PAGE of *P.pastoris* human recombinant and plasma clusterin with and without treatment with N-glycosidase F

A. Approximately 150 ng of immunoaffinity purified plasma clusterin (lanes 1,2,5,6) or recombinant clusterin prepared by ethanol precipitation from conditioned BMMY (lanes 3,4,7,8) were separated under reducing and non-reducing conditions on 12% and 11% SDS polyacrylamide gels, respectively and either stained with silver (lanes 1,3,5,7) or transferred to nitrocellulose and probed with α chain specific monoclonal antibodies G7 and 78E (lanes 2,4,6,8). The positions of molecular weight standards run in parallel are indicated.

B. Approximately 10 μg of recombinant clusterin (lane 1,2,5,7) or plasma clusterin (lane 3,4,6,8) prepared as in A. were denatured in SDS and treated with (+) or without (-) N-glycosidase F, separated under reducing or non-reducing conditions on 12% and 10% SDS polyacrylamide gels, respectively and stained with Coomassie Blue. Bands identified as 1 through 9 in lane 1 were electroblotted to PVDF membranes and subjected to N-terminal sequencing (Table 4.2). The positions of molecular weight standards run in parallel are indicated. The position of N-glycosidase F is given by the asterisk.

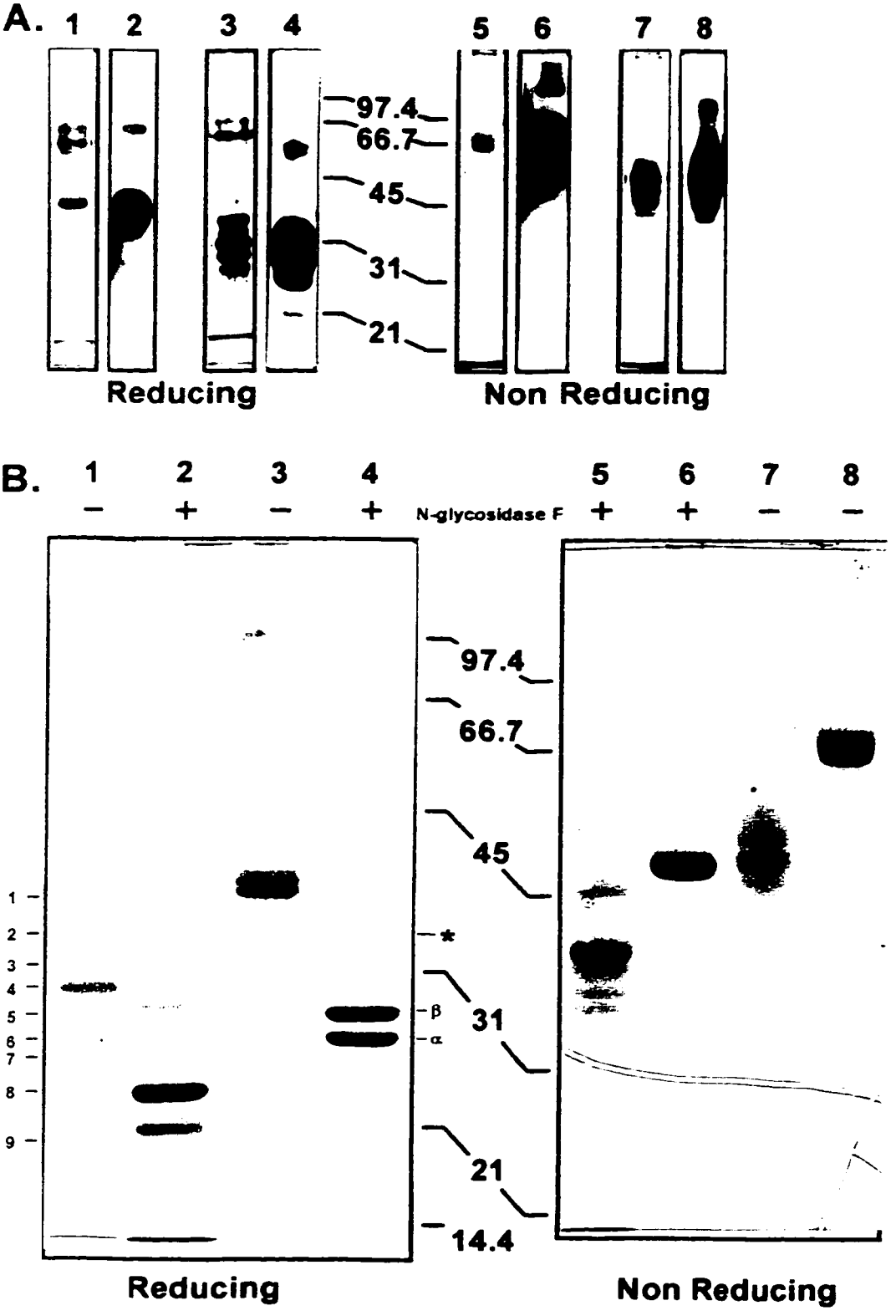
A.
1
2
3
4
5
6
7
8
97.4
66.7
45
31
21
Reducing
Non Reducing
B.
1
2
3
4
5
6
7
8
−
+
−
+
N-glycosidase F
+
+
−
−
97.4
66.7
45
*
β
α
31
21
14.4
1
2
3
4
5
6
7
8
9
Reducing
Non Reducing

that hydrolyzes all known peptidyl N-linked glycans, converted the 68-70 kDa band to primarily 48 kDa (Fig. 4.1B, lane 6). Under reducing conditions the 37-39 kDa bands were converted to two prominent bands, staining with equal intensity, at 28 and 26 kDa (Fig. 4.1B, lane 4). When N-deglycosylated preparations were separated under non-reducing conditions in the first dimension then reduced *in situ* and separated in the second dimension, the 48 kDa band in the first dimension dissociated predominantly to 28 and 26 kDa bands in the second (Fig. 4.2A). G7/78E, detected both the 48 kDa band under non-reducing conditions (Fig. 4.2B, bottom panel) and the 26 kDa N-deglycosylated band under reducing conditions (Fig. 4.2B, left panel). Thus, the 68-70 kDa band corresponds to the N-glycosylated disulfide linked clusterin heterodimer and the 37-39 kDa bands to the constitutive N-glycosylated α and β chains. The 48 kDa band corresponds to the N-deglycosylated form of the 68-70 kDa band and is a disulfide linked dimer of 28 and 26 kDa polypeptides. The 28 kDa N-deglycosylated band corresponds to the β chain (222 amino acids; calculated molecular weight 25,883 daltons) while the 26 kDa band corresponds to the α chain (205 amino acids; calculated molecular weight 24,197 daltons) as previously described (Burkey et al., 1991). The epitopes for G7 and 78E have not been previously described. These results suggest that on reducing Western blots G7 and/or 78E epitopes are localized mainly to the α chain.

In immunoaffinity preparations of human serum/plasma clusterin several other minor polypetides are consistently observed with higher protein loads by SDS PAGE. A number of these correspond to minor forms of clusterin and were detected by G7/78E. On long exposures of western blots under non-reducing conditions a band of approximately

Figure 4.2. 2D SDS PAGE of plasma clusterin treated with N-glycosidase F

A. 20 μg of immunoaffinity purified human plasma clusterin was treated with N-glycosidase F in the absence of reducing agents then separated by two dimensional non-reducing by reducing SDS PAGE as described in Methods and Materials and stained with Coomassie Blue. The positions of molecular weight standards run in parallel are indicated at the top and right for the indicated dimension. The left and bottom panels are one dimensional Coomassie Blue stained gels of 5 μg each of N-deglycosylated plasma clusterin separated under reducing and non-reducing conditions, respectively. The position of N-glycosidase F is indicated by an asterisk.

B. Reproduction of A. Boxed areas are processed disulfide linked heterodimers and unprocessed proprotein. Numbers external to these boxes indicate the relative molecular weight of the polypeptides in the associated dimension. Of the disulfide linked heterodimers (vertically colinear spots) only the full length α (26 kDa, blue) and β (28 kDa, red) have been identified. At the left and bottom panels are one dimensional Western blots as for A. above probed with monoclonal antibodies G7 and 78E. Lines show the estimated correspondance of the position of immunoreactive bands with the two dimensional gel. Short and long exposures are shown for the non-reducing Western blot (bottom). Note the doublet at about 94 kDa kDa evident in longer exposure of this blot.

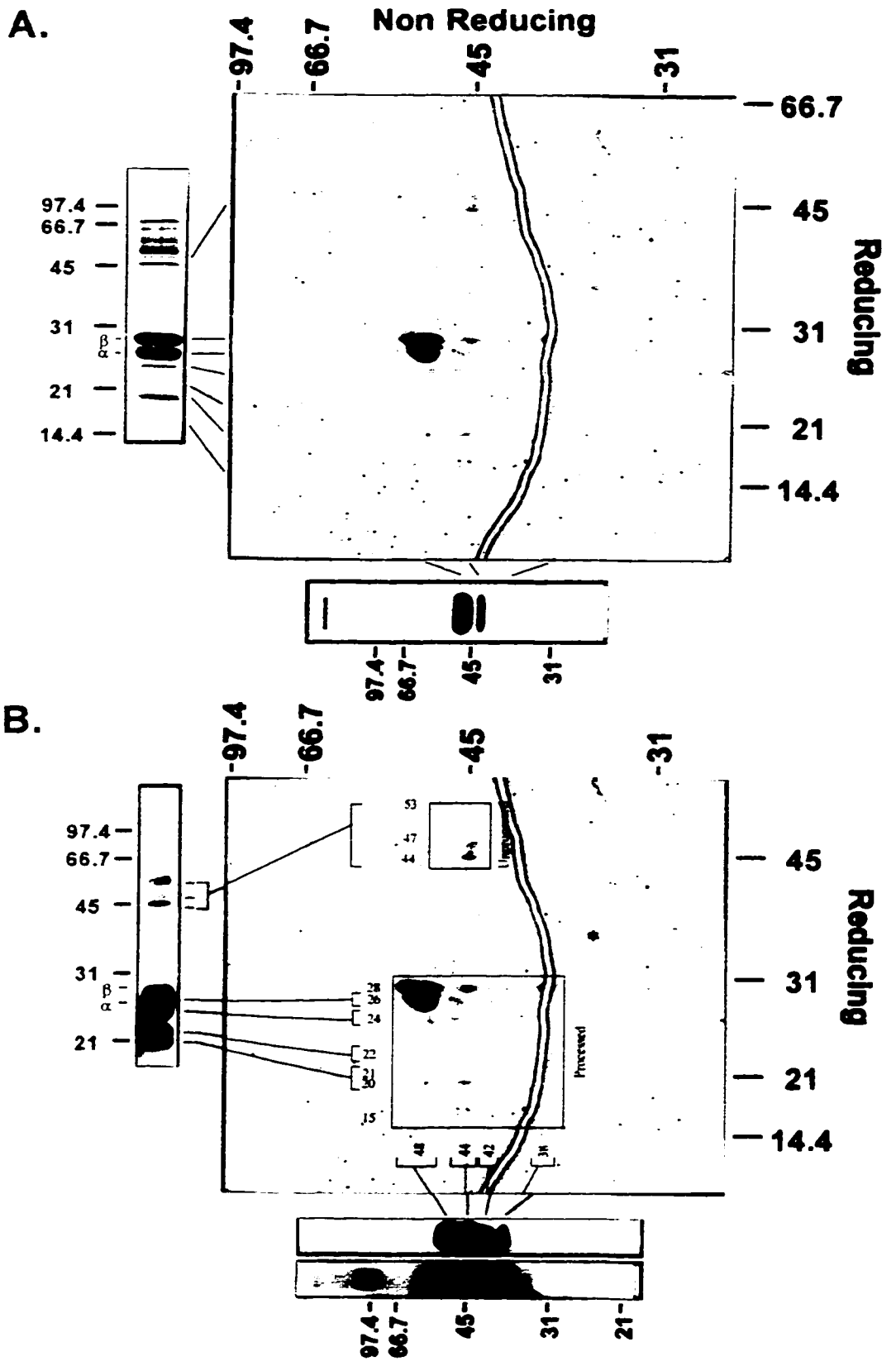
A.
Non Reducing
97.4
66.7
45
31
66.7
45
31
21
14.4
Reducing
97.4
66.7
45
31
β
α
21
14.4
97.4
66.7
45
31
B.
97.4
66.7
45
31
45
31
21
14.4
Reducing
97.4
66.7
45
31
β
α
21
Processed
97.4
66.7
45
31
21

148 kDa (Fig. 4.1A, lane 6 and Appendix, Fig. 6.3, fractions 13 to 15) may correspond to an immunoreactive doublet at about 94 kDa following treatment with N-glycosidase F (Fig. 4.2B, bottom panel) and may be a dimeric form of the clusterin heterodimer. Since this band is absent under reducing contions it is likely to be a disulfide linked form of this heterodimer. Under reducing conditions immunoreactive bands at 67 to 88 kDa (Fig. 4.1A, lane 2) are probably precursors to bands at 44, 47, and 53 kDa following treatment with N-glycosidase F (Fig. 4.2B, left panel) and are likely to be disulfide linked forms of the proprotein which have not been processed between the cysteine rich domains. After N-deglycosylation under non-reducing conditions minor new bands with a molecular weight less than 48 kDa, particularly at 44, and 38 kDa are apparent on both Coomassie Blue stained gels and western blots (Fig. 4.2A and B, bottom panels). Under reducing conditions minor N-deglycosylated bands of 24, 22, 21, 20, 16 and 15 kDa are observed on Coomassie blue stained gels (Fig. 4.2A, left panel) with 24 to 20 kDa bands immunoreactive with G7/78E and likely to be minor proteolytic derivatives of the α chain (Fig. 4.2B, left panel). On two dimensional gels the non-reduced bands in the range 44 to 38 kDa are constituted of a variety of clusterin forms in the reducing dimension (Fig. 4.2A and B). 44 and 47 kDa bands in the second dimension correspond to unprocessed forms of the clusterin heterodimer while several proteolytic derviatives of the (α205-β1) processed clusterin heterodimer are also identifiable as colinear pairs of equivalently staining spots (Fig. 4.2A and B).

The Triton X-100 washed immunoaffinity preparations did not contain apoAI (28 kDa; reducing and non-reducing) (Jenne et al., 1991) or serum paraoxonase (44 kDa;

reducing and non-reducing) (Blatter et al., 1993; Kelso et al., 1994).

1.1.2. Expression of human clusterin as a secreted protein in *Pichia pastoris*

Human clusterin is subject to extensive post-translational modifications during biosynthesis including disulfide bond formation, addition of complex N-linked carbohydrates, and partial proteolysis to generate the heterodimer. To obtain a recombinant form of clusterin, human clusterin was expressed as a secreted protein in the methylotrophic yeast *Pichia pastoris*. The full length human clusterin cDNA, including the N-terminal secretory signal sequence, was placed under control of the methanol inducible AOX1 promoter in the plasmid pHIL-D2, yielding the construct pD2HT7. pD2HT7 was integrated into the *P. pastoris* genome both at the *AOX1* and *HIS4* loci. Integration at the former replaces the AOX1 coding sequence, while integration at the latter occurs with duplication of the HIS4 gene without affecting the AOX1 gene. Only the latter can grow on media with methanol as the sole carbon source.

Secretion of human clusterin was induced by transfer of *HIS+ P. pastoris* (strain GS115) transformants of pD2HT7 to methanol containing medium, and detected by G7 immunoreactivity, specifically to conditioned medium applied to nitrocellulose (data not shown). Expression was considerably higher for transformants expected to integrate at the *HIS4* than the *AOX1* locus (data not shown). The level of expression of recombinant human clusterin from the former was estimated at 17 ± 3 μg/mL of conditioned medium by a quantitative dot blot immunoassay developed using G7 as detecting antibody and purified human plasma clusterin applied in parallel as a standard (data not shown).

1.1.3. Structure of recombinant human clusterin

A series of bands, the majority of which ranged from 42 to 56 kDa were present in conditioned medium from the highest expressing pD2HT7 clone but not vector only transformants when analyzed by non-reducing SDS PAGE (data not shown). Visual estimation of expression levels, based on the relative intensity of Coomassie Blue stained gels of recombinant and serum/plasma clusterin run in parallel, was on the same order of magnitude as that estimated by the G7 dot blot immunoassay. This agreement suggested that the G7 conformational epitope is preserved in most molecules of recombinant clusterin.

Precipitation with ethanol was developed as a rapid method to concentrate recombinant clusterin from conditioned medium for further structural analysis. Clusterin was quantitatively precipitated from conditioned medium using either 35% ethanol at pH 6.5 or 25% ethanol at pH 5.5 and both conditions were used at different times (data not shown). Ethanol precipitates contained the same 42 to 56 kDa non-reduced bands as conditioned medium (Fig. 4.1A, lane 7). These were the major polypeptides present, and all appeared to be reactive with monoclonal antibodies G7/78E (Fig. 4.1A, lane 8) suggesting that recombinant clusterin in these preparations was substantially pure. Under reducing conditions most of these polypeptides shifted to lower molecular weights, migrating predominately as a series of bands in the range 26 to 36 kDa (Fig. 4.1A, lane 3). Although with higher protein loads, and/or in different experiments, larger numbers of minor bands within the range 26 to 36 kDa were observed, on most gels six or so discrete bands of approximately 36, 34, 32, 30, 28, and 26 kDa within that range were resolvable

by SDS PAGE (Fig. 4.1B, lane 1, numbers 1-6). Minor bands were observed at about 24, 23, and 20 kDa (Fig. 4.1B, lane 1, numbers 7-9). G7/78E immunoreactivity was observed with all bands in the range 34 to 26 kDa as well as at 24 and 20 kDa (Fig. 4.1A, lane 4 and Table 4.2). There was no apparent immunoreactivity with the 36 kDa band and although reactivity overlapped the 34 and 30 kDa bands it was not commensurate with the relative proportions of these bands estimated from silver and Coomassie Blue staining, suggesting that most of the protein at these positions does not contain the α epitope of either G7 or 78E.

The molecular weights of recombinant clusterin under non-reducing and reducing conditions were consistent with the structure of a disulfide linked dimer quantitatively processed by proteolysis between the cysteine rich domains. To examine this possibility further ethanol precipitates were separated by SDS PAGE under reducing conditions and transferred to PVDF membranes for N-terminal sequencing of the 6 major and 3 minor polypeptides identified above. The sequences were variably "noisy" although through 15 cycles three clusterin N-termini were clearly distinguishable (Table 4.2). Not unexpectedly, given the apparent overlap between α specific G7/78E immunoreactivity and unreactive polypeptides most of the polypeptides resolved by reducing SDS PAGE yielded more than one of these N-termini. The 36 kDa band yielded only, and the 34 kDa band as a small contaminating signal, the β N-terminal sequence (S_1LMP...) corresponding to the β N-terminus in human serum clusterin (Kirszbaum et al., 1989) suggesting some functional conservation of proteolytic processing in *P.pastoris*. The predominant β N-terminus however, corresponded to a 36 amino acid N-terminal

Table 4.2. N-terminal sequence, Western blot reactivity, and silver staining of N-glycosylated polypeptides from *P. pastoris* recombinant human clusterin separated by reducing SDS PAGE

Band[a]	MW (kDa)	α DQTV...[b]	β SLMP...[b]	β SPAF...[b]	G7/78E[c]	Grey-Green[d]	Brown[d]
1	36	-	+	-	-		+
2	34	+/-	+	++	+/-		+
3	32	++	-	+	+	+	
4	30	++	-	+++	+		+
5	28	+++	-	+	++	+	
6	26	++	-	++	+		+
7	24	+/-	-	-	+/-	?	?
8	23	+	-	+	-	?	?
9	20	+/-	-	-	+/-	?	?

[a] Numbers correspond to those given in Fig. 4.1 indicating the positions of bands excised from PVDF electroblots.

[b] The α or β N-terminal sequence of the excised bands. +++, ++, +, +/-, and - indicate that the associated N-terminus, estimated from yields per cycle through up to 15 sequencing cycles is present at very high, high, moderate, weak, and undetectable levels, respectively.

[c] Western blots using monoclonal antibody 78E or a mixture of 78E and G7 showing the level of reactivity ++, +, +/-, and - . The distribution of Western blot immunoreactivity is consistent with the α subunit.

[d] Correspondance between identity of band and color after silver staining. Informative bands are 1, 2, and 4 in which β N-termini are in excess over α, and 3 and 5 in which α are in excess over β and suggest that the β subunit stains brown and the α grey-green. Question marks; uncertain assignment.

truncation (S_{37}PAF...) and was present as the major constituent of bands at 34, and 30 kDa and in approximately equivalent yields to α at 26 kDa. Most of this β N-terminus, approximately 50 to 60%, was however, present at 34 kDa. Minor amounts were obtained as a background signal in the 32, 28, and 24 kDa bands. Only one N-terminus obtained from the α chain was detected, namely that predicted from cleavage of the N-terminal secretory signal sequence (D_1QTV....) by signal peptidase. This was the major N-terminus corresponding to the 32 and 28 kDa bands and was present as a significant background signal at 30 and 26 kDa. Most of this α N-terminus, approximately 40 to 50%, was present at 28 kDa. Minor yields were detectable in all other bands except that at 36 kDa. As expected there was a good correspondence in position and intensity between G7/78E immunoreactivity and those bands that have α N-termini.

The identification of β N-termini was consistent with the synthesis and secretion of recombinant human clusterin as a disulfide linked heterodimer. To confirm this heterodimeric structure ethanol precipitates were treated with N-glycosidase F prior to analysis by one and two dimensional SDS PAGE. Following N-deglycosylation 42 to 56 kDa non-reduced polypeptides shifted to 33 to 48 kDa (Fig. 4.1B, lane 5) and 26 to 36 kDa reduced polypeptides to 14 to 28 kDa (Fig. 4.1B, lane 2 and Fig. 4.3E, lane 1). Thus, most if not all recombinant clusterin appears to be modified by N-linked glycosylation. Only a very minor amount comigrated with N-deglycosylated serum/plasma clusterin under non-reducing conditions (compare lanes 5 and 6, Fig. 4.1B) and with the β chain under reducing conditions (compare lanes 2 and 4, Fig. 4.1B and lanes 1 and 2, Fig. 4.3E) while the majority under either condition was of much lower

Figure 4.3. 2D SDS PAGE of recombinant clusterin from conditioned BMMY treated with N-glycosidase F

A. 20 μg of recombinant clusterin prepared by ethanol precipitiation of conditioned BMMY was treated with N-glycosidase F and separated by two dimensional non-reducing by reducing SDS PAGE and stained with Coomassie Blue as described in Materials and Methods. The positions of molecular weight standards run in parallel are indicated at the top and left for the indicated dimension.

B. As in A but separated polypeptides were electroblotted to nitrocellulose and probed with α chain specific antibodies G7 and 78E. The blot is aligned with A. in the reducing dimension. The positions of molecular weight standards run in parallel in the non-reducing dimension are indicated at the top.

C. Longer exposure of B showing additional high molecular weight forms of clusterin at approximately 70 kDa in the non-reducing dimension, and the unprocessed forms along the diagonal of equal molecular weight in both dimensions. The blot is aligned with A in the non-reducing dimension. The positions of molecular weight standards run in parallel in the reducing dimension are indicated to the right.

D. Reproduction of A showing the principal pattern of αβ structures inferred by combining data from A, B, and C. The boxed areas represent disulfide linked heterodimers cut at least once between the cysteine rich domains (processed); an area representing polypeptides lying on the diagonal (equal relative molecular weight in both dimensions) representing unprocessed proprotein forms (unprocessed); and low molecular weight polypeptides that migrate at the dye front in the non-reducing dimension and may be non covalently associated clusterin derived polypeptides (clusterin peptides). Of the processed forms blue and green spots are immunoreactive in B identifying them as α derivatives while red and purple spots are unreactive identifying them as β derivatives. Numbers outside the box corresponding to processed forms indicate the relative molecular weight of spots in the associated dimension. Lower case letters in the reducing dimension identify known and hypothesized proteolytic cleavage events in Fig. 4.4 associated with the corresponding spots and relative molecular weights. The position of N-glycosidase F in A is indicated by the asterisk.

E. Coomassie Blue stained gel of ethanol precipitated recombinant clusterin (lane 1) and immunoaffinity purified plasma clusterin (lane 2) treated with N-glycosidase F showing comigration of the 28 kDa recombinant polypeptide with the full length β chain from the plasma protein. Only a lightly stained band in the non recombinant preparation comigrates with the full length 26 kDa α chain. Most recombinant polypeptides are proteolytic derivatives of the full length α or β chains.

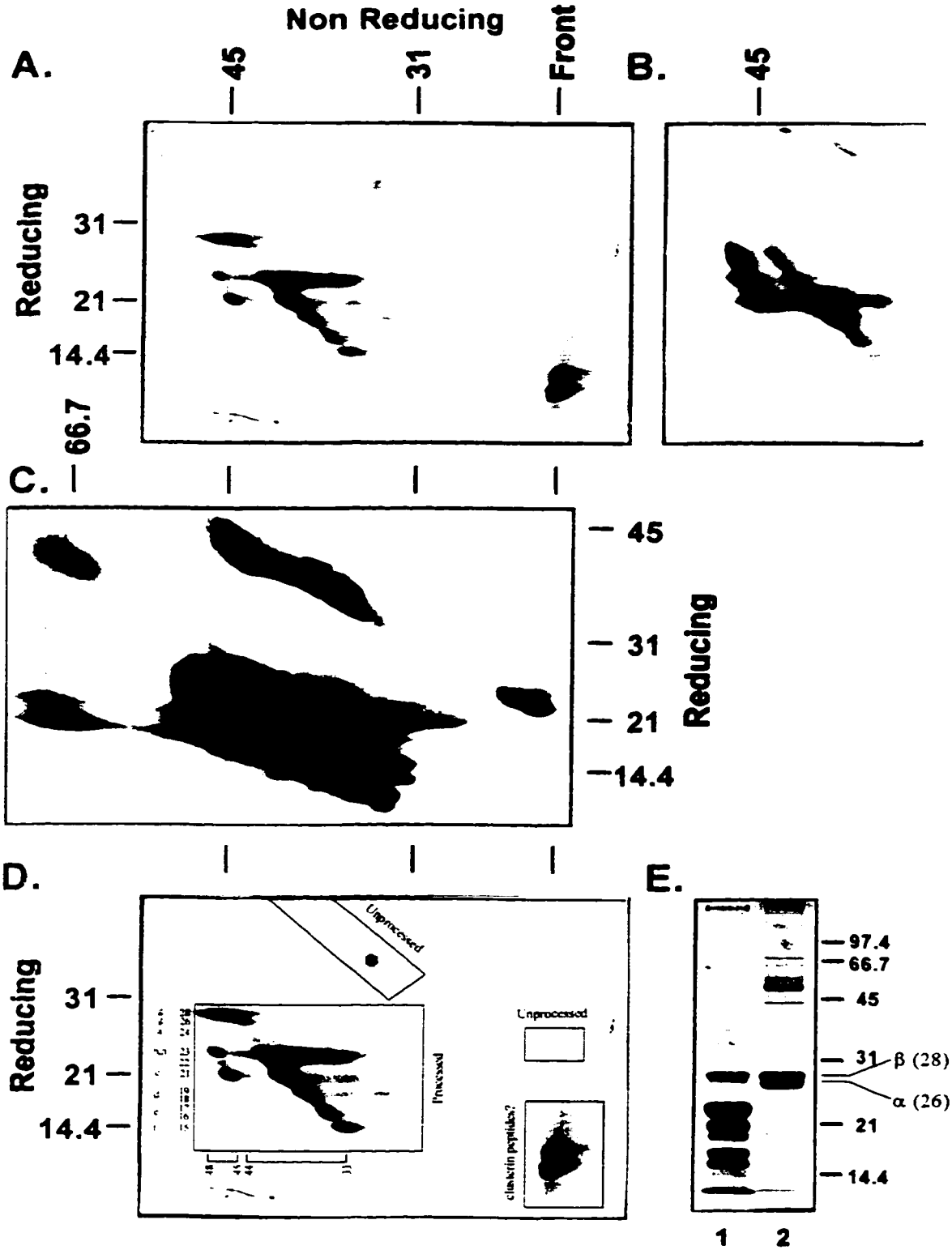
Non Reducing
A.
45
31
Front
B.
45
Reducing
31
21
14.4
66.7
C.
45
31
21
14.4
Reducing
D.
Reducing
31
21
14.4
Unprocessed
Processed
Unprocessed
clathrin peptides?
E.
97.4
66.7
45
31
β (28)
α (26)
21
14.4
1
2

molecular weight suggesting that most recombinant clusterin chains were related to those of serum/plasma clusterin by proteolytic truncations. The two dimensional analysis when combined with Western blotting using G7/78E resolved some of this complexity (Fig. 4.3A and B). Bands in the range 48 to 45 kDa in the non-reducing dimension were dissociated in the reducing dimension into a 28 kDa non-immunoreactive elongated spot consistent with the β chain (Fig. 4.3D, red), and more spherical immunoreactive spots of 26, 24, 23, 22, and, 21 consistent with α chain derivatives (Fig. 4.3D, blue). The spot shape, dimension, Coomassie Blue staining intensity, colinearity and chain identity are consistent with heterodimeric disulfide linked structures of α26:β28, α24:β28, α23:β28 (major), α22:β28, and α21:β28 (major). Bands in the range 45 to 33 kDa in the non-reducing dimension dissociated in the reducing dimension predominately into a 23 kDa non immunoreactive elongated spot (immunoreactivity at the 45 kDa end of this 23 kDa band is compatible with a comigrating α chain derivative) consistent with a β chain derivative (purple, Fig. 4.3D), and more spherical immunoreactive spots of 26, 24, 23, 22, 21, 19, 18, 17, 16, and 15 consistent with α chain derivatives (green, Fig. 4.3D). Again spot shape, intensity, colinearity and chain identity were consistent with heterodimeric disulfide linked structures of α26:β23, α24:β23, α23:β23, α22:β23, α21:β 23, α19:β23, α18:β23, α17:β23, α16:β23, and α15:β23. Other spots apparent on Coomassie Blue or G7/78E immunoblots fall within the boxed area in Fig. 4.3D, and correspond to minor forms of processed disulfide linked heterodimers. These lie for the most part to the right of the main diagonal of staining and immunoreactivity in Fig. 4.3A and B and it is likely that these correspond to dimers of at least one other truncated form of the β chain.

The N-deglycosylated 28 kDa form of the β chain from the recombinant clusterin preparation comigrates with that of serum/plasma clusterin and is presumptively full length. A truncation of 36 amino acids to give the alternate β N-terminus probably accounts for the 23 kDa form. This suggests that two proteolytic events account for (at least) the majority of the β forms. In contrast there are a large number of proteolytic events that produce truncations of various lengths of the α chain. Since the only α N-terminus identified is that resulting from signal peptidase cleavage, and the collective yield of polypeptides with this N-terminus was roughly equivalent to the sum of yields for the two β chains most, if not all, of these α truncations are presumed to lie at the C-terminus of the α chain. The localization of these sites was estimated from the relative molecular weight of the corresponding N-deglycosylated band and mapped onto the linear antiparallel model of clusterin structure (Fig. 4.4). All of the major proteolytic sites are predicted to lie within sequences encoded by exon 5. Essentially no truncations of the α chain greater than approximately 5 kDa, corresponding to the 21 kDa derivative (Fig. 4.4, a through c) are observed paired with β28 while β23 is associated in addition with truncations up to approximately 11 kDa of the α (Fig. 4.4, d through f). Notably, in the model there is a rough colinearity between the localization of the proteolytic site in the β chain and that in the α corresponding to the maximum associated truncation (Fig. 4.4, g and c, and h and f).

Several other minor spots outside the area corresponding to α:β disulfide linked processed forms were evident on the two dimensional Coomassie blue stained gels and western blots. Polypeptides comigrating with the dye front (< 21 kDa) in the non-

Figure 4.4. Location of major sites of proteolysis associated with expression of clusterin in *P. pastoris* on the linear antiparallel structural model

Human clusterin α and β chains are presented as given in Figure 3.6 with putative coiled-coil (blue boxes) and exon 5 encoded (green boxes) amphipathic α helices as redefined in Chapter 3. Purple lines indicate the location of proline residues in human clusterin. Arrows indicate known (solid) or estimated (broken) sites of proteolysis associated with expression of clusterin in *P. pastoris*. The location of sites of proteolysis in the α chain was estimated from relative molecular weights of the corresponding polypetides by reducing SDS PAGE of N-glycosidase F treated preparations (a to f). a, b, and c have the α chain N-terminus and thus correspond to C-terminal truncations only. d, e, and f were estimated based on the assumption that they have the mature α N-terminus but this is not known directly. Sites of proteolysis in the β chain are known directly from N-terminal sequence analysis (g and h). The letters identify the corresponding truncated chains in the reducing dimension in Fig. 4.3D and Fig. 4.5B.

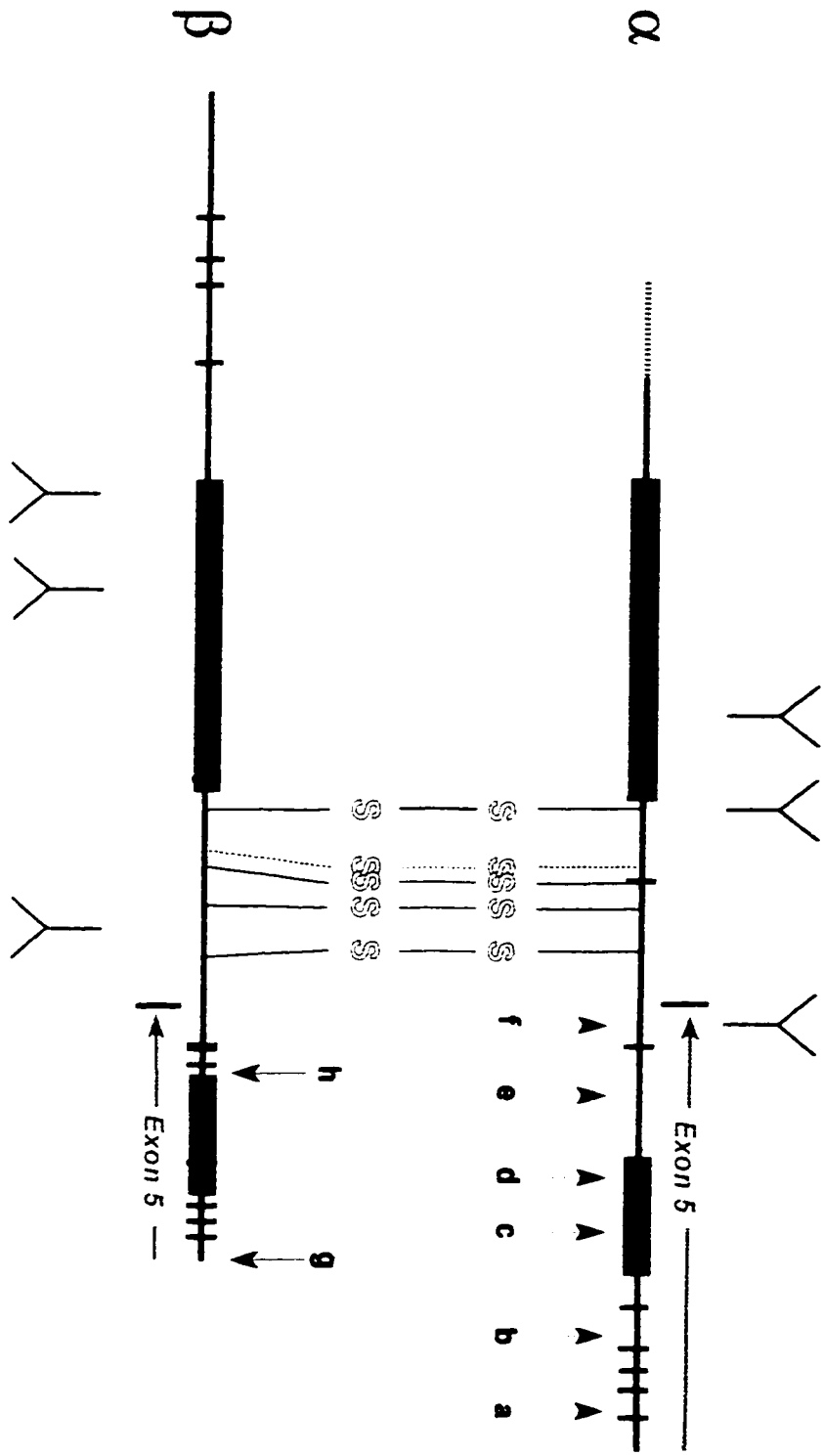
α
β
Exon 5
Exon 5
a
b
c
d
e
f
g
h

reducing dimension were resolved into a series of spots of less than 14.4 kDa in the reducing dimension (Fig. 4.3A corresponding to boxed area in Fig. 4.3D). Based on their small size and quantity they might plausibly correspond to short non covalently associated clusterin polypeptides released as a result of proteolytic events yielding the various heterodimers.

A more or less continuous line of Coomassie Blue staining was also observed following a diagonal of approximately equal molecular weight in both reducing and non-reducing dimensions beginning at approximately 46 kDa and ending at approximately 34 kDa. This was identified with clusterin on the basis of a coincident line of G7/78E immunoreactivity on longer exposures of westen blots (Fig. 4.3C) and are probably proteolytic derivatives of the unprocessed proprotein.

Still a third set of spots is observed corresponding to a molecular weight of about 66 to 70 kDa in the non-reducing dimension that resolved in the reducing dimension into Coomassie Blue stained spots of 28, 23, and 21 kDa and G7/78E immunoreactivity as a smear from 46 to 43 kDa, and as discrete bands at 23 and 21 kDa (Fig. 4.3C). The band above 97.4 kDa on non-reducing Western blots of N-glycosylated polypeptides likely corresponds to these forms of recombinant clusterin (Fig. 4.1A, lane 8). These may represent disulfide linked combinations of derivatives the α and/or β chains with an unprocessed form of the heterodimer.

1.1.4. Casein improves the stability and/or biosynthesis of recombinant clusterin

The observation that recombinant human clusterin is a disulfide linked heterodimer suggests that it has to some significant extent the tertiary structure characteristic of the serum/plasma protein. However, *P. pastoris* protease(s) clearly cleave the recombinant protein at aberrant sites such that very little full length heterodimer can be observed in these preparations. To improve recombinant stability, inducing medium was supplemented with casein to a final concentration of 10 mg/mL, as a possible competitor for extracellular proteolysis. To estimate the levels of expression in this protein-rich medium a competitive antigen capture assay was developed. Binding of a fixed amount of a biotinylated, ethanol-precipitated preparation of recombinant clusterin, to G7 immobilized on a microtitre plate, was competed by conditioned medium containing unlabeled recombinant clusterin or purified serum/plasma clusterin, in parallel, as a standard. This estimated a level of expression of about 88 μg recombinant clusterin/mL of medium, approximately 5.2 times the level of expression in the absence of casein (data not shown). As ethanol precipitation of clusterin from modified medium was complicated by coprecipitation of casein, recombinant clusterin in this medium was purified by immunoaffinity chromatography. Yields were in close agreement with expectations of the estimates of expression levels from the antigen capture assay using subsaturating loads of conditioned medium. Amino acid analysis of the two preparations used in the course of this study gave similar estimates of the difference in experimental composition from known composition but were slightly higher than those of serum/plasma clusterin (Table 4.1, average 16.3%).

The structure of immunoaffinity purified recombinant clusterin was analyzed by one and two dimensional SDS PAGE with and without N-deglycosylation, Western blotting with G7/78E and N-terminal sequencing of PVDF electroblots. The results of these analyses are summarized in Fig. 4.5 and Table 4.3. Relative to ethanol precipitates from unsupplemented, conditioned medium, in the one and two dimensional analysis of N-deglycosylated immunoaffinity preparations from supplemented medium, there is a proportional increase in β28 (Fig. 4.5B, red spots), and decrease in β23 (Fig. 4.5B, purple spots) kDa forms. Similarly there are proportional increases in α26, α24, and α21 kDa forms (Fig. 4.5B, blue spots) and decreases in all other forms especially those less than 21 kDa (Fig. 4.5B, green spots). Expressed in terms of heterodimers there are proportional increases in α26:β28, α24:β28, α21:β28, α26:β23, and α24:β23 with α21:β 23 remaining a significant dimeric form. N-terminal sequencing of PVDF blots of the two dimensional gels confirmed that the 28 kDa spot had the same β N-terminus as that of serum/plasma clusterin while the 23 kDa spot had the β N-terminus arising from the 36 amino acid N-terminal truncation (Table 4.3). The 26, 24, and 21 kDa spots had the N-terminus of the mature α chain (Table 4.3). These data confirmed the assignment of the composition and structure of heterodimers from ethanol preparations and suggested that the casein supplement had at least some of the desired effect on limiting extracellular proteolysis.

1.1.5. Heterogeneous glycosylation of recombinant clusterin

It is likely that some of the heterogeneity in molecular weight of N-glycosylated recombinant preparations is the consequence of heterogeneity in N-linked glycosylation

Figure 4.5. 2D SDS PAGE of recombinant clusterin immunoaffinity purified from casein supplemented BMMY and treated with N-glycosidase F

A. 25 μg of immunoaffinity purified recombinant clusterin was treated with N-glycosidase F, separated by two dimensional non-reducing by reducing SDS PAGE, and stained with Coomassie Blue as described in Methods and Materials. Molecular weight markers run in parallel in the associated dimension are indicated at the top and right of the figure. Left panel; 5 μg of immunoaffinity purified recombinant clusterin treated with N-glycosidase F, and separated by SDS PAGE under reducing conditions and either stained with Coomassie Blue (lane 1) or electroblotted to nitrocellulose and probed with α chain specific monoclonal antibodies G7 and 78E (lane 2). Bottom panel; 5 μg of immunoaffinity purified recombinant clusterin treated with N-glycosidase F, and separated by SDS PAGE under non-reducing conditions and stained with Coomassie Blue. Lines from left and bottom to center panel identify corresponding bands in each dimension.

B. Reproduction of A. with boxed areas as in Fig. 4.3. The identities of polypetides corresponding to α (blue and green) and β (red and purple) chains are indicated. Numbers outside the box corresponding to processed forms indicate the relative molecular weight of spots in the associated dimension, and lower case letters in the reducing dimension identify known and hypothesized proteolytic cleavage events in Fig. 4.4 associated with the corresponding spots and relative molecular weights. The position of N-glycosidase F in A is indicated by the asterisk. A duplicate of A was electroblotted to PVDF membranes and circled spots analyzed by N-terminal sequencing. The associated numbers identify the spots with the N-terminal sequencing data given in Table 4.3

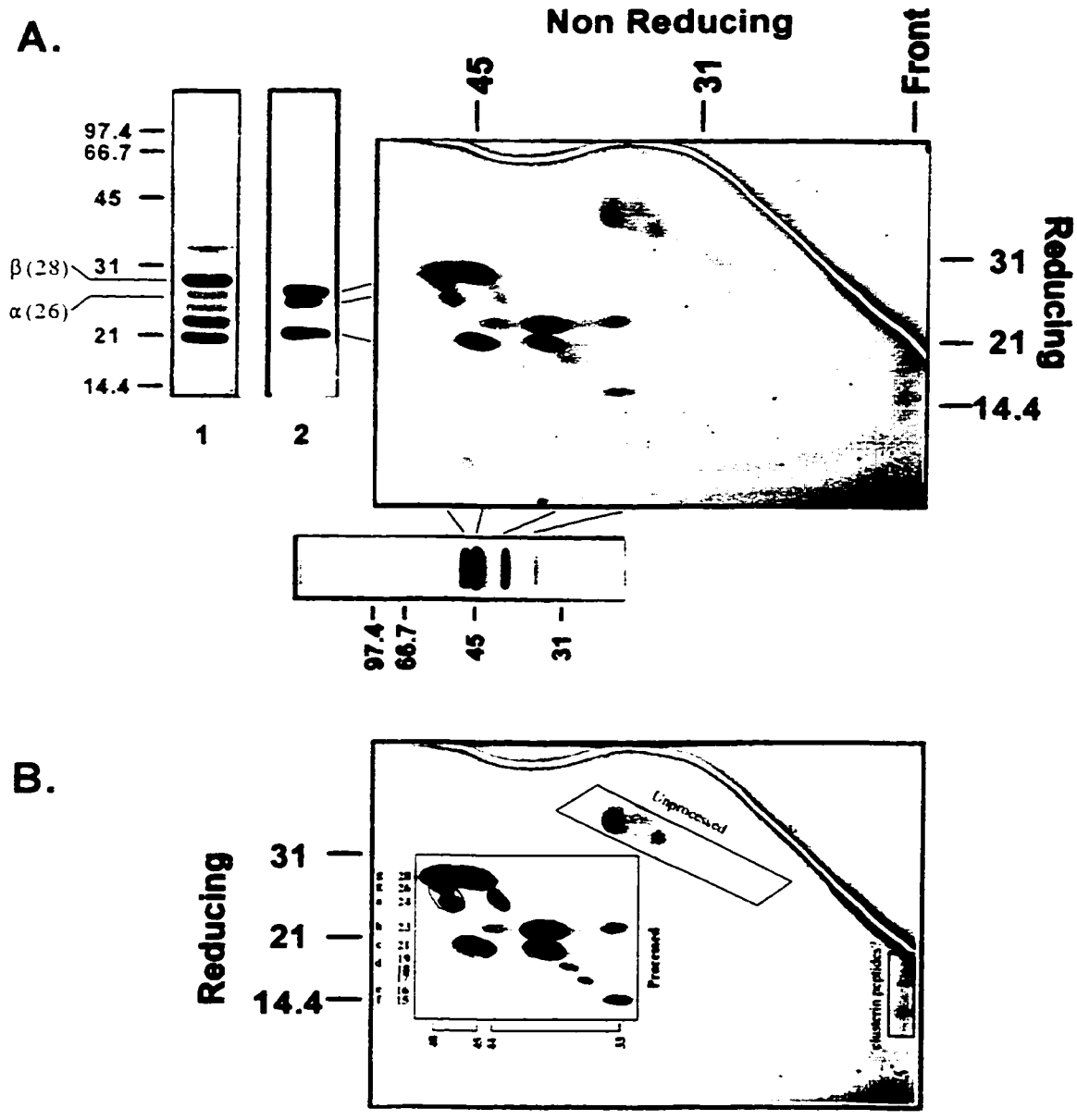
A.
Non Reducing
45
31
Front
97.4
66.7
45
β(28)
31
α(26)
21
14.4
1
2
Reducing
31
21
14.4
97.4
66.7
45
31
B.
Reducing
31
21
14.4
Unprocessed
Processed

Table 4.3. N-terminal Edman sequencing of immunoaffinity purified N-deglycosylated recombinant clusterin separated by 2D SDS PAGE

Cycle	Spot 1[a]		Spot 2[a]		Spot 3[a]		Spot 4[a]	Spot 5[a]	Spot 6[a]
1	- S	1.28 D	4.41 S	*1.38* D	2.81 S	*2.03* D	3.10 D	*11.2* D	*7.42* D
2	3.20 L	0.84 Q	5.46 L	0.32 Q	4.13 P	0.76 Q	2.63 Q	6.12 Q	4.02 Q
3	2.75 M	- T	3.61 M	- T	3.67 A	- T	0.70 T	1.90 T	1.36 T
4	3.78 P	1.02 V	5.71 P	0.34 V	2.91 F	0.38 V	1.17 V	3.24 V	2.01 V
5	3.44 F	- S	3.93 F	- S	3.48 Q	- S	0.76 S	1.58 S	1.35 S
6	- S	0.63 D	1.60 S	*0.97* D	- H	*1.08* D	1.01 D	*5.77* D	*4.27* D
7	3.19 P	0.68 N	3.85 P	0.43 N	3.26 P	- N	1.08 N	8.50 N	2.55 N
8	1.97 Y	1.03 E	3.11 Y	0.81 E	4.13 P	1.03 E	1.21 E	3.64 E	2.44 E
9	2.37 E	1.06 L	4.36 E	0.18 L	0.79 T	- L	0.53 L	2.01 L	1.21 L
10	2.94 P	0.69 Q	3.14 P	0.45 Q	3.00 E	0.53 Q	0.97 Q	2.78 Q	1.91 Q
Mean[b]	2.96± 0.58	0.90± 0.23	3.92± 1.19	0.42± 0.21	3.13± 1.00	0.68± 0.28	1.32± 0.85	3.72± 2.41	2.11± 0.92

[a] pmol of indicated PTH amino acid for the indicated sequencing cycle. Numbers refer to spots identified in Fig. 4.5B.

[b] average pmol\cycle ± one standard deviation for the 10 sequencing cycles. Some of the D yields are *italicized.* These values were not considered in calculation of the mean as there was an error in calibration of the Asp PTH standard in these runs. Similarly '-' indicates that the expected peak was either not detected or was not identified by the instrument, and was also not considered in this calculation.

and not merely the consequence of proteolysis. For example, the N-terminally truncated β chain was of a singular molecular weight when N-deglycosylated and yet in reduced N-glycosylated preparations corresponded to several species of distinct molecular weight (Table 4.2). A partial analysis of this heterogeneity was facilitated by fractionation of immunoaffinity purified recombinant preparations by RP-HPLC. Elution of bound clusterin with a sufficiently shallow gradient of acetonitrile resolved the recombinant protein into two overlapping sets of peaks (Fig. 4.6A). Treatment of fractions from these peak(s) with N-glycosidase F demonstrated that the early eluting set of peaks (Fractions 56 to 59) corresponded to dimers consisting of primarily of β23 kDa while the later eluting set of peaks (Fractions 60 to 63) dimers consisting primarily of β28 (Fig. 4.6B). In several of these fractions the dimers present were pure with respect to a single proteolytic form of one or other chain. Fraction 57 consisted predominantly of dimers of β23, fractions 61 to 63 inclusive of β28 and fractions 62 and 63 of α21. Hence, N-glycosylated polypeptides in these fractions associated with the homogeneous chain give some idea of the heterogeneity in N-linked carbohydrate modifications. Fractions 56 to 63 were separated by SDS PAGE under reducing conditions without prior treatment with N-glycosidase F and stained with silver (Fig. 4.6C). We have observed that the β chain is more strongly stained with silver than the α in agreement with previous reports (James et al., 1988). In our hands the α chain stained a light greyish-green while the β chain a strong dark brown (Table 4.2). This observation was used to assign N-glycosylated polypeptides to the particular N-deglycosylated form of one or other chain in these HPLC fractions. The result of this analysis is shown in Fig. 4.6D. In fraction 57 three major brown staining bands were present at about 26, 30 and 33 kDa and are presumed

Figure 4.6. RP HPLC analysis of immunoaffinity purified recombinant clusterin

A. 100 μg of recombinant clusterin immunoaffinity purified from casein supplemented BMMY was separated by RP-HPLC on a Vydac C4 column monitored at 230 nm collecting 1 mL fractions as described in Methods and Materials.

B. Approximately 40% of concentrated neutralized fractions 56 to 63 were treated with N-glycosidase F as described in Methods and Materials and separated on a 12% SDS polyacrylamide gel under reducing conditions and stained with Coomassie Blue. Indicated to the right is the chain, N-terminus and molecular weight in parenthesis of the three polypeptides considered in D which could be assigned to N-glycosylated polypeptides.

C. Representation of the major banding patterns of N-glycosylated polypeptides from 18 to 45 kDa in the fractions 56 to 63 ordered as given in B separated by electrophoresis under reducing conditions on a 11% SDS polyacrylamide gel and stained with silver. This gel did not photograph well and is represented schematically with an approximation of the coloration of bands used to identify α and β chains.

D. Informative fractions in the identification of the major silver stained N-glycosylated polypeptides in C. with particular N-deglycosylated polypeptides in B. and only these latter are shown. Informative fractions were 57 for β23, 61 to 63 inclusive for β28, and 62 to 63 inclusive for α21 deemed as essentially pure with respect to that chain and N-deglycosylated form. Tentative identification between bands in B and C was made primarily on the basis of silver stained coloration (Table 4.2). Numbers 0 to 3 to the right of each lane in D represent polypeptides that may correspond to addition at 0 to 3 consensus sites of N-linked glycosylation in each chain of an average high mannose carbohydrate in *P.pastoris*; $Man_{8-14}GlcNAc_2$ (approximately 2 to 3.2 kDa) (Grinna and Tschopp, 1989).

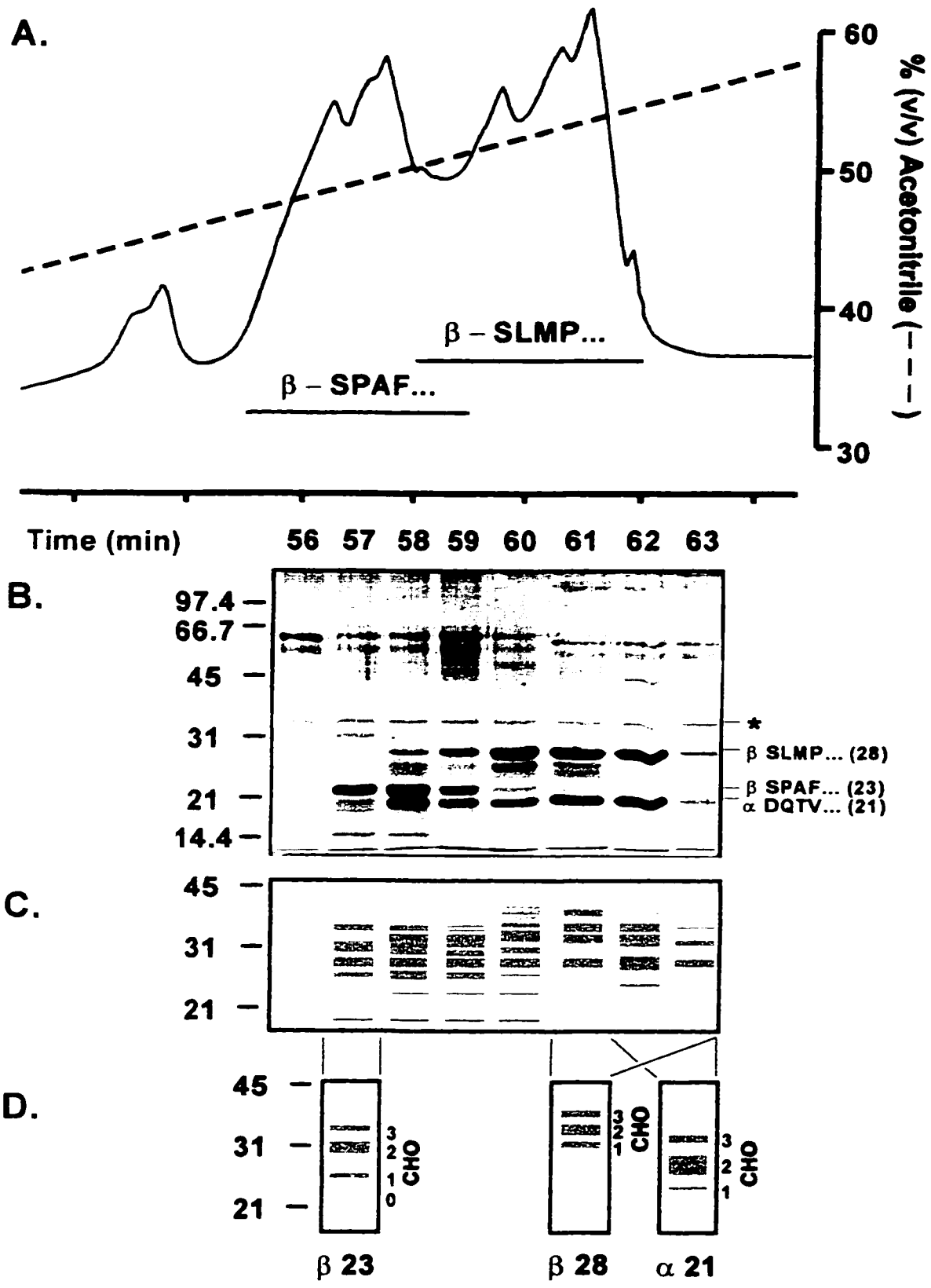
A.
60
50
40
30
% (v/v) Acetonitrile (– – –)
β – SLMP...
β – SPAF...
Time (min)
56 57 58 59 60 61 62 63
B.
97.4
66.7
45
31
21
14.4
*
β SLMP... (28)
β SPAF... (23)
α DQTV... (21)
C.
45
31
21
D.
45
31
21
3
2
1
0
CHO
3
2
1
CHO
3
2
1
CHO
β 23
β 28
α 21

glycoforms of β23. Similarly in fraction 61 to 63 three such bands were present collectively at 36, 34, and 31 kDa and are presumed glycoforms of β28. In fraction 62 and 63 two major grey-green bands present at 28 and 32kDa are presumed to be glycoforms of α21.

It is possible that each glycoform for each chain specific proteolytic form represents N-glycosylation at all three potential sites with successive discrete increases in the average molecular weight of 2 to 4 kDa. However, it is interesting that differences on the order of 2 to 4 kDa within each set are close to estimations of the molecular weight of an average N-linked high mannose carbohydrate on *P.pastoris* secreted glycoproteins ($Man_{8-14}GlcNAc_2$, calculated molecular mass of 2 to 3.2 g/mol) (Grinna and Tschopp, 1989). Thus, it is likely that each set of discrete bands corresponds to the addition or elaboration beyond the trimannosyl core of a typical high mannose N-linked carbohydrate at one, two, or three conserved positions, respectively of the given polypeptide core. In the case of the two forms of the β chain significant yields are obtained for one, two, and three N-linked carbohydrates though proportionately, as indicated from the highest PVDF sequencing yields of the N-terminally truncated β chain at about 30 kDa, modification at two sites is by far most frequent. Only minor amounts of dark to brown staining bands at around 22-23 kDa for β 23 or 28 kDa for β28, in any of the corresponding RP HPLC fractions, may represent β polypeptides secreted without N-linked carbohydrate. Of the glycoforms of α21, the 28 kDa form is proportionally most abundant, followed by the 32 kDa form, while bands that might correspond to the denuded 21 kDa and singly N-glycosylated 24 kDa forms are relatively minor. Thus, the

α chain is also appears to be N-glycosylated in most cases at two of the three consensus sites in *P. pastoris*.

1.1.6. Functional analysis of recombinant and serum/plasma clusterin

Two questions related to the activity of clusterin were pursued in parallel. First, we compared the binding properties of immunoaffinity purified *P. pastoris* recombinant human clusterin with those of the serum/plasma protein to determine whether it would serve as a model source for the analysis of the relationship between structure and function using a mutagenic approach. Second, we sought evidence for physically distinct binding sites for LRP2 and a possibly promiscuous binding site for hydrophobic/amphipathic ligands and for pH regulation of the latter by means of histidine ionization.

Based on the two binding site model (Chapter 3) it seemed appropriate to compare recombinant to serum/plasma clusterin with respect to interactions with putative ligands of these two sites. Representative hydrophobic/amphipathic ligands included complement C9, and $A\beta_{1-40}$. Because purified IgG was inexpensive and readily available in large quantities, comparative binding to this ligand was also assessed. In light of the suggestion that the hydrophobic/amphipathic ligand binding site of clusterin is promiscuous it is possible that the interaction between clusterin and IgG also reflects the activity of this site. Lastly, the LRP2 binding interaction was compared based on specific binding to the surface of differentiated F9 cells which express high levels of this receptor (Kounnas et al., 1995).

1.1.1. Binding of clusterin to Zn^{+2} polymerized C9, $A\beta_{1-40}$, and IgG at acidic pH

The interaction between clusterin and hydrophobic/amphipathic ligands was analyzed using solid phase binding assays in which clusterin in solution bound to ligands immobilized to 96 well polystyrene microtitre plates. The assay system used was a modification of the assay developed to study the interaction of clusterin with immobilized IgG (Wilson and Easterbrook-Smith, 1992).

Immunoaffinity purified serum/plasma clusterin was labeled with biotin and complexes formed between solution phase clusterin and immobilized ligands (IgG, $A\beta_{1-40}$, or Zn^{+2} polymerized complement C9) were detected with streptavidin and biotin labeled horseradish peroxidase. In my hands polymerized preparations of monomeric C9, induced by incubation with Zn^{+2}, gave a significantly higher clusterin binding signal, per unit concentration of coating ligand, than monomeric C9 (data not shown). This is consistent with the assertion that the clusterin binding site on C9 is exposed by activation (Tschopp et al., 1993; McDonald and Nelsestuen, 1997), although other explanations such as differences in density of bound C9, or the facilitation of multivalent interactions with clusterin oligomers by C9 polymerization cannot be excluded. Because of this Zn^{+2} polymerized C9 (poly C9) was used in all subsequent experiments.

If the ionization of histidine on clusterin regulates interactions with hydrophobic/amphipathic ligands it is possible that changing the binding pH over the range expected for imidazole titration in these *in vitro* binding assays will affect the formation of stable clusterin ligand complexes. Thus, the binding pH was varied from 5

to 7.5. There is an increase, which displayed a good approximation to a linear relationship, in binding of labeled clusterin with increasing concentration at all pHs over a range of 1 to 40 nM for each ligand (Fig. 4.7, insets), indicating that under these conditions, concentrations are subsaturating. Slopes of best fit regression lines were used to compare changes in binding as a function of pH. Changes in binding pH had differential effects on the number of stable complexes formed between clusterin and each ligand. Stable binding to immobilized $A\beta_{1-40}$ (Fig. 4.7A) displayed evidence of a well defined optimum (pH 5.8-5.9), and from pH 7.5 to the optimum a sigmoidal shape and very large 19 fold increase in stable binding. Binding to immobilized IgG (Fig. 4.7B) showed little evidence of an optimum, a less pronounced sigmoidal shape between pH 7.5 and the optimum, and a more modest 3.1 fold increase in stable binding from pH 7.5 to the optimum. Finally binding to poly C9 (Fig. 4.7C) showed the highest binding, with only small differences over the range pH 5 to 7.5 indicated by a 1.6 fold increase from pH 7.5 to the optimum (pH 6.3). Binding to BSA coated wells was negligible over the range of clusterin concentrations used in these experiments at pH 7.5 and 7, indicating that at these pH binding is specific for the target ligand (data not shown). However, binding to BSA coated wells was observed to show small, but reproducible increases at pH 6 (data not shown). At pH 6 under the conditions of the experiment in Fig. 4.7 binding to BSA might account for an estimated 4.3% of total binding to wells coated with poly C9, 5.6% to wells coated with $A\beta_{1-40}$, and 9.9% to wells coated with IgG, indicating that most of the measured binding was also specific for the target ligand at this pH. Thus, most of the increase in stable ligand binding, particularly to $A\beta_{1-40}$ and IgG, measured between pH 7.5 and 6, is specific to these ligands. A minimal increase from pH 7.5 to 6

Figure 4.7. Binding of labeled human clusterin to $A\beta_{1-40}$, IgG, and Zn^{+2} polymerized C9 as a function of pH

Biotin labeled human clusterin at the indicated concentrations (insets) was incubated at pH 7.5 (red circles and lines), 7 (green circles and lines), 6.5 (yellow circles and lines), 6 (dark blue circles and lines), 5.5 (purple circles and lines), or 5 (light blue circles and lines) in 96 well polystyrene plates coated with 4 μg/mL $A\beta_{1-40}$ (A), 5 μg/mL IgG (B), or 4 μg/mL Zn^{+2} polymerized complement C9 (C). Bound biotin labeled clusterin was detected as described in Methods and Materials. After subtraction of the assay response in the absence of labeled clusterin the data at each pH were fitted using a linear least squares regression analysis and the slopes of these lines plotted as a function of pH for each ligand.

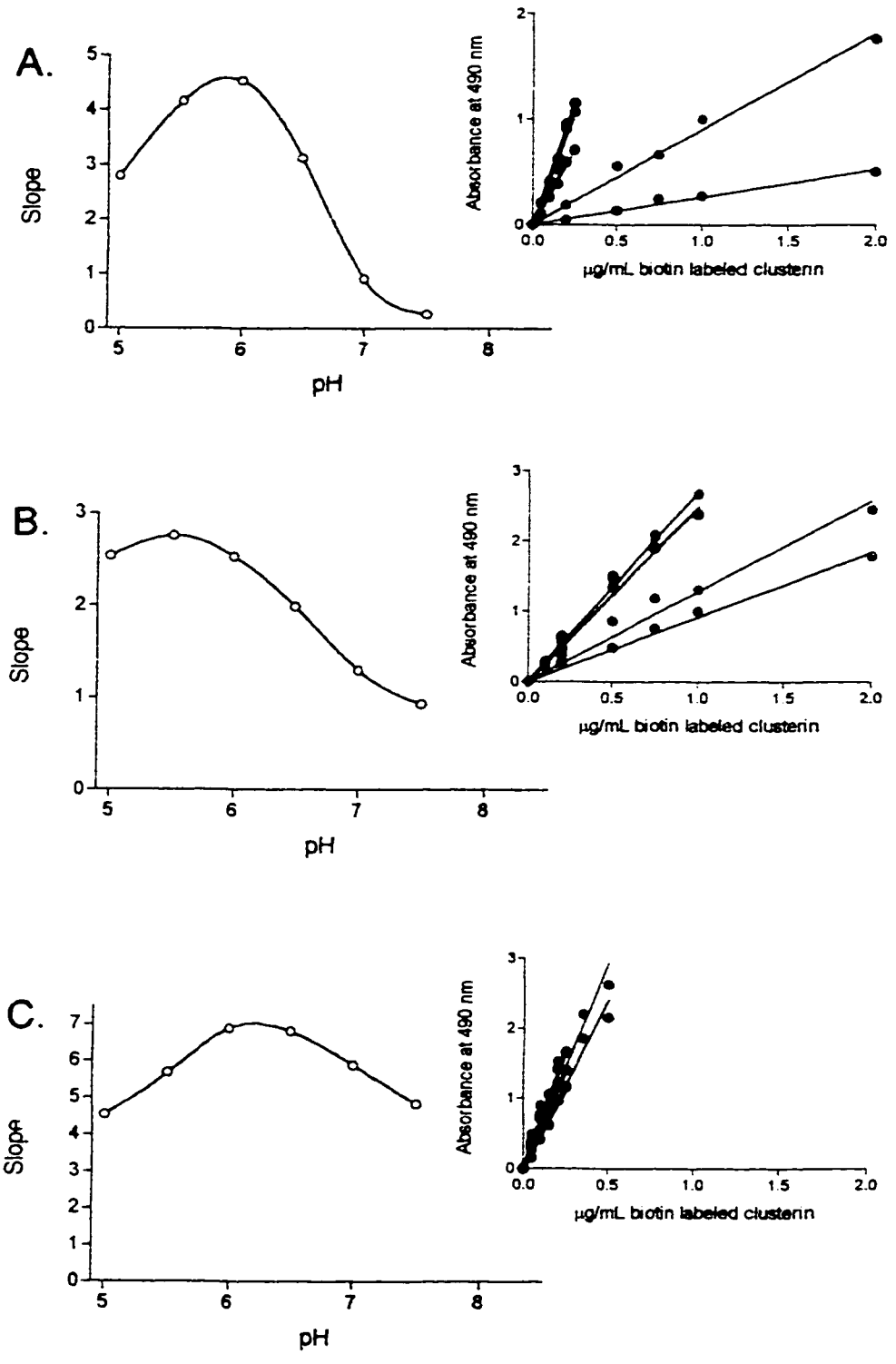
A.
Slope
pH
Absorbance at 490 nm
µg/mL biotin labeled clusterin
B.
Slope
pH
Absorbance at 490 nm
µg/mL biotin labeled clusterin
C.
Slope
pH
Absorbance at 490 nm
µg/mL biotin labeled clusterin

which can be ascribed solely to the specific interaction of clusterin with the target ligand is 16.3 fold for $A\beta_{1-40}$, 2.4 fold for IgG, and 1.4 fold for poly C9. Specific increases in binding as a function of pH between pH 7.5 to 6, and the order of sensitivity ($A\beta_{1-40}$ >> IgG > poly C9) were also confirmed in experiments in which complexes of unlabeled clusterin with immobilized ligands were detected with monoclonal antibody G7 (data not shown). Since room temperature washes with PBS-BSA containing 0.1% Triton X-100 and subsequent incubations with detecting reagents in PBS-BSA are at neutral pH, it is apparent that under the conditions of these experiments increases in stable binding at mildly acidic pH are not significantly reversed by subsequent incubations at neutral pH.

1.1.8. Specific activity of recombinant and serum/plasma clusterin in interactions with Zn^{+2} polymerized complement C9, $A\beta_{1-40}$, and IgG

The specificity, affinity, and saturability of binding of labeled clusterin at neutral and mildly acidic pH was determined by competition with unlabeled clusterin at pH 6 and 7. Unlabeled serum/plasma clusterin was a high affinity specific competitor for binding of labeled clusterin to $A\beta_{1-40}$, poly C9, and IgG at both pH 6 and 7 (closed circles in Fig. 4.8A-F). The half maximal inhibitory concentration of binding (IC_{50}s) was estimated from best fits of single site competitive binding curves. The IC_{50} for serum/plasma clusterin binding to $A\beta_{1-40}$ was calculated to be 36 nM at pH 7 and 104 nM at pH 6. In the binding to poly C9 it was calculated to be 19 nM at pH 7 and 96 nM at pH 6 and for binding to IgG, 41 nM at pH 7 and 159 nM at pH 6 (Table 4.4). These data indicate that binding of labeled serum/plasma clusterin at neutral and mildly acidic pH to all three ligands was specific, of high affinity, and saturable. The differences in IC_{50}

Figure 4.8. Competitive binding assay to measure relative affinities of *P.pastoris* human recombinant and plasma clusterin to $A\beta_{1-40}$, IgG, and Zn^{+2} polymerized C9

biotin labeled human clusterin (200 ng/mL; A, C, E) or (500 ng/mL; B, D, F) was incubated at pH 6 (A, C, E) or 7 (B, D, F) with the indicated concentrations of unlabeled immunoaffinity purified *P. pastoris* human recombinant (open circles in B, D, F) or plasma clusterin (closed circles in A - F) in 96 well polystyrene plates coated with 4 (A) or 1 μg/mL (B) $A\beta_{1-40}$ (A), 5 (C) or 1.5 μg/mL (D) IgG, or 4 (E) and 1 μg/mL (F) Zn^{+2} polymerized C9. Bound labeled clusterin was detected as described in Methods and Materials. Data were fitted to the equation of a competitive inhibitor for one site binding. IC_{50}s estimated from these competitive inhibition binding curves are given in Table 4.4.

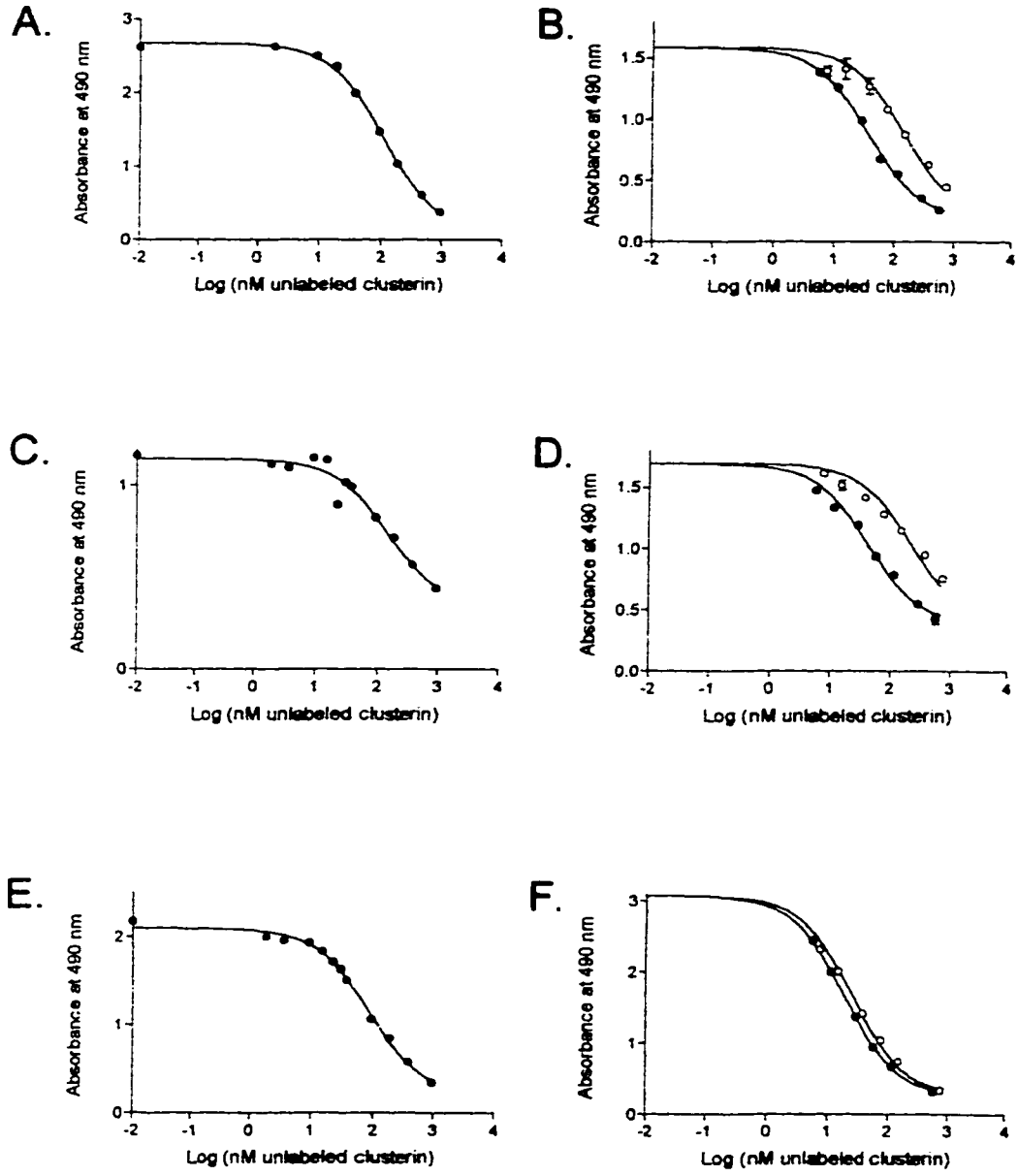
A.
B.
C.
D.
E.
F.
Absorbance at 490 nm
Log (nM unlabeled clusterin)

Table 4.4. Estimated IC_{50}s for immunoaffinity purified human recombinant and serum\plasma clusterin in competitive binding assays

Ligand	Plasma or Serum Clusterin		Recombinant Clusterin	
	IC_{50}, nM[a]	95% Confidence Interval	IC_{50}, nM[a]	95% Confidence Interval
Poly C9	18.8[b]	$18.2 \leq IC_{50} \leq 19.5$	25.6[b]	$23.4 \leq IC_{50} \leq 27.9$
	96[c]	$94.7 \leq IC_{50} \leq 97.6$	-	-
$1\beta_{1-40}$	36.1[b]	$33.7 \leq IC_{50} \leq 38.7$	142.4[b]	$119.3 \leq IC_{50} \leq 170.1$
	103[c]	$103.3 \leq IC_{50} \leq 103.9$	-	-
IgG	41.3[b]	$36.1 \leq IC_{50} \leq 47.2$	219.2[b]	$179.5 \leq IC_{50} \leq 267.6$
	713[c]	$698 \leq IC_{50} \leq 727$	-	-
Differentiated F9 Cells	9.9[d]	$5.1 \leq IC_{50} \leq 19.2$	10.3[c]	$7.1 \leq IC_{50} \leq 15.1$

[a] IC_{50}, concentration of unlabeled clusterin obtaining 50% inhibition of specific binding of labeled clusterin estimated from a best fit, non-linear regression analysis assuming a one binding site competition of unlabeled ligand with a fixed concentration of labeled ligand.

[b] Unlabeled immunoaffinity purified *P. pastoris* recombinant preparation II compared to human serum preparation IV at pH 7.

[c] Unlabeled immunoaffinity purified human EDTA plasma preparation V at pH 6.

[d] Unlabeled immunoaffinity purified *P. pastoris* recombinant preparation I compared to human EDTA plasma preparation II.

between pH 6 and 7 are not directly comparable since different preparations of human serum/plasma clusterin were used as were different concentrations of coating ligands.

Unlabeled immunoaffinity purified recombinant human clusterin was also a high affinity specific competitor at pH 7 for binding of labeled serum/plasma clusterin to $A\beta_{1-40}$ (IC_{50} = 142 nM), poly C9 (IC_{50} = 26 nM), and IgG (IC_{50} = 219.2 nM), although the IC_{50} was 3.9, 1.3, and 5.3 fold greater, respectively than that of non recombinant clusterin (Fig. 4.8B, D, and F, open circles).

These results, indicating that recombinant clusterin is a less effective specific competitive inhibitor of the binding interaction between labeled serum/plasma clusterin with IgG, $A\beta_{1-40}$, and poly C9, were confirmed by comparison of the binding of unlabeled clusterin to immobilized ligands, detected with monoclonal antibody G7. G7-immunoreactive complexes increase with increasing concentration of recombinant clusterin over a range of the order of 10 to 100 nM for poly C9 (Fig. 4.9A, closed circles), and 100 to 500 nM for $A\beta_{1-40}$ (Fig. 4.9B, closed circles), and IgG (Fig. 4.9C, closed circles) and showed evidence of saturation at higher concentrations. This binding is significantly greater than the binding to BSA (Fig. 4.9A, B, and C, closed squares) at any concentration, indicating that binding is specific and of relatively high affinity However, in agreement with the results of competitive inhibition binding assays, the binding of recombinant clusterin was significantly lower than that for serum/plasma clusterin (Fig. 4.9A, B, and C, open circles) at the same subsaturating concentrations Moreover, the magnitude of differences with respect to each ligand appeared to follow

Figure 4.9. Comparative binding of human recombinant and plasma clusterin to IgG, $A\beta_{1-40}$, and Zn^{+2} Polymerized C9 detected with G7

Unlabeled immunoaffinity purified *P. pastoris* human recombinant (solid circles and squares) and plasma clusterin (open circles and squares) were incubated at the indicated concentrations in 96 well polystyrene microtitre plates coated with 1 μg/mL Zn^{+2} polymerized C9 (circles in A), 1 μg/mL $A\beta_{1-40}$ (circles in B), 10 μg/mL IgG (circles in C) or 1% BSA (squares in A, B, C) at pH 6 (A, B) or pH 7 (C). Bound clusterin was detected with G7 as described in Methods and Materials. A. and B. are endpoint absorbance at 490 nm while in C. development of the assay was followed kinetically at 490 nm and presented as initial rate of change of absorbance.

A.

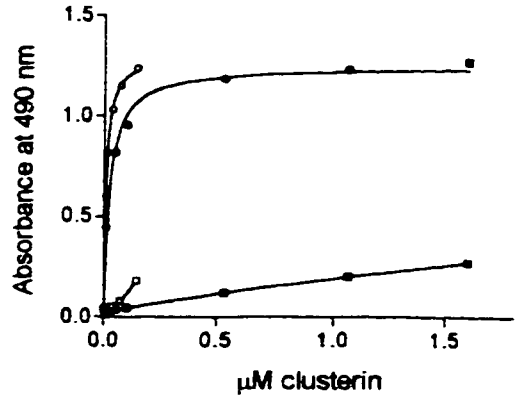
Absorbance at 490 nm
1.5
1.0
0.5
0.0
0.0
0.5
1.0
1.5
μM clusterin

B.

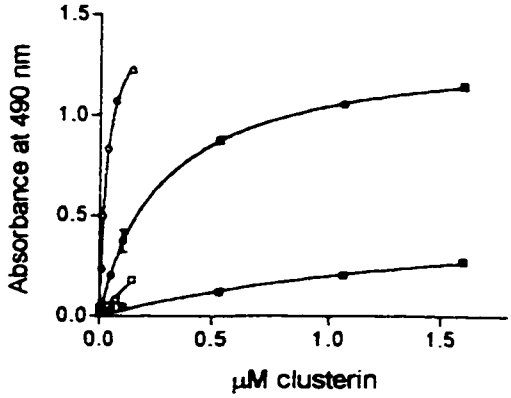
Absorbance at 490 nm
1.5
1.0
0.5
0.0
0.0
0.5
1.0
1.5
μM clusterin

C.

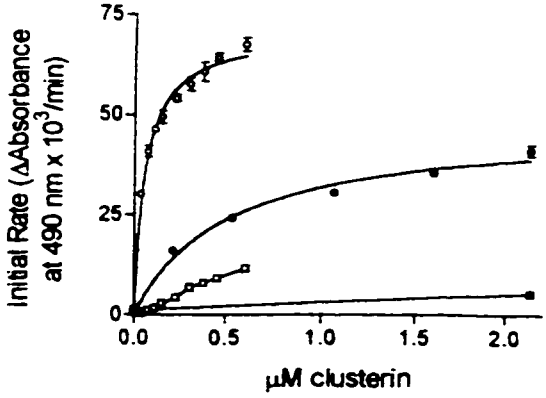
Initial Rate (ΔAbsorbance at 490 nm x 10³/min)
75
50
25
0
0.0
0.5
1.0
1.5
2.0
μM clusterin

the order seen in the competitive binding assays, that is a significantly smaller difference is observed between recombinant and serum/plasma clusterin for poly C9, followed by much larger differences for $A\beta_{1-40}$ and IgG.

1.1.9. Incorporation of recombinant clusterin into sC5b-9

To determine if recombinant clusterin is capable of interacting with ligands in solution as well as to immobilized ligands, a rapid assay was developed to determine the capacity of clusterin to become incorporated into the soluble complement attack complex (sC5b-9) formed spontaneously in serum using inulin to activate the alternative pathway. Clusterin is incorporated in this complex under these conditions, and can be copurified with it (Jenne et al., 1985; Choi et al., 1989; Jenne and Tschopp, 1989) (Appendix, Fig. 6.2 and 6.3, Appendix). A single spin through a 10 to 40% (w/w) linear sucrose gradient effectively separates clusterin incorporated into sC5b-9 from unincorporated clusterin in human serum (Appendix, Fig. 6.4). Clusterin copurified with sC5b-9 sediments to a position in the gradient ≥ 33% sucrose, peaking at about 35 to 36% sucrose. G7 detects at least five fold more clusterin in these fractions from inulin treated serum than from untreated serum, indicating that changes in clusterin present in these fractions are an effective measure of the incorporation of clusterin into sC5b-9. To determine whether *P. pastoris* recombinant clusterin is capable of interacting with complement components in serum, immunoaffinity purified preparations were labeled with biotin and added back to serum, which was subsequently treated with or without inulin. Fig. 4.10 shows that both biotin labeled recombinant and serum/plasma clusterin are substantially increased in fractions ≥ 33% sucrose and peaking at 35 to 36% sucrose from serum treated with inulin

Figure 4.10. Incorporation of biotin labeled *P.pastoris* human recombinant and plasma clusterin into sC5b-9 in inulin activated serum

Biotin labeled immunoaffinity purified human plasma (left two figures) or *P. pastoris* recombinant human clusterin (right two figures), was added exogenously to a 1:1 dilution of freshly prepared human serum and incubated with (bottom two figures) or without (top two figures) inulin for 6 to 8 h to activate sC5b-9 formation. Serum was fractionated by centrifugation through 10 to 40% (w/w) linear sucrose gradients as described in Methods and Materials. 5 µL of the bottom most successive 6 to 7 fractions, corresponding to the indicated gradient positions, were separated by electrophoresis under reducing conditions on 11% SDS polyacrylamide gels, blotted to nitrocellulose, and probed for biotin-labeled proteins with streptavidin HRP. Molecular weight markers in kDa are to the right. 5 ng of biotin labeled plasma or recombinant clusterin were run in parallel. Top brackets are positions in the gradient at which the majority of sC5b-9 is found.

Please note that sucrose concentration of fractions increases from left to right for biotin labeled human plasma clusterin and from right to left for recombinant human clusterin.

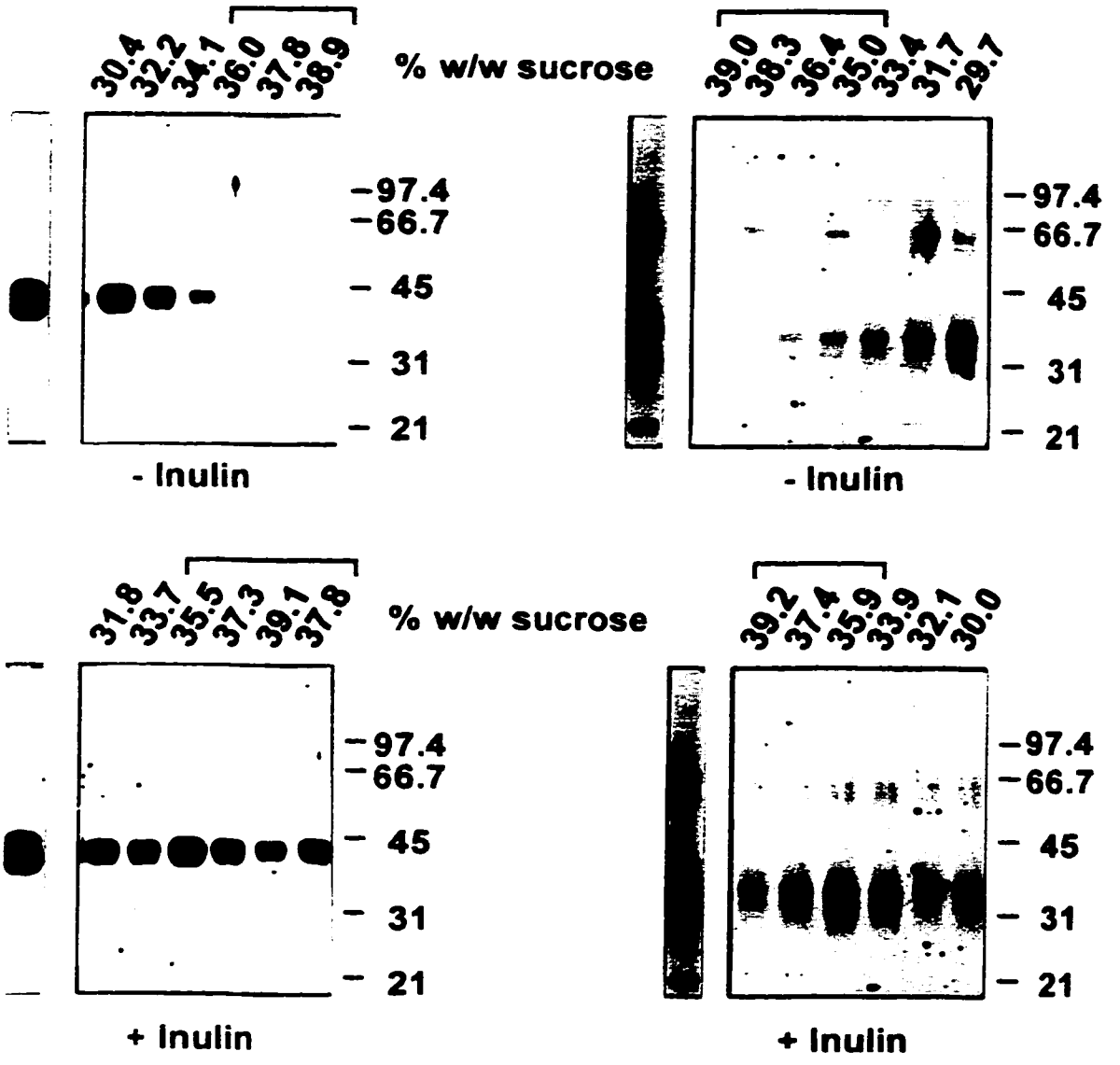
30.4
32.2
34.1
36.0
37.8
38.9
% w/w sucrose
39.0
38.3
36.4
35.0
33.4
31.7
29.7
97.4
66.7
45
31
21
- Inulin
- Inulin
31.8
33.7
35.5
37.3
39.1
37.8
% w/w sucrose
39.2
37.4
35.9
33.9
32.1
30.0
97.4
66.7
45
31
21
+ Inulin
+ Inulin

relative to the same fractions from untreated serum indicating that recombinant clusterin is capable of interacting with complement components in solution.

1.1.10. Specific binding of recombinant clusterin to LRP2 on differentiated F9 cells

I have hypothesized that LRP2 binds to a site distinct from that of presumed hydrophobic/amphipathic ligands. To determine whether decreases in the specific activity of recombinant clusterin in the interaction with presumed hydrophobic/amphipathic ligands would also be observed with LRP2, cell surface binding was measured to murine F9 teratocarcinoma cells differentiated *in vitro* with retinoic acid and dibutyryl cAMP. When treated over several days these cells undergo both molecular and morphological changes (Strickland and Mahdavi, 1978; Strickland et al., 1980) including a dramatic upregulation in the expression of LRP2 at the cell surface (Kounnas et al., 1995). In my hands, differentiated cells displayed morphological changes previously described including, at early times, colonies of flattened triangular shaped cells with refractile perinuclear granules and, at later times, ball-like nodules (Strickland and Mahdavi, 1978; Strickland et al., 1980). Fig. 4.11A shows that LRP2 expression is increased in differentiated F9 cells as previously described (Kounnas et al., 1995). Binding of ^{125}I labeled serum/plasma clusterin at 4° C to differentiated F9 cells is specific and of high affinity as shown by competition with unlabeled recombinant (Fig. 4.11B, open circles) and serum/plasma clusterin (Fig. 4.11B, closed circles), despite the observation of high proportional non specific binding (55 to 65% of total bound counts). Although reflecting larger experimental uncertainties, 95% confidence intervals are comparatively wide, unlabeled serum/plasma clusterin and recombinant clusterin are not measurably different

Figure 4.11. Competitive binding assay to measure the relative affinity of *P.pastoris* human recombinant and plasma clusterin for binding sites on differentiated F9 cells

A. Lysates were prepared from F9 cells grown for 8 days in the presence or absence of 0.1 μM retinoic acid (RA), and 0.2 μM dibutyryl cAMP (dB-cAMP) and 150 μg total protein from each was separated by electrophoresis on discontinuous 4 to 12% linear gradient SDS polyacrylamide gels, electroblotted to nitrocellulose and probed for the presence of LRP2 using the anti-rat LRP2 mouse monoclonal 1H2. The position of molecular weight standards (in kDa) run in parallel are indicated on the right and the immunoreactive band corresponding to LRP2 by the arrow.

B. ^{125}I labeled immunoaffinity purified human plasma clusterin (7.5 nM) was incubated at 4°C in the presence of the indicated concentrations of unlabeled immunoaffinity purified *P. pastoris* human recombinant (open circles) or plasma clusterin (closed circles) in gelatin coated 24 well plates containing $5x10^5$ differentiated F9 cells. After subtraction of bound counts in the presence of 100 fold molar excess of unlabeled competitor, data were normalized to cell number and fitted to the equation of a competitive inhibitor for one site binding.

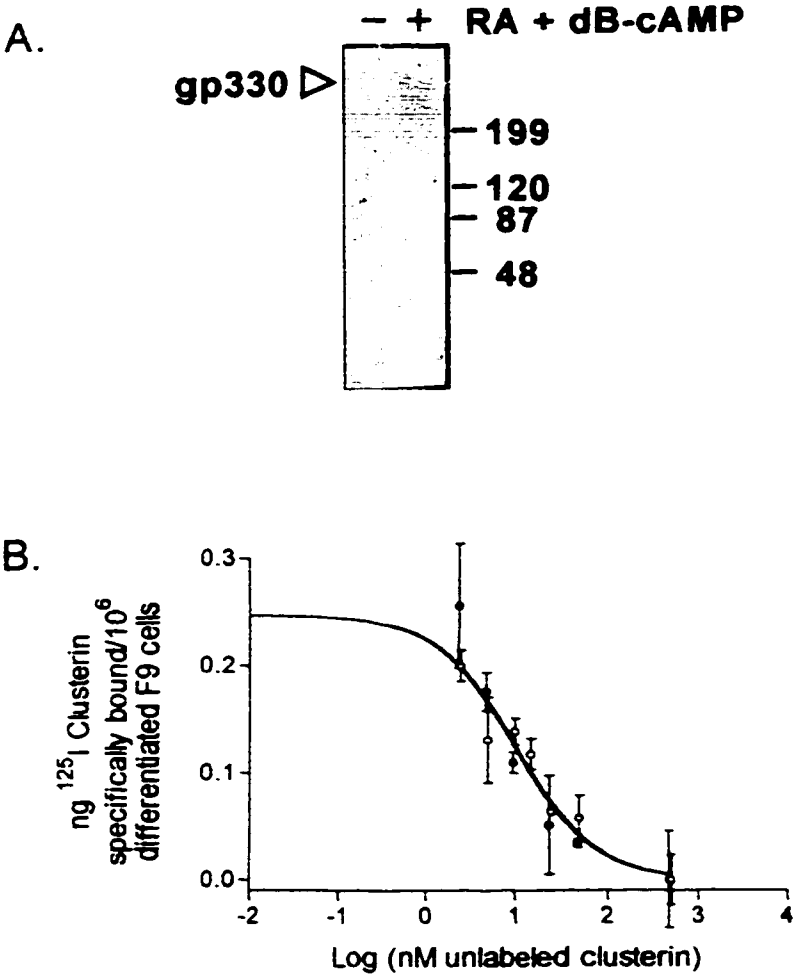
A.
− + RA + dB-cAMP
gp330
199
120
87
48
B.
ng 125I Clusterin specifically bound/10^6 differentiated F9 cells
0.3
0.2
0.1
0.0
-2
-1
0
1
2
3
4
Log (nM unlabeled clusterin)

as specific competitive inhibitors, with estimated IC_{50}s of 9.9 nM and 10.3 nM, respectively (Table 4.4).

1.1.11. Heterologous competition with Zn^{+2} polymerized C9 and $A\beta_{1-40}$

To test directly whether binding to $A\beta_{1-40}$, poly C9, and IgG might reflect a binding site that is shared or overlapping the ability of solution phase $A\beta_{1-40}$ and poly C9 to compete for binding of clusterin to immobilized ligands in heterologous competitions was assessed. Poly C9 in solution is a high affinity specific inhibitor for the binding of serum/plasma clusterin to all three immobilized ligands with an IC_{50} of 160 nM in the homologous competition (Fig. 4.12A, closed circles), 210 nM for IgG (Fig. 4.12A, open squares), and 250 nM for $A\beta_{1-40}$ (Fig. 4.12A, open circles) at pH 6. The effectiveness of $A\beta_{1-40}$ in solution as competitor was determined at both pH 6 (Fig. 4.12B, C, and D, closed circles) and pH 7 (Fig. 4.12B, C, and D, open circles). On a molar basis $A\beta_{1-40}$ is a less effective specific inhibitor than poly C9, but showed evidence of specific inhibition of binding to all three immobilized ligands, particularly at pH 6. In agreement with the observations of the effect of pH on clusterin binding to immobilized $A\beta_{1-40}$ it is a much less effective specific inhibitor at pH 7. The IC_{50} in the homologous competition is estimated at no more than 1.1 μM at pH 6 and 3.1 μM at pH 7 (Fig. 4.12B), 1.5 μM at pH 6 and 7.3 μM at pH 7 for IgG (Fig. 4.12C), and 1.2 μM at pH 6 and 10.8 μM at pH 7 for poly C9 (Fig. 4.11D). The IC_{50} for homologous competition with solution phase $A\beta_{1-40}$ is 50 times higher than that reported previously (Matsubara et al., 1995). However, these workers used a different protocol for their inhibition assays. In the experiments performed here significant differences may include shorter times of preincubation with

Figure 4.12. $A\beta_{1-40}$, and Zn^{+2} polymerized C9 as heterologous competitors of the interaction of clusterin with IgG, $A\beta_{1-40}$, Zn^{+2} polymerized C9

A. 1 μg/mL human plasma clusterin was preincubated for 45 min at 37°C in the presence of the indicated concentrations of Zn^{+2} polymerized C9 then added to 96 well polystyrene microtitre plates coated with 2.5 μg/mL IgG (open squares), 2 μg/mL $A\beta_{1-40}$ (open circles), or 1 μg/mL Zn^{+2} polymerized complement C9 (closed circles) at pH 6. Bound clusterin was detected with G7 as described in Methods and Materials. Data were normalized to binding in the absence of competitor and fitted to the equation of a competitive inhibitor for one site binding.

B. to D. 200 ng/mL (closed circles) or 500 ng/mL (open circles) of biotin labeled human plasma clusterin was preincubated for 45 min at 37°C with twice the indicated concentrations of $A\beta_{1-40}$ at pH 6 (closed circles) or 7 (open circles) in a buffer lacking BSA or Triton X-100. After preincubation samples were diluted by two fold with a buffer containing BSA and Triton X-100 to obtain final concentrations of 1% BSA and 0.1% Triton X-100 at the corresponding pH, and added to wells coated with 4 μg/mL $A\beta_{1-40}$ (B), 4 μg/mL IgG (C), or 5 μg/mL Zn^{+2} polymerized complement C9 (D). Bound labeled clusterin was detected as described in Methods and Materials. Data were normalized to the binding in the absence of competitor and fitted to the equation of a competitive inhibitor for one site binding.

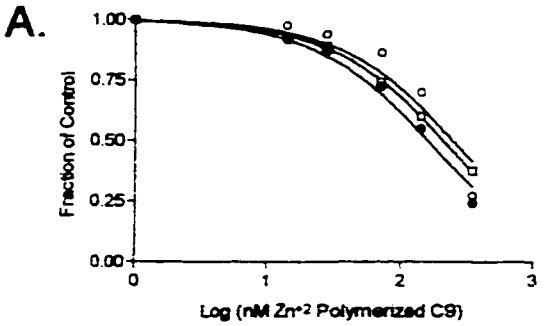
A.
1.00
0.75
0.50
0.25
0.00
Fraction of Control
0
1
2
3
Log (nM Zn+2 Polymerized C9)

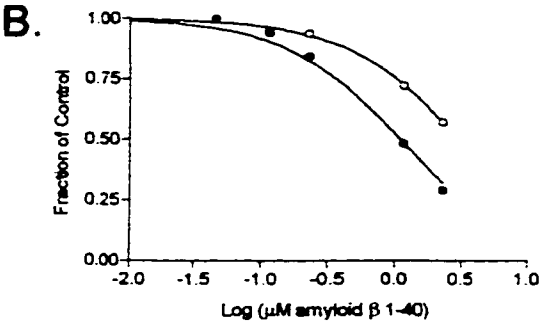
B.
1.00
0.75
0.50
0.25
0.00
Fraction of Control
-2.0
-1.5
-1.0
-0.5
0.0
0.5
1.0
Log (μM amyloid β 1-40)

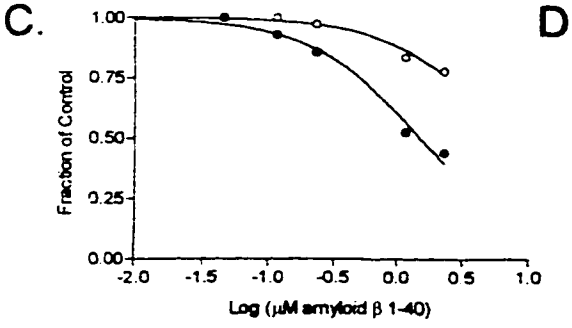
C.
1.00
0.75
0.50
0.25
0.00
Fraction of Control
-2.0
-1.5
-1.0
-0.5
0.0
0.5
1.0
Log (μM amyloid β 1-40)

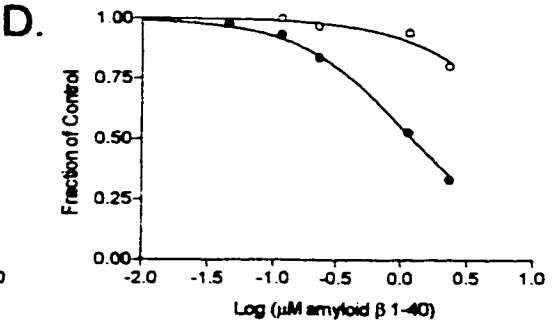
D.
1.00
0.75
0.50
0.25
0.00
Fraction of Control
-2.0
-1.5
-1.0
-0.5
0.0
0.5
1.0
Log (μM amyloid β 1-40)

solution phase peptide prior to addition to $A\beta_{1-40}$ coated wells, and coincubation in coated wells in the presence of BSA and Triton X-100 in contrast to physiological saline used in the previous study. Additionally, the history of the peptide may be significant. Aggregated $A\beta_{1-40}$ is a less effective solution phase inhibitor of clusterin binding to immobilized peptide than fresh, unaggregated peptide (Matsubara et al., 1995) and different sources of $A\beta_{1-40}$ differing by an order of magnitude in estimated β sheet content have been observed to give a corresponding order of magnitude difference in IC_{50} (1 to >10 μM) as inhibitors of binding of apoE3 to immobilized peptide (Golabek et al., 1996). In the experiments reported here no measurement of the state of aggregation or specific conformational content of the peptide used were made. However, regardless of the reason for differences in the observed magnitude of the effect, it is apparent that $A\beta_{1-40}$ is a specific heterologous competitor to binding of clusterin to IgG and poly C9.

1.1.12. Monoclonal antibody G7 inhibits binding to differentiated F9 cells

The monolconal antibody, G7 at 50 μg/mL (40 fold molar excess to ^{125}I-labeled clusterin) was found to inhibit essentially 100% of specific binding of ^{125}I-labeled clusterin to differentiated F9 cells (Fig. 4.13A). However, G7 is able to detect clusterin bound to $A\beta_{1-40}$, IgG, and poly C9 suggesting that the G7 epitope is distinct from the binding site for these ligands. This was confirmed by showing that over a concentration range at which G7 in solution was a high affinity competitive inhibitor of the binding of biotin labeled serum/plasma clusterin to immobilized G7 (IC_{50} = 3 μg/mL or 20 nM assuming a molecular weight of 150 kDa for IgG) (Fig. 4.13B, C, and D, open circles) there was little or no effect on binding to immobilized IgG (Fig. 4.13C), $A\beta_{1-40}$ (Fig.

Figure 4.13. G7 as a differential inhibitor of the interaction of clusterin with binding sites on differentiated F9 cells and IgG, $A\beta_{1-40}$, and Zn^{+2} polymerized C9

A. ^{125}I labeled immunoaffinity purified human plasma clusterin (7.5 nM) was preincubated for 1 h at 4°C with or without 52.5 µg/mL G7 in binding buffer then incubated in gelatin coated 24 well plates containing approximately $5x10^5$ differentiated F9 cells each. In parallel, differentiated F9 cells were incubated with labeled clusterin in the presence of 100 fold molar excess of unlabeled clusterin. After subtraction of bound counts in the presence of 100 fold molar excess of unlabeled clusterin, data were normalized to the number of cells per well.

B. to D. Biotin labeled immunoaffinity purified human plasma clusterin (500 ng/mL) was preincubated for 30 min at room temperature with G7 at the indicated concentrations then added to 96 well polystyrene microtitre plates coated with 2 µg/mL G7 (open circles in B, C, D), 4 µg/mL $A\beta_{1-40}$ (closed circles in B), 5 µg/mL IgG (closed circles in C), or 1.5 µg/mL Zn^{+2} polymerized complement C9 (closed circles in D) at pH 7. Bound labeled clusterin was detected as described in Methods and Materials. Data for inhibition of labeled clusterin binding to immobilized G7 by solution phase G7 were fitted to the equation of a competitive inhibitor for one site binding.

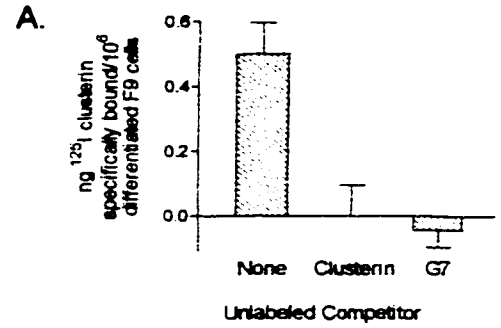
A.
ng ^{125}I clusterin specifically bound/10^6 differentiated F9 cells
0.6
0.4
0.2
0.0
None
Clusterin
G7
Unlabeled Competitor

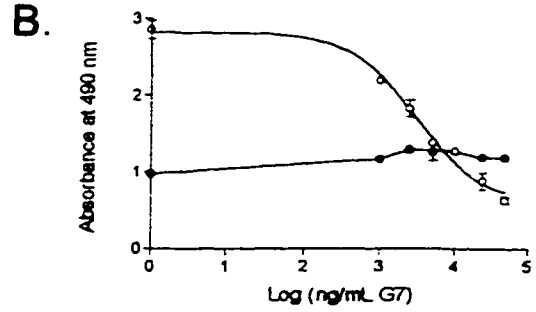
B.
Absorbance at 490 nm
3
2
1
0
0
1
2
3
4
5
Log (ng/mL G7)

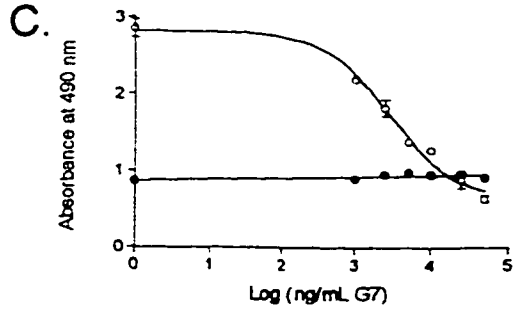
C.
Absorbance at 490 nm
3
2
1
0
0
1
2
3
4
5
Log (ng/mL G7)

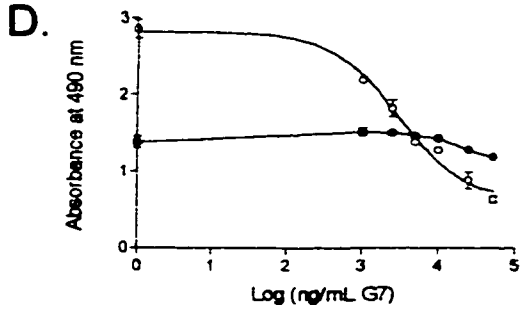
D.
Absorbance at 490 nm
3
2
1
0
0
1
2
3
4
5
Log (ng/mL G7)

4.13B), or poly C9 (Fig. 4.13D). For comparison with the inhibition of cell surface ligand binding, in the microtitre plate assay 50 μg/mL G7 inhibits essentially all epitope specific binding of a similar concentration of biotin labeled clusterin to immobilized G7 without effect on ligand binding to $A\beta_{1-40}$, poly C9, and IgG. These data suggest that the binding sites for G7 and LRP2 are the same or nearby and are distinct from those for $A\beta_{1-40}$, poly C9 and IgG.

1.1.13. Effect of chemical modification by DEPC on the interaction of clusterin with Zn^{+2} polymerized complement C9, IgG and $A\beta_{1-40}$

The role of histidine(s) in the binding of clusterin to immobilized ligands was investigated further using the histidine modification reagent diethyl pyrocarbonate (DEPC). Experimentally DEPC is relatively specific for histidine in the pH range 6 to 8, reacting with the deprotonated form of the imidazole ring to produce N-carbethoxy adducts (Miles, 1977). We reasoned that the N-carbethoxy adducts may affect binding properties by a steric mechanism and/or changes in imidazole pK_a. In model systems a difference absorption maximum in the region of 240 nm is observed between imidazole and N-carbethoxy imidazole side chains with $\varepsilon_{\Delta 240}$ = 3200/M-cm, which has been used to estimate the stoichiometry of modification of histidine residues in proteins (Miles, 1977). In initial experiments serum/plasma clusterin, at concentrations ranging from 1.5 to 3 μM was modified with DEPC at 0.1 to 1 mM over a pH range of 6 to 7, to determine optimal reaction conditions. The Δ240 nm progress curve for DEPC treatment of clusterin is approximately hyperbolic, typical of a rapid initial reaction slowing at later times presumably due to a combination of completion of the reaction and DEPC hydrolysis

Figure 4.14. Effect of DEPC modification on the interaction of clusterin with $A\beta_{1-40}$, IgG, and Zn^{+2} Polymerized C9

A. Human clusterin (1.5 μM) was modifed at room temperature in 15 mM K_2HPO_4-KH_2PO_4 pH 6, 50 mM NaCl with DEPC at concentrations of 0.1 mM (blue), 0.3 mM (purple), 0.5 mM (yellow), 0.7 mM (green) , and 1 mM (red) and the change in absorbance at 240 nm recorded as a function of time after DEPC addition.

B. Human clusterin (2.1 μM) was modified at room temperature with 0.3 mM DEPC in 30 mM K_2HPO_4-KH_2PO_4, 100 mM NaCl pH 6 (blue), 6.25 (purple), 6.5 (yellow), 6.75 (green) and 7 (red) and the change in absorbance at 240 nm recorded as a function of time after DEPC addition.

C. to G human clusterin (2.3 μM) was modified at room temperature with 0.5 mM DEPC in 20 mM K_2HPO_4-KH_2PO_4, 50 mM NaCl pH 6 (closed circles in C, D, E, F, and G) and 7 (open circles in C, D, E, F, and G). At various times after addition aliquots were withdrawn from the reaction, and the reaction stopped as described in Methods and Materials. The 0 time point was withdrawn prior to addition of DEPC. Modified clusterin at a final concentation of 10 μg/mL was used to compete 500 ng/mL of biotin labeled plasma clusterin in 96 well polystyrene microtitre plates coated with 1 μg/mL Zn^{+2} polymerized C9 (C, and red circles and lines in G), 1 μg/mL $A\beta_{1-40}$ (D, and green circles and lines in G), or 2 μg/mL IgG (E, and purple circles and lines in G). Bound clusterin was detected as described in Methods and Materials. Red broken lines in C, D, and E indicate the absorbance at 490 nm for competition by 10 μg/mL (100%), 7.5 μg/mL (75%), 5 μg/mL (50%), 2.5 μg/mL (25%), and 0 μg/mL (0%) of unlabeled, unmodified clusterin as estimated from competition curves prepared in parallel. F, time course of the change in absorbance at 240 nm after DEPC treatment at pH 6 (closed circles) and 7 (open circles) measured in parallel. Absorbance data for DEPC modified clusterin in C, D, and E, were converted to effective concentrations using the parallel competition curves for each ligand with unlabeled, unmodified human clusterin as standards and plotting this as a function of the corresponding change in absorbance at 240 nm estimated from F. Linear regression analysis was used to fit lines to the data at each pH of modification and for each ligand (pH 6, solid lines; pH 7, broken lines).

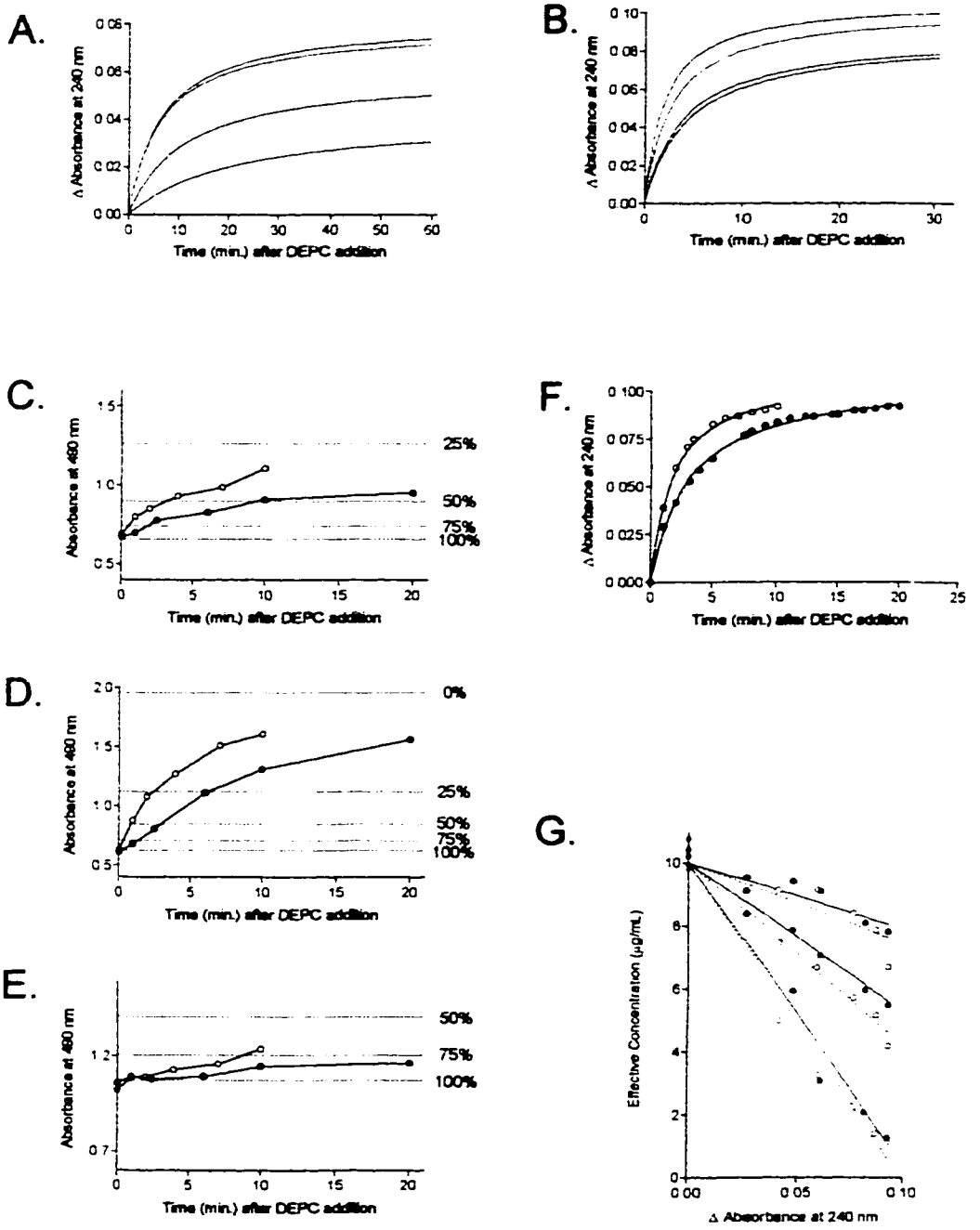
A.
Δ Absorbance at 240 nm
Time (min.) after DEPC addition
B.
Δ Absorbance at 240 nm
Time (min.) after DEPC addition
C.
Absorbance at 480 nm
25%
50%
75%
100%
Time (min.) after DEPC addition
F.
Δ Absorbance at 240 nm
Time (min.) after DEPC addition
D.
Absorbance at 480 nm
0%
25%
50%
75%
100%
Time (min.) after DEPC addition
G.
Effective Concentration (μg/mL)
Δ Absorbance at 240 nm
E.
Absorbance at 480 nm
50%
75%
100%
Time (min.) after DEPC addition

(Fig. 4.14A). Using 1.5 μM clusterin at pH 6 the initial rate and extent of reaction increase rapidly between 0.1 and 0.5 mM DEPC, more gradually above 0.5 mM and is virtually identical at 0.7 and 1 mM, suggesting that DEPC concentrations are not rate limiting at the higher concentrations but become so between 0.7 and 0.5 mM. At concentrations of clusterin to DEPC that were rate limiting with respect to DEPC there are also increases in the initial rate and extent of reaction as the pH is increased from 6 to 7, as expected for the greater reactivity of deprotonated imidazole side chains (Fig. 4.14B). No significant changes are observed in the absorbance at 280 nm that would suggest O-carbethoxylation of tyrosine (data not shown), so that most changes in absorbance observed at 240 nm may be ascribed to modification of histidine residues in particular (Miles, 1977).

To study the effect of DEPC modification on clusterin binding activity concentrations of clusterin and DEPC were chosen that were intermediate in terms of rate and extent at pH 6 and 7, to facilitate isolation of intermediate states of modification. Samples of clusterin withdrawn at intervals after initiation of modification were terminated by dilution into a stop/binding buffer at a fixed final concentration determined previously to obtain a level of competition with the binding of labeled clusterin to immobilized $A\beta_{1-40}$, poly C9, and IgG, lying within the descending segment of the competition curve where changes in the assay response are most sensitive to the concentration of unlabeled, unmodified competitor. The competition was measured at pH 7 using a concentration of labeled clusterin that gave only a small binding to BSA coated wells. Increases in assay response corresponding to a decrease in relative effectiveness as

an unlabeled competitor are observed for all three ligands as a function of time after addition of DEPC and degree of modification (Fig. 4.14C, D, and E). Decreases in relative competitive effectiveness are more rapid when modified at pH 7 than 6 but when expressed as a function of degree of modification no apparent difference was observed between modification at pH 6 and 7 for each ligand (Fig. 4.14 G, compare solid and open circles). There is no evidence of more than one phase to the relationship between relative competitive effectiveness and degree of modification for each ligand, particularly for $A\beta_{1-40}$ and poly C9. There are however, considerable differences among the three ligands with respect to sensitivity of clusterin binding to DEPC modification. At maximal levels of modification clusterin competed with the labeled form for binding to immobilized $A\beta_{1-40}$ at a level equivalent to 10 to 20% of its nominal concentration (Fig. 4.14D, and Fig. 4.14G, green), 45 to 55% to poly C9 (Fig. 4.14C, and Fig. 4.14G, red), and 80 to 85% to IgG (Fig. 4.14E, and Fig. 4.14G, purple).

1.3. Discussion

1.3.1. Structure of human serum/plasma clusterin

Human clusterin was purified to homogeneity from serum/plasma using immunoaffinity chromatogaphy. As reported a Triton X-100 wash of the column prior to low pH dissociation of clusterin antibody complexes obtained eluates essentially free of copurifying apoAI-HDL (Jenne et al., 1991). However, small amounts of copurifiying IgG were present, which may represent IgG bound non covalently to clusterin or small amounts of G7 bleeding from the column. By SDS PAGE the majority of human clusterin in these preparations was a 67-68 kDa band constituted of a disulfide linked

dimer of approximately 37 to 39 kDa chains. Both chains were N-glycosylated and when associated carbohydrate was enzymatically removed denuded polypeptides of 26 (α) and 28 kDa (β) were revealed.

1.3.2. Structure of recombinant human clusterin secreted by *P. pastoris*

To develop a system in which hypotheses concerning clusterin structure and activity could be studied human clusterin was expressed as a recombinant protein in the methylotrophic yeast *P.pastoris*. The full length human cDNA was placed under control of the methanol inducible AOX1 promoter, assuming that the clusterin secretory signal sequence would direct expression along the constitutive secretory pathway. High levels of human clusterin were measured in conditioned medium in the presence of methanol and were recovered in a relatively pure state by ethanol precipitation from unmodified medium or by G7 immunoaffinity chromatography of a modified medium containing 10 mg/mL casein. Based on N-terminal sequencing results that detected only the α N-terminus corresponding to removal of the secretory signal peptide, the presence of N-linked carbohydrate on the majority of recombinant clusterin polypeptides, and identification of a disulfide linked heterodimer, most if not all clusterin recovered is secreted via the constitutive secretory pathway. The occurence of an α/β heterodimeric disulfide linked structure for most of recombinant clusterin is a surprise as it suggests that unknown yeast protease(s) must efficiently cleave the polypeptide at least once between the cysteine rich domains. Two sites of proteolysis have been identified in the β chain and appear to account for the two major forms of this chain; the full length 28 kDa (N-deglycosylated) form having the N-terminus of the secreted heterodimer isolated from

natural sources and a 23 kDa form produced by a 36 amino acid N-terminal truncation of the full length form. It is likely that minor dimeric forms also consist of a further truncation of the β chain. Preliminary analysis of deglycosylated, ethanol-precipitated preparations of *P. pastoris* recombinant rat clusterin α and β chains, using liquid chromatography mass spectrometry (LCMS) and N-terminal sequencing have identified minor amounts of a C-terminal β derived peptide corresponding to 326 to 447 of the rat clusterin preproprotein (Personal Communication, Dr. Jim Kapron). A similar cleavage event may also generate further minor truncated forms of the human recombinant β chain.

In contrast smaller amounts of the full length 26 kDa (N-deglycosylated) α chain are present, with most of the α chains cleaved at one or more additional sites to generate a larger number of truncated forms. The minor 24 and more abundant 21 kDa forms have the mature α N-teminus and thus correspond solely to C-terminal truncations. Most of the larger truncations, corresponding to forms of 15 to 21 kDa (N-deglycosylated) may also correspond solely to C-terminal truncations although at present this is not based on direct N-terminal sequencing of deglycosylated preparations separated on two dimensional gels. Rather it is based on the failure to detect evidence of any other N-terminus other than that of the mature α N-terminus from sequencing of the major N-glycosylated reduced polypeptides separated by SDS PAGE. Since these PVDF sequences were somewhat "noisy", and only discrete and discontinuous positions between 36 and 20 kDa were sampled for sequencing, it remains possible that some of these α forms are the result of a combination of N and C-terminal truncations, the N-termini of which are either not

clearly distinguishable or lie at one or more unsampled positions in blots. LCMS and N-terminal sequence analysis of recombinant rat clusterin α and β chains have identified several fractions corresponding to polypeptides with the mature α N-terminus that give rise to major ion species that can be related to the molecular weight of identifiable α N-terminal fragments (Personal communication, Dr. Jim Kapron). These include α1-119 ($M_{obs.}$ 15276.21 Da; SD = 4.55; 3 ion species; compare $M_{calc.}$ 15273.4 Da), α1-148 ($M_{obs.}$ 17531.17 Da; SD = 6.24; 3 ion species; compare $M_{calc.}$ 17533.8 Da), α1-171 ($M_{obs.}$ 20136.65 Da; SD = 3.02; 4 ion species compare $M_{calc.}$ 20137.7 Da), α1-172 ($M_{obs.}$ 20285.84 Da; SD = 1.04; 4 ion species compare $M_{calc.}$ 20284.9 Da), and α1-195 ($M_{obs.}$ 23094.42 Da; SD = 2.75; 2 ion species compare $M_{calc.}$ 23094.1 Da). The position of the implied proteolytic cleavage sites all lie within exon 5 and are very close to some of those estimated from molecular weights of recombinant human clusterin separated by SDS PAGE. In particular, probable rat recombinant α N-terminal fragments with mass less than approximately 20.5 kDa are consistent with the identification of at least some if not all human recombinant α chain forms less than 20.5 kDa on SDS PAGE with solely C-terminal truncations.

1.1.3. Implications of patterns of limited proteolysis in recombinant clusterin

If all forms of the α chain are related to the full length chain solely as C-terminal truncations the corresponding sites of proteolysis may be estimated, based on the size of the N-deglycosylated form on SDS PAGE (Fig. 4.4). From this analysis most if not all cleavage events are likely to occur within sequences encoded by exon 5 under the conditions prevailing during expression. The observation that no significant degradation

of the protein appears to take place beyond the β23:α15 kDa heterodimer suggests that what remains represents a structually resistant core consisting of the disulfide linked domain, the proposed coiled-coil and the domain encoded by exon 8. Proteolytic sensitivity in folded proteins is determined by the sequence specificity of the protease and by the conformational accessiblity of the target bond to the catalytic site of the protease. The sensitivity of exon 5 encoded sequences to *P. pastoris* proteases may reflect surface association of these sequences and/or a high degree of chain flexibility. Exon 5 encodes sequences that are less well conserved and feature the largest number of gaps to optimize alignments (Fig. 1.1), structural properties that suggest surface associated connecting elements between regular pieces of secondary structure. In addition exon 5 encoded sequences are relatively rich in proline residues (Fig. 4.4), which by disrupting regular secondary structure may render these sequences flexible and proteolytically sensitive. By contrast, resistance of the remainder of the protein may be a direct consequence of conformational rigidity resulting from a high degree of regular secondary structure, such as might be expected in particular for the disulfide and coiled-coil domains. This differential sensitivity is similar to that noted for newly synthesized canine clusterin in the endoplasmic reticulum (Wada et al., 1994). Non oxidized, unprocessed, unfolded clusterin associated with calnexin in the endoplasmic reticulum is rapidly degraded by proteinase K with no evidence of resistant domains. This pattern changes however, shortly after formation of disulfide bonds. In particular, the pattern of proteinase K sensitivity is most compatible with cleavage first within exon 5 encoded sequences to generate an array of disulfide linked dimers (Wada et al., 1994). It is notable that these observations echo the domain model proposed in Chapter 3 and may imply that

these domains are to some extent structurally independent. Interestingly, the minor β C-terminal peptide identified by LCMS in recombinant rat clusterin implies cleavage at a site two amino acids N-terminal to the coding junction of exons 7 and 8 of the rat gene and constitutes all of the coding potential of exon 8. This may reflect the proteolytic sensitivity of junctional sequences that connect structurally distinct and resistant domains formed from exon 8 encoded sequences and the putative coiled-coil.

In addition to these observations, the pattern of α/β dimers resulting from proteolysis suggests that events in each chain may not be independent. Essentially, no dimers consisting of the full length 28 kDa β chain are observed with forms of α less than 21 kDa while β23 is associated with additional α forms less than 21 kDa down to and including 15 kDa. This suggests an interdependence of the proteolytic events that result in β23 and those that result in α forms less than 21 kDa and supports the suggestion of an overall structural fold featuring important mutual non-covalent interactions between chains rather than one in which the chains fold more or less independently. Limited proteolysis may follow a sequential course when one event is required to render another sensitive and the association of α proteolytic sites with the site of proteolysis in the β chain may reflect such a sequential pathway. Comparison of patterns of proteolysis in the presence and absence of casein appears to support this conclusion. Under otherwise similar conditions of expression, for which it is assumed that there are comparable times of exposure to and levels of extracellular proteases, in the presence of casein there were proportional increases of α26, 24 and 21 kDa and β28 kDa, in association with proportional decreases in α19 to 15 kDa and β23 kDa bands that

predominate in the absence of casein, suggesting that the former group have a precursor-product relationship to the latter. A sequential proteolytic pathway consistent with these observations is for disulfide linked dimers with the structure α26:β28, α24.4:β28 and α 20.5:β28 to be cleaved at βH36-αS37 to produce dimers of the form α26:β22.7, α24.4:β 22.7 and α20.5:β22.7 and for this proteolytic event to subsequently dispose the protein to proteolysis at sites which generate α forms less than 20.5 kDa. Because most secreted clusterin is processed between the cysteine rich domains and no processing event appears to yield forms of either the α or β chain that are greater than 26 and 28 kDa, respectively, whether in the presence or absence of casein, limited proteolysis at the natural site, α R205-βS1 must occur with a high degree of efficiency. Given the many-fold dilution of clusterin and proteases following secretion and the presence of casein as competitor, such efficiency seems incompatible with extracellular proteolysis and likely occurs intracellularly. Clusterin may be processed at this site by an endoprotease, prior to secretion, with a specificity similar to that of mammals and birds.

Interestingly, when mapped onto the linear antiparallel model of clusterin structure in Chapter 3, the estimated site of the proteolytic event giving rise to the 21 kDa α form (Fig. 4.4, c) is very nearly colinear with the natural β N-terminus while that giving rise to the 15 kDa α form (Fig. 4.4, f) may be colinear with the N-terminus of β23. This spatial correspondence between structurally "communicating" sites suggests that there is some physical meaning to the literal development of the implications of the model along the lines of local interactions in the exon 5 encoded domain, in addition to those known in the disulfide domain and hypothesized in the coiled-coil domain.

1.1.4. Implications of *P. pastoris* recombinant clusterin binding activities and heterologous ligand competitions for ligand binding sites

Recombinant human clusterin purified from casein-supplemented conditioned medium is functional in the interaction with several clusterin ligands including IgG, $A\beta_{1-40}$, poly C9 and LRP2. It is a high affinity competitive inhibitor of the binding of labeled serum/plasma clusterin to each ligand, and forms specific and stable complexes with IgG, $A\beta_{1-40}$, and poly C9, as shown by detecting such complexes with monoclonal antibody G7. In addition, the recombinant protein specifically incorporates into newly forming sC5b-9 in serum.

The specific activity of recombinant clusterin in the competitive binding assay to differentiated F9 cells is not significantly different from serum/plasma clusterin. Recombinant clusterin is slightly less effective as a specific inhibitor in competitive binding assays to poly C9 but substantially less effective as a specific inhibitor in binding assays to IgG and $A\beta_{1-40}$. Similar results are obtained using G7 to directly detect stably bound complexes. Whereas at the same subsaturating concentration slightly less recombinant than serum/plasma clusterin is stably bound to poly C9, much less is stably bound at the same concentration to IgG and $A\beta_{1-40}$.

Most recombinant clusterin has an α/β disulfide linked heterodimeric structure and was purified using a monoclonal antibody affinity column with a reactivity dependent upon appropriate chain associations. Thus, differences in activity are not likely to be the consequence of large scale structural changes associated with misfolding. While

it is possible that heterogeneity in the addition reported here, and/or known differences between *P. pastoris* and mammalian cells in the structure and composition of N-linked glycans, might contribute to these differences, it is interesting that recombinant preparations are also characterized by endoproteolysis within exon 5 encoded sequences that give rise to a heterogeneous mix of dimers. In particular, major sites of proteolysis affect the hypothesized hydrophobic/amphipathic ligand binding site. The 36 amino acid N-terminal truncation of the β chain includes all of the predicted Domain 3 β chain amphipathic α helix, and the proteolytic site accounting for the major 20.5 kDa α form may lie in the middle of the corresponding α chain amphipathic α helix (Fig. 4.4). Similar large decreases in the specific activity of recombinant preparations in binding to IgG and $A\beta_{1-40}$ are consistent with the proposed localization of a promiscuous binding site for such ligands in these sequences.

Contrary to expectation however, partial proteolysis within exon 5 encoded sequences was not associated with similarly dramatic effects on the interaction with poly C9. This suggests that the binding site for C9 on clusterin may be distinct from that of both IgG, and $A\beta_{1-40}$, and may not correspond to exon 5 encoded amphipathic α helices. On the other hand, poly C9 is an effective heterologous competitor of the interaction of clusterin with both IgG and $A\beta_{1-40}$. In addition $A\beta_{1-40}$, particularly at pH 6, inhibits the interaction of clusterin with poly C9 and IgG. It is possible that the poly C9 and the $A\beta_{1-40}$/IgG binding sites are situated closely in space and competition is based on a steric mechanism rather than strict competition for the same site. Recent results suggest that clusterin may bind to activated C9 principally at a site other than the amphipathic

membrane binding site of C9. Clusterin reportedly binds to the denatured 20 kDa C-terminal tryptic fragment of the C9b thrombolytic fragment, in addition to the 50 kDa N-terminal fragment that contains the putative amphipathic α helices that constitute the presumed membrane binding site (Tschopp et al., 1993). Moreover, incubation of sC5b-9 with deoxycholate dissociates only a small proportion of clusterin incorporated into the complex, suggesting that the physicochemical basis of the interaction may not be hydrophobic (Tschopp et al., 1993). Perhaps most significantly, clusterin can bind to complement complexes already assembled on membranes by means of a C9 binding site on bound C8 or C9 despite the likelihood that their respective membrane binding sites are already occupied by interactions with the target membrane (McDonald and Nelsestuen, 1997). These authors have recently suggested that clusterin may inhibit complement complex assembly at two levels (McDonald and Nelsestuen, 1997). Inhibition at the level of C7 may involve binding of clusterin to the membrane binding site of C7 in metastable fluid phase C5b-7 prior to assembly with target membranes. Such an interaction may involve the proposed promiscuous hydrophobic/amphipathic ligand binding site encoded by exon 5 in clusterin. Clusterin inhibition of C9 assembly into membrane bound C5b-8 and C5b-9_n may involve binding to a site in assembled C8 or C9 critical to the protein-protein interactions necessary for subsequent C9 incorporation, and may involve a distinct site on clusterin. Thus, clusterin binding to Zn^{+2} polymerized C9 *in vitro*, in which C9 is thought to be structurally analogous to its state in C5b-9_n (Podack and Tschopp, 1982; Tschopp, 1984), may represent primarily the latter interaction, although the absence of target cell membranes may permit some interaction between the membrane binding sites of poly C9 and the exon 5 encoded hydrophobic/amphipathic

ligand binding site of clusterin. The 20 kDa tryptic fragment of thrombolytic C9b contains a cysteine rich EGF-like domain and may represent the principal clusterin binding site on C9 (Esser, 1994). Limited homology to part of the N-terminal thrombospondin like repeat of C7, C8α, C8β, and C9 and a central portion of the cysteine rich domain of the α chain of clusterin has been suggested (Kirszbaum et al., 1989) and may reflect a C8/C9 binding site on clusterin. The structural stability of this domain in recombinant clusterin is certainly consistent with the relatively high specific activity of recombinant preparations in interactions with poly C9. The implication of a distinct binding site for C9 supports a specific physiological relation to C9 and argues against a strictly general protective role for clusterin as a promiscuous binding protein for structurally diverse hydrophobic/amphipathic ligands.

The similar apparent affinities of recombinant and serum/plasma clusterin in binding to differentiated F9 cells is also notably associated with the structural stability of the putative coiled-coil domain, consistent with the localization of the LRP2 binding site to this domain. The clusterin binding site on LRP2 is likely to be the second cluster of cysteine rich low density lipoprotein receptor (LDLR) related ligand binding repeats, based on studies identifying this as the binding site for apoE (Orlando et al., 1997), a heterologous competitor for the binding of clusterin to LRP2 (Kounnas et al., 1995). Interestingly, C9 contains a single LDLR related ligand binding repeat suggesting the possibility that the clusterin LRP2 binding site may bind this repeat in C9 (Esser, 1994). However, monoclonal antibody G7 specifically inhibited binding to differentiated F9 cells, but had no effect on binding to poly C9 arguing that the C9 and LRP2 binding sites

are distinct. This agrees with studies showing that clusterin does not bind to the denatured C9a thrombolytic fragment that contains the LDLR related binding repeat (Tschopp et al., 1993). Thus, there may be three distinct ligand binding sites on clusterin. The separation of the LRP2 binding site from other clusterin ligands is consistent with the hypothesis that LRP2 is a clearance and/or transport receptor for clusterin ligand complexes as implied by recent studies showing that $A\beta_{1-40}$ binding to, and endocytosis by, a receptor immunologically related to LRP2 is clusterin dependent (Zlokovic et al., 1996b).

The clusterin-LRP2 inhibitory binding activity of G7 suggests that the G7 epitope is proximal to the LRP2 binding site. Although sensitive recognition of clusterin by G7 requires appropriate α and β interchain interactions it appears to weakly recognize the α subunit by Western blot (Fig. 6.1, Appendix). Thus, the epitope may lie largely within the α chain but require β chain interactions to efficiently assume the appropriate conformation. Western blots of N-deglycosylated recombinant clusterin suggest that G7 recognizes at least the α21 kDa fragment indicating that the G7 epitope lies towards the α N-terminus and the proposed LRP2 binding, predominately α chain, cationic domain. However, G7 does not appear to recognize α derived polypeptides of molecular weight less than 21 kDa on Western blot (Fig. 6.1, Appendix), despite the fact that if exclusively C-terminal none of these truncations is estimated to extend into the LRP2 binding site. If these truncations eliminate the G7 epitope then the LRP2 binding site may be misassigned or the G7 epitope and LRP binding site may be proximal but not identical. Alternatively, this may be an issue of sensitivity since G7 immunoaffinity preparations of

recombinant clusterin contain small yields of heterodimers of the form α(19 to 15):β23 suggesting that these α derived fragments may contain the epitope. A more complete and refined mapping of this epitope and of the conditions of its recognition by G7 should contribute to an understanding of the location, structure and activity of clusterin binding sites.

1.1.5. *P. pastoris* as a host for recombinant human clusterin expression

As a model organism for the high level expression of mammalian clusterin *P. pastoris* presents both advantages and disadvantages. Expression levels are very high, the organism is simple to culture, and transform and offers a rapid turnaround time for the preparation and analysis of specifically introduced mutations. Secreted recombinant clusterin retains structural and functional hallmarks of the serum/plasma protein including a disulfide linked heterodimeric structure, conformation dependent immunoreactivity, and ligand binding acitivity. In the case of complement C9 and LRP2, the specific binding activity is similar to that of the non recombinant protein implying that *P. pastoris* is a suitable host for mutagenic based structure/function studies related to these ligands. However, similar studies of the interaction with IgG, or $A\beta_{1-40}$ may encounter interpretive difficulties related to heterogeneity in proteolytic processing, unless a method to purify appropriately processed dimers is developed. It may be possible to use a ligand based method, such as an $A\beta_{1-40}$ affinity matrix, or a chromatographic method based on hydrophobicity. For example, RP-HPLC of recombinant immunoaffinity preparations was shown to resolve, as a later eluting set of peaks, dimers containing the intact β chain from those in which the 36 amino acid

amphipathic N-terminal peptide had been truncated. Of itself, limited proteolysis accompanying expression in *P. pastoris* may be turned to further advantage in developing more refined structure/function maps. For example, a more accurate quantification of particular dimers in individual preparations may be obtained by phosphorimaging of N-deglycosylated, metabolically labeled clusterin resolved on two dimensional gels. Measurement of activities associated with such preparations could allow the identification of correlations with particular proteolytic events. In addition, the differential activity of these recombinant preparations should find experimental utility in classifying the structural basis of other clusterin activities such as cell aggregation (Blaschuk et al., 1983; Fritz et al., 1983), cholesterol efflux (Gelissen et al., 1998), and protection against atherogenic conditioning of LDL (Navab et al., 1997), which are currently poorly understood in these terms.

1.1.6. Histidine ionization and pH regulation of clusterin ligand binding activity

In Chapter 3 I hypothesized that ionization of histidine residues may serve a role in regulation of clusterin activity. This has potential (patho)physiological significance since clusterin is found and/or expressed in constitutively and/or transiently in acidified environments. One possibility, given the localization of histidines in, or adjacent to, exon 5 encoded amphipathic α helices, is that ionization might affect ligand binding activity, particularly of hydrophobic/amphipathic ligands. For this reason I studied the variation in binding to IgG, $A\beta_{1-40}$, and poly C9 as a function of pH. I anticipated that similarities in behavior as a function of pH would suggest a common mode of regulation attributable to a common binding site on clusterin.

There is however, a wide variation observed in changes in the degree of stable clusterin binding to IgG, $A\beta_{1-40}$, and poly C9 as a function of pH over a range of 7.5 to 5. These are consistent whether measured as biotin-labeled or G7-immunoreactive clusterin bound. High levels of clusterin are stably bound to poly C9 at all pH and relative to these, changes observed over this pH range were small and thus unlikely to be significant. In contrast, stable binding to both IgG and $A\beta_{1-40}$, increases, dramatically for the latter, as the pH was lowered from 7.5 to 6. Below pH 6 binding to $A\beta_{1-40}$ decreases again while that to IgG remains relatively stable to pH 5. In light of the suggestion that the principal C9 binding site may be distinct, these differences between IgG and $A\beta_{1-40}$, and poly C9 might be expected.

To investigate further a possible role for histidine residues in clusterin ligand binding, the effect of N-carbethoxylation of the imidazole side chains with DEPC on binding to IgG, poly C9 and $A\beta_{1-40}$ was studied. Modification with DEPC variably diminishes the specific interaction of clusterin with all three ligands. The decrease in effective competitiveness appears to be well correlated with the difference in absorbance at 240 nm and is not significantly different when clusterin was modified at pH 6 or pH 7, despite the fact that the reaction proceeds at a slower rate at pH 6 due to the lower reactivity of protonated imidazole side chains. The absorbance difference at 240 nm appears to reflect only the contribution of histidines as there were no observed change in absorbance at 280 nm attributable to O-carbethoxylation of tyrosine (Miles, 1977). Thus, decreases in activity for all three ligands are likely to be causally related to modification of histidine(s). It is not clear which specific histidine(s) might be related to these activity

changes and whether each ligand shares the same one(s). In the case of poly C9 and $A\beta_{1-40}$ at least, there appears to be a linear relationship between the relative effective competitiveness and the difference in absorbance at 240 nm over the entire range of the latter. Although multiple distinct models relating modification to decreases in activity might be fit to this observation, the simplest model is one in which modification of a small subset of all histidines, having no unusually pronounced reactivity, has a deterministic effect on binding affinity.

There is however, no simple correlation between the effect of pH on stable binding of clusterin to ligands and the effects of DEPC modification of histidine residues. Binding of poly C9 is relatively unaffected by mild acidification and yet is intermediate in sensitivity to DEPC modification of clusterin. Binding to IgG shows intermediate increases in binding in response to mild acidification yet is least affected by DEPC modification of clusterin. Separate binding sites may explain the differences between poly C9 and $A\beta_{1-40}$ and IgG. If, as suggested by heterologous competition, these sites are closely situated in space, it is possibile that the same DEPC modified histidine(s) may have both direct and indirect effects on each site. However, the differences between $A\beta_{1-40}$ and IgG seem more problematic in light of a simple hypothesis that clusterin histidine ionization might regulate hydrophobic/amphipathic ligand binding in a general way, and that both ligands use the same site. The profound sensitivity of the clusterin-$A\beta_{1-40}$ interaction to DEPC modification may argue for interactions mediated by clusterin histidine(s) specific for $A\beta_{1-40}$.

One possibility for the marked pH dependence of the clusterin-$A\beta_{1-40}$ interaction is that the relevant event(s) mediating these changes take place not only on clusterin but on $A\beta_{1-40}$. Aggregation of Aβ4 synthetic petides *in vitro* is dependent on pH and is markedly enhanced at mildly acidic pH (Burdick et al., 1992). This is in part due to isoelectric precipitation. Maximal levels of clusterin bound to $A\beta_{1-40}$ correspond to an acidic pH at which both clusterin and $A\beta_{1-40}$ are predicted to be near their isoelectric points, suggesting that increases in stable binding may be the result, in part, of a decrease in ionic repulsion.

However, it is unclear that such a mechanism can account for such a dramatic increase in stable binding of clusterin to $A\beta_{1-40}$ at low pH. Moreover, it is also unclear as to why the interaction should demonstrate such a profound sensitivity to the modification of clusterin by DEPC. These results may be more compatible with the binding of clusterin to a specific pH-induced conformational form of $A\beta_{1-40}$ involving one or more specific (clusterin) imidazole-($A\beta_{1-40}$) carboxylate salt bridges. pH induced conformational changes have been described for Aβ4 derived peptides, and proposed to account in large part for the pH dependence of fibrillogenesis (Kelly, 1996). Using ^1H NMR, $A\beta_{10-35}$ has been shown to be unstructured at pH 2.1 but to assume a specific conformation at pH 5.6 (Lee et al., 1995). This change is associated with an increase in fibrillogenic capacity of the peptide between pH 4 and pH 5.6 to pH 9 (Lee et al., 1995). The pH dependence of $A\beta_{9-25}$ fibrillogenesis measured by flourescence energy transfer is compatible with four acid/base equilibria proposed to correspond to ionization of two histidines, H13 and H14 (predicted pK_as of 5.86 and 7.6), and to two acidic side chains of

E11, E22 or D23 (predicted pK_a of 3.96 for both) in the peptide (Jackson Huang et al., 1997). Fibrillogenesis increases dramatically as the pH decreases from neutral to the maximum observed at pH 5 when all four species are predicted to be ionized. The effect of ionic strength on the pH dependence of fibrillogenesis of this peptide is more compatible with screening of a pair of specific imidazole-carboxylate salt bridges per monomer stabilizing the monomer in the fibril than with isoelectric precipitation solely (Jackson Huang et al., 1997). The ^1H NMR study also obtained evidence of a stabilizing imidazole-carboxylate salt bridge in the fibrillogenically active peptide (Lee et al., 1995). Thus, it is possible that much of the increase in stable binding of clusterin to $A\beta_{1-40}$ is a consequence of a conformational change in the immobilized peptide. Moreover, this may be a fibrillogenically active form of the peptide. In this regard it is notable that imidazole-carboxylate salt bridges are implicated in stabilizing Aβ fibrils since the studies reported here on the DEPC modification of clusterin implicate an imidazole(s) on clusterin in the interaction with $A\beta_{1-40}$. Interestingly, H13D and H14D substitutions in $A\beta_{11-25}$ have been shown to substantially impair fibrillogenesis without significantly changing the β sheet conformation of these peptides (Fraser et al., 1994) suggesting that fibril-stabilizing imidazole-carboxylate salt bridges may be inter-monomeric. Thus, an imidazole on clusterin may substitute for an $A\beta_{1-40}$ monomer imidazole in an interaction with an $A\beta_{1-40}$ carboxylate.

Clusterin is reported to bind Aβ peptide derivatives 1-28 and 17-28 in addition to 1–40, but not 1-16 (Choi-Miura et al., 1994) suggesting that the clusterin binding site is localized to residues 17-28. This sequence, LVFFAEDVGSNK, contains hydrophobic

amino acids as well as the two acidic residues that have been implicated in fibril imidazole-carboxylate salt bridges. It is possible that binding to clusterin involves both hydrophobic interactions with the non polar faces of exon 5 encoded amphipathic α helices, as well as electrostatic interactions between clusterin imidazole(s) and these Aβ peptide acidic side chains. In this regard I noted in Chapter 3 that of the stronger acid/base amino acid side chains exon 5 encoded helices have a conserved preference for acidic side chains. It may be possible that these also make salt bridges with imidazole(s) of Aβ4 peptides. Thus, in its interactions with Aβ4 peptides clusterin may recapitulate many of the binding interactions of another monomer in a stable fibril and inhibit Aβ4 fibrillogenesis by interactions both with free Aβ4 peptides and sites on growing fibrils necessary for fibril growth. If such specific interactions can be substantiated, rather than exon 5 encoded amphipathic α helices corresponding to a promiscuous binding site for hydrophobic/amphipathic ligands it is tempting to see tailoring of a specific fit between clusterin and $A\beta_{1-40}$ or a similar ligand.

1.1.7. Pathophysiological implications of the clusterin Aβ4 interaction

A possible pH dependent interaction between clusterin and Aβ4 peptides may have previously unappreciated (patho)physiological consequences. Complexes of clusterin and Aβ4 peptides exist in serum and cerebro-spinal fluid (Ghiso et al., 1993; Koudinov et al., 1994; Golabek et al., 1995) but it is not known where or when these complexes are first formed. In cells in which clusterin and amyloid precursor protein (APP) are co-expressed it is possible that acidification late in the constitutive secretory pathway may induce an association of clusterin with the amyloidogenic domain of APP

and this may influence the relative outcomes of nearby α and β secretase cleavages. Alternatively, APP C-terminal membrane associated fragments generated by α and/or β secretase cleavage may meet clusterin in an acidic lysosomal compartment and an induced association may influence cleavage by γ secretase and/or protect the resulting peptides from further degradation. Thus, clusterin may modulate production of Aβ4 peptides. The recent observation that clusterin and Aβ4 peptides newly synthesized and secreted by HepG2 cells in culture appear to be associated together in lipoprotein particles (Koudinov and Koudinova, 1997) may reflect a cellular origin for clusterin-Aβ4 peptide complexes. The consequences of clusterin overexpression in cells producing Aβ4 peptides may provide an obvious test of this hypothesis.

The pathogenesis of autosomal dominant hereditary cereberal hemorrhage with amyloidosis of the Dutch type (HCHWA-D), also has a possible specific relationship to the nature of clusterin Aβ4 interactions proposed here. Neuropathologically and clinically, HCHWA-D is distinct from Alzheimer's disease (Selkoe, 1994). HCHWA-D features heavy β amyloid deposition of primarily $A\beta_{1-40}$ in meningeal and cerebral microvessels, which are presumed to underlie a clinical course suggesting hemorrhage as the primary cause of neurological symptoms and ultimate fatality (Selkoe, 1994). By contrast progressive cognitive dysfunction in AD is presumed to result from formation of parenchymal deposits of $A\beta_{1-42}$ (Selkoe, 1994; Hardy, 1997). The difference in the major forms of Aβ peptides in vascular (1-40) and parenchymal (1-42) deposits suggests distinct cellular origins of these peptides. $A\beta_{1-40}$ is the principal form of soluble Aβ peptides in CSF and plasma (Selkoe, 1994) and clusterin-$A\beta_{1-40}$ complexes may be

transported across the blood-brain barrier by a receptor immunologically related to LRP2 on brain microvessels (Zlokovic et al., 1996b). Thus, vascular deposits of Aβ in the brain may be derived from $A\beta_{1-40}$ in plasma transported in association with clusterin. On the basis of the model of clusterin binding to $A\beta_{1-40}$ described here clusterin may have an important role in the etiology of HCHWA-D. HCHWA-D is genetically associated with two APP mutations which convert the glutamate residue within the putative clusterin binding site to a neutral amino acid (glutamine or glycine) (Selkoe, 1994). Substitution with a neutral amino acid may prevent formation of the hypothetical salt bridge with the ionized imidazole side chain on clusterin. The result may be a decrease in complex stability following acidification of transcytotic vesicles, resulting in dissociation of the complex and release of the free peptide. It will be interesting to determine whether and with what affinity clusterin binds to these mutant forms of $A\beta_{1-40}$ and how pH affects this binding.

1.4. Summary

This chapter described the expression, purification, and structural and functional characterization of human clusterin synthesized in the yeast *Pichia pastoris*. The recombinant protein was secreted at high levels, and had many of the structural hallmarks of the serum/plasma protein. It had the α chain N-terminus predicted from N-terminal secretory signal sequence cleavage by signal peptidase, was modified heterogeneously by N-linked carbohydrate addition and was quantitatively cleaved between the α and β chain cysteine rich domains, which included the site of endoproteolytic processing observed in mammalian and avian cells, to yield an α/β disulfide linked heterodimer. The

recombinant protein was efficiently recognized by G7, a monoclonal antibody with high affinity for a conformational epitope dependent on appropriate α and β chain interactions, permitting purification to homogeneity by immunoaffinity chromatography. These preparations demonstrated interactions, specifically, and with high affinity, to reported clusterin ligands including sC5b-9, complement C9, $A\beta_{1-40}$, IgG and LRP2 espressed on the surface of differentiated F9 cells. Taken together with high levels of expression, ease and rapidity of growth and transformation, and low cost, this suggests that *P. pastoris* will be a useful host for preparation of wild type and mutant forms of clusterin. Proteolysis at aberrant sites primarily within sequences encoded by exon 5, accompanies recombinant expression, resulting in a heterogeneous mix of heterodimers, which may however, impose some limits on particular experimental uses of this model source.

In and of itself characterization of aberrant proteolysis in recombinant human clusterin has important implications for structure, and the relationship of structure to function. The sensitivity of exon 5 encoded sequences to proteases and the contrasting stability of the remainder of the protein is evocative of the proposed domain structure developed for clusterin in Chapter 3. In addition, evidence that proteolysis in exon 5 encoded sequences of the β chain might be causally linked to proteolysis in exon 5 encoded sequences of the α chain echoed the proposal that segments of the α and β chain colinear in the linear antiparallel model were physically interactive and mutually stabilizing. I suggest that these proteolytic patterns are largely a direct consequence of the specific structural relationships detailed in the model developed in Chapter 3.

Aberrant proteolysis is also associated with differential effects on the specific binding activity of recombinant preparations. Proteolysis in exon 5 encoded sequences, is known or predicted to affect the amphipathic α helices in each chain proposed as elements of a promiscuous binding site for hydrophobic/amphipathic ligands and is associated with dramatic decreases in interactions with IgG and $A\beta_{1-40}$. By contrast, the stability of the putative antiparallel coiled-coil is associated with a specific activity for the interaction with LRP2 indistinguishable from the serum/plasma protein. I suggest that differences in the specific binding activity of recombinant preparations to these ligands is causally related to differential proteolysis of the respective ligand binding domains.

Several observations are surprising in light of the general consensus view of clusterin structure-function. Comparatively small decreases in the specific acitivity of recombinant preparations in the interaction with Zn^{+2} polymerized complement C9 are not expected if C9 is an archetypal hydrophobic/amphipathic ligand. Thus, there may be a nearby, but distinct, high affinity binding site specific for complement C9 (and possibly C8). This is in aggreement with the suggestions of recent studies of the interaction of clusterin with C9 (McDonald and Nelsestuen, 1997). Despite the presence of an LDLR ligand binding repeat in C9, the differential effect of G7 in inhibiting clusterin binding to LRP2 but not Zn^{+2} polymerized C9 suggests that the C9 binding site is distinct from that of LRP2. Specificity may also exist in the interaction of clusterin with $A\beta_{1-40}$. The dramatic increase in stable binding of clusterin to $A\beta_{1-40}$ in response to mild acidification, and effective decrease as a specific competitive inhibitor of this interaction when clusterin is modified by DEPC is thought to reflect an electrostatic interaction between an

ionized clusterin histidine(s) and an acidic amino acid(s) in the juxtamembrane domain of $A\beta_{1-40}$, in addition to hydrophobic interactions and that might parallel inter monomeric stabilizing interactions in Aβ fibrils. The identification of a specific binding site for C9 and specificity in the interaction with $A\beta_{1-40}$ suggests that the physiological role of clusterin may relate to interactions with specific ligands rather than as a general protective protein in the neutralization of a broad range of hydrophobic surface active molecules.

CHAPTER FIVE

4. *Monoclonal antibodies to rat clusterin : reagents for identifying clusterin ligand interactions in rat tissues*

4.1. Background

The physiological function of clusterin in the apparently diverse biological contexts in which it is expressed is unknown. It has been assumed that this function depends upon the properties of clusterin as a binding protein. As described, a number of clusterin ligands including apoAI-HDL, serum paraoxonase, terminal complement complexes, Aβ4 peptides, immunoglobulins, and LRP2 have been identified by chromatography of human plasma, cereberal spinal fluid, and milk on either ligand or antibody affinity matrices. However, the lack of useful reagents, in particular high affinity monoclonal antibodies that recognize clusterin under non denaturing conditions in a more experimentally tractable species have limited attempts to identify particular clusterin ligand complexes in other tissues.

Our laboratory has been interested in particular, in the function of clusterin in the rat ventral prostate following castration. Following castration, and temporally associated with involution of the organ (Tenniswood et al., 1992; Colombel and Buttyan, 1995) the distal epithelial cells of the rat ventral prostate are the sites of a dramatic upregulation in clusterin mRNA (Rouleau et al., 1990; Guenette et al., 1994a). Clusterin is not likely to be a direct regulator and/or obligatory component of the apoptotic cell death pathway. However, clusterin may play supporting and/or protective roles in involution of the organ that are important in tissue reorganization. Newly synthesized clusterin may act as a late stage complement inhibitor, limiting development of an inflammatory response. Alternatively, it may serve as a transport protein removing and/or redistributing lipids from dying cells, or may serve some function not yet appreciated. The purification and

characterization of putative clusterin ligand complexes from the regressing rat prostate may help to clarify its specific function in the prostate and may provide some fundamental insights into the biology of the prostate.

1.2. Objectives

To identify clusterin ligand complexes present in the rat ventral prostate following castration we decided to prepare murine monoclonal antibodies that would bind to rat clusterin with high affinity under non denaturing conditions. These could then be used as immunoaffinity reagents to rapidly and specifically copurify rat clusterin and associated ligands from the involuting prostate under mild conditions. The preparation and immunological characterization of a number of murine rat clusterin specific monoclonal antibodies, including antibodies that immunoprecipitate clusterin from the rat ventral prostate, is described in this chapter.

1.3. Results

1.3.1. Structural characterization of rat clusterin expressed in *P. pastoris*

The high levels of expression of human clusterin in *P.pastoris* suggests that it may serve as an efficient host for the high level expression of the rat homolog to be used as an immunogen and screening antigen in the preparation of monoclonal antibodies. In addition the demonstration that recombinant preparations of human clusterin have many of the important structural and functional hallmarks of the serum protein suggests that biosynthesis in *P. pastoris* produces a largely native structure which one might expect to direct the production of high affinity antibodies to native epitopes.

An expression construct for rat clusterin was developed that was completely analogous to that for human clusterin. The full length rat cDNA, including the N-terminal secretory signal sequence was amplified by PCR and subcloned into a *P. pastoris* expression vector under control of the methanol inducible AOX1 promoter. The rat expression construct was integrated by homologous recombination at the *HIS4* locus of the *P. pastoris* genome in light of the lower levels of secretion obtained for the human construct when recombined at *AOX1* relative to *HIS4* loci.

As for the human protein, rat clusterin was present at similarly high levels in unsupplemented medium conditioned by *P.pastoris* transformants when induced to express with methanol (Fig. 5.1A). By SDS PAGE, recombinant rat clusterin migrates as a series of bands from about 57 to 42 kDa under non-reducing conditions, and as a series of prominent discrete bands from 40 to 23 kDa under reducing conditions, suggesting that it is also a disulfide linked dimer proteolytically processed between the cysteine rich domains in each chain. Rat clusterin was quantitatively precipitated from conditioned medium by ethanol precipitation with an estimated purity of greater than 90% (compare Western analysis using anti-rat Sertoli cell SGP-2; Fig. 5.1B, lane W to a Coomassie Blue stain of the same preparation; Fig. 5.1B, lane 2, C) and this method was use to concentrate and partially purify recombinant rat clusterin for use as immunogen and screening antigen. Treatment of this preparation with N- glycosidase F shifts the relative molecular weight of rat clusterin to a series of bands from 50 to 35 kDa under non-reducing conditions and to principal bands of 28, 23, 21, 20, and 16 kDa under reducing conditions (Fig. 5.1B, lane 4). Thus, the majority of rat recombinant clusterin is N-

Figure 5.1. Secretion of rat clusterin expressed in *P.pastoris*

A. 25 µL of BMMY media conditioned by a *P.pastoris HIS+* transformant with pD217H (lane 2) or pHIL-D2 vector alone (lane 1) were separated by electrophoresis on 12% SDS polyacrylamide gels under reducing and non-reducing conditions as indicated. Separated polypeptides were visualized by staining with Coomassie Blue (C). The position of molecular weight markers (in kDa) run in parallel is indicated at the side of each figure.

B. 2 µL per lane of an ethanol precipitated preparation of *P. pastoris* recombinant rat clusterin (concentrated ≥ 100 fold) (lanes 2, and 4) or 2 µg per lane of immunoaffinity purified human serum clusterin (Lanes 1, and 3) were treated with (lanes 3, and 4) or without (lanes 1, and 2) N-glycosidase F. Samples were separated on 11% SDS polyacrylamide gels under reducing and non-reducing conditions as indicated and stained with Coomassie Blue (C). In lanes designated 'W' 0.5 µL of the rat clusterin preparation were run in parallel, transferred to nitrocellulose, and probed with anti-rat clusterin polyclonal antibody SGP-2. The position of molecular weight markers (in kDa) run in parallel is indicated at the center of the figure.

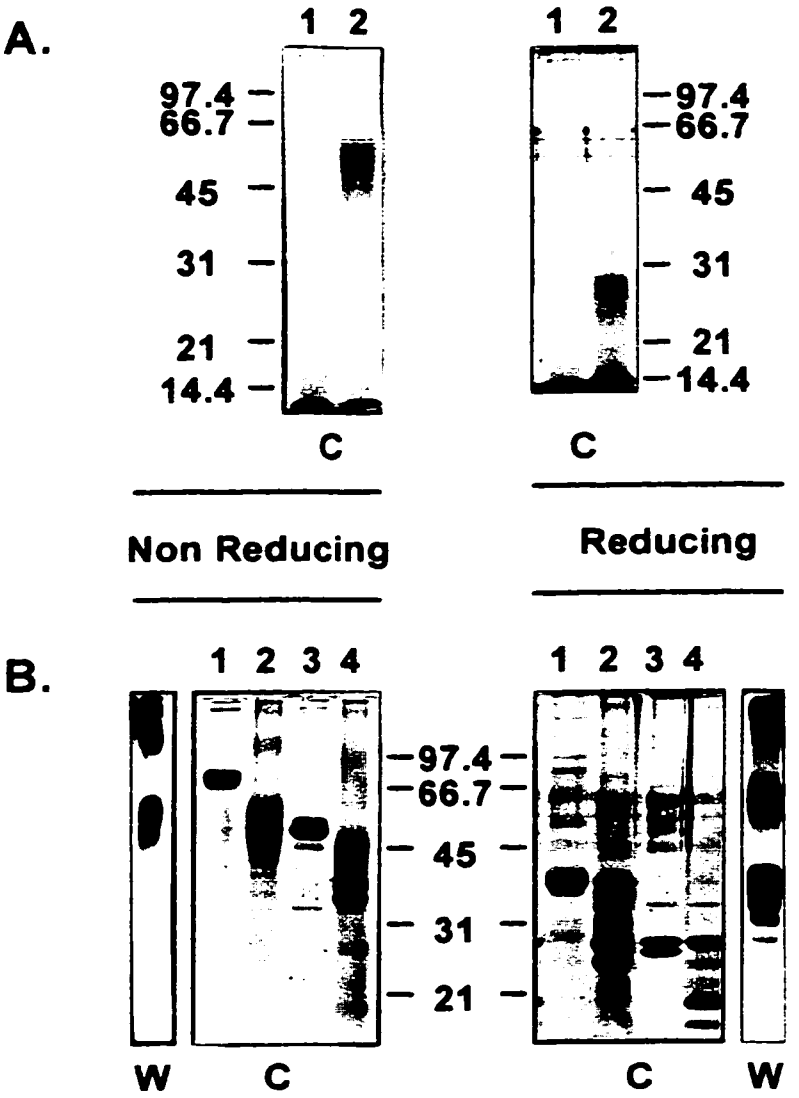
A.
1 2
97.4
66.7
45
31
21
14.4
C
Non Reducing
1 2
97.4
66.7
45
31
21
14.4
C
Reducing
B.
1 2 3 4
97.4
66.7
45
31
21
W
C
1 2 3 4
C
W

glycosylated and is probably secreted via the normal secretory pathway. The 28 kDa band comigrated with the N-deglycosylated β chain of human serum clusterin while only a minor 26 kDa band comigrated with the N-deglycosylated human serum α chain (Fig. 5.1B). Rat and human sequences are 77% identical overall, and the α chains are of equal length and the β chain of the rat sequence is only one amino acid smaller than the human. In consequence the human chains serve equally well for recombinant rat clusterin as chain molecular weight markers in deglycosylation experiments. The profile both before and after N-deglycosylation of the rat preparation strongly resembles that of recombinant human clusterin expressed in the absence of casein suggesting that proteolysis occurs both at the authentic site (αR205-βS1) as well as at aberrant sites. Like the human these latter sites may be proximal to αR205-βS1 and within exon 5 encoded sequences. Thus, recombinant rat clusterin likely resembles in large part its natural counterpart in respect of tertiary structure.

1.1.2. Preparation and characterization of anti-rat clusterin monoclonal antibodies

A single fusion of splenocytes from a mouse immunized and screened by ELISA with the ethanol precipitate yielded 25 positive hybridomas. Of the original isolates 12 were recovered as positive sublines following expansion and a single round of cloning by limiting dilution. Although a number of these gave a heterogeneous response when rescreened by ELISA during cloning, suggesting that the initial isolate was heterogeneous, a single immunoglobulin type in most cases was obtained for expanded positive sublines, suggesting that most of these sublines are pure (Table 5.1). Eight gave strong reactivity in ELISA while 2 were moderate and 2 weak (Table 5.1).

Table 5.1. Summary of murine anti-rat clusterin hybridoma immunoreactivity

Hybri-doma[a]	Class	ELISA[b]	Immunoppt.[c]	Western Analysis[d]					Group
				MalE-αβ	MalE-α	MalE-β	Serum	Day 4 RVP	
2D9	IgG_1, κ	++	ND	++	++	+/-	ND	+/- NR (65) +/- (α,β) R	1
1F8	IgG_{2b}, λ	++	ND	+/-	+/-	+/-	ND	ND	2?
2F6	IgG_1, κ	++	+	+/-	+/-	+/-	+ NR - R	+ NR (65) - R	2
4A7	IgG_1, κ	+	ND	+/-	+/-	+/-	ND	ND	?
2A10	IgG_1, κ	++	+	+/-	+/-	+/-	+ NR, - R	+ NR (65) +/- (β) R	2
6F4	IgG_1, κ	++	+	ND	ND	ND	+ NR - R	+ NR (65) +/- (β) R	2?
6E9	IgG_1, κ	++	+	+	-	+	- NR +/-(β) R	+/- NR (65) +/- (β) R	3
7A8	IgG_1, κ	++	-	++	-	++	+/- NR + (β) R	+ NR (67-43) + (β) R	4
2B5	IgM, κ	+	ND	ND	ND	ND	ND	ND	?
6F3	IgG_1, κ	+/-	ND	ND	ND	ND	ND	ND	?
6A6	IgG_1, κ	++	ND	ND	ND	ND	ND	ND	?
6G6	IgG_1, κ	+/-	ND	ND	ND	ND	ND	ND	?

++, Strong; +, Moderate; +/-, Weak; -, Not Reactive; ND, Not Determined

[a] All hybridomas listed were obtained as ELISA positive sublines. All assays used conditioned media from cloned sublines.

[b] ELISA with *P. pastoris* rat recombinant clusterin partially purified from conditioned media by ethanol precipitation.

[c] Immunoprecipitation of clusterin from rat ventral prostate homogenates 4 days after castration

[d] Western analysis of rat clusterin from the indicated sources. MalE-α, MalE-β, and MalE-αβ are recombinant fusion proteins expressed in *E. coli*. Serum and day 4 post castrate rat ventral prostate (RVP) lysates were run under non reducing (NR) and reducing (R) conditions. α and/or β in parenthesis indicates subunit reactivity under reducing conditions. Under non reducing conditions in day 4 RVP the relative molecular weight of the major reactive band(s) are indicated in parenthesis.

The reactivity of a number of the hybridomas was further characterized to identify monoclonal antibodies that are specific for rat clusterin and not to either a yeast protein contaminant or to a yeast specific post-translational modification. For this purpose both recombinant and natural sources of rat clusterin were chosen. Natural sources included both rat serum, in which clusterin is present at 20 to 45 μg/mL (Grima et al., 1990) as well as lysates of the rat ventral prostate prepared on days 0 to 4 following orchidectomy (Grima et al., 1990; Sensibar et al., 1993). In addition to *P. pastoris* recombinant clusterin, lysates of recombinant *E.coli* expressing fusions of the maltose binding protein (MalE) with the rat αβ proprotein, or of each of the independent chains were useful in verifying specificity and in defining corresponding epitopes.

Of the 12 hybridomas yielding positive sublines by ELISA, eight are specific for one or more additional sources of rat clusterin by one or more immunological methods (Table 5.1). In the following discussion four of these are described in particular, including 7A8, 2A10, 6E9 and 2D9, as representative of at least four distinguishable reactivities corresponding to distinct configurational and/or conformational rat clusterin epitopes (Table 5.1). All are among those strongly reactive with the recombinant rat preparation by ELISA and, with the exception of 2A10, give a homogeneous response in ELISA when cloned, providing additional confidence that the expanded sublines represent pure clones. 2A10 gave a heterogeneous response when cloned, but a strong reactive subline was clonally pure with respect to immunoglobulin type and in all of the following assays this subline shows a consistent reactivity.

Hybridoma 7A8 proved consistently to be the most sensitive for the recognition of clusterin from several sources separated under both reducing and non-reducing conditions on Western blots. The α and β chains of rat clusterin have mobilities of approximately 36 and 43 kDa, respectively on SDS PAGE (Collard and Griswold, 1987). The mobility of α and β chains is shown for rat serum detected by anti-rat Sertoli cell SGP-2 (Fig. 5.2). This polyclonal contains both α and β specific reactivities as shown by its reactivity with α and β chains from rat tissues (Sensibar et al., 1993). 7A8 reacts specifically with the β but not α chain of serum (Fig. 5.2). Under non-reducing conditions a single immunoreactive band was observed at 65 kDa from serum, corresponding to the mature disulfide linked heterodimer (Fig. 5.2). In lysates of ventral prostate 7A8 reacts with the uncleaved αβ proprotein at 57 kDa in addition to the β chain under reducing conditions (Fig. 5.3A and B). In the ventral prostate the level of these two immunoreactive bands increased progressively from day 0 to 4 following castration (Fig. 5.3A) mirroring the kinetics of induction of clusterin mRNA (Montpetit et al., 1986; Léger et al., 1987; Wong et al., 1993). Under non-reducing conditions a number of immunoreactive bands are observed ranging from 43 to 67 kDa (Fig. 5.3). Bands of molecular weight less than 65 kDa are reproducible and increase with similar kinetics following castration suggesting that they are specifically related to clusterin. 7A8 also reacts strongly and specifically with the β chain and αβ proprotein but not the α chain MalE fusion from recombinant *E.coli* lysates confirming the identification of a β restricted reactivity (Fig. 5.4).

Although 2A10 displays a nearly comparable and in some cases stronger

Figure 5.2. Monoclonal and polyclonal reactivity to rat serum clusterin by Western blot

2 μL per lane of rat serum was separated by electrophoresis on 12% or 10% SDS polyacrylamide gels under reducing (R) and non-reducing (NR) conditions, respectively, transferred to nitrocellulose, and clusterin detected with the indicated antibodies as described in Methods and Materials. α and β chains of reduced rat serum clusterin are indicated. The position of molecular weight markers (in kDa) run in parallel is indicated at the center of each figure.

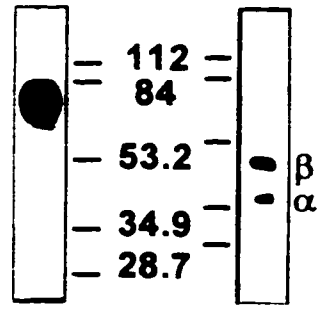

Anti SGP-2

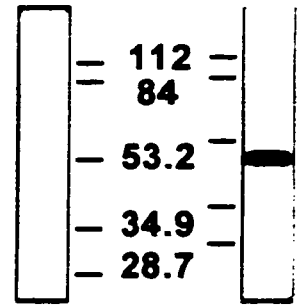

7A8

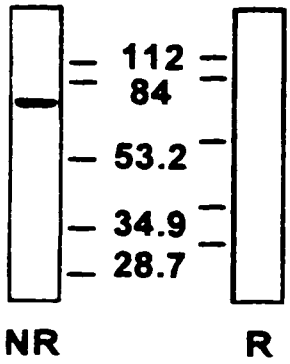

2A10

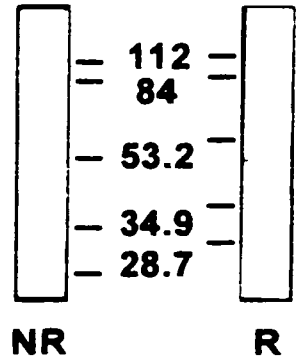

6E9

Figure 5.3. Monoclonal reactivity to clusterin in post castrate rat ventral prostate by Western blot

A. Time course of expression of clusterin in the rat ventral prostate following castration. 100 μg total protein per lane from lysates of ventral prostates prepared from uncastrated (day 0), and from day 1 to 4 after orchiectomy were separated on 7.5% SDS polyacrylamide gels under reducing and non-reducing conditions, transferred to nitrocellulolse and probed in parallel with hybridoma 7A8 or 2A10 conditioned media. In non-reducing blots the range of molecular weights (in kDa) of immunoreactive products is given to the right of the figure. In reducing blots, arrowheads indicate the rat clusterin β chain and unprocessed αβ proprotein.

B. 100 μg total protein per lane from lysates of rat ventral prostates prepared from day 4 after castration were separated on 12% and 10% SDS polyacrylamide gels under reducing and non-reducing conditions, respectively, transferred to nitrocellulose and probed in parallel with hybridoma 2D9, 2A10, 6E9, or 7A8 conditioned media, representative of reactivity groups 1, 2, 3, and 4 (Table 5.1). In reducing blots the α and β chains of rat clusterin and unprocessed αβ proprotein are indicated to the right of the figure. The positions of molecular weight standards (in kDa) run in parallel is indicated to the right of each figure.

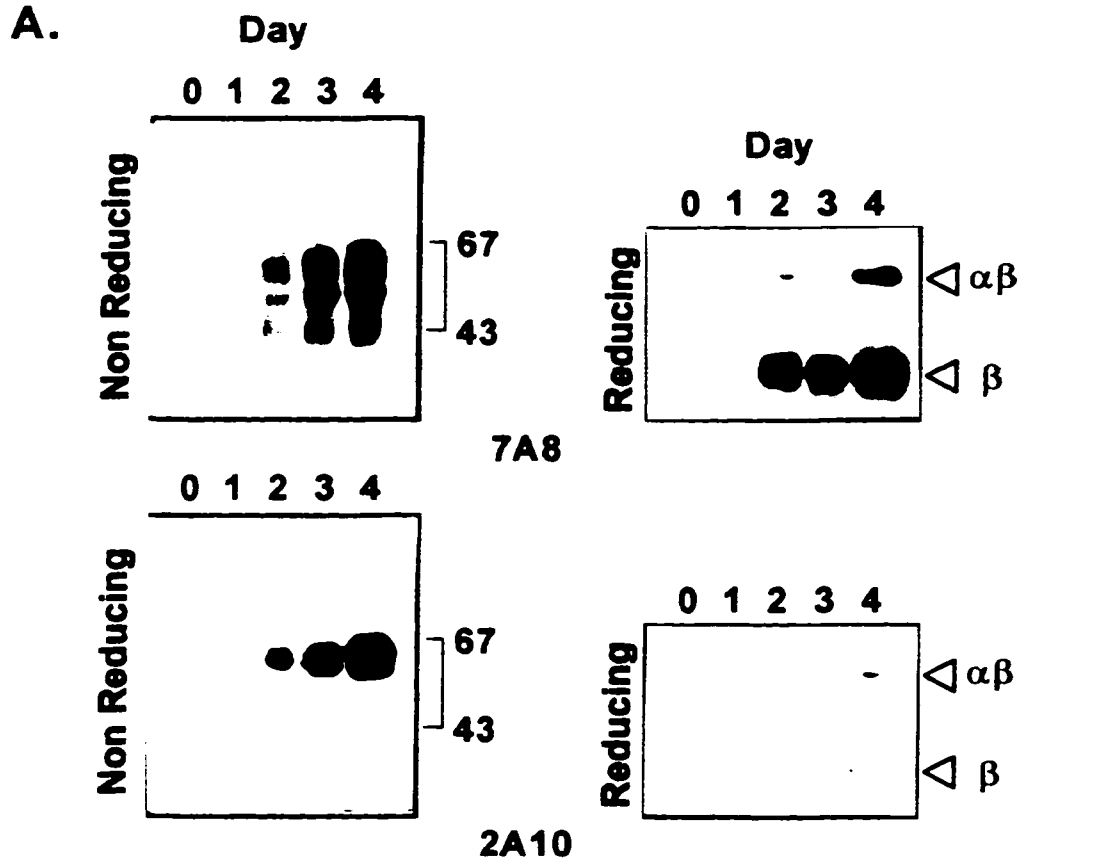
A.
Day
0 1 2 3 4
Non Reducing
67
43
7A8
Day
0 1 2 3 4
Reducing
αβ
β
0 1 2 3 4
Non Reducing
67
43
2A10
0 1 2 3 4
Reducing
αβ
β

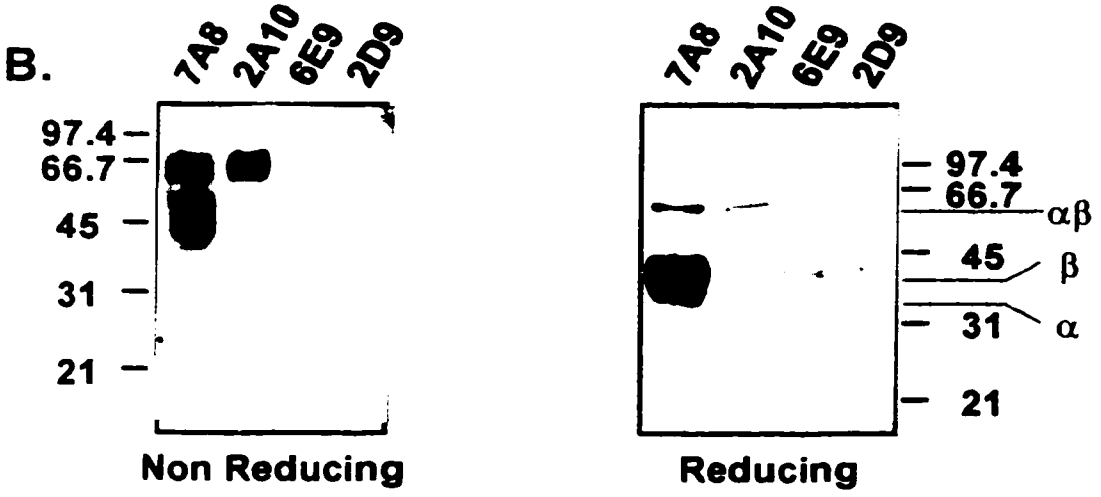
B.
7A8
2A10
6E9
2D9
97.4
66.7
45
31
21
Non Reducing
7A8
2A10
6E9
2D9
97.4
66.7
αβ
45
β
31
α
21
Reducing

Figure 5.4. Western blot monoclonal and polyclonal reactivity to MalE -rat clusterin α, β, and αβ proprotein fusions expressed in *E.coli*

Log phase *E. coli* transformed with pMalpRI (v), pMalpα (α), pMalpβ (β), or pMalpαβ (αβ), induced with IPTG to express respectively MalE-lacz, and MalE-rat clusterin α, β, and αβ proprotein fusions, were lysed in SDS and 35 μg of total protein from each separated on 10% SDS polyacrylamide gels under reducing conditions. Gels were either fixed and stained with Coomassie Blue as indicated or polypeptides were transferred to nitrocellulose and rat clusterin detected in parallel with the indicated antibodies. The position of molecular weight standards (in kDa) run in parallel is indicated to the right of each group of aligned figures.

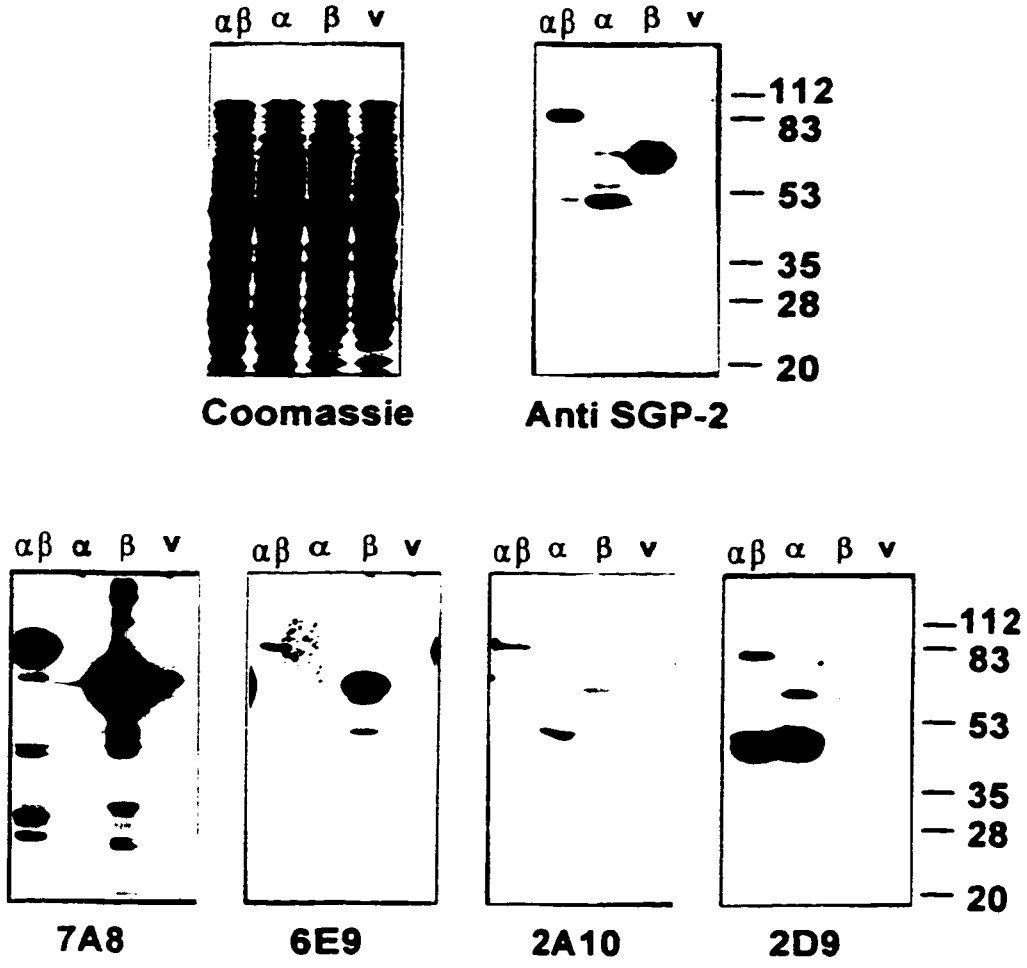
αβ α β v
αβ α β v
112
83
53
35
28
20
Coomassie
Anti SGP-2
αβ α β v
αβ α β v
αβ α β v
αβ α β v
112
83
53
35
28
20
7A8
6E9
2A10
2D9

reactivity to rat clusterin to non-reduced samples than 7A8 when used under identical conditions it is distinct in having a much higher avidity for non-reduced relative to reduced clusterin from all sources. Fig. 5.2 shows this difference for rat serum, and Fig. 5.3A and B for day 0 to 4 post castrate ventral prostate lysate samples processed simultaneously and equalized with respect to protein load. Reduction of clusterin results in the near elimination of reactivity with any clusterin polypeptide by Western blot. This is most convincingly shown for lysates of ventral prostate in which 2A10 detects the 65 kDa heterodimeric form of clusterin in non-reduced samples by day 2 following castration but only weakly detects the αβ proprotein present in lysates from day 4 samples (Fig. 5.3A). When used for Western analysis of lysates from rat ventral prostate or serum separated under reducing conditions, no signal was consistently obtained to either the separated α or β chains. However, when used for Western blots against reduced lysates of recombinant *E.coli* MalE fusions, 2A10 weakly detected both of the individual α and β chains as well as the αβ proprotein (Fig. 5.4). This was not due to cross reactivity to MalE as no band was detected in the vector alone control (Fig. 5.4). It is possible that the much higher surface antigen densities enabled by overexpression in bacteria (note the prominent fusion protein bands in a Coomassie Blue stain of bacterial lysates; Fig. 5.4) enables bivalent binding of sufficient affinity to a weak monovalent epitope to obtain detection, which is not possible with the lower surface antigen densities in serum and ventral prostate lysates. The reactivity of 2A10 with MalE fusions however, suggests that the corresponding epitope may be either shared by both α and β chains, despite a lack of extensive sequence homology between them, or is constituted of amino acids from both chains. Western blot reactivity with both N-deglycosylated chains has

been described independently for the mAb11 monoclonal antibody to human serum clusterin, suggesting that such specificity is possible (de Silva et al., 1990c).

6E9 had some variably weak avidity for both reduced and non-reduced clusterin which appeared to favor reduction when equivalent protein loads were processed simultaneously (Fig. 5.2, and 5.3B). 6E9 weakly detected the β chain of clusterin from serum under reducing conditions but did not react with non-reduced serum clusterin (Fig. 5.2). However, it specifically detects the 43 kDa β chain and weakly the upper 65 kDa heterodimer from reduced and non-reduced lysates from ventral prostate 4 days after castration, respectively (Fig. 5.3B). As for 7A8 it reacts specifically with the β chain and αβ proprotein but not the α chain MalE fusion from recombinant *E. coli* lysates confirming the assignment of a β restricted reactivity (Fig. 5.4).

2D9 is the only hybridoma to show an α chain specificity in reducing samples of natural rat tissues. It detects the 36 kDa α chain in addition to weak reactivity to the 43 kDa β chain in reduced lysates from the ventral prostate on day 4 following castration (Fig. 5.3B), suggesting that as for 2A10, the corresponding epitope may be either shared by both α and β chains or constituted of amino acids from both chains. This is confirmed by Western blot of MalE clusterin fusions, but under identical conditions 2D9 demonstrates a much stronger avidity for the α chain fusion than 2A10 (Fig. 5.4), in keeping with its somewhat different reactivity with natural sources. In general however, it appears to be the weakest hybridoma on Western blots of either reduced or non-reduced clusterin from any source.

The generally weak reactivity of 2A10, and 6E9 on Western blot suggests that they might recognize native epitopes. To determine if specifically, these hybridomas have high affinity for such an epitope, they were assayed for the ability to immunoprecipitate clusterin solubilized under mild conditions. Individual ventral prostates excised from rats 4 days after castration were homogenized on ice in PBS glycerol and insoluble proteins removed by ultracentrifugation at 100000xg. The supernatant contained soluble clusterin and was used as a source for immunoprecipitations (Fig. 5.5A). 2A10 and 6E9, but not 7A8 immunoprecipitate clusterin from this supernatant as shown by the presence and absence, respectively of a series of bands at around 65 kDa on silver stained (Fig. 5.5B) gels or on Western blot (Fig. 5.5C). The failure of isotype matched 7A8 or Protein G alone to immunoprecipitate clusterin indicates that the interaction with 2A10 and 6E9 is specific.

It was also of interest to determine if any of the hybridomas demonstrate utility in immunohistochemistry. Fig. 5.6 shows the reactivity of 2A10, 6E9, and 7A8 to paraffin sections of the rat ventral prostate on day 0 and day 4 after castration. No immunoperoxidase reactivity was detected in the ventral prostate on day 0 with any of the hybridomas. However, on day 4 following castration there was marked punctate reactivity for all three, primarily localized to the apical regions of the majority of epithelial cells. No reactivity was observed with stromal cells at either time point. The day 4 reactivity of 7A8 is weaker than that for either 2A10 or 6E9, an observation which may relate to either a lower affinity and/or relative accessibility of its respective epitope. This is the pattern of reactivity observed previously with a polyclonal antibody to rat

Figure 5.5. Relative capacity of monoclonals to immunoprecipitate clusterin from post castrate rat ventral prostate

A. Individual rat ventral prostates from day 4 post castrates were homogenized either in RIPA or in PBS-glycerol. PBS-glycerol homogenates were subjected to a 10 min spin at full speed in a microfuge yielding pellet (P1) and supernatant (S1) fractions. S1 was further centrifuged for 30 min at 100000xg yielding pellet (P2) and supernatant (S2). Pellet fractions were washed and then extracted with 2% SDS and 8 M urea to solubilize proteins. 100 µg of total protein from a RIPA homogenate or in fractions from differential centrifugation of the PBS glycerol homogenate were separated by electrophoresis on a 12% SDS polyacrylamide gel under reducing conditions, transferred to nitrocellulose, and probed with hybridoma 7A8 conditioned media. The position of molecular weight standards (in kDa) is indicated at the right of the figure.

B. 500 µg total protein each of S2 fraction diluted into 500 µL PBS were incubated with or without (Protein G) or anti-rat clusterin monoclonal antibodies 2A10, 6E9, or 7A8 conjugated to Protein G agarose by preincubation with hybridoma conditioned media. After washing beads extensively, bound proteins were eluted by heating in non-reducing SDS PAGE sample buffer and separated on a 7.5% to 15% linear gradient SDS polyacrylamide gel under non-reducing conditions and silver stained. The arrowhead indicates a 67 kDa band corresponding to eluted rat clusterin. The position of molecular weight standards (in kDa) is indicated to the right of the figure.

C. As in B. but eluted proteins were separated on a 7.5% SDS polyacrylamide gel under non-reducing conditions, transferred to nitrocellulose and probed with hybridoma 2A10 conditioned media. 100 µg total protein of a RIPA homogenate from a day 4 post castrate ventral prostate (Day 4 RVP) was run in parallel as a positive control. Arrowheads indicate immunoreactive bands corresponding to rat clusterin and coeluted IgG.

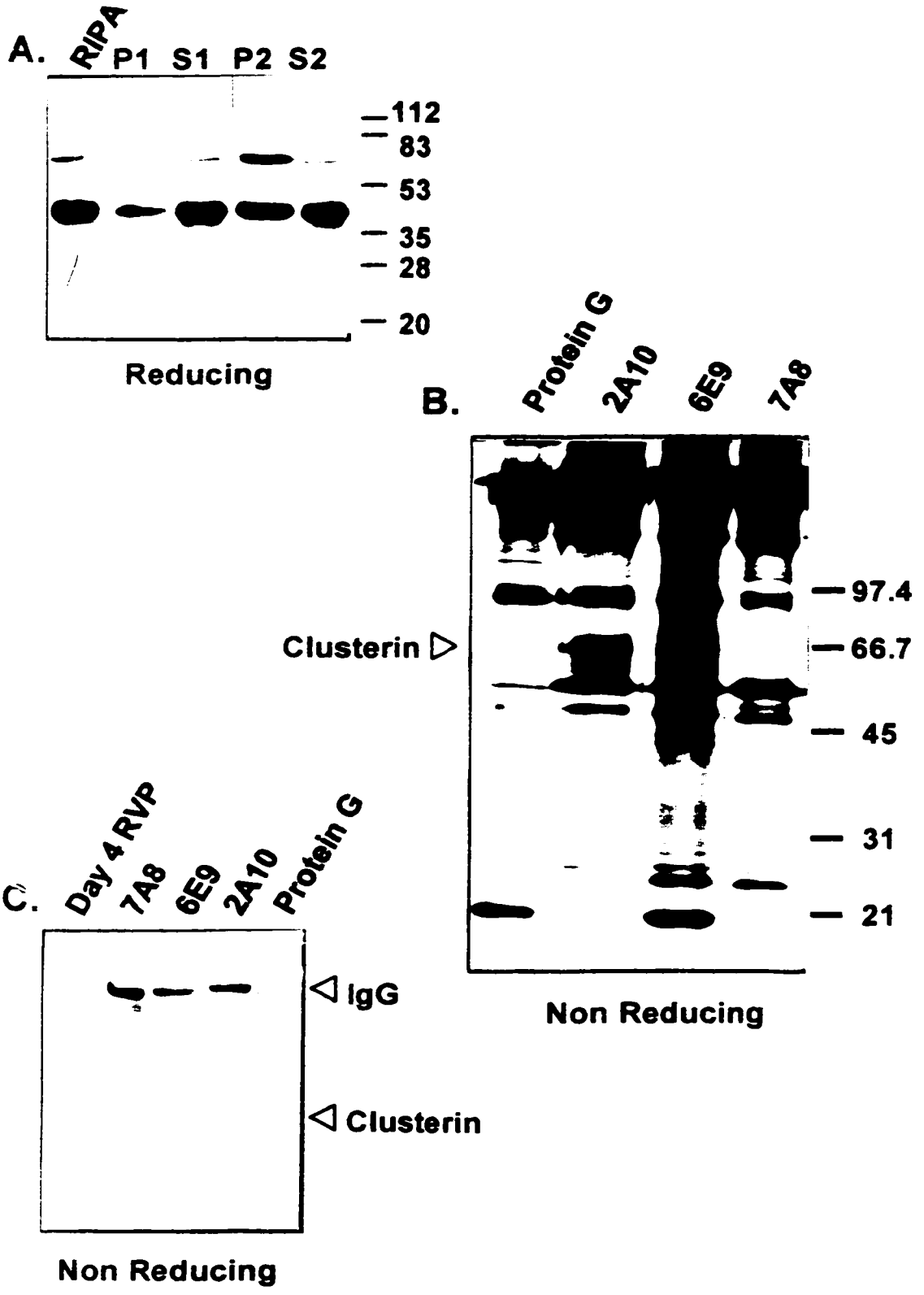
A.
RIPA
P1
S1
P2
S2
112
83
53
35
28
20
Reducing
B.
Protein G
2A10
6E9
7A8
Clusterin
97.4
66.7
45
31
21
Non Reducing
C.
Day 4 RVP
7A8
6E9
2A10
Protein G
IgG
Clusterin
Non Reducing

Figure 5.6. Immunohistochemical analysis of clusterin in post castrate ventral prostate using monoclonals

Sections from the ventral prostate of control rats (day 0) or rats on day 4 after castration were prepared and clusterin detected with hybridoma 7A8, 6E9, or 2A10 conditioned media as described in Methods and Materials. Peroxidase activity localizes to the apical pole of lumenal epithelial cells in the day 4 castrates in sections stained with all three monoclonal antibodies. L, lumen; E, epithelia; and S, stroma.

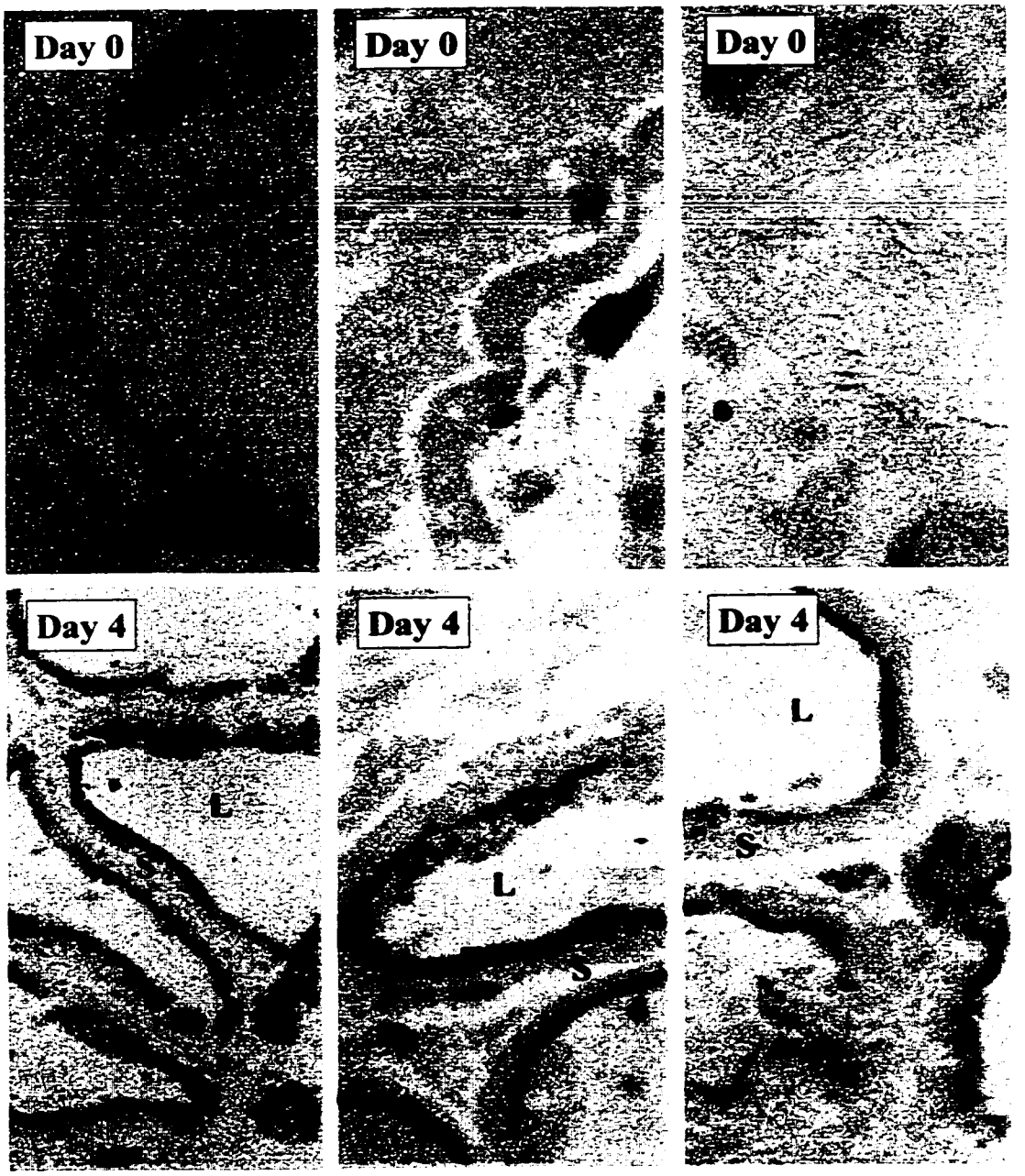

7A8 6E9 2A10

Sertoli cell SGP-2 (Sensibar et al., 1991). Furthermore *in situ* hybridization showed that the distal prostatic epithelium is the specific site of *de novo* clusterin synthesis in the ventral prostate following castration (Rouleau et al., 1990; Guenette et al., 1994a). This concordance suggests that the immunoperoxidase reactivity directed by 2A10, 6E9, and 7B8 is specific for clusterin, and clearly indicates their potential utility in immunohistochemistry.

5.4. Discussion

5.4.1. Structure of recombinant rat clusterin

Recombinant rat clusterin, obtained as a methanol inducible secreted protein from transformants of the yeast *P. pastoris* and partially purified by ethanol precipitation of conditioned medium, was used effectively as an immunogen and primary screening antigen for the development of a versatile panel of hybridomas producing monospecific monoclonal antibodies to both natural and recombinant proteins. *P. pastoris* recombinant rat clusterin resembles the natural protein structurally in a number of important respects. It is extensively modified by addition of N-linked carbohydrate, and relative molecular weights of polypeptides on SDS PAGE both before and after treatment with N-glycosidase F, with or without disulfide reduction, are most compatible with a disulfide linked, presumably $\alpha\beta$ heterodimeric structure. This is supported by the isolation of monoclonal antibodies to this preparation with high affinity for one or more native epitopes on rat clusterin from the ventral prostate, with, in the case of 2A10, properties consistent with a conformational dependence on appropriate interchain associations. However, while recombinant and natural rat clusterin are to a large extent analogous at a

tertiary structural level, as for the human recombinant protein, sensitivity to yeast proteases generates a heterogeneous mixture of dimers related as truncations to the natural protein.

5.4.2. Classification of hybridoma immunological reactivity

Four hybridomas of the eight with some demonstrable specificity for rat clusterin, were more thoroughly characterized by Western analysis, immunoprecipitation, and immunohistochemistry using several recombinant and natural sources. Although all of these hybridomas secrete murine IgG_1 with kappa light chains, the pattern of reactivity obtained suggests that these represent at least four different monoclonals with different specificities. 7A8 is consistently the best hybridoma for Western analysis and unique in its high avidity for reduced and separated chains with a β restricted reactivity, while retaining good reactivity with non-reduced clusterin. In addition, qualitatively, it displayed unique reactivity with several clusterin related polypeptides. These include-castration induced bands of less than 65 kDa from non-reduced homogenates of the rat ventral prostate, and full length and truncated MalE αβ proprotein and β chain fusions from reduced lysates of the respective recombinant *E. coli*. Furthermore, it is unable to immunoprecipitate clusterin from ventral prostate solubilized under conditions expected to preserve the native structure, and under which 2A10 and 6E9 are effective. On the basis of these observations it is clear that 7A8 is a distinct monoclonal with distinct specificity.

2A10 and 6E9, although equivalent in their capacity to immunoprecipitate

clusterin under native conditions, represent two distinct monoclonals with distinct specificities on the basis of patterns of reactivity on Western blots. 2A10 displayed a remarkably higher avidity to non-reduced relative to reduced clusterin and detected both α and β chain containing MalE fusions. 6E9 in contrast, although weakly, has a higher apparent avidity for reduced rat clusterin. In lysates prepared from rat ventral prostates 4 days after castraction, it reproducably detects the 43 kDa β chain, and unambiguously displays a β chain restricted reactivity to MalE fusions.

Lastly 2D9, although not yet assayed for its ability to immunoprecipitate clusterin under mild conditions, is clearly distinct in its avidity for the reduced and separated α chain in both lysates prepared from prostates 4 days after castration, and in its high avidity for the MalE α chain in addition to weak reactivity to the MalE β chain fusion.

5.4.3. Structural implications of 2A10 immunological reactivity

The behavior of 2A10 resembles that of the anti-human clusterin monoclonal G7 in having a high affinity for a native epitope and on Western blot a much higher avidity for non-reduced protein. This pattern is suggestive of a conformational epitope dependent upon appropriate interchain associations. In Chapter 3 it was shown that the non-reduced human heterodimer is rapidly and reversibly denaturable in urea. Maintenance of the disulfide structure may facilitate renaturation in large part by holding in register segments of the α and β chain outside this domain that physically associate, in particular the putative antiparallel α helical coiled-coil. On Western blot, maintenance of this association by disulfides may facilitate renaturation of the 2A10 or G7 epitope after

initial denaturation in SDS. Reduction and chain separation would render such interactions impossible, and in consequence also renaturation and effective epitope recognition. The observation that on reducing blots of lysates prepared from prostates 4 days after castration, 2A10 had higher avidity for the unprocessed αβ proprotein despite the fact that quantitatively most clusterin is processed to the heterodimeric form is significant, because it suggests the importance of chain separation in addition to reduction. It is possible that despite reduction of disulfide bonds the unprocessed proprotein can renature, albeit much less effectively, owing to maintenance of a physical linkage between the chains. Interestingly, the polyclonal anti-rat Sertoli cell SGP-2, raised against the disulfide linked heterodimer, also displayed a generally higher avidity for non-reduced clusterin on Western blot (Fig. 5.2), suggesting that the antibody immune response to native dimeric clusterin may in general be dominated by antibodies with this property. It is tempting to speculate that the isolation of antibodies with these properties implies the existence of a structure whose stability is dominated by covalent and non-covalent interchain associations along the lines set out by the linear antiparallel model in Chapter 3 rather than one in which the two chains essentially fold independently and maintain only a limited interchain physicochemical association.

5.4.4. Preliminary analysis of clusterin coimmunoprecipitating polypeptides in the castrated rat ventral prostate

Two monoclonal antibodies, 2A10 and 6E9 were obtained that are capable of immunoprecipitating rat clusterin solubilized from the castrated rat ventral prostate under mild conditions. These two antibodies had markedly different immunological reactivity

and may thus bind to distinct epitopes, increasing the chances that at least one antibody recognizes an epitope that is not sterically hindered by clusterin ligand interactions. In preliminary experiments 2A10 and 6E9 coimmunoprecipitating polypeptides have been sought from lysates of the ventral prostate prepared in PBS glycerol (Fig. 5.5B). Of the large number of silver stained polypeptides eluted from monoclonals non covalently bound to Protein G agarose, none appear as yet to be specifically associated with 2A10 or 6E9 immunoprecipitates from day 4 post castrate lysates (Fig. 5.5C). This analysis has however, been complicated by co-eluting immunoglobulins and other nonspecifically associated proteins that may have obscured small amounts of specifically associated proteins. To reduce the number of co-eluting polypeptides, 2A10 and 6E9 will need to be prepared at preparative levels and covalently linked to a support matrix. In addition, Western blots of clusterin immunoprecipitates with antibodies to known clusterin ligands may identify the existence of the corresponding clusterin ligand complex. Alternatively, clusterin in the rat ventral prostate may be associated with lipids.

5.5. Summary

A panel of murine anti-rat clusterin monoclonal antibodies was prepared to rat clusterin expressed as a secreted protein in *P. pastoris*, and partially purified from conditioned medium by ethanol precipitation. Among the different monoclonal antibodies obtained, four distinct immunological reactivities have been characterized and antibodies useful for immunohistochemistry, Western analysis, and immunoprecipitation of clusterin from rat tissues identified. Two monoclonal antibodies having distinct reactivity are capable of immunoprecipitating clusterin from the castrated rat ventral

prostate under mild conditions. One or both of these should be useful for the identification of specific clusterin-ligand complexes in the involuting rat ventral prostate, and clarification of the role of clusterin in the complex tissue reorganization associated with this process.

APPENDIX

6. *Appendix*

Figure 6.1. Reactivity of G7 and 78E anti human clusterin monoclonal antibodies to *P. pastoris* recombinant human clusterin

20 μL of BMMY conditioned by a *P. pastoris* transformant of pD2HT7 expressing high levels of human clusterin was denatured in SDS and treated with or without N-glycosidase F. As a control for the action of proteases present in conditioned media an identical sample was denatured and immediately frozen at -20°C. Following separation by electrophoresis on a 12% SDS polyacrylamide gel under reducing conditions resolved polypeptides were electroblotted to nitrocellulose and probed in parallel with hybridoma G7 and 78E conditioned media secreting anti–human clusterin monoclonal antibodies. G7 and 78E detected many of the same polypeptides. The molecular weight of these immunoreactive bands corresponds to the distribution of clusterin α subunit N-termini from sequence analysis of PVDF blots of N-glycosylated preparations (Table 4.2) and of α26, α24, and α21 following treatment with N-glycosidase F (Fig. 4.3 and 4.5). However, G7 and 78E show distinct reactivities. G7 is much less sensitive in recognition of denatured, reduced, and separated chains indicated by the fact that the exposure time for the G7 blot was 15 minutes while that for 78E was 5 seconds. Longer exposures of the 78E blot also detected N-glycosylated bands at 24 and 20 kDa as well as N-deglycosylated bands from 15 to 21 kDa whereas under the conditions of this experiment no reactivity was detected to these bands with G7. Sensitivity of detection with G7 was considerably greater on Western blots of non-reduced clusterin and significantly on reduced blots, although proportionally much lower in abundance, appeared to recognize unprocessed forms of the αβ proprotein (relative molecular mass at about 45 kDa) with equal or greater sensitivity than the far more abundant processed forms. Together with the fact that G7 has high affinity for clusterin present in solution under mild conditions suggests that G7 recognizes a conformational epitope largely confined to the α chain but dependent upon appropriate interactions with the β chain.

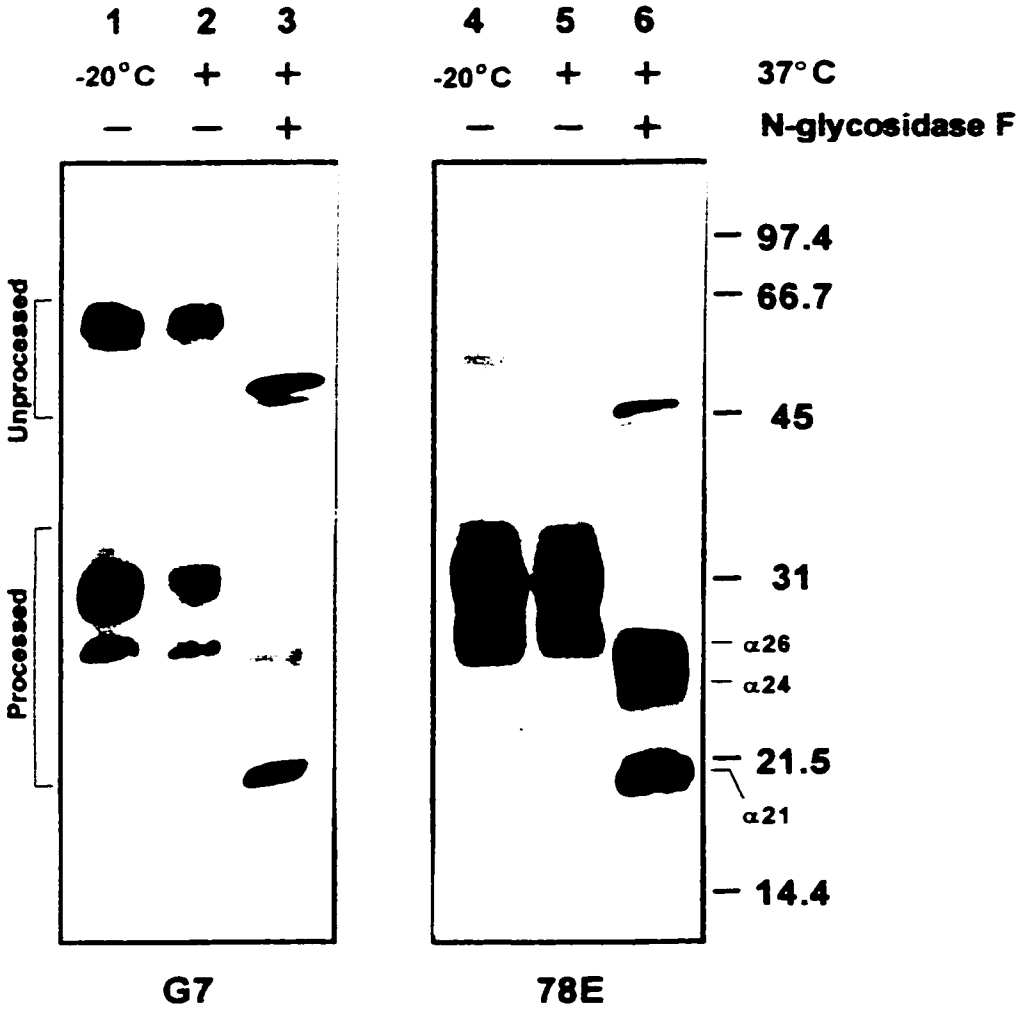
1 2 3
4 5 6
-20°C + +
-20°C + +
37°C
— — +
— — +
N-glycosidase F
Unprocessed
Processed
97.4
66.7
45
31
α26
α24
21.5
α21
14.4
G7
78E

Figure 6.2. DEAE sephacel chromatography of PEG precipitate from inulin activated human serum

Proteins precipitating between 5 and 10% (w/v) PEG from 75 mL of inulin activated human serum were redissolved in 25 mM veronal-HCl, 100 mM NaCl pH 7 and fractionated by ion exchange chromatography on DEAE Sephacel using a linear gradient of 50 to 500 mM NaCl collecting 9 mL fractions. Bottom: chromatogram developed as absorbance at 280 nm. Top: 36 μL of indicated fractions separated under non-reducing conditions by electrophoresis on an 8% SDS polyacrylamide gel and stained with Coomasie blue. The position of C5b and the locations of C6, C7, C8αγ, C8β, and C9 (C6-C9) of sC5b-9 are indicated to the right. sC5b-9 elutes between 9 to 14 mmho/cm (estimated at 220 to 410 mM NaCl) (Bhakdi and Roth, 1981). Fractions in this range demonstrating the distinctive polypeptide composition of sC5b-9 were pooled as indicated and concentrated for further purification by sucrose gradient ultracentrifugation.

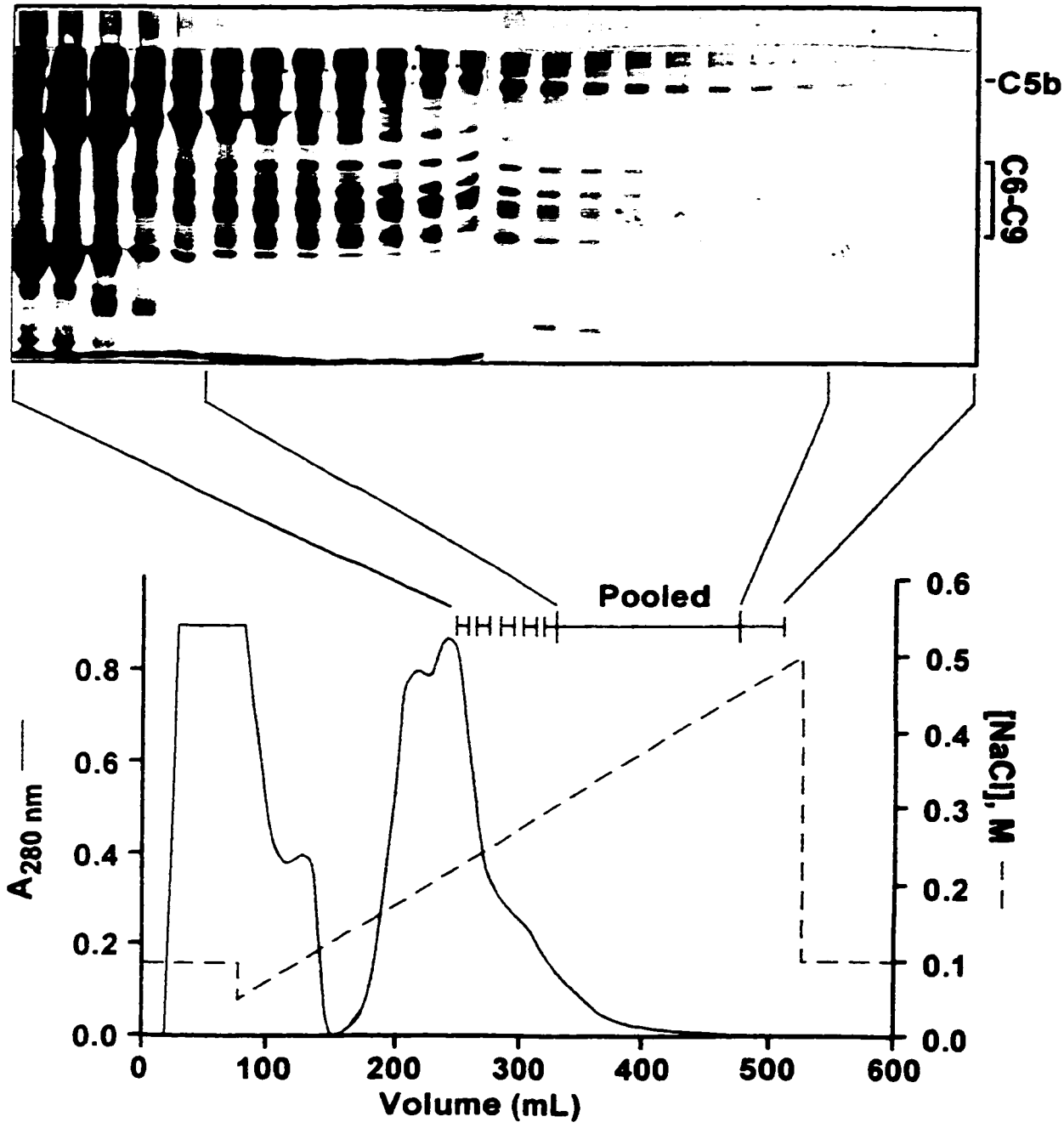
C5b
C6-C9
Pooled
0.8
0.6
0.4
0.2
0.0
A280 nm
0.6
0.5
0.4
0.3
0.2
0.1
0.0
[NaCl], M
0
100
200
300
400
500
600
Volume (mL)

Figure 6.3. Sucrose gradient ultracentrifugation of sC5b-9 from pooled DEAE sephacel fractions

1 mL aliquots of pooled, concentrated, and spin dialyzed DEAE sephacel fractions separated by sedimentation through 11.3 mL 10 to 43% (w/v) linear sucrose gradients, and fractionated from the top. Top: concentration of protein and sucrose in each fraction. Middle: 36 μL of indicated fractions separated under non-reducing conditions by electrophoresis on an 8% SDS polyacrylamide gel and stained with Coomassie blue. Molecular weight markers run in parallel are indicated to the outside right and left and the constituents of sC5b-9: C5b, C6, C7, C8αγ, C8β, and C9 are indicated in the center. Bottom: Western analysis of 20 μL of each fraction separated by electrophoresis under non-reducing conditons on a 10% SDS polyacrylamide gel and probed for clusterin with monoclonal antibody G7 (arrowhead). Fractions 13 (25.31% (w/v) sucrose) to 16 (32.6% (w/v) sucrose) inclusive were pooled and concentrated.

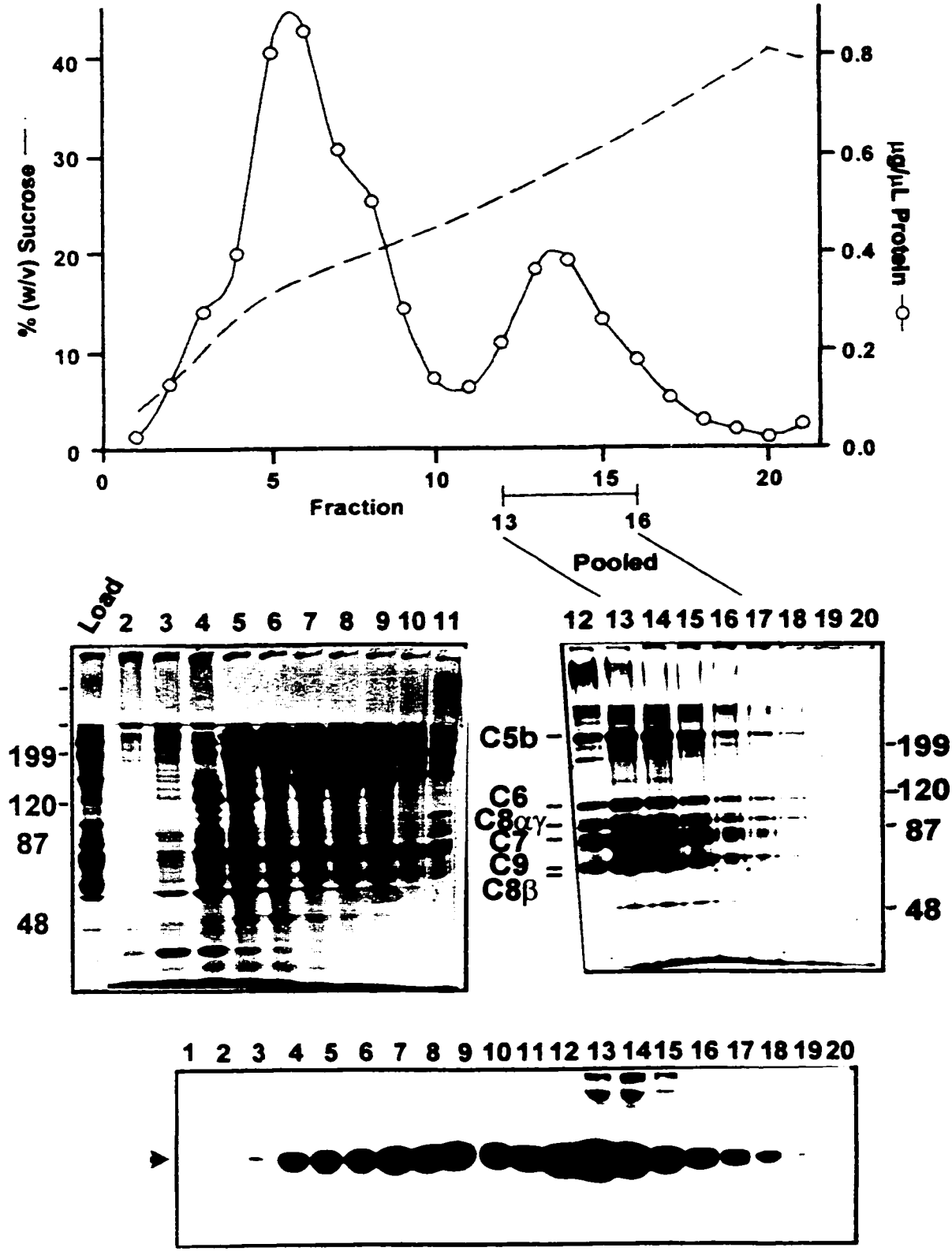
% (w/v) Sucrose
Fraction
μg/mL Protein
Pooled
Load
C5b
C6
C8αγ
C7
C9
C8β
199
120
87
48

Figure 6.4. Separation of clusterin associated with sC5b-9 by single step sedimentation of serum through 10 to 40% (w/w) linear sucrose gradients

19 μg of purified sC5b-9 or 30 μL of inulin treated or untreated human serum separated by sedimentation through 5.2 mL 10 to 40% (w/w) linear sucrose gradients and fractionated from the top. Aliqouts of the 8 successive bottom most fractions with indicated % (w/w) sucrose were dotted to nitrocellulose and probed for clusterin with monoclonal antibody G7. Clusterin associated with sC5b-9 can be separated from unassociated clusterin in serum by means of this single fractionation step.

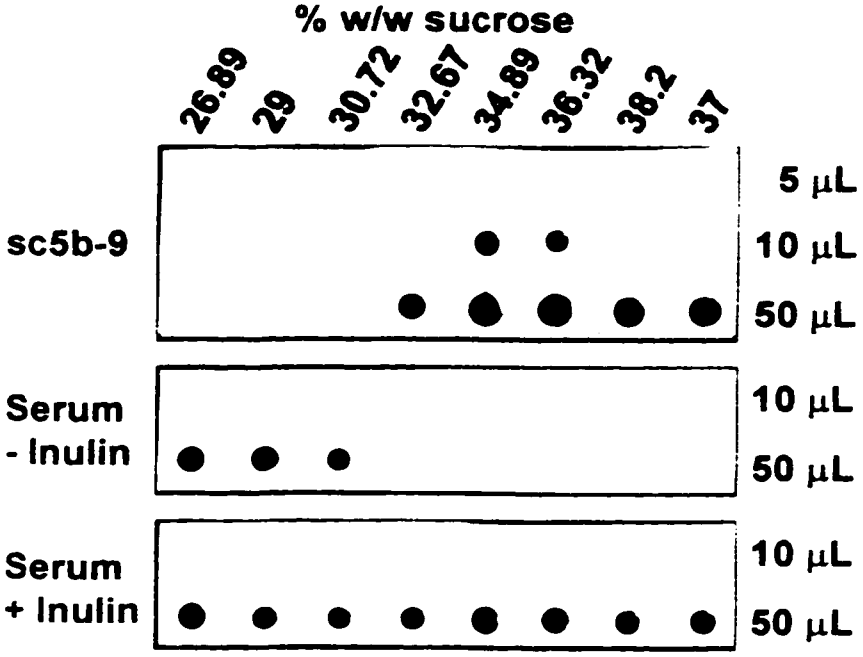
% w/w sucrose
26.89
29
30.72
32.67
34.89
36.32
38.2
37
sc5b-9
5 µL
10 µL
50 µL
Serum
- Inulin
10 µL
50 µL
Serum
+ Inulin
10 µL
50 µL

REFERENCES

7. *References*

Agarwal, N., Jomary, C., Jones, S. E., O'Rourke, K., Chaitin, M., Wordinger, R. J. and Murphy, B. F. (1996). Immunocytochemical colocalization of clusterin in apoptotic photoreceptor cells in retinal degeneration slow rds mutant mouse retinas. Biochem Biophys Res Commun 225: 84-91.

Ahuja, H. S., Tenniswood, M., Lockshin, R. and Zakeri, Z. F. (1994). Expression of clusterin in cell differentiation and cell death. Biochem Cell Biol 72: 523-530.

Ahuja, H.S., Tenniswood, M. and Zakeri, Z.F. (1996). Differential expression of clusterin in the testis and epididymis of postnatal and germ cell deficient mice. J Androl 17: 491-501.

Akesson, P., Sjoholm, A. G. and Bjorck, L. (1996). Protein SIC, a novel extracellular protein of streptococcus pyogenes interfering with complement function. J Biol Chem 271: 1081-1088.

Appel, D., Pilarsky, C., Graichen, R. and Koch-Brandt, C. (1996). Sorting of gp80 (GPIII, clusterin), a marker protein for constitutive apical secretion in Madin-Darby canine kidney (MDCK) cells, into the regulated pathway in the pheochromocytoma cell line PC12. Eur J Cell Biol 70: 142-149.

Aronow, B. J., Lund, S. D., Brown, T. L., Harmony, J. A. and Witte, D. P. (1993). Apolipoprotein J expression at fluid-tissue interfaces: potential role in barrier cytoprotection. Proc Natl Acad Sci U S A 90: 725-729.

Aronow, B. J. (1997). Preliminary observations on the phenotype of clusterin knockout mice. Third International Workshop on Clusterin, Villars-sur-Ollon, Switzerland.

Aulitzky, W. K., Schlegel, P. N., Wu, D. F., Cheng, C. Y., Chen, C. L., Li, P. S., Goldstein, M., Reidenberg, M. and Bardin, C. W. (1992). Measurement of urinary clusterin as an index of nephrotoxicity. Proc Soc Exp Biol Med 199: 93-96.

Berge, V., Johnson, E. and Hogasen, K. (1997). Clusterin and the terminal complement pathway synthesized by human umbilical vein endothelial cells are closely linked when detected on co-cultured agarose beads. Apmis 105: 17-24.

Bernstein, H. D., Poritz, M. A., Strub, K., Hoben, P. J., Brenner, S. and Walter, P. (1989). Model for signal sequence recognition from amino-acid sequence of 54K subunit of signal recognition particle. Nature 340: 482-486.

Bhakdi, S. and Roth, M. (1981). Fluid-phase SC5b-8 complex of human complement: generation and isolation from serum. J Immunol 127: 576-580.

Birkenmeier, E. H., Letts, V. A., Frankel, W. N., Magenheimer, B. S. and Calvet, J. P. (1993). Sulfated glycoprotein-2 (Sgp-2) maps to mouse chromosome 14. Mamm Genome

4: 131-132.

Blaschuk, O., Burdzy, K. and Fritz, I. B. (1983). Purification and characterization of a cell-aggregating factor (clusterin), the major glycoprotein in ram rete testis fluid. J Biol Chem 258: 7714-7720.

Blatter, M. C., James, R. W., Messmer, S., Barja, F. and Pometta, D. (1993). Identification of a distinct human high-density lipoprotein subspecies defined by a lipoprotein-associated protein, K-45. Identity of K-45 with paraoxonase. Eur J Biochem 211: 871-879.

Boggs, L. N., Fuson, K. S., Baez, M., Churgay, L., McClure, D., Becker, G. and May, P. C. (1996). Clusterin (Apo J) protects against in vitro amyloid-β (1-40) neurotoxicity. J Neurochem 67: 1324-1327.

Borghini, I., Barja, F., Pometta, D. and James, R. W. (1995). Characterization of subpopulations of lipoprotein particles isolated from human cerebrospinal fluid. Biochim Biophys Acta 1255: 192-200.

Burdick, D., Soreghan, B., Kwon, M., Kosmoski, J., Knauer, M., Henschen, A., Yates, J., Cotman, C. and Glabe, C. (1992). Assembly and aggregation properties of synthetic Alzheimer's A4/β amyloid peptide analogs. J Biol Chem 267: 546-554.

Burkey, B. F., deSilva, H. V. and Harmony, J. A. (1991). Intracellular processing of apolipoprotein J precursor to the mature heterodimer. J Lipid Res 32: 1039-1048.

Burkey, B. F., Stuart, W. D. and Harmony, J. A. (1992). Hepatic apolipoprotein J is secreted as a lipoprotein. J Lipid Res 33: 1517-1526.

Calvet, J. P. and Chadwick, L. J. (1994). Primary and secondary genetic responses after folic acid-induced acute renal injury in the mouse. J Am Soc Nephrol 5: 1324-1332.

Cardin, A. D., Demeter, D. A., Weintraub, H. J. and Jackson, R. L. (1991). Molecular design and modeling of protein-heparin interactions. Methods Enzymol 203: 556-583.

Chen, H., Tritton, T. R., Kenny, N., Absher, M. and Chiu, J. F. (1996). Tamoxifen induces TGF-β1 activity and apoptosis of human MCF- 7 breast cancer cells in vitro. J Cell Biochem 61: 9-17.

Cheng, C. Y., Chen, C. L., Feng, Z. M., Marshall, A. and Bardin, C. W. (1988a). Rat clusterin isolated from primary Sertoli cell-enriched culture medium is sulfated glycoprotein-2 (SGP-2). Biochem Biophys Res Commun 155: 398-404.

Cheng, C. Y., Mathur, P. P. and Grima, J. (1988b). Structural analysis of clusterin and its subunits in ram rete testis fluid. Biochemistry 27: 4079-4088.

Chiesa, R., Angeretti, N., Lucca, E., Salmona, M., Tagliavini, F., Bugiani, O. and Forloni, G. (1996). Clusterin (SGP-2) induction in rat astroglial cells exposed to prion protein fragment 106-126. Eur J Neurosci 8: 589-597.

Choi, N. H., Mazda, T. and Tomita, M. (1989). A serum protein SP-40,40 modulates the formation of membrane attack complex of complement on erythrocytes. Mol Immunol 26: 835-840.

Choi, N. H., Nakano, Y., Tobe, T., Mazda, T. and Tomita, M. (1990). Incorporation of SP-40,40 into the soluble membrane attack complex (SMAC, SC5b-9) of complement. Int Immunol 2: 413-417.

Choi-Miura, N. H., Takahashi, Y., Nakano, Y., Tobe, T. and Tomita, M. (1992a). Identification of the disulfide bonds in human plasma protein SP-40,40 (apolipoprotein-J). J Biochem (Tokyo) 112: 557-561.

Choi-Miura, N. H., Ihara, Y., Fukuchi, K., Takeda, M., Nakano, Y., Tobe, T. and Tomita, M. (1992b). SP-40,40 is a constituent of Alzheimer's amyloid. Acta Neuropathol (Berl) 83: 260-264.

Choi-Miura, N. H., Sakamoto, T., Tobe, T., Nakano, Y. and Tomita, M. (1993a). The role of HDL consisting of SP-40,40, apo A-I, and lipids in the formation of SMAC of complement. J Biochem (Tokyo) 113: 484-487.

Choi-Miura, N. H., Sakamoto, T., Ohtaki, S., Nakamura, H., Ishizawa, S., Takagi, Y., Gomi, K. and Tomita, M. (1993b). Elevated complement activities of sera from patients with high density lipoprotein deficiency (Tangier disease): the presence of normal level of clusterin and the possible implication in the atherosclerosis. Clin Exp Immunol 93: 242-247.

Choi-Miura, N., Matsubara, E., Oda, E., Ghiso, J., Frangione, B. and Tomita, M. (1994). Clusterin is complexed to Alzheimer's amyloid b peptide. The Second Clusterin Workshop, Coeur d'Alene, Idaho.

Clark, A. M. and Griswold, M. D. (1997a). Expression of clusterin/sulfated glycoprotein-2 under conditions of heat stress in rat Sertoli cells and a mouse Sertoli cell line. J Androl 18: 257-263.

Clark, A. M., Maguire, S. M. and Griswold, M. D. (1997b). Accumulation of clusterin/sulfated glycoprotein-2 in degenerating pachytene spermatocytes of adult rats treated with methoxyacetic acid. Biol Reprod 57: 837-846.

Cohen, C. and Parry, D. A. D. (1986). α-helical coiled coils-a widespread motif in proteins. Trends Biochem Sci 11: 245-248.

Collard, M. W. and Griswold, M. D. (1987). Biosynthesis and molecular cloning of sulfated glycoprotein 2 secreted by rat Sertoli cells. Biochem 26: 3297-3303.

Colombel, M. C. and Buttyan, R. (1995). Hormonal control of apoptosis: the rat prostate gland as a model system. Methods Cell Biol 46: 369-385.

Cornette, J. L., Cease, K. B., Margalit, H., Spouge, J. L., Berzofsky, J. A. and DeLisi, C. (1987). Hydrophobicity scales and computational techniques for detecting amphipathic structures in proteins. J Mol Biol 195: 659-685.

Correa-Rotter, R., Hostetter, T. H., Manivel, J. C., Eddy, A. A. and Rosenberg, M. E. (1992a). Intrarenal distribution of clusterin following reduction of renal mass. Kidney Int 41: 938-950.

Correa-Rotter, R., Hostetter, T. H., Nath, K. A., Manivel, J. C. and Rosenberg, M. E. (1992b). Interaction of complement and clusterin in renal injury. J Am Soc Nephrol 3: 1172-1179.

Cotman, C. W., Tenner, A. J. and Cummings, B. J. (1996). β-Amyloid converts an acute phase injury response to chronic injury responses. Neurobiol Aging 17: 723-731.

Creighton, T. E. (1979). Electrophoretic analysis of the unfolding of proteins by urea. J Mol Biol 129: 235-264.

Cyr, D. G. and Robaire, B. (1992). Regulation of sulfated glycoprotein-2 (clusterin) messenger ribonucleic acid in the rat epididymis. Endocrinol 130: 2160-2166.

Daly, N. L., Scanlon, M. J., Djordjevic, J. T., Kroon, P. A. and Smith, R. (1995). Three-dimensional structure of a cysteine-rich repeat from the low-density lipoprotein receptor. Proc Natl Acad Sci U S A 92: 6334-6338.

Danik, M., Chabot, J.G., Mercier, C., Benabid, A.L., Chauvin, C., Quirion, R. and Suh, M. (1991). Human gliomas and epileptic foci express high levels of a mRNA related to rat testicular sulfated glycoprotein 2, a purported marker of cell death. Proc Natl Acad Sci U S A 88: 8577-8581.

Danik, M., Chabot, J. G., Hassan-Gonzalez, D., Suh, M. and Quirion, R. (1993). Localization of sulfated glycoprotein-2/clusterin mRNA in the rat brain by in situ hybridization. J Comp Neurol 334: 209-227.

Darnell, J., Lodish, H. and Baltimore, D. (1986). Assembly of organelles. in: Molecular Cell Biology. New York, NY, Scientific American Books, Inc . 911-979.

Day, J. R., Laping, N. J., McNeill, T. H., Schreiber, S. S., Pasinetti, G. and Finch, C. E. (1990). Castration enhances expression of glial fibrillary acidic protein and sulfated

glycoprotein-2 in the intact and lesion- altered hippocampus of the adult male rat. Mol Endocrinol 4: 1995-2002.

de Silva, H. V., Harmony, J. A., Stuart, W. D., Gil, C. M. and Robbins, J. (1990a). Apolipoprotein J: structure and tissue distribution. Biochem 29: 5380-5389.

de Silva, H. V., Stuart, W. D., Duvic, C. R., Wetterau, J. R., Ray, M. J., Ferguson, D. G., Albers, H. W., Smith, W. R. and Harmony, J. A. (1990b). A 70-kDa apolipoprotein designated ApoJ is a marker for subclasses of human plasma high density lipoproteins. J Biol Chem 265: 13240-13247.

de Silva, H. V., Stuart, W. D., Park, Y. B., Mao, S. J., Gil, C. M., Wetterau, J. R., Busch, S. J. and Harmony, J. A. (1990c). Purification and characterization of apolipoprotein J. J Biol Chem 265: 14292-14297.

Diemer, V., Hoyle, M., Baglioni, C. and Millis, A. J. (1992). Expression of porcine complement cytolysis inhibitor mRNA in cultured aortic smooth muscle cells. Changes during differentiation in vitro. J Biol Chem 267: 5257-5264.

Dietzsch, E., Murphy, B. F., Kirszbaum, L., Walker, I. D. and Garson, O. M. (1992). Regional localization of the gene for clusterin (SP-40,40; gene symbol CLI) to human chromosome 8p12-->p21. Cytogenet Cell Genet 61: 178-179.

Duguid, J. R., Bohmont, C. W., Liu, N. G. and Tourtellotte, W. W. (1989). Changes in brain gene expression shared by scrapie and Alzheimer disease. Proc Natl Acad Sci U S A 86: 7260-7264.

Dvergsten, J., Manivel, J. C., Correa-Rotter, R. and Rosenberg, M. E. (1994). Expression of clusterin in human renal diseases. Kidney Int 45: 828-835.

Eddy, A. A. and Fritz, I. B. (1991). Localization of clusterin in the epimembranous deposits of passive Heymann nephritis. Kidney Int 39: 247-252.

Ehnholm, C., Bozas, S. E., Tenkanen, H., Kirszbaum, L., Metso, J., Murphy, B. and Walker, I. D. (1991). The apolipoprotein A-I binding protein of placenta and the SP-40, 40 protein of human blood are different proteins which both bind to apolipoprotein A-I. Biochim Biophys Acta 1086: 255-260.

Esser, A. F. (1994). The membrane attack complex of complement. Assembly, structure and cytotoxic activity. Toxicology 87: 229-247.

Farquhar, M. G., Kerjaschki, D., Lundstrom, M. and Orlando, R. A. (1994). gp330 and RAP: the Heymann nephritis antigenic complex. Ann N Y Acad Sci 737: 96-113.

Fink, T. M., Zimmer, M., Tschopp, J., Etienne, J., Jenne, D. E. and Lichter, P. (1993).

Human clusterin (CLI) maps to 8p21 in proximity to the lipoprotein lipase (LPL) gene. Genomics 16: 526-528.

Flach, R., Cattaruzza, M. and Koch-Brandt, C. (1995). Clusterin gene expression in apoptotic MDCK cells is dependent on the apoptosis-inducing stimulus. Biochim Biophys Acta 1268: 325-328.

Fraser, P. E., McLachlan, D. R., Surewicz, W. K., Mizzen, C. A., Snow, A. D., Nguyen, J. T. and Kirschner, D. A. (1994). Conformation and fibrillogenesis of Alzheimer Aβ peptides with selected substitution of charged residues. J Mol Biol 244: 64-73.

French, L. E., Tschopp, J. and Schifferli, J. A. (1992a). Clusterin in renal tissue: preferential localization with the terminal complement complex and immunoglobulin deposits in glomeruli. Clin Exp Immunol 88: 389-393.

French, L. E., Polla, L. L., Tschopp, J. and Schifferli, J. A. (1992b). Membrane attack complex (MAC) deposits in skin are not always accompanied by S-protein and clusterin. J Invest Dermatol 98: 758-763.

French, L. E., Wohlwend, A., Sappino, A. P., Tschopp, J. and Schifferli, J. A. (1994). Human clusterin gene expression is confined to surviving cells during in vitro programmed cell death. J Clin Invest 93: 877-884.

Fritz, I. B., Burdzy, K., Setchell, B. and Blaschuk, O. (1983). Ram rete testis fluid contains a protein (clusterin) which influences cell-cell interactions in vitro. Biol Reprod 28: 1173-1188.

Fritz, I. B. and Burdzy, K. (1989). Novel action of carnitine: inhibition of aggregation of dispersed cells elicited by clusterin in vitro. J Cell Physiol 140: 18-28.

Fritz, I. B., Wong, K. and Burdzy, K. (1991). Clustering of erythrocytes by fibrinogen is inhibited by carnitine: evidence that sulfhydryl groups on red blood cell membranes are involved in carnitine actions. J Cell Physiol 149: 269-276.

Furuya, Y., Isaacs, J. T. and Shimazaki, J. (1995). Induction of programmed death/apoptosis androgen-dependent mouse mammary tumor cell line (Shionogi Carcinoma 115) by androgen withdrawal. Jpn J Cancer Res 86: 1159-1165.

Garden, G. A., Bothwell, M. and Rubel, E. W. (1991). Lack of correspondence between mRNA expression for a putative cell death molecule (SGP-2) and neuronal cell death in the central nervous system. J Neurobiol 22: 590-604.

Gelissen, I. C., Hochgrebe, T., Wilson, M. R., Easterbrook-Smith, S. B., Jessup, W., Dean, R. T. and Brown, A. J. (1998). Apolipoprotein J (clusterin) induces cholesterol export from macrophage-foam cells: a potential anti-atherogenic function? Biochem J

331: 231-237.

Gellman, S. H. (1991). On the role of methionine residues in the sequence-independent recognition of nonpolar protein surfaces. Biochem 30: 6633-6636.

Ghiso, J., Matsubara, E., Koudinov, A., Choi-Miura, N. H., Tomita, M., Wisniewski, T. and Frangione, B. (1993). The cerebrospinal-fluid soluble form of Alzheimer's amyloid β is complexed to SP-40,40 (apolipoprotein J), an inhibitor of the complement membrane-attack complex. Biochem J 293: 27-30.

Golabek, A., Marques, M. A., Lalowski, M. and Wisniewski, T. (1995). Amyloid β binding proteins in vitro and in normal human cerebrospinal fluid. Neurosci Lett 191: 79-82.

Golabek, A. A., Soto, C., Vogel, T. and Wisniewski, T. (1996). The interaction between apolipoprotein E and Alzheimer's amyloid β-peptide is dependent on β-peptide conformation. J Biol Chem 271: 10602-10606.

Goldenberg, D. P. (1989). Analysis of protein conformation by gel electrophoresis. in: Protein structure: a practical approach. Eds.: T. E. Creighton. Eynsham, Oxford, England, IRL Press at Oxford University Press. 225-250.

Goldner-Sauve, A., Szpirer, C., Szpirer, J., Levan, G. and Gasser, D. L. (1991). Chromosome assignments of the genes for glucocorticoid receptor, myelin basic protein, leukocyte common antigen, and TRPM2 in the rat. Biochem Genet 29: 275-286.

Grima, J., Zwain, I., Lockshin, R. A., Bardin, C. W. and Cheng, C. Y. (1990). Diverse secretory patterns of clusterin by epididymis and prostate/seminal vesicles undergoing cell regression after orchiectomy. Endocrinol 126: 2989-2997.

Grima, J., Pineau, C., Bardin, C. W. and Cheng, C. Y. (1992). Rat Sertoli cell clusterin, α2-macroglobulin, and testins: biosynthesis and differential regulation by germ cells. Mol Cell Endocrinol 89: 127-140.

Grinna, L. S. and Tschopp, J. F. (1989). Size distribution and general structural features of N-linked oligosaccharides from the methylotrophic yeast, Pichia pastoris. Yeast 5: 107-115.

Griswold, M. D., Roberts, K. and Bishop, P. (1986). Purification and characterization of a sulfated glycoprotein secreted by Sertoli cells. Biochem 25: 7265-7270.

Guenal, I. and Mignotte, B. (1995). Studies of specific gene induction during apoptosis of cell lines conditionally immortalized by SV40. FEBS Lett 374: 384-386.

Guenette, R. S., Daehlin, L., Mooibroek, M., Wong, K. and Tenniswood, M. (1994a).

Thanatogen expression during involution of the rat ventral prostate after castration. J Androl 15: 200-211.

Guenette, R. S., Corbeil, H. B., Léger, J., Wong, K., Mezl, V., Mooibroek, M. and Tenniswood, M. (1994b). Induction of gene expression during involution of the lactating mammary gland of the rat. J Mol Endocrinol 12: 47-60.

Hammad, S. M., Ranganathan, S., Loukinova, E., Twal, W. O. and Argraves, W. S. (1997). Interaction of apolipoprotein J amyloid b-peptide complex with low density lipoprotein receptor-related protein-2/megalin. A mechanism to prevent pathological accumulation of amyloidβ- peptide. J Biol Chem 272: 18644-18649.

Hardardottir, I., Kunitake, S. T., Moser, A. H., Doerrler, W. T., Rapp, J. H., Grunfeld, C. and Feingold, K. R. (1994). Endotoxin and cytokines increase hepatic messenger RNA levels and serum concentrations of apolipoprotein J (clusterin) in Syrian hamsters. J Clin Invest 94: 1304-1309.

Harding, M. A., Chadwick, L. J., Gattone, V. H. and Calvet, J. P. (1991). The SGP-2 gene is developmentally regulated in the mouse kidney and abnormally expressed in collecting duct cysts in polycystic kidney disease. Dev Biol 146: 483-490.

Hardy, J. (1997). Amyloid, the presenilins and Alzheimer's disease. Trends Neurosci 20: 154-159.

Harlow, E. and Lane, D. (1988). Antibodies: a laboratory manual. Cold Spring Harbor Laboratory, Cold Spring Harbor, NY.

Hartmann, K., Rauch, J., Urban, J., Parczyk, K., Diel, P., Pilarsky, C., Appel, D., Haase, W., Mann, K., Weller, A. and et al. (1991). Molecular cloning of gp80, a glycoprotein complex secreted by kidney cells in vitro and in vivo. A link to the reproductive system and to the complement cascade. J Biol Chem 266: 9924-9931.

Herault, Y., Chatelain, G., Brun, G. and Michel, D. (1992). V-src-induced-transcription of the avian clusterin gene. Nucl Acids Res 20: 6377-6383.

Hermo, L., Wright, J., Oko, R. and Morales, C. R. (1991). Role of epithelial cells of the male excurrent duct system of the rat in the endocytosis or secretion of sulfated glycoprotein- 2 (clusterin). Biol Reprod 44: 1113-1131.

Hinton, B. T. (1995). What does the epididymis do and how does it work? in Handbook of Andrology.Eds.: B. Robaire, J. Pryor and J. Trasler. Lawrence, KS, Allen Press, Inc. 18-20.

Hochgrebe, T., Humphreys, D., Wilson, M. R. and Easterbrook-Smith, S. B. (1997). Clusterin does not regulate complement activation under physiologically relevant

conditions. Third International Clusterin Workshop, Villars-sur-Ollon, Switzerland.

Hugly, S., Roberts, K. and Griswold, M. D. (1988). Transferrin and sulfated glycoprotein-2 messenger ribonucleic acid levels in the testis and isolated Sertoli cells of hypophysectomized rats. Endocrinol 122: 1390-1396.

Humphreys, D., Hochgrebe, T. T., Easterbrook-Smith, S. B., Tenniswood, M. P. and Wilson, M. R. (1997). Effects of clusterin overexpression on TNFα- and TGFβ-mediated death of L929 cells. Biochem 36: 15233-15243.

Hunter, W. M. and Greenwood, F. C. (1962). Preparation of Iodine-131 labeled human growth hormone of high specific activity. Nature 194: 495-496.

Igdoura, S. A., Hermo, L. and Morales, C. R. (1994). Sulfated glycoprotein-2 synthesized by nonciliated cells of the efferent ducts is targeted to the lysosomal compartment. Microsc Res Tech 29: 468-480.

Jackson Huang, T. H., Fraser, P. E. and Chakrabartty, A. (1997). Fibrillogenesis of Alzheimer Aβ peptides studied by flouresence energy transfer. J Mol Biol 269: 214-224.

James, R. W., Hochstrasser, A. C., Borghini, I., Martin, B., Pometta, D. and Hochstrasser, D. (1991). Characterization of a human high density lipoprotein-associated protein, NA1/NA2. Identity with SP-40,40, an inhibitor of complement-mediated cytolysis. Arterioscler Thromb 11: 645-652.

James, R. W., Hochstrasser, D., Tissot, J. D., Funk, M., Appel, R., Barja, F., Pellegrini, C., Muller, A. F. and Pometta, D. (1988). Protein heterogeneity of lipoprotein particles containing apolipoprotein A-I without apolipoprotein A-II and apolipoprotein A-I with apolipoprotein A-II isolated from human plasma. J Lipid Res 29: 1557-1571.

Jenkins, S. H., Stuart, W. D., Bottoms, L. A. and Harmony, J. A. (1996). Quantitation of plasma apolipoprotein J. Methods Enzymol 263: 309-316.

Jenne, D., Hugo, F. and Bhakdi, S. (1985). Monoclonal antibodies to human plasma protein X alias complement S-protein. Biosci Rep 5: 343-352.

Jenne, D. E. and Tschopp, J. (1989). Molecular structure and functional characterization of a human complement cytolysis inhibitor found in blood and seminal plasma: identity to sulfated glycoprotein 2, a constituent of rat testis fluid. Proc Natl Acad Sci U S A 86: 7123-7127.

Jenne, D. E., Lowin, B., Peitsch, M. C., Bottcher, A., Schmitz, G. and Tschopp, J. (1991). Clusterin (complement lysis inhibitor) forms a high density lipoprotein complex with apolipoprotein A-I in human plasma. J Biol Chem 266: 11030-11036.

Jomary, C., Ahir, A., Agarwal, N., Neal, M. J. and Jones, S. E. (1995). Spatio-temporal pattern of ocular clusterin mRNA expression in the rd mouse. Brain Res Mol Brain Res 29: 172-176.

Jones, D. H. and Howard, B. H. (1991). A rapid method for recombination and site-specific mutagenesis by placing homologous ends on DNA using polymerase chain reaction. Biotech 10: 62-66.

Jones, S. E., Meerabux, J. M., Yeats, D. A. and Neal, M. J. (1992). Analysis of differentially expressed genes in retinitis pigmentosa retinas. Altered expression of clusterin mRNA. FEBS Lett 300: 279-282.

Jordan-Starck, T. C., Lund, S. D., Witte, D. P., Aronow, B. J., Ley, C. A., Stuart, W. D., Swertfeger, D. K., Clayton, L. R., Sells, S. F., Paigen, B. and et al. (1994). Mouse apolipoprotein J: characterization of a gene implicated in atherosclerosis. J Lipid Res 35: 194-210.

Kamboh, M. I., Harmony, J. A., Sepehrnia, B., Nwankwo, M. and Ferrell, R. E. (1991). Genetic studies of human apolipoproteins. XX. Genetic polymorphism of apolipoprotein J and its impact on quantitative lipid traits in normolipidemic subjects. Am J Hum Genet 49: 1167-1173.

Kapron, J. T., Hilliard, G. M., Lakins, J. N., Tenniswood, M. P., West, K. A., Carr, S. A. and Crabb, J. W. (1997). Identification and characterization of glycosylation sites in human serum clusterin. Protein Sci 6: 2120-2133.

Kelly, J. W. (1996). Alternative conformations of amyloidogenic proteins govern their behavior. Curr Opin Struct Biol 6: 11-17.

Kelso, G. J., Stuart, W. D., Richter, R. J., Furlong, C. E., Jordan-Starck, T. C. and Harmony, J. A. (1994). Apolipoprotein J is associated with paraoxonase in human plasma. Biochem 33: 832-839.

Kimura, K. and Yamamoto, M. (1996). Modification of the alternative splicing process of testosterone- repressed prostate message-2 (TRPM-2) gene by protein synthesis inhibitors and heat shock treatment. Biochim Biophys Acta 1307: 83-88.

Kirszbaum, L., Sharpe, J. A., Murphy, B., d'Apice, A. J., Classon, B., Hudson, P. and Walker, I. D. (1989). Molecular cloning and characterization of the novel, human complement-associated protein, SP-40,40: a link between the complement and reproductive systems. EMBO J 8: 711-718.

Kirszbaum, L., Bozas, S. E. and Walker, I. D. (1992). SP-40,40, a protein involved in the control of the complement pathway, possesses a unique array of disulphide bridges. FEBS Lett 297: 70-76.

Kissinger, C., Skinner, M. K. and Griswold, M. D. (1982). Analysis of Sertoli cell-secreted proteins by two-dimensional gel electrophoresis. Biol Reprod 27: 233-240.

Koudinov, A., Matsubara, E., Frangione, B. and Ghiso, J. (1994). The soluble form of Alzheimer's amyloid β protein is complexed to high density lipoprotein 3 and very high density lipoprotein in normal human plasma. Biochem Biophys Res Commun 205: 1164-1171.

Koudinov, A. R. and Koudinova, N. V. (1997). Alzheimer's soluble amyloid β protein is secreted by HepG2 cells as an apolipoprotein. Cell Biol Int 21: 265-271.

Kounnas, M. Z., Stefansson, S., Loukinova, E., Argraves, K. M., Strickland, D. K. and Argraves, W. S. (1994). An overview of the structure and function of glycoprotein 330, a receptor related to the α2-macroglobulin receptor. Ann N Y Acad Sci 737: 114-123.

Kounnas, M. Z., Loukinova, E. B., Stefansson, S., Harmony, J. A., Brewer, B. H., Strickland, D. K. and Argraves, W. S. (1995). Identification of glycoprotein 330 as an endocytic receptor for apolipoprotein J/clusterin. J Biol Chem 270: 13070-13075.

Kyprianou, N. and Isaacs, J. T. (1989). "Thymineless" death in androgen-independent prostatic cancer cells. Biochem Biophys Res Commun 165: 73-81.

Kyprianou, N., English, H. F. and Isaacs, J. T. (1990). Programmed cell death during regression of PC-82 human prostate cancer following androgen ablation. Cancer Res 50: 3748-3753.

Kyprianou, N., English, H. F., Davidson, N. E. and Isaacs, J. T. (1991a). Programmed cell death during regression of the MCF-7 human breast cancer following estrogen ablation. Cancer Res 51: 162-166.

Kyprianou, N., Alexander, R. B. and Isaacs, J. T. (1991b). Activation of programmed cell death by recombinant human tumor necrosis factor plus topoisomerase II-targeted drugs in L929 tumor cells. J Natl Cancer Inst 83: 346-350.

Kyprianou, N., Bains, A. K. and Jacobs, S. C. (1994). Induction of apoptosis in androgen-independent human prostate cancer cells undergoing thymineless death. Prostate 25: 66-75.

Laemmli, U. K. (1970). Cleavage of structural proteins during the assembly of the head of bacteriophage T4. Nature 227: 680-685.

Lampert-Etchells, M., McNeill, T. H., Laping, N. J., Zarow, C., Finch, C. E. and May, P. C. (1991). Sulfated glycoprotein-2 is increased in rat hippocampus following entorhinal cortex lesioning. Brain Res 563: 101-106.

Laping, N. J., Nichols, N. R., Day, J. R. and Finch, C. E. (1991). Corticosterone differentially regulates the bilateral response of astrocyte mRNAs in the hippocampus to entorhinal cortex lesions in male rats. Brain Res Mol Brain Res 10: 291-297.

Laslop, A., Steiner, H. J., Egger, C., Wolkersdorfer, M., Kapelari, S., Hogue-Angeletti, R., Erickson, J. D., Fischer-Colbrie, R. and Winkler, H. (1993). Glycoprotein III (clusterin, sulfated glycoprotein 2) in endocrine, nervous, and other tissues: immunochemical characterization, subcellular localization, and regulation of biosynthesis. J Neurochem 61: 1498-1505.

Law, G. L. and Griswold, M. D. (1994). Activity and form of sulfated glycoprotein 2 (clusterin) from cultured Sertoli cells, testis, and epididymis of the rat. Biol Reprod 50: 669-679.

Lee, J. P., Stimson, E. R., Ghilardi, J. R., Mantyh, P. W., Lu, Y. A., Felix, A. M., Llanos, W., Behbin, A., Cummings, M., Van Criekinge, M. and et al. (1995). 1H NMR of Aβ amyloid peptide congeners in water solution. Conformational changes correlate with plaque competence. Biochem 34: 5191-5200.

Lee, K. H., Ji, Y. M., Lim, H. M., Lee, S. C. and You, K. H. (1993). Molecular cloning and sequencing of sulfated glycoprotein-2 cDNA from testis of mouse: implications of two different mRNAs of SGP-2. Biochem Biophys Res Commun 194: 1175-1180.

Léger, J. G., Montpetit, M. L. and Tenniswood, M. P. (1987). Characterization and cloning of androgen-repressed mRNAs from rat ventral prostate. Biochem Biophys Res Commun 147: 196-203.

Léger, J. G., Le Guellec, R. and Tenniswood, M. P. (1988). Treatment with antiandrogens induces an androgen-repressed gene in the rat ventral prostate. Prostate 13: 131-142.

Lim, V. I. (1978). Polypeptide chain folding through a highly helical intermediate as a general principle of globular protein structure formation. FEBS Lett 89: 10-14.

Liu, L., Tornqvist, E., Mattsson, P., Eriksson, N. P., Persson, J. K., Morgan, B. P., Aldskogius, H. and Svensson, M. (1995). Complement and clusterin in the spinal cord dorsal horn and gracile nucleus following sciatic nerve injury in the adult rat. Neurosci 68: 167-179.

Lupas, A., Van Dyke, M. and Stock, J. (1991). Predicting coiled coils from protein sequences. Science 252: 1162-1164.

Mackness, B., Hunt, R., Durrington, P. N. and Mackness, M. I. (1997). Increased immunolocalization of paraoxonase, clusterin, and apolipoprotein A-I in the human artery wall with the progression of atherosclerosis. Arterioscler Thromb Vasc Biol 17:

1233-1238.

Margalit, H., Spouge, J. L., Cornette, J. L., Cease, K. B., DeLisi, C. and Berzofsky, J. A. (1987). Prediction of immunodominant helper T cell antigenic sites from the primary sequence. J Immunol 138: 2213-2229.

Margalit, H., Fischer, N. and Ben-Sasson, S. A. (1993). Comparative analysis of structurally defined heparin binding sequences reveals a distinct spatial distribution of basic residues. J Biol Chem 268: 19228-19231.

Martin, D. P., Ito, A., Horigome, K., Lampe, P. A. and Johnson, E. M., Jr. (1992). Biochemical characterization of programmed cell death in NGF- deprived sympathetic neurons. J Neurobiol 23: 1205-1220.

Matsubara, E., Frangione, B. and Ghiso, J. (1995). Characterization of apolipoprotein J-Alzheimer's Aβ interaction. J Biol Chem 270: 7563-7567.

Matsubara, E., Soto, C., Governale, S., Frangione, B. and Ghiso, J. (1996). Apolipoprotein J and Alzheimer's amyloid β solubility. Biochem J 316: 671-679.

Mattmueller, D. R. and Hinton, B. T. (1991). In vivo secretion and association of clusterin (SGP-2) in luminal fluid with spermatozoa in the rat testis and epididymis. Mol Reprod Dev 30: 62-69.

May, P. C., Lampert-Etchells, M., Johnson, S. A., Poirier, J., Masters, J. N. and Finch, C. E. (1990). Dynamics of gene expression for a hippocampal glycoprotein elevated in Alzheimer's disease and in response to experimental lesions in rat. Neuron 5: 831-839.

May, P. C., Robison, P., Fuson, K., Smalstig, B., Stephenson, D. and Clemens, J. A. (1992). Sulfated glycoprotein-2 expression increases in rodent brain after transient global ischemia. Brain Res Mol Brain Res 15: 33-39.

McDonald, J. F. and Nelsestuen, G. L. (1997). Potent inhibition of terminal complement assembly by clusterin: characterization of its impact on C9 polymerization. Biochem 36: 7464-7473.

McGeer, P. L., Kawamata, T. and Walker, D. G. (1992). Distribution of clusterin in Alzheimer brain tissue. Brain Res 579: 337-341.

Michel, D., Gillet, G., Volovitch, M., Pessac, B., Calothy, G. and Brun, G. (1989). Expression of a novel gene encoding a 51.5 kD precursor protein is induced by different retroviral oncogenes in quail neuroretinal cells. Oncogene Res 4: 127-136.

Michel, D., Chatelain, G., Herault, Y. and Brun, G. (1995). The expression of the avian clusterin gene can be driven by two alternative promoters with distinct regulatory

elements. Eur J Biochem 229: 215-223.

Michel, D., Chatelain, G., North, S. and Brun, G. (1997a). Stress-induced transcription of the clusterin/apoJ gene. Biochem J 328: 45-50.

Michel, D., Moyse, E., Trembleau, A., Jourdan, F. and Brun, G. (1997b). Clusterin/ApoJ expression is associated with neuronal apoptosis in the olfactory mucosa of the adult mouse. J Cell Sci 110: 1635-1645.

Miles, E. W. (1977). Modification of histidyl residues in proteins by diethylpyrocarbonate. Methods Enzymol 47: 431-442.

Moestrup, S. K., Christensen, E. I., Nielsen, S., Jorgensen, K. E., Bjrn, S. E., Rigaard, H. and Gliemann, J. (1994). Binding and endocytosis of proteins mediated by epithelial gp330. Ann N Y Acad Sci 737: 124-137.

Monera, O. D., Zhou, N. E., Kay, C. M. and Hodges, R. S. (1993). Comparison of antiparallel and parallel two-stranded α-helical coiled-coils. Design, synthesis, and characterization. J Biol Chem 268: 19218-19227.

Monera, O. D., Kay, C. M. and Hodges, R. S. (1994). Electrostatic interactions control the parallel and antiparallel orientation of α-helical chains in two-stranded α-helical coiled-coils. Biochem 33: 3862-3871.

Montpetit, M. L., Lawless, K. R. and Tenniswood, M. (1986). Androgen-repressed messages in the rat ventral prostate. Prostate 8: 25-36.

Morales, C. R., Igdoura, S. A., Wosu, U. A., Boman, J. and Argraves, W. S. (1996). Low density lipoprotein receptor-related protein-2 expression in efferent duct and epididymal epithelia: evidence in rats for its in vivo role in endocytosis of apolipoprotein J/clusterin. Biol Reprod 55: 676-683.

Muller-Eberhard, H. J. (1986). The membrane attack complex of complement. Ann Rev Immunol 4: 503-528.

Muller-Eberhard, H. J. (1988). Molecular organization and function of the complement system. Ann Rev Biochem 57: 321-347.

Murphy, B. F., Kirszbaum, L., Walker, I. D. and d'Apice, A. J. (1988). SP-40,40, a newly identified normal human serum protein found in the SC5b-9 complex of complement and in the immune deposits in glomerulonephritis. J Clin Invest 81: 1858-1864.

Murphy, B. F., Saunders, J. R., O'Bryan, M. K., Kirszbaum, L., Walker, I. D. and d'Apice, A. J. (1989). SP-40,40 is an inhibitor of C5b-6-initiated haemolysis. Int Immunol 1: 551-554.

Myoken, Y., Okamoto, T., Osaki, T., Yabumoto, M., Sato, G. H., Takada, K. and Sato, J. D. (1989). An alternative method for the isolation of NS-1 hybridomas using cholesterol auxotrophy of NS-1 mouse myeloma cells. In Vitro Cell Dev Biol 25: 477-480.

Narvaez, C. J., Vanweelden, K., Byrne, I. and Welsh, J. (1996). Characterization of a vitamin D3-resistant MCF-7 cell line. Endocrinol 137: 400-409.

Nath, K. A., Dvergsten, J., Correa-Rotter, R., Hostetter, T. H., Manivel, J. C. and Rosenberg, M. E. (1994). Induction of clusterin in acute and chronic oxidative renal disease in the rat and its dissociation from cell injury. Lab Invest 71: 209-218.

Navab, M., Hama-Levy, S., Van Lenten, B. J., Fonarow, G. C., Cardinez, C. J., Castellani, L. W., Brennan, M. L., Lusis, A. J. and Fogelman, A. M. (1997). Mildly oxidized LDL induces an increased apolipoprotein J/paraoxonase ratio. J Clin Invest 99: 2005-2019.

O'Bryan, M. K., Baker, H. W., Saunders, J. R., Kirszbaum, L., Walker, I. D., Hudson, P., Liu, D. Y., Glew, M. D., d'Apice, A. J. and Murphy, B. F. (1990). Human seminal clusterin (SP-40,40). Isolation and characterization. J Clin Invest 85: 1477-1486.

Oda, T., Pasinetti, G. M., Osterburg, H. H., Anderson, C., Johnson, S. A. and Finch, C. E. (1994). Purification and characterization of brain clusterin. Biochem Biophys Res Commun 204: 1131-1136.

Oda, T., Wals, P., Osterburg, H. H., Johnson, S. A., Pasinetti, G. M., Morgan, T. E., Rozovsky, I., Stine, W. B., Snyder, S. W., Holzman, T. F. and et al. (1995). Clusterin (apoJ) alters the aggregation of amyloid β-peptide (Aβ1-42) and forms slowly sedimenting Aβ complexes that cause oxidative stress. Exp Neurol 136: 22-31.

Oritani, K. and Kincade, P. W. (1996). Identification of stromal cell products that interact with pre-B cells. J Cell Biol 134: 771-782.

Orlando, R. A., Exner, M., Czekay, R. P., Yamazaki, H., Saito, A., Ullrich, R., Kerjaschki, D. and Farquhar, M. G. (1997). Identification of the second cluster of ligand-binding repeats in megalin as a site for receptor-ligand interactions. Proc Natl Acad Sci U S A 94: 2368-2373.

Palmer, D. J. and Christie, D. L. (1990). The primary structure of glycoprotein III from bovine adrenal medullary chromaffin granules. Sequence similarity with human serum protein-40,40 and rat Sertoli cell glycoprotein. J Biol Chem 265: 6617-6623.

Pankhurst, G. J., Bennett, C. A. and Easterbrook-Smith, S. B. (1997). Clusterin is a heparin-binding protein. Third International Workshop on Clusterin, Villars-sur-Ollon, Switzerland.

Partridge, S. R., Baker, M. S., Walker, M. J. and Wilson, M. R. (1996). Clusterin, a putative complement regulator, binds to the cell surface of Staphylococcus aureus clinical isolates. Infect Immun 64: 4324-4329.

Pasinetti, G. M. and Finch, C. E. (1991). Sulfated glycoprotein-2 (SGP-2) mRNA is expressed in rat striatal astrocytes following ibotenic acid lesions. Neurosci Lett 130: 1-4.

Pasinetti, G. M., Cheng, H. W., Morgan, D. G., Lampert-Etchells, M., McNeill, T. H. and Finch, C. E. (1993). Astrocytic messenger RNA responses to striatal deafferentation in male rat. Neurosci 53: 199-211.

Pike, C. J., Burdick, D., Walencewicz, A. J., Glabe, C. G. and Cotman, C. W. (1993). Neurodegeneration induced by β-amyloid peptides in vitro: the role of peptide assembly state. J Neurosci 13: 1676-1687.

Podack, E. R. and Tschopp, J. (1982). Circular polymerization of the ninth component of complement. Ring closure of the tubular complex confers resistance to detergent dissociation and to proteolytic degradation. J Biol Chem 257: 15204-15212.

Polihronis, M., Paizis, K., Carter, G., Sedal, L. and Murphy, B. (1993). Elevation of human cerebrospinal fluid clusterin concentration is associated with acute neuropathology. J Neurol Sci 115: 230-233.

Popper, P., Farber, D. B., Micevych, P. E., Minoofar, K. and Bronstein, J. M. (1997). TRPM-2 expression and tunel staining in neurodegenerative diseases: studies in wobbler and rd mice. Exp Neurol 143: 246-254.

Punnia-Moorthy, A. (1988). Buffering capacity of normal and inflamed tissues during the injection of local anaesthetic solutions. Br J Anaesth 61: 154-159.

Purrello, M., Bettuzzi, S., Di Pietro, C., Mirabile, E., Di Blasi, M., Rimini, R., Grzeschik, K. H., Ingletti, C., Corti, A. and Sichel, G. (1991). The gene for SP-40,40, human homolog of rat sulfated glycoprotein 2, rat clusterin, and rat testosterone-repressed prostate message 2, maps to chromosome 8. Genomics 10: 151-156.

Reddy, K. B., Jin, G., Karode, M. C., Harmony, J. A. and Howe, P. H. (1996a). Transforming growth factor β (TGF β)-induced nuclear localization of apolipoprotein J/clusterin in epithelial cells. Biochem 35: 6157-6163.

Reddy, K. B., Karode, M. C., Harmony, A. K. and Howe, P. H. (1996b). Interaction of transforming growth factor β receptors with apolipoprotein J/clusterin. Biochem 35: 309-314.

Reeder, D. J., Stuart, W. D., Witte, D. P., Brown, T. L. and Harmony, J. A. (1995). Local synthesis of apolipoprotein J in the eye. Exp Eye Res 60: 495-504.

Rennie, P. S., Bruchovsky, N., Buttyan, R., Benson, M. and Cheng, H. (1988). Gene expression during the early phases of regression of the androgen-dependent Shionogi mouse mammary carcinoma. Cancer Res 48: 6309-6312.

Roeth, P. J. and Easterbrook-Smith, S. B. (1996). C1q is a nucleotide binding protein and is responsible for the ability of clusterin preparations to promote immune complex formation. Biochim Biophys Acta 1297: 159-166.

Rosemblit, N. and Chen, C. L. (1994). Regulators for the rat clusterin gene: DNA methylation and cis- acting regulatory elements. J Mol Endocrinol 13: 69-76.

Rosenberg, M. E. and Paller, M. S. (1991). Differential gene expression in the recovery from ischemic renal injury. Kidney Int 39: 1156-1161.

Rosenberg, M. E., Manivel, J. C., Carone, F. A. and Kanwar, Y. S. (1995a). Genesis of renal cysts is associated with clusterin expression in experimental cystic disease. J Am Soc Nephrol 5: 1669-1674.

Rosenberg, M. E. and Silkensen, J. (1995b). Clusterin: physiologic and pathophysiologic considerations. Int J Biochem Cell Biol 27: 633-645.

Rouleau, M., Léger, J. and Tenniswood, M. (1990). Ductal heterogeneity of cytokeratins, gene expression, and cell death in the rat ventral prostate. Mol Endocrinol 4: 2003-2013.

Rozovsky, I., Morgan, T. E., Willoughby, D. A., Dugichi-Djordjevich, M. M., Pasinetti, G. M., Johnson, S. A. and Finch, C. E. (1994). Selective expression of clusterin (SGP-2) and complement C1qB and C4 during responses to neurotoxins in vivo and in vitro. Neurosci 62: 741-758.

Russo, P., Warner, J. A., Huryk, R., Perez, G. and Heston, W. D. (1994). TRPM-2 gene expression in normal rat ventral prostate following castration and exposure to diethylstilbestrol, flutamide, MK-906 (finasteride), and coumarin. Prostate 24: 237-243.

Saito, A., Pietromonaco, S., Loo, A. K. and Farquhar, M. G. (1994). Complete cloning and sequencing of rat gp330/"megalin," a distinctive member of the low density lipoprotein receptor gene family. Proc Natl Acad Sci U S A 91: 9725-9729.

Sato, J. D., Kawamoto, T. and Okamoto, T. (1987). Cholesterol requirement of P3-X63-Ag8 and X63-Ag8.653 mouse myeloma cells for growth in vitro. J Exp Med 165: 1761-1766.

Saunders, J. R., Aminian, A., McRae, J. L., O'Farrell, K. A., Adam, W. R. and Murphy, B. F. (1994). Clusterin depletion enhances immune glomerular injury in the isolated perfused kidney. Kidney Int 45: 817-827.

Sawczuk, I. S., Hoke, G., Olsson, C. A., Connor, J. and Buttyan, R. (1989). Gene expression in response to acute unilateral ureteral obstruction. Kidney Int 35: 1315-1319.

Schiffer, M. and Edmundson, A. B. (1967). Use of helical wheels to represent the structures of proteins and to identify segments with helical potential. Biophys J 7: 121-135.

Schreiber, S. S., Tocco, G., Najm, I. and Baudry, M. (1993). Seizure activity causes a rapid increase in sulfated glycoprotein-2 messenger RNA in the adult but not the neonatal rat brain. Neurosci Lett 153: 17-20.

Schumer, M., Colombel, M. C., Sawczuk, I. S., Gobe, G., Connor, J., O'Toole, K. M., Olsson, C. A., Wise, G. J. and Buttyan, R. (1992). Morphologic, biochemical, and molecular evidence of apoptosis during the reperfusion phase after brief periods of renal ischemia. Am J Pathol 140: 831-838.

Schwochau, G. B., Nath, K. A. and Rosenberg, M. E. (1997). Promotion of cell interactions by clusterin protects renal tubular epithelial cells from oxidant damage. Third International Workshop on Clusterin, Villars-sur-Ollon, Switzerland.

Scoazec, J. Y., Borghi-Scoazec, G., Durand, F., Bernuau, J., Pham, B. N., Belghiti, J., Feldmann, G. and Degott, C. (1997). Complement activation after ischemia-reperfusion in human liver allografts: incidence and pathophysiological relevance. Gastroenterol 112: 908-918.

See, Y. P. and Jackowski, G. (1989). Estimating molecular weights of polypeptides by SDS gel electrophoresis. in: Protein structure: a practical approach. Ed.: T. E. Creighton. Eynsham, Oxford, England, IRL Press. 1-19.

Selkoe, D. J. (1991). The molecular pathology of Alzheimer's disease. Neuron 6: 487-498.

Selkoe, D. J. (1994). Cell biology of the amyloid β-protein precursor and the mechanism of Alzheimer's disease. Ann Rev Cell Biol 10: 373-403.

Sensibar, J. A., Griswold, M. D., Sylvester, S. R., Buttyan, R., Bardin, C. W., Cheng, C. Y., Dudek, S. and Lee, C. (1991). Prostatic ductal system in rats: regional variation in localization of an androgen-repressed gene product, sulfated glycoprotein-2. Endocrinol 128: 2091-2102.

Sensibar, J. A., Qian, Y., Griswold, M. D., Sylvester, S. R., Bardin, C. W., Cheng, C. Y. and Lee, C. (1993). Localization and molecular heterogeneity of sulfated glycoprotein-2 (clusterin) among ventral prostate, seminal vesicle, testis, and epididymis of rats. Biol Reprod 49: 233-242.

Sensibar, J. A., Sutkowski, D. M., Raffo, A., Buttyan, R., Griswold, M. D., Sylvester, S. R., Kozlowski, J. M. and Lee, C. (1995). Prevention of cell death induced by tumor necrosis factor α in LNCaP cells by overexpression of sulfated glycoprotein-2 (clusterin). Cancer Res 55: 2431-2437.

Silkensen, J., Skubitz, K. and Rosenberg, M. E. (1994). The effect of clusterin on renal epithelial cell aggregation and adhesion. The Second Workshop on Clusterin Coeur d'Alene, Idaho.

Silkensen, J. R., Schwochau, G. B. and Rosenberg, M. E. (1994). The role of clusterin in tissue injury. Biochem Cell Biol 72: 483-488.

Simboli-Campbell, M., Narvaez, C. J., Tenniswood, M. and Welsh, J. (1996). 1,25-Dihydroxyvitamin D3 induces morphological and biochemical markers of apoptosis in MCF-7 breast cancer cells. J Steroid Biochem Mol Biol 58: 367-376.

Sklar, G. N., Eddy, H. A., Jacobs, S. C. and Kyprianou, N. (1993). Combined antitumor effect of suramin plus irradiation in human prostate cancer cells: the role of apoptosis. J Urol 150: 1526-1532.

Slawin, K., Sawczuk, I. S., Olsson, C. A. and Buttyan, R. (1990). Chromosomal assignment of the human homologue encoding SGP-2. Biochem Biophys Res Commun 172: 160-164.

Smith, P. K., Krohn, R. I., Hermanson, G. T., Mallia, A. K., Gartner, F. H., Provenzano, M. D., Fujimoto, E. K., Goeke, N. M., Olson, B. J. and Klenk, D. C. (1985). Measurement of protein using bicinchoninic acid. Anal Biochem 150: 76-85.

Smith, S. B., Bora, N., McCool, D., Kutty, G., Wong, P., Kutty, R. K. and Wiggert, B. (1995). Photoreceptor cells in the vitiligo mouse die by apoptosis. TRPM- 2/clusterin expression is increased in the neural retina and in the retinal pigment epithelium. Invest Ophthalmol Vis Sci 36: 2193-2201.

Speicher, D. W. (1989). Microsequencing with PVDF membranes: efficient electroblotting, direct protein adsorption and sequencer program modifications . Orlando, FL, Academic Press, Inc. 24-35.

Strickland, S. and Mahdavi, V. (1978). The induction of differentiation in teratocarcinoma stem cells by retinoic acid. Cell 15: 393-403.

Strickland, S., Smith, K. K. and Marotti, K. R. (1980). Hormonal induction of differentiation in teratocarcinoma stem cells: generation of parietal endoderm by retinoic acid and dibutyryl cAMP. Cell 21: 347-355.

Stuart, W. D., Krol, B., Jenkins, S. H. and Harmony, J. A. (1992). Structure and stability

of apolipoprotein J-containing high- density lipoproteins. Biochem 31: 8552-8559.

Swertfeger, D. K., Witte, D. P., Stuart, W. D., Rockman, H. A. and Harmony, J. A. (1996). Apolipoprotein J/clusterin induction in myocarditis: A localized response gene to myocardial injury. Am J Pathol 148: 1971-1983.

Sylvester, S. R., Skinner, M. K. and Griswold, M. D. (1984). A sulfated glycoprotein synthesized by Sertoli cells and by epididymal cells is a component of the sperm membrane. Biol Reprod 31: 1087-1101.

Sylvester, S. R., Morales, C., Oko, R. and Griswold, M. D. (1991). Localization of sulfated glycoprotein-2 (clusterin) on spermatozoa and in the reproductive tract of the male rat. Biol Reprod 45: 195-207.

Tenniswood, M. P., Guenette, R. S., Lakins, J., Mooibroek, M., Wong, P. and Welsh, J. E. (1992). Active cell death in hormone-dependent tissues. Cancer Metastasis Rev 11: 197-220.

Thomas-Salgar, S. and Millis, A. J. (1994). Clusterin expression in differentiating smooth muscle cells. J Biol Chem 269: 17879-17885.

Tschopp, J. (1984). Circular polymerization of the membranolytic ninth component of complement. Dependence on metal ions. J Biol Chem 259: 10569-10573.

Tschopp, J., Chonn, A., Hertig, S. and French, L. E. (1993). Clusterin, the human apolipoprotein and complement inhibitor, binds to complement C7, C8β, and the b domain of C9. J Immunol 151: 2159-2165.

Tschopp, J., Jenne, D. E., Hertig, S., Preissner, K. T., Morgenstern, H., Sapino, A. P. and French, L. (1993). Human megakaryocytes express clusterin and package it without apolipoprotein A-1 into a-granules. Blood 82: 118-125.

Tsuruta, J. K., Wong, K., Fritz, I. B. and Griswold, M. D. (1990). Structural analysis of sulphated glycoprotein 2 from amino acid sequence. Relationship to clusterin and serum protein 40,40. Biochem J 268: 571-578.

Tung, P. S., Burdzy, K., Wong, K. and Fritz, I. B. (1992). Competition between cell-substratum interactions and cell-cell interactions. J Cell Physiol 152: 410-421.

Urban, J., Parczyk, K., Leutz, A., Kayne, M. and Kondor-Koch, C. (1987). Constitutive apical secretion of an 80-kD sulfated glycoprotein complex in the polarized epithelial Madin-Darby canine kidney cell line. J Cell Biol 105: 2735-2743.

Vaishnav, M. Y. and Moudgal, N. R. (1991). Effect of specific FSH or LH deprivation on testicular function of the adult rat. Ind J Biochem Biophys 28: 513-520.

Vakeva, A., Laurila, P. and Meri, S. (1993). Co-deposition of clusterin with the complement membrane attack complex in myocardial infarction. Immunol 80: 177-182.

Vakeva, A., Meri, S., Lehto, T. and Laurila, P. (1995). Activation of the terminal complement cascade in renal infarction. Kidney Int 47: 918-926.

van Boeckel, C. A., Grootenhuis, P. D. and Haasnoot, C. A. (1991). Specificity in the recognition process between charged carbohydrates and proteins. Trends Pharmacol Sci 12: 241-243.

Wada, I., Ou, W. J., Liu, M. C. and Scheele, G. (1994). Chaperone function of calnexin for the folding intermediate of gp80, the major secretory protein in MDCK cells. Regulation by redox state and ATP. J Biol Chem 269: 7464-7472.

Walton, M., Young, D., Sirimanne, E., Dodd, J., Christie, D., Williams, C., Gluckman, P. and Dragunow, M. (1996). Induction of clusterin in the immature brain following a hypoxic- ischemic injury. Brain Res Mol Brain Res 39: 137-152.

Warri, A. M., Huovinen, R. L., Laine, A. M., Martikainen, P. M. and Harkonen, P. L. (1993). Apoptosis in toremifene-induced growth inhibition of human breast cancer cells in vivo and in vitro. J Natl Cancer Inst 85: 1412-1418.

Weisgraber, K. H. (1994). Apolipoprotein E: structure-function relationships. Adv Protein Chem 45: 249-302.

Wiessner, C., Back, T., Bonnekoh, P., Kohno, K., Gehrmann, J. and Hossmann, K. A. (1993). Sulfated glycoprotein-2 mRNA in the rat brain following transient forebrain ischemia. Brain Res Mol Brain Res 20: 345-352.

Wilson, C., Wardell, M. R., Weisgraber, K. H., Mahley, R. W. and Agard, D. A. (1991). Three-dimensional structure of the LDL receptor-binding domain of human apolipoprotein E. Science 252: 1817-1822.

Wilson, M. R., Roeth, P. J. and Easterbrook-Smith, S. B. (1991). Clusterin enhances the formation of insoluble immune complexes. Biochem Biophys Res Commun 177: 985-990.

Wilson, M. R. and Easterbrook-Smith, S. B. (1992). Clusterin binds by a multivalent mechanism to the Fc and Fab regions of IgG. Biochim Biophys Acta 1159: 319-326.

Wilson, M. R., Easterbrook-Smith, S. B., Lakins, J. and Tenniswood, M. P. R. (1995). Mechanisms of induction and function of clusterin at sites of cell death. in: Clusterin : Role in Vertebrate Development, Function and Adaptation. Ed.: J. A. K. Harmony. Austin, TX, R G Landes. 75-91.

Witte, D. P., Aronow, B. J., Stauderman, M. L., Stuart, W. D., Clay, M. A., Gruppo, R. A., Jenkins, S. H. and Harmony, J. A. (1993). Platelet activation releases megakaryocyte-synthesized apolipoprotein J, a highly abundant protein in atheromatous lesions. Am J Pathol 143: 763-773.

Wong, P., Pineault, J., Lakins, J., Taillefer, D., Léger, J., Wang, C. and Tenniswood, M. (1993). Genomic organization and expression of the rat TRPM-2 (clusterin) gene, a gene implicated in apoptosis. J Biol Chem 268: 5021-5031.

Wong, P., Taillefer, D., Lakins, J., Pineault, J., Chader, G. and Tenniswood, M. (1994a). Molecular characterization of human TRPM-2/clusterin, a gene associated with sperm maturation, apoptosis and neurodegeneration. Eur J Biochem 221: 917-925.

Wong, P., Kutty, R. K., Darrow, R. M., Shivaram, S., Kutty, G., Fletcher, R. T., Wiggert, B., Chader, G. and Organisciak, D. T. (1994b). Changes in clusterin expression associated with light-induced retinal damage in rats. Biochem Cell Biol 72: 499-503.

Wong, P., Borst, D. E., Farber, D., Danciger, J. S., Tenniswood, M., Chader, G. J. and van Veen, T. (1994c). Increased TRPM-2/clusterin mRNA levels during the time of retinal degeneration in mouse models of retinitis pigmentosa. Biochem Cell Biol 72: 439-446.

Wright, P. S., Cross-Doersen, D., Th'ng, J. P., Guo, X. W., Crissman, H. A., Bradbury, E. M., Montgomery, L. R., Thompson, F. Y., Loudy, D. E., Johnston, J. O. and Bitonti, A. J. (1996). A ribonucleotide reductase inhibitor, MDL 101,731, induces apoptosis and elevates TRPM-2 mRNA levels in human prostate tumor xenografts. Exp Cell Res 222: 54-60.

Zakeri, Z., Curto, M., Hoover, D., Wightman, K., Engelhardt, J., Smith, F. F., Kierszenbaum, A. L., Gleeson, T. and Tenniswood, M. (1992). Developmental expression of the S35-S45/SGP-2/TRPM-2 gene in rat testis and epididymis. Mol Reprod Dev 33: 373-384.

Zheng, G., Bachinsky, D. R., Abbate, M., Andres, G., Brown, D., Stamenkovic, I., Niles, J. L. and McCluskey, R. T. (1994a). gp330: receptor and autoantigen. Ann N Y Acad Sci 737: 154-162.

Zheng, G., Bachinsky, D. R., Stamenkovic, I., Strickland, D. K., Brown, D., Andres, G. and McCluskey, R. T. (1994b). Organ distribution in rats of two members of the low-density lipoprotein receptor gene family, gp330 and LRP/α2MR, and the receptor-associated protein (RAP). J Histochem Cytochem 42: 531-542.

Zlokovic, B. V. (1996a). Cerebrovascular transport of Alzheimer's amyloid β and apolipoproteins J and E: possible anti-amyloidogenic role of the blood-brain barrier. Life Sci 59: 1483-1497.

Zlokovic, B. V., Martel, C. L., Matsubara, E., McComb, J. G., Zheng, G., McCluskey, R. T., Frangione, B. and Ghiso, J. (1996b). Glycoprotein 330/megalin: probable role in receptor-mediated transport of apolipoprotein J alone and in a complex with Alzheimer disease amyloid β at the blood-brain and blood- cerebrospinal fluid barriers. Proc Natl Acad Sci U S A 93: 4229-4234.

CURRICULUM VITAE

NAME: JOHNATHON NEIL LAKINS

DATE OF BIRTH: 10th of March, 1963

PLACE OF BIRTH: Burton-upon-Trent, Staffordshire, UK

CITIZENSHIP: Canadian

EDUCATION:

St. John's Ravenscourt
Winnipeg, Manitoba (Grades 10-12)

University of Ottawa
Ottawa, Ontario
B.Sc. (Hons) Biochemistry, 1990

University of Ottawa
Ottawa, Ontario
Ph.D. (Biochemistry) registered 1990-present

AWARDS:

Medical Research Council Student Fellowship, 1990-1995
University of Ottawa Entrance Scholarship, 1990-1995
University of Ottawa Merit Scholarship, 1987-1990
NSERC Summer Studentship, 1989

EXPERIENCE:

Lab Demonstrator, University of Ottawa 1990-1994
3rd Year Physical Biochemistry
3rd Year Molecular Biology
4th Year Biotechnology

Research Assistant – Dr. Ruth Lupu
Lawrence Berkeley National Labs., 1997-1998

Scientist
Marin Biologic Laboratories
3152 Paradise Dr.
Tiburon, CA, 1998-Present

PUBLICATIONS AND ABSTRACTS:

(1) Research papers published or in press:

Lakins, J., Bennett, S.A.L., Chen, J., Arnold, J.M., Morrissey, C., Wong, P., O'Sullivan, J., and Tenniswood, M. (1998) Clusterin biogenesis is altered during apoptosis in the regressing rat ventral prostate. J. Biol. Chem.; In press

Kapron J.T., Hilliard, G.M., Lakins, J.N., Tenniswood, M.P., West, K.A., Carr, S.A., and Crabb, J.W. (1997) Identification and characterization of glycosylation sites in human serum clusterin. Protein Sci.; **6(10)**: 2120-2133

Nitsche, E.M., Moquin, A., Adams, P.S., Guenette, R.S., Lakins, J.N., Sinnecker, G.H., Kruse, K., and Tenniswood, M.P.R. (1996) Differential display RT PCR from human foreskin fibroblasts for investigation of androgen-dependent gene expression. Am. J. Med. Genet.; **63(1)**: 231-238

Savory, J.G., May, D., Reich, T., La Casse, E.C., Lakins, J., Tenniswood, M., Raymond, Y., Hache, R.J., Sikorska, M., and Lefebvre, Y.A. (1995) 5 α-reductase type 1 is localized to the outer nuclear membrane. Mol. Cell. Endocrinol.; **110(1-2)**: 137-147

Wong, P., Taillefer, D., Lakins, J., Pineault, J., Chader, G., and Tenniswood, M. (1994) Molecular characterization of human TRPM-2/clusterin, a gene associated with sperm maturation, apoptosis, and neurodegeneration. Eur. J. Biochem.; **221(3)**: 917-925

Wong, P., Pineault, J., Lakins, J., Taillefer, D., Leger, J., Wang, C., and Tenniswood, M. (1993) Genomic organization and expression of the rat TRPM-2 (clusterin) gene, a gene implicated in apoptosis. J. Biol. Chem.; 5021-5031

(2) Reviews published or in press:

Wilson, M.R., Easterbrook-Smith, S.B., Lakins, J., and Tenniswood, M.P.R. (1995) Mechanisms of induction and function of clusterin at sites of cell death. In: Clusterin: Role in Vertebrate Development, Function and Adaptation, Ed.: J.A.K. Harmony, R.G. Landes Co., Austin, Texas: 75-91

Tenniswood, M., Taillefer, D., Lakins, J., Guenette, R.S., Mooibroek, M., Daehlin, L., and Welsh, J.E. (1994) Control of gene expression during apoptosis in hormone-dependent tissues. In: Apoptosis II: The molecular basis of apoptosis in disease, Eds. L.D. Tomei and R.O. Cope, Cold Spring Harbor Laboratory Press, Cold Spring Harbor, NY: 283-311

Tenniswood, M.P.R., Guenette, R.S., Lakins, J., Mooiebroek, M., Wong, P., and Welsh, J.E. (1992) Active cell death in hormone-dependent tissues. Cancer Metastasis Rev.; **11(2)**: 197-220

(3) Research papers and reviews submitted or in preparation:

Morrissey, C., Lakins, J., Moquin, A., Tenniswood, M., and Hussain, M. (1998) Serum clusterin concentrations do not alter in prostate cancer. Submitted to Clin. Cancer Res.

Valdusic, E.A., Hornby, A.E., Guerra-Vladusic, F.K., Lakins, J., and Lupu, R. (1998) Expression and regulation of a novel estrogen receptor (ERβ) in breast cancer cell lines and tumors. Submitted to Cancer Res.

Tenniswood, M., Wang, Z., Lakins, J., Morrissey, C., O'Sullivan, J., and Tang, H. (1998) Clusterin in the male reproductive tract. Review submitted to J. Androl.

Lakins, J. and Tenniswood, M. (1998) Secretion, purification, and characterization of human clusterin expressed as a recombinant protein in *Pichia pastoris*; partial proteolysis suggests distinct binding sites for hydrophobic ligands complement C9 and Alzheimer's amyloid β peptide. In preparation.

(4) Abstracts:

Lakins, J. and Tenniswood, M. (1997) An integrated model of human clusterin structure and function: Framework for more refined studies. Oral presentation at: Third International Workshop on Clusterin; Villars-sur-Ollon, Switzerland

Nitsche, E.M., Adams, P.S., Taillefer, D., Lakins, J., Guenette, R.S., and Tenniswood, M. (1995) Investigation of androgen regularion of genes in genital skin fibroblasts by differential display RT PCR. Poster presentation at: Canadian Federation of Biological Sciences; Saskatoon, Saskatchewan, Canada

Nitsche, E.M., Taillefer, D., Lakins, J., Guenette, R.S., and Tenniswood, M. (1995) Expression of androgen regulared genes in genital skin fibroblasts *in vitro*. Poster presentation at: The Endocrine Society; Washington DC, USA

Hilliard, G.M., Kapron, J.T., West, K., Lakins, J., Tenniswood, M., Carr, S.A., and Crabb, J.W. (1995) Characterization of carbohydrate on human clusterin. Poster presentation at: The Protein Society; Boston, Mass., USA

Lakins, J., Tang, H., Wilson, M., and Tenniswood, M. (1994) Expression of human clusterin in *Saccharomyces cerevisiae* and *Pichia pastoris*. Poster presentation at: Second International Workshop on Clusterin; Coeur d'Alene, Idaho, USA

Wong, P., Lakins, J., Taillefer, D., Putlina, T., Chader, G., and Tenniswood, M. (1993) Human TRPM-2: Isolation and molecular characterization. Poster presentation at: Keystone Symposia on Molecular and Cellular Biology of Ageing: Lake Tahoe, California, USA

Lakins, J., and Tenniswood, M. (1992) Characterization of MalE clusterin subunit and proprotein fusions expressed in *E.coli*. Oral presentation at: First International Workshop on Clusterin; Cambridge, UK

Lakins, J., and Tenniswood, M. (1990) Gene expression in Ca^{+2} ionophore treated RDE cells. Poster presentation at: Canadian Federation of Biological Sciences; Halifax, Nova Scotia, Canada